

Synthesis and Reactions of Iridium(III) and
Rhodium(III) Complexes containing Terminal
Difluoro- and Dichloro-phosphino Groups

Neil Thomas McManus

Presented for the degree of
Doctor of Philosophy
University of Edinburgh
1982



ACKNOWLEDGEMENTS

I would like to thank my supervisors Professor E.A.V. Ebsworth and Dr. D.W.H. Rankin for their help and guidance throughout my period of research. I would also like to thank all other members of the Inorganic research group for their assistance and in particular Mr. S.G.D. Henderson for his helpful advice and material assistance. I am grateful to Mr. J. Miller, Dr. A. Boyd, Mr. L. Bell and Dr. D. Reed for recording n.m.r. spectra and Mr. J. Grunbaum for obtaining elemental analysis. I thank the S.E.R.C. for provision of a Studentship and the University of Edinburgh for laboratory facilities. Finally, I would like to thank Miss A. Erskine for typing this thesis.

To my family, and friends
who won't understand the remainder
of this work

CONTENTS

| | | |
|------------------|---|----|
| | Summary | |
| <u>Chapter 1</u> | Introduction | 1 |
| | 1.1 Reactions of $\text{MX}(\text{CO})(\text{PR}_3)_2$ [M=Ir, Rh; X=Cl, Br, I] | 2 |
| | 1.2 Metal-fluorophosphine chemistry | 13 |
| | 1.3 Transition metal complexes with trivalent Group VB ligands | 20 |
| <u>Chapter 2</u> | The Reactions of Hydrido- and halo-difluoro- phosphines with $\text{IrY}(\text{CO})(\text{PEt}_3)_2$ [Y=Cl, Br, I] | 28 |
| | 2.1 Introduction | 29 |
| | 2.2 The reaction of HPF_2 with $\text{IrI}(\text{CO})(\text{PEt}_3)_2$ | 29 |
| | 2.3 The reaction of HPF_2 with $\text{IrBr}(\text{CO})(\text{PEt}_3)_2$ | 38 |
| | 2.4 The reaction of HPF_2 with $\text{IrCl}(\text{CO})(\text{PEt}_3)_2$ | 39 |
| | 2.5 The reactions of PF_2X with $\text{IrX}(\text{CO})-$ $(\text{PEt}_3)_2$ [X=Cl, Br, I] | 39 |
| | 2.6 The reactions of PF_2X with $\text{IrY}(\text{CO})(\text{PEt}_3)_2$ [X≠Y=Cl, Br, I] | 41 |
| | 2.7 Discussion for n.m.r. parameters | 44 |
| | 2.8 Conclusions | 54 |
| <u>Chapter 3</u> | Reactions of $\text{Ir}(\text{PF}_2)(\text{CO})(\text{PEt}_3)_2\text{X}_2$ | 57 |
| | 3.1 Reactions of $\text{Ir}(\text{PF}_2)(\text{CO})(\text{PEt}_3)_2\text{X}_2$ with non-metal substrates | 58 |
| | 3.1.1 The reaction of diborane with $\text{Ir}(\text{PF}_2)(\text{CO})(\text{PEt}_3)_2\text{X}_2$ [X=Cl, I] | 58 |

| | |
|---|-----|
| 3.1.2 The Reaction of HCl with $\text{Ir}(\text{PF}_2)(\text{CO})-(\text{PEt}_3)_2\text{Cl}_2$ | 64 |
| 3.1.3 The reactions of group VIB elements with $\text{Ir}(\text{PF}_2)(\text{CO})(\text{PEt}_3)_2\text{Cl}_2$ | 67 |
| 3.1.4 The reaction of dichlorine with $\text{Ir}(\text{PF}_2)(\text{CO})(\text{PEt}_3)_2\text{Cl}_2$ | 82 |
| 3.1.5 The reactions of H_2E with $\text{Ir}(\text{PF}_2)(\text{CO})-(\text{PEt}_3)_2\text{Cl}_2$ [E=O,S,Se] | 92 |
| 3.1.6 The reaction of excess PF_2Cl with $\text{Ir}(\text{PF}_2)(\text{CO})(\text{PEt}_3)_2\text{Cl}_2$ | 102 |
| 3.2 The reactions of $\text{Ir}(\text{PF}_2)(\text{CO})(\text{PEt}_3)_2\text{Cl}_2$ with transition metal substrates | 106 |
| 3.2.1 Introduction | 106 |
| 3.2.2 The reactions of $\text{Ir}(\text{PF}_2)(\text{CO})(\text{PEt}_3)_2\text{Cl}_2$ with $\text{MCl}_2(\text{COD})$ [M=Pd,Pt; COD=1,5-cyclooctadiene] | 110 |
| 3.2.3 The reactions of $\text{Ir}(\text{PF}_2)(\text{CO})(\text{PEt}_3)_2\text{Cl}_2$ with $[\text{MCl}_2 \text{ arene}]_2$ | 123 |
| 3.3 General Discussion of Experimental Data Relating to the derivatives of $\text{Ir}(\text{PF}_2)(\text{CO})(\text{PEt}_3)_2\text{Cl}_2$ | 131 |
| 3.3.1 X-ray crystal structure data | 131 |
| 3.3.2 Nuclear magnetic resonance data | 133 |
| 3.3.3 Infra-red data | 134 |
| 3.4 Conclusions and some suggestions for future work | 134 |

| | | |
|------------------|--|-----|
| <u>Chapter 4</u> | Synthesis and some reactions of iridium and rhodium complexes containing terminal dichlorophosphino groups | 136 |
| 4.1 | Synthesis | 137 |
| 4.2 | Some reactions of $M(PCl_2)(CO)(PEt_3)_2Cl_2$ [M=Ir, Rh] | 141 |
| 4.2.1 | The reaction of $Rh(PCl_2)(CO)(PEt_3)_2Cl_2$ with $IrCl(CO)(PEt_3)_2$ | 141 |
| 4.2.2 | The reaction of HCl with $Ir(PCl_2)(CO)-(PEt_3)_2Cl_2$ | 144 |
| 4.2.3 | The reactions of the group VIB elements with $Ir(PCl_2)(CO)(PEt_3)_2Cl_2$ | 145 |
| 4.2.4 | The reactions of $Ir(PCl_2)(CO)(PEt_3)_2Cl_2$ with H_2E (E=O, S, Se) | 147 |
| 4.2.5 | The reaction of methanol with $Ir(PCl_2)-(CO)(PEt_3)_2Cl_2$ | 161 |
| 4.2.6 | The reaction of dichlorine with $Ir(PCl_2)(CO)(PEt_3)_2Cl_2$ | 161 |
| 4.3 | Conclusions and suggestions for further work | 165 |
| <u>Chapter 5</u> | The Reactions of Halodifluorophosphines with $RhY(CO)(PEt_3)_2$ [Y=Cl, Br, I] | 170 |
| 5.1 | Introduction | 171 |
| 5.2 | The reactions of PF_2X with $RhY(CO)(PEt_3)_2$ [X=Y=Cl, Br, I] | 172 |
| 5.3 | The reaction of PF_2Cl with $RhCl(CO)-(PEt_3)_2$ | 177 |

| | | |
|-------------------|--|-----|
| 5.4 | Discussion of n.m.r. parameters | 183 |
| 5.5 | Conclusions | 189 |
| <u>Chapter 6</u> | Experimental | 191 |
| 6.1 | Vacuum line techniques | 192 |
| 6.2 | Handling air sensitive solids | 192 |
| 6.3 | Instruments | 193 |
| 6.4 | Reactions in sealed n.m.r. tubes | 194 |
| 6.5 | Experimental relating to reactions described in Chapter 2 | 195 |
| 6.6 | Experimental relating to reactions described in Chapter 3 | 200 |
| 6.7 | Experimental relating to reactions described in Chapter 4 | 207 |
| 6.8 | Experimental relating to reactions described in Chapter 5 | 213 |
| <u>Appendix I</u> | Reactions of some aminodifluorophosphines with $\text{IrX}(\text{CO})(\text{PEt}_3)_2$ [X = Cl, Br, I] | 215 |
| AI.1 | Introduction | 216 |
| AI.2 | The reactions of PF_2NMe_2 with $\text{IrX}(\text{CO})(\text{PEt}_3)_2$ [X=Cl,Br,I] | 216 |
| AI.3 | The reaction of PF_2NHMe with $\text{IrI}(\text{CO})(\text{PEt}_3)_2$ | 220 |
| AI.4 | The reaction of PF_2NHMe with $\text{IrCl}(\text{CO})(\text{PEt}_3)_2$ | 222 |
| AI.5 | The reactions of PF_2NH_2 with $\text{IrX}(\text{CO})(\text{PEt}_3)_2$ [X=Cl,Br] | 226 |

| | | |
|---------------------|---|-----|
| AI.6 | The reaction of PF_2NH_2 with $\text{IrI}(\text{CO})(\text{PEt}_3)_2$ | 227 |
| AI.7 | The reaction of PF_2NMe_2 with $\text{IrCl}(\text{CO})(\text{PEt}_3)_2$ | 228 |
| AI.8 | The reaction of a large excess of PF_2NMe_2 with $\text{IrI}(\text{CO})(\text{PEt}_3)_2$ | 228 |
| AI.9 | Experimental | 233 |
| AI.10 | Conclusions | 238 |
| <u>Appendix II</u> | The reaction of PF_3 with $\text{IrCl}(\text{CO})(\text{PEt}_3)_2$ | 240 |
| <u>Appendix III</u> | Published material | 243 |
| References | | 245 |
| Courses Attended | | 256 |

SUMMARY

This thesis describes the formation and structure of iridium(III) and rhodium(III) complexes containing terminal difluoro- and dichloro-phosphino groups. The complexes were synthesised by the oxidative addition of halodifluorophosphines and trichlorophosphine to $MY(CO)(PEt_3)_2$ [$M = Ir, Rh$; $Y = Cl, Br, I$].

Reactions of these species with a variety of non metal substrates, such as B_2H_6 , group VB elements and H_2E , have yielded a number of interesting conversions of the phosphino moieties.

Reactions of $Ir(PF_2)(CO)(PEt_3)_2Cl_2$ with transition metal substrates have been utilised to synthesise mixed metal PF_2 bridged complexes.

Appendices 1 and 2 describe some novel reactions of amino difluorophosphines and trifluorophosphine with $IrX(CO)(PEt_3)_2$ which yield an interesting variety of different five-coordinate iridium(I) complexes with coordinated fluoro-phosphine ligands.

All the complexes described in this thesis have been characterised by n.m.r. spectroscopy and where applicable micro elemental analyses and i.r. spectra of the products have been obtained, and in three cases X-ray crystal structures of complexes have been obtained.

CHAPTER 1

INTRODUCTION

INTRODUCTION

This chapter will provide a brief discussion of chemistry relevant to this work.

I.1 Reactions of $\text{MX}(\text{CO})(\text{PR}_3)_2$ [M = Ir, Rh; X = Cl, Br or I]

The majority of the reactions carried out on this class of complexes fall into two main categories:

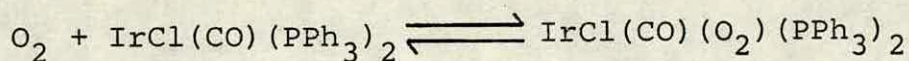
(a) The formation of five-coordinate donor adducts with small molecules.

(b) The oxidative addition of small molecules across the metal centre.

Although the dividing line between the two categories of reaction is at times indistinct, each will be dealt with separately in this introduction.

I.1(a) The Formation of Donor Adducts with Small Molecules

Work in this field was first stimulated by Vaska's discovery that carbonylchlorobistriphenylphosphine iridium(I), "Vaska's compound", added dioxygen⁽¹⁾ to form what was postulated as a five-coordinate donor adduct.



Although this complex is being discussed here as a donor adduct there is some doubt regarding this classification; this reaction can probably be regarded as lying on the border line between donor addition and oxidative addition.

Since Vaska reported this reaction, a large number of small molecules have been shown to react with Vaska's compound to yield adducts e.g. $\text{CO}^{(2)}$, $\text{SO}_2^{(3)}$, $\text{C}_2\text{H}_4^{(4)}$, $\text{BF}_3^{(5,6)}$ and $\text{SnCl}_4^{(7)}$.

The formation of the adducts has been shown to depend on mainly two factors:

(i) Weak donation from filled atomic or molecular orbitals on the ligand to unfilled d orbitals on the metal.

(ii) Acceptance of electron density from metal d orbitals by unfilled p or π orbitals on the ligand.

The degree of ligand-to-metal interactions is difficult to follow experimentally but an excellent empirical method for determining the degree of metal-to-ligand interaction is by measuring ν_{CO} of the adducts and comparing this value to that of the starting material⁽⁸⁾. A high degree of metal-to-ligand electron donation correlates with a relatively high ν_{CO} ; this results from the proportional decrease in metal-carbonyl d- π backbonding. With this method it has been shown that there is high metal-to-ligand donation in the $\text{BF}_3^{(6)}$ adduct (this is not surprising given that BF_3 is a strong Lewis acid) and that there is only weak interaction in the SO_2 adduct.

X-ray crystallographic studies have supported the postulate that there is significant metal to ligand interaction in the adducts. X-ray crystal structures of the O_2 and C_2H_4 adducts

showed this in the fact that the O-O and C-C distances respectively were greater than those of the free molecules⁽⁹⁾.

It has been shown that the most stable adducts with respect to loss of the small molecule are those of the strong π acceptor ligands⁽⁶⁾. The evidence put forward showed that dioxygen and sulphur dioxide, which have low electron affinities, formed adducts with relatively high dissociation pressures, whereas the BF_3 adduct did not exhibit a noticeable vapour pressure. Vaska showed a similar trend in a comparison of the association constants of adducts of substituted ethylenes⁽⁸⁾ the adducts of ethylenes with electron-withdrawing substituents (e.g. F, CN) had greater association constants than that of the ethylene adduct.

Reactions of BF_3 with $\text{IrCl}(\text{CO})\text{L}_2$ ⁽⁵⁾ ($\text{L} = \text{PEt}_2\text{Ph}$ or PMePh_2) gave rise to adducts with greater association constants than those of the adduct formed from Vaska's compound. The interpretation of this result is that the more basic phosphines give rise to a greater basicity at the metal centre; this gives rise to even stronger interactions from the metal to the ligand, although, the possibility that steric factors had caused the difference were not ruled out.

These observations suggest that the major factor determining the stability of the five coordinate adducts is not the degree of ligand-to-metal donation but the degree of metal-to-ligand back donation.

Work on the corresponding rhodium complexes has been less extensively reported but it has been shown that they do form adducts with the strong Lewis acids BCl_3 and BBr_3 ⁽¹⁰⁾. The fact that they formed adducts only with strong acids followed from the fact that the rhodium complexes are inherently less basic than their iridium analogues.

1.1(b) The Oxidative Addition of Small Molecules

Oxidative addition⁽¹¹⁾ is the generic name for a large group of reactions whereby the central atom of a compound simultaneously increases its coordination number and oxidation state by two on reaction with another molecule. The expression for the reaction can be written generally as



(The reverse reaction is termed reductive elimination).

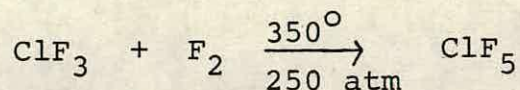
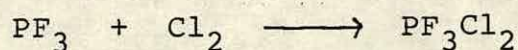
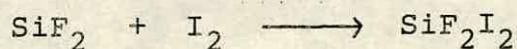
For addition reactions to proceed, the central atom M must possess:

- (a) non-bonding electron density
- (b) vacant coordination sites.

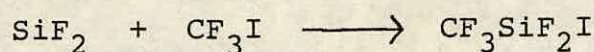
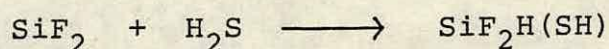
Although most of the research into oxidative addition reactions has been carried out on transition metal centres, certain compounds of main group elements are able to undergo reactions which can be regarded as oxidative additions.

A variety of higher oxidation state halides of groups IVB, VB, VIB and VIIB have been produced by the oxidative addition of the appropriate dihalogen or interhalogen to

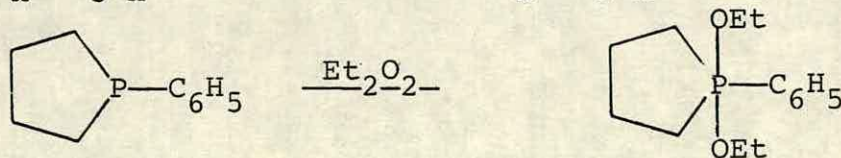
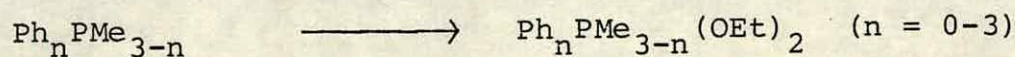
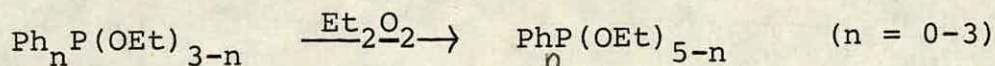
compounds of that group with a lower oxidation state. Examples of this are shown below⁽¹¹⁻¹⁴⁾:



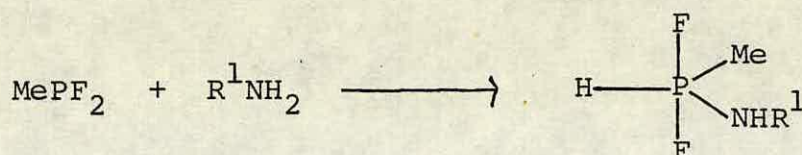
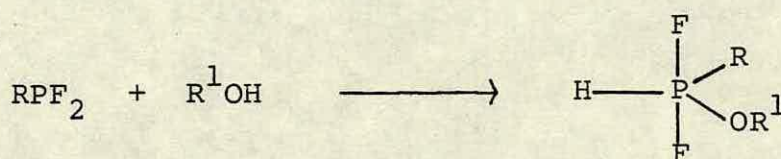
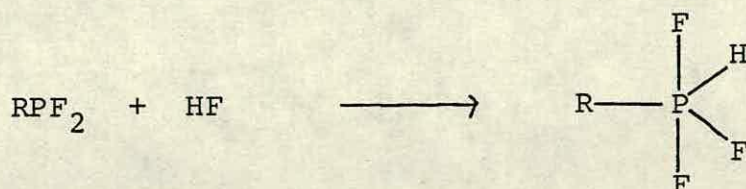
Oxidative addition reactions of main group compounds are not limited to the addition of halogens e.g. SiF_2 can add oxidatively H_2S ⁽¹⁵⁾ and CF_3I ⁽¹⁶⁾.



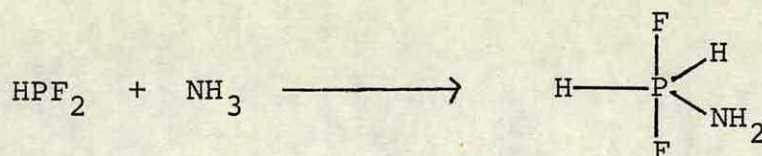
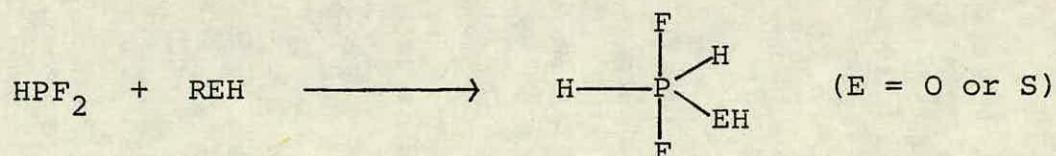
With regard to oxidative addition reactions on compounds of the main group elements, probably the most widely studied involve phosphorus(III) systems⁽¹⁸⁾. Oxidative addition reactions of halogens across phosphorus, as exemplified above, are known for many different fluorophosphines^(17,19). Phosphorus (III) compounds also undergo oxidative addition reactions with other compounds; examples of this are the reactions of phosphines and phosphites with diethylperoxide^(20,21)



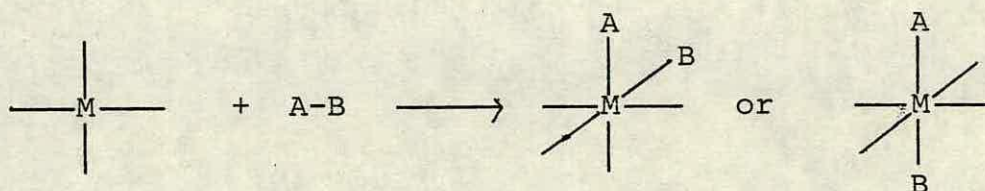
Fluorophosphines also undergo oxidative addition reactions with molecules besides halogens. Aryl- and alkyl-difluorophosphines have been shown to add oxidatively molecules such as H-F, alcohols and secondary amines⁽¹⁷⁾.



Difluorophosphine itself has been shown to react with alcohols, thiols⁽²²⁾ and ammonia⁽²³⁾.



Much of the work on the study of oxidative addition to transition metal centres has been carried out on square planar d^8 complexes (16 electron systems) which usually produce d^6 octahedral complexes on oxidative addition (18 electron systems).



The position of the equilibrium is largely dependent on two factors:

(i) The metal; in particular the energy required to raise its oxidation state by two.

(ii) The nature of A-B; primarily the strength of the A-B bond but also the strength of the M-A and M-B bond.

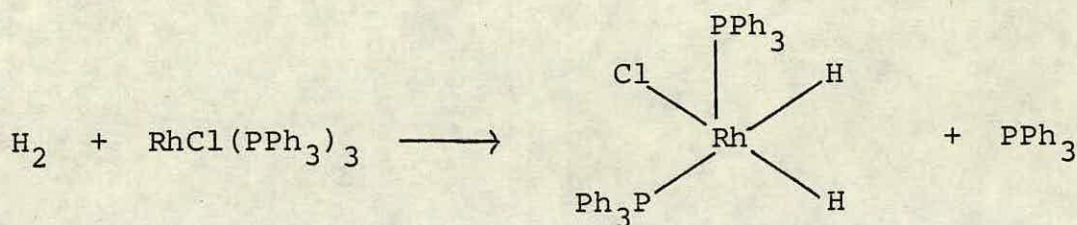
The first factor dictates that heavier metals in a triad form more stable adducts than the lighter ones, e.g. Ir(III) complexes are more stable than Rh(III), and, going across a group, the metals to the left form the more stable adducts, e.g. Ir(III) complexes are more stable than Pt(IV).

The importance of the nature of A-B is fairly self-evident: a high A-B bond strength will favour reductive elimination because of the difficulty in breaking the A-B bond and high M-A and M-B bond energies will similarly favour the oxidative addition reaction.

One factor not mentioned above because it does not effect the reaction directly is the nature of the ligands bound to the metal

centre. The reactivity of the four-coordinate complexes is enhanced by electron donating ligands which can help stabilise a high oxidation state.

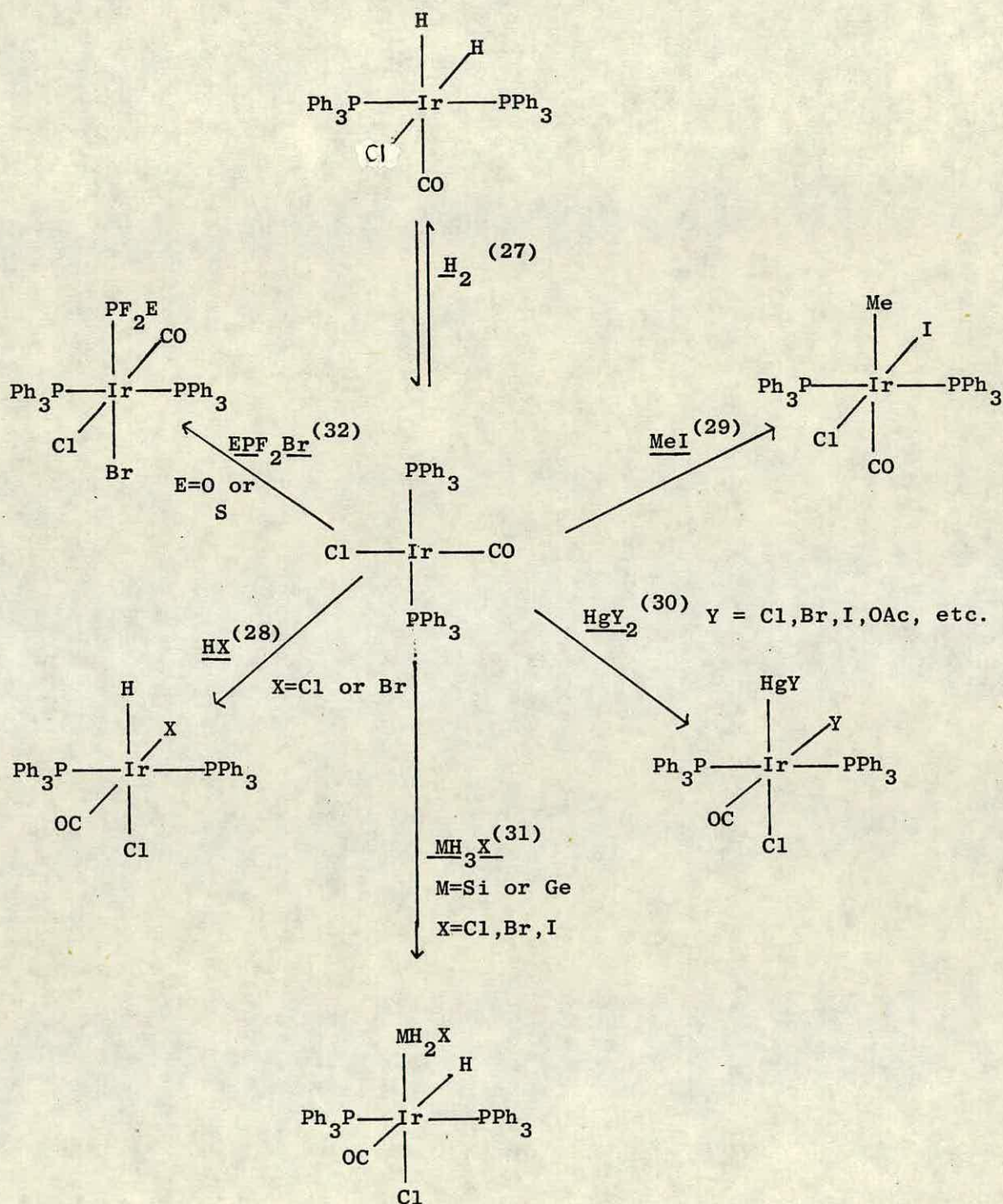
One of the main reasons for the great volume of research carried out on oxidative addition to metal d^8 complexes is its importance in many homogeneous catalytic systems⁽²⁴⁾, for instance of crucial importance in the catalytic hydrogenation of alkenes by $\text{RhCl}(\text{PPh}_3)_3$, 'Wilkinson's catalyst'⁽²⁵⁾, is the initial oxidative addition of H_2 to rhodium; in this case the oxidative addition is accompanied by a loss of phosphine.



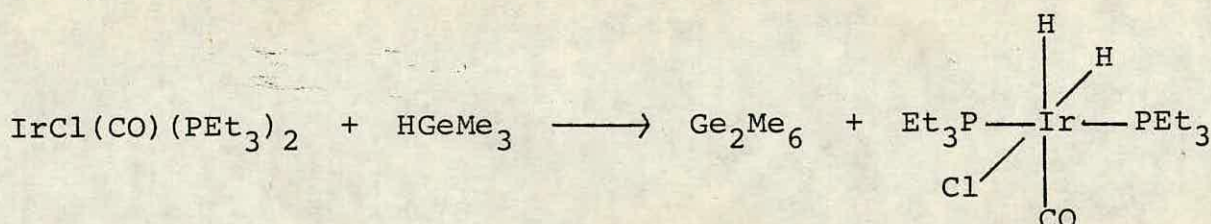
The oxidative addition effectively activates the hydrogen by breaking the H-H bond prior to reaction with the alkene which binds to rhodium in a subsequent stage of the mechanism. A similar oxidative addition of H_2 to rhodium is involved in the catalysis of hydroformylation by $\text{HRh}(\text{CO})(\text{PPh}_3)_3$ ⁽²⁶⁾.

Attention was drawn to the possibilities of the activation of hydrogen by oxidative addition to metal complexes by Vaska⁽²⁷⁾ who discovered that H_2 oxidatively added to Vaska's compound (it was later found that Vaska's compound could catalyse the hydrogenation of ethylene⁽⁴⁾). It has been found that Vaska's compound oxidatively adds an amazingly large variety of different molecules. Figure 1.1.1 summarises but a few of these reactions and gives some idea of the range of different compounds that are able to undergo oxidative addition reactions to metal centres.

Figure 1.1.1 Oxidative Addition Reactions to Vaska's Compound



Although by far the greatest volume of work into the oxidative additions reactions of $\text{IrX}(\text{CO})\text{L}_2$ ($\text{L} = \text{PR}_3$, AsR_3) has been carried out on Vaska's compound there has been work on complexes containing other phosphines. Exhaustive studies have been made on the addition of silyl and germyl compounds (MH_3X ; $\text{M} = \text{Si}, \text{Ge}$; $\text{X} = \text{Cl}, \text{Br}, \text{I}, \text{NR}_2$ etc.) to the triethylphosphine analogue⁽³³⁾. These reactions yielded stable six coordinate iridium-silyl or -germyl complexes. The production of stable iridium(III) complexes seems to be dependent on the ligand added, as the reaction of $\text{IrCl}(\text{CO})(\text{PEt}_3)_2$ with trimethyl germane⁽³⁴⁾ did not yield a stable iridium(III) germyl complex.



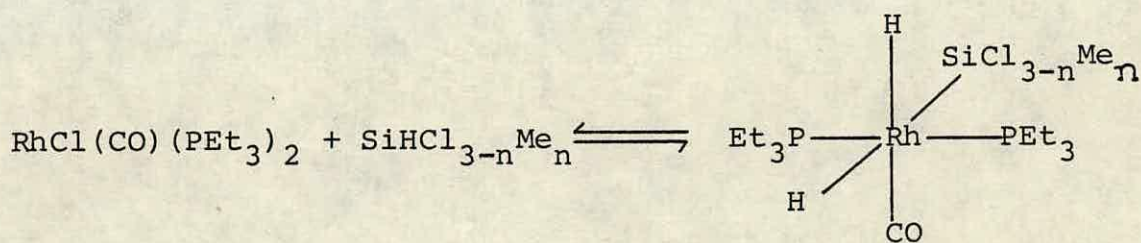
Clearly the formation of stable iridium(III) adducts is dependent on a fine balance between electron withdrawing and electron donating effects of all the ligands. Recent studies of the reactions of main group chlorides with $\text{IrCl}(\text{CO})(\text{PEt}_3)_2$ ⁽³⁵⁾ have shown that stable products of oxidative addition are obtained in many cases, e.g. SCl_2 , AsCl_3 , SnCl_4 and GeCl_4 .

It was found in the studies involving the oxidative addition of silyls and germyls to iridium that better characterisations of products were obtained for the systems containing PEt_3 because of the greater solubility of complexes

in the reaction media which meant that a complete characterisation of products was possible by ^{31}P and ^1H nmr.

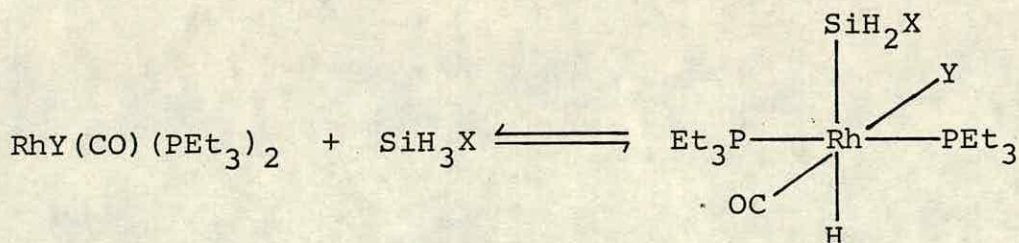
Oxidative addition reactions of analogous rhodium four coordinate complexes are also known. In fact Vallerino reported the oxidative addition of the dihalogens to $\text{RhX}(\text{CO})(\text{PPh}_3)_2$ ⁽³⁶⁾ some time before Vaska published the early reports of oxidative addition to the iridium complex. Work by Heck⁽²⁹⁾ showed that activated organic halides oxidatively add to $\text{RhCl}(\text{CO})(\text{PPh}_3)_2$ but the adducts were seen to be unstable, reductive elimination of the organic halides occurring readily.

Wilkinson and co-workers, in an attempt to produce stable rhodium(III)silyl complexes, found that SiHCl_3 and SiHCl_2Me ⁽³⁷⁾ oxidatively added across rhodium in $\text{RhCl}(\text{CO})(\text{PEt}_3)_2$ to yield adducts which dissociated readily in solution at room temperature.



(n = 0, 1)

The reactions of silyl and germyl compounds $[\text{MH}_3\text{X}]$, $\text{M} = \text{Si}, \text{Ge}; \text{X} = \text{H}, \text{Cl}, \text{I}$ with $\text{RhY}(\text{CO})(\text{PEt}_3)_2$ ^(38,39) [$\text{Y} = \text{Cl}, \text{I}$] showed the equilibrium in these reactions was very sensitive to the Group X on the Group IVB metal. The reaction of silane ($\text{X} = \text{H}$) with $\text{RhY}(\text{CO})(\text{PEt}_3)_2$ results in the production of an oxidative adduct at 198 K which decomposes to starting materials at room temperature.



(Y = Cl, I; X = Cl, I, H)

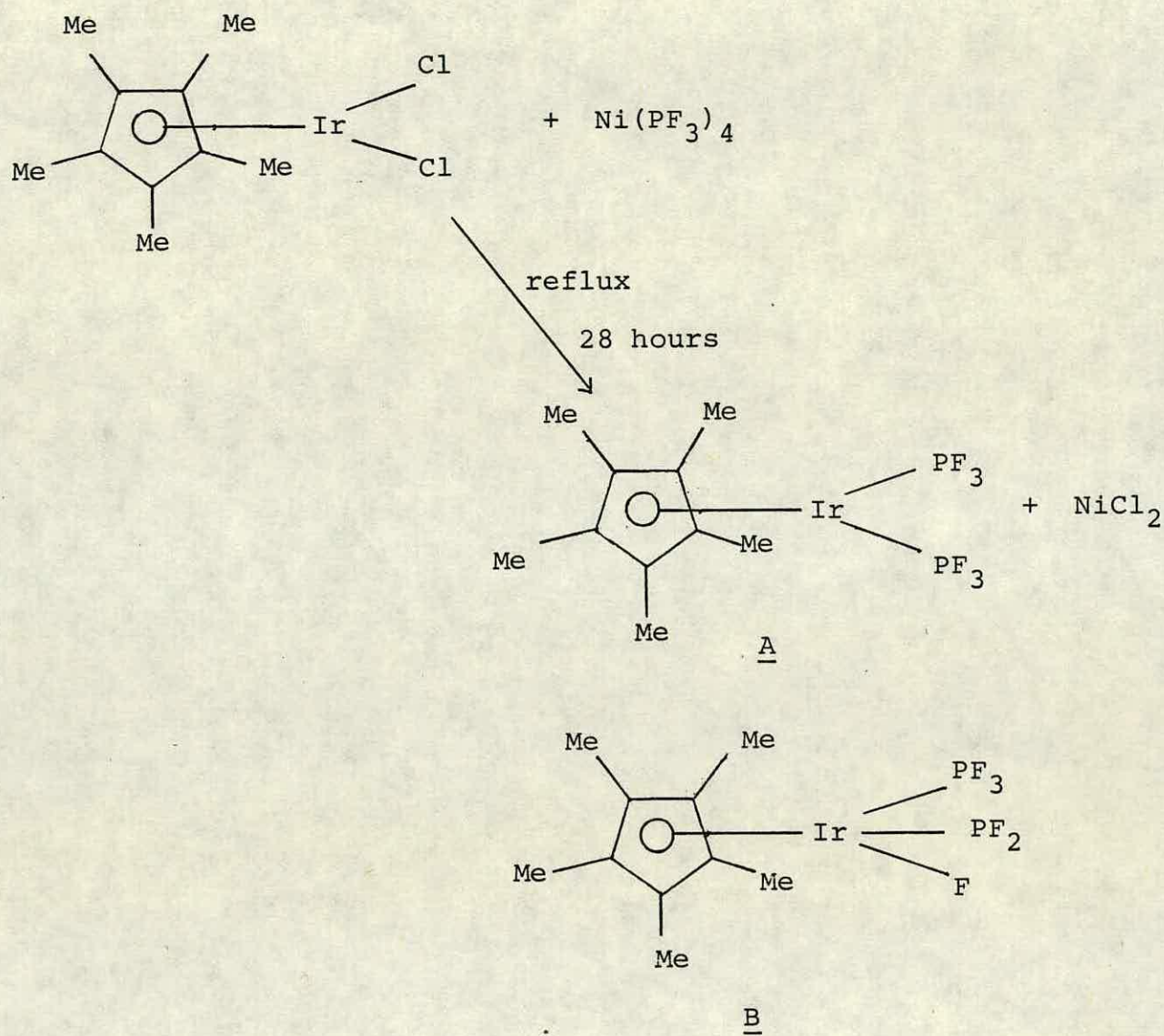
The corresponding adducts of iodo- and chloro-silane were stable at room temperature, as were adducts of chlorogermane and various organosilanes $[\text{SiH}_3\text{R}, \text{R} = \text{C}_2\text{H}_5, \text{C}_3\text{H}_7, \text{Ph}]$. The results implied that stable adducts were obtained when X was an electron-withdrawing substituent; conversely, the result obtained by Wilkinson *et al* concerning the addition of $\text{SiCl}_{3-n}\text{Me}_n$ ⁽³⁷⁾ [n = 0,1] showed that ligands with too great an electron-withdrawing effect also results in adducts that are unstable at room temperature.

Rhodium(III) adducts are generally less stable than the analogous iridium complexes in keeping with the fact that the stability of Ir(III) relative to Ir(I) is greater than that of Rh(III) to Rh(I). The relative instability of Rh(III) accounts partly for the great success of rhodium complexes as catalysts.

1.2 Metal Fluorophosphine Chemistry

A vast amount of work has been carried out on the synthesis, structure and reactions of metal-fluorophosphines ⁽¹⁷⁾. However, up until the time of this work there have been no reported examples of fully characterised metal fluorophosphine complexes containing a terminal difluorophosphino moiety.

King claimed to have synthesised an iridium difluorophosphino⁽⁴⁰⁾ complex as a byproduct in the reaction of $\text{Ni}(\text{PF}_3)_4$ with an iridium-arene complex:



Comparison of the n.m.r. data cited for compound B with values obtained in this work cast some doubt on this structural assignment ; this will be discussed in a later chapter.

Metal fluorophosphine chemistry to date, has been dominated by study of the interaction of trifluorophosphine with metals^(17,41). A sizable amount of work has also been carried out on metal-PF₂R compounds (R = CF₃, CCl₃, NR₂, CH₂Cl, etc.).^(17,42)

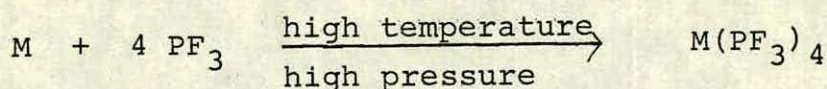
Interest in the interaction of fluorophosphines with metals stemmed from the belief that they possessed coordinating properties similar to carbon monoxide. Indeed many fluorophosphine complexes have metal-carbonyl analogues, e.g. Ni(PF₃)₄ and Ni(CO)₄.

It is believed that bonding in metal-fluorophosphine and metal-carbonyl complexes results from a balance of two factors:

- (i) σ bond donation from the lone pair on phosphorus
- (iii) $d\pi - d\pi$ bonding involving electrons from metal d orbitals to vacant d orbitals on phosphorus.

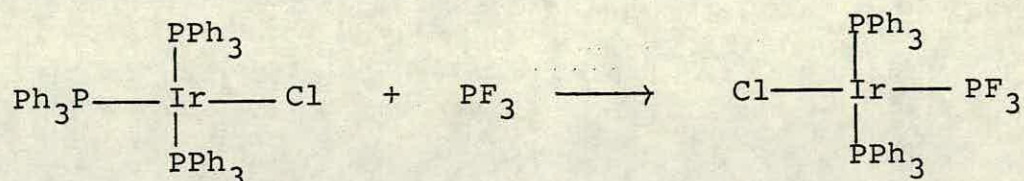
For metal fluorophosphine complexes, the degree of back-bonding depends on the 'R' group attached to phosphorus, as well as the oxidation state of the metal.

Metal-fluorophosphine complexes have been formed by a number of different methods. Some use extremely harsh reaction conditions in which the fluorophosphine is reacted with the metal at very high temperature and pressure⁽⁴³⁾.

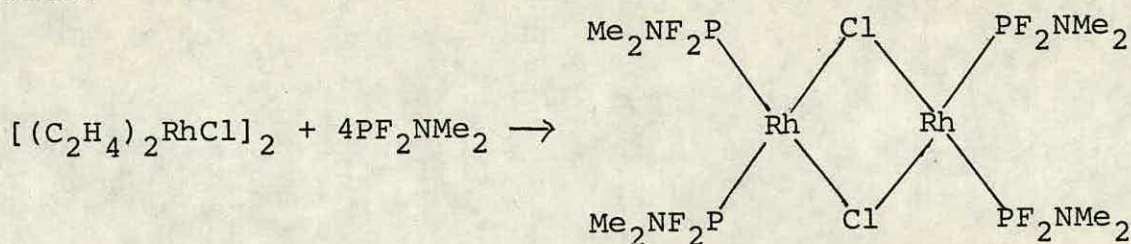


(M = Ni, Pd or Pt)

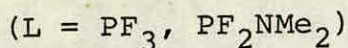
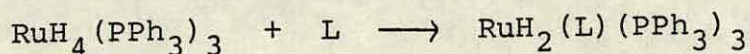
Another common method is by displacement of other ligands on the metal, such as in the example below where a triphenyl phosphine is displaced yielding a PF_3 analogue of Vaska's compound⁽⁴⁴⁾.



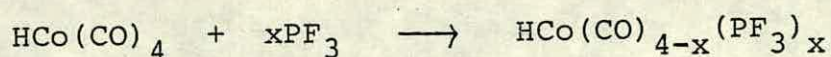
Other ligand displacement reactions, such as displacement of olefins from metal centres, have been utilised in the synthesis of metal fluorophosphine complexes as exemplified below⁽⁴⁵⁾.



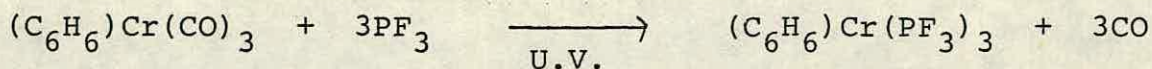
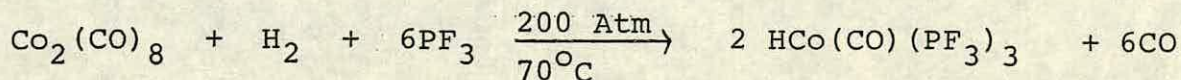
More recently dihydrogen has been used as a leaving group in the production of some ruthenium fluorophosphine complexes⁽⁴⁶⁾.



Many methods of synthesis involve displacement of carbon monoxide from metal carbonyls. Some of these reactions such as the example below proceed under very mild conditions⁽⁴⁷⁾.



However, most carbonyl displacement reactions do not proceed under such mild conditions and have to be thermally or photochemically induced⁽¹⁷⁾:

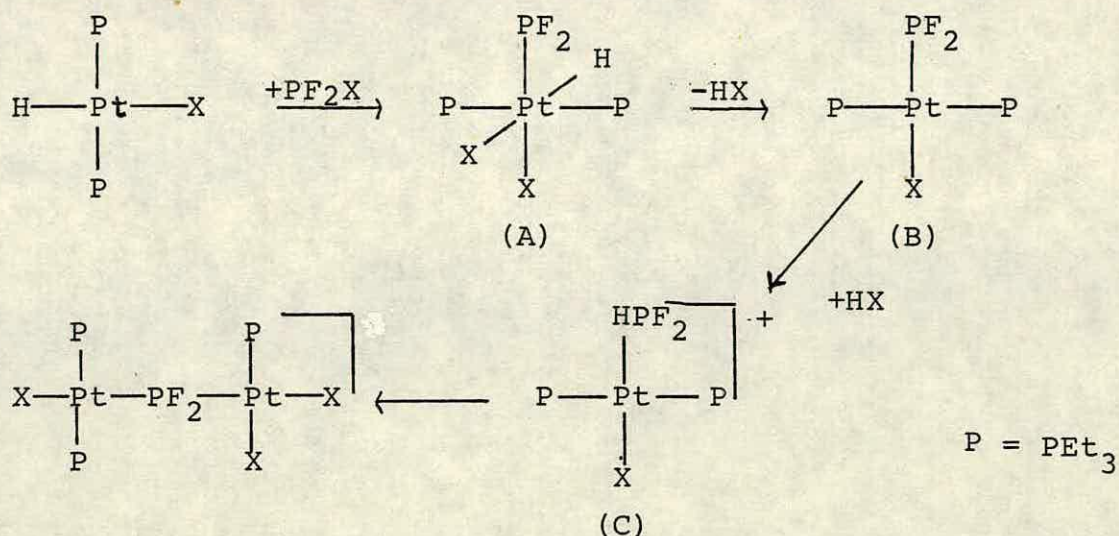


The examples given above are only a small sample of the available syntheses for metal difluorophosphine complexes. However, they do give some idea of the variety of preparative routes.

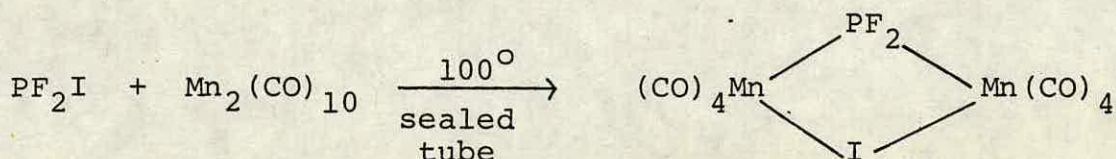
Although there are a great many examples of metal fluorophosphine complexes containing PF_2R ligands [$\text{R} = \text{F}, \text{CF}_3, \text{CCl}_3, \text{NR}_2$ etc.] there are comparatively few reported examples of reactions, and metal complexes, of halodifluorophosphines [PF_2X , $\text{X} = \text{Cl}, \text{Br}, \text{I}$] or hydridodifluorophosphine [HPF_2].

The reactions of PF_2X with halohydridobistriethylphosphine platinum(II) $[\text{PtHX}(\text{PEt}_3)]_2$ have been reported⁽⁴⁸⁾. The reactions ultimately yield PF_2 -bridged binuclear platinum(II) complexes. The postulated mechanism (see Figure 1.2.1) is of interest in that the reaction is believed to proceed via oxidative addition of PF_2X yielding a platinum-terminal PF_2 complex (A) which rapidly decomposes through a four-coordinate platinum(II) terminal PF_2 complex (B) to a four-coordinate platinum(II) HPF_2 (C) complex. The reactions were studied by ^{31}P , ^{19}F and ^1H n.m.r.; the results from these techniques did not produce direct evidence of either of the terminal PF_2 complexes but signals were detected for the species containing

the coordinated HPF_2 ligand. The proposed mechanism has been supported by results in this work.



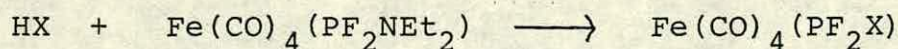
Another reaction of PF_2X with a metal substrate to produce a PF_2 bridged species was that of PF_2I with dimanganese decacarbonyl⁽⁴⁹⁾.



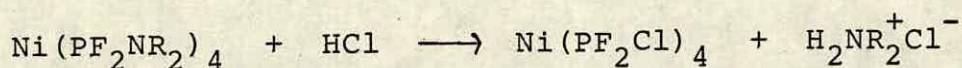
PF_2X has been used as a coordinating ligand in much the same way as PF_3 in a few complexes; for instance, direct reaction of PF_2Cl with platinum dichloride⁽⁵⁰⁾ produces a bis PF_2Cl platinum complex.



Other complexes containing PF_2X ligands have been produced by a different route; by the deamination of amino-difluorophosphine ligands bound to metals^(51,52).



(X = Cl, Br)

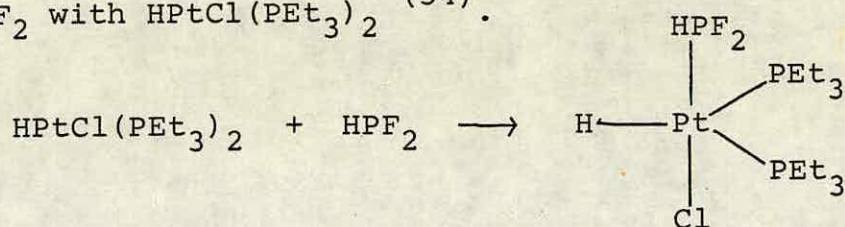


Complexes containing HPF_2 as a ligand have been even less well reported. One reported example was the product of a very interesting reaction; that of HPF_2 with nickel atoms⁽⁵³⁾.



The complex was found to be reasonably stable at room temperature but far less stable than $\text{Ni}(\text{PF}_3)_4$.

The only other example of a metal HPF_2 complex was a platinum(II) five coordinate species formed in the reaction of HPF_2 with $\text{HPtCl}(\text{PEt}_3)_2$ ⁽⁵⁴⁾.



This complex was characterised from its ^{31}P , ^{19}F and ^1H n.m.r. at low temperature (ca. 203 K) as it decomposed at ambient temperatures.

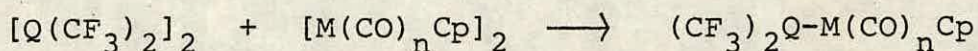
It is a little strange that there has been so little work carried out on studies into the interactions of metals with PF_2X and PF_2H when compared to the volume of research into metal complexes of other types of fluorophosphines. Perhaps the metal phosphorus bonds formed with such ligands are weaker as a result of the lesser π acidity of the PF_2X ligands when compared to PF_3 ; this would result in weaker metal to phosphorus backbonding, and therefore less stable complexes.

I.3 Transition Metal Complexes with Trivalent Group VB Ligands

Although many metal complexes containing Group VB ligands, such as phosphines and arsines, exist, there are comparatively few complexes containing trivalent ligands. Alternatively one could say there are comparatively few trivalent Group VB compounds with transition metal substituents.

The synthetic routes to these compounds are reasonably varied.

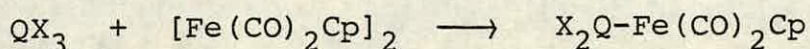
Trivalent phosphorus and arsenic compounds with metal group attached have been synthesised by the reactions of tetrakis(trifluoromethyl)-diphosphine⁽⁵⁵⁾ and -diarsine⁽⁵⁶⁾ with binuclear metal complexes.



(Cp = cyclopentadienyl; Q = P; M = Fe, n = 2

Q = As; M = Fe, n = 2; M = Mo, n = 3)

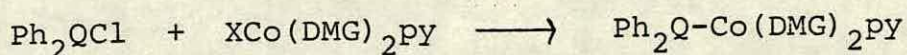
Cullen et al^(57,58) found that the reactions of Group VB halides (QX_3 ; Q = As, Sb, Bi; X = Cl, Br, I) with similar binuclear metal carbonyls also yielded complexes with trivalent Group VB centres.



(Q = As, X = Cl, Br; Q = Sb, X = Cl, Br, I;

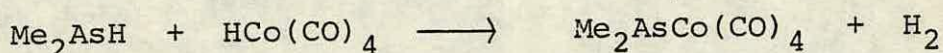
Q = Bi, X = Cl)

Schrauzer et al ⁽⁵⁹⁾ were able to produce diarylmetal-antimony and bismuth compounds by the reaction of diaryl chlorostibines and bismuthines with a cobalt complex containing a labile halide group.



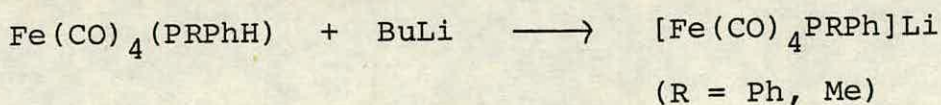
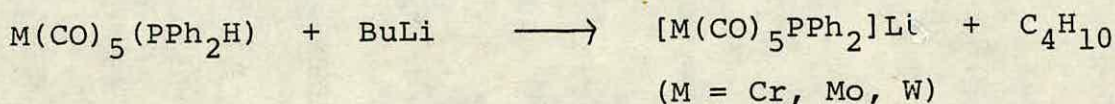
(DMG = Dimethylglyoxime; py = pyridine; Q = Sb or Bi)

The driving force of the reaction was the loss of dihalogen. A similar driving force is utilised in the reaction of dimethylarsine with a hydride carbonyl cobalt complex to produce a terminal dimethylarsine complex ⁽⁶⁰⁾.



This complex was not fully characterised as it decomposed rapidly with loss of carbonyl.

Treichel et al produced a series of transition metal dialkyl- or aryl-phosphide compounds by the deprotonation of secondary phosphines bound to various metals ⁽⁶¹⁾.

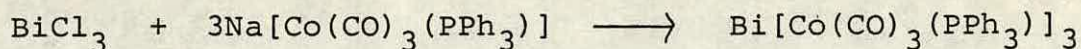


The most widely used method of synthesis involves the elimination of alkali metal salts in reactions between halides of Group VB elements and anionic metal complexes.

Nesmayanov et al⁽⁶²⁾ were probably the first group to utilise with any success, this type of reaction with a Group VB compound (previously this type of reaction had been successfully used to synthesise transition metal-group IVB compounds⁽⁶³⁾). By this method they synthesised a rhenium complex containing a terminal BiPh₂ grouping.



Cullen et al were able to produce trivalent arsenic and bismuth compounds, with iron and cobalt groups attached by this method⁽⁵⁸⁾. (The displacement of mercuric chloride in reaction with mercuric compounds was also used).



By far the largest number of Group VB compounds with metal substituents have been synthesised using salts of the type $[\text{M}(\text{CO})_n\text{Cp}]\text{Na}$ [$\text{M} = \text{Cr}, \text{Mo}, \text{W}, n = 3$; $\text{M} = \text{Fe}, n = 2$]. Reactions utilising these salts were carried by Cooke et al in 1968⁽⁶⁴⁾ to make $(\text{C}_6\text{F}_5)_2\text{Q-metal}$ compounds; however the full exploitation of this type of system was the work Malisch and co-workers from 1973 onwards. Figure 1.3.1 illustrates the use of these salts in the preparation of Group VB compounds with these metal carbonyl substituents.

One example of the opposite type of salt elimination, that is the reaction of a metal halide with an anionic group VB species, has been reported⁽⁷⁵⁾.

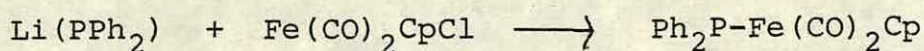
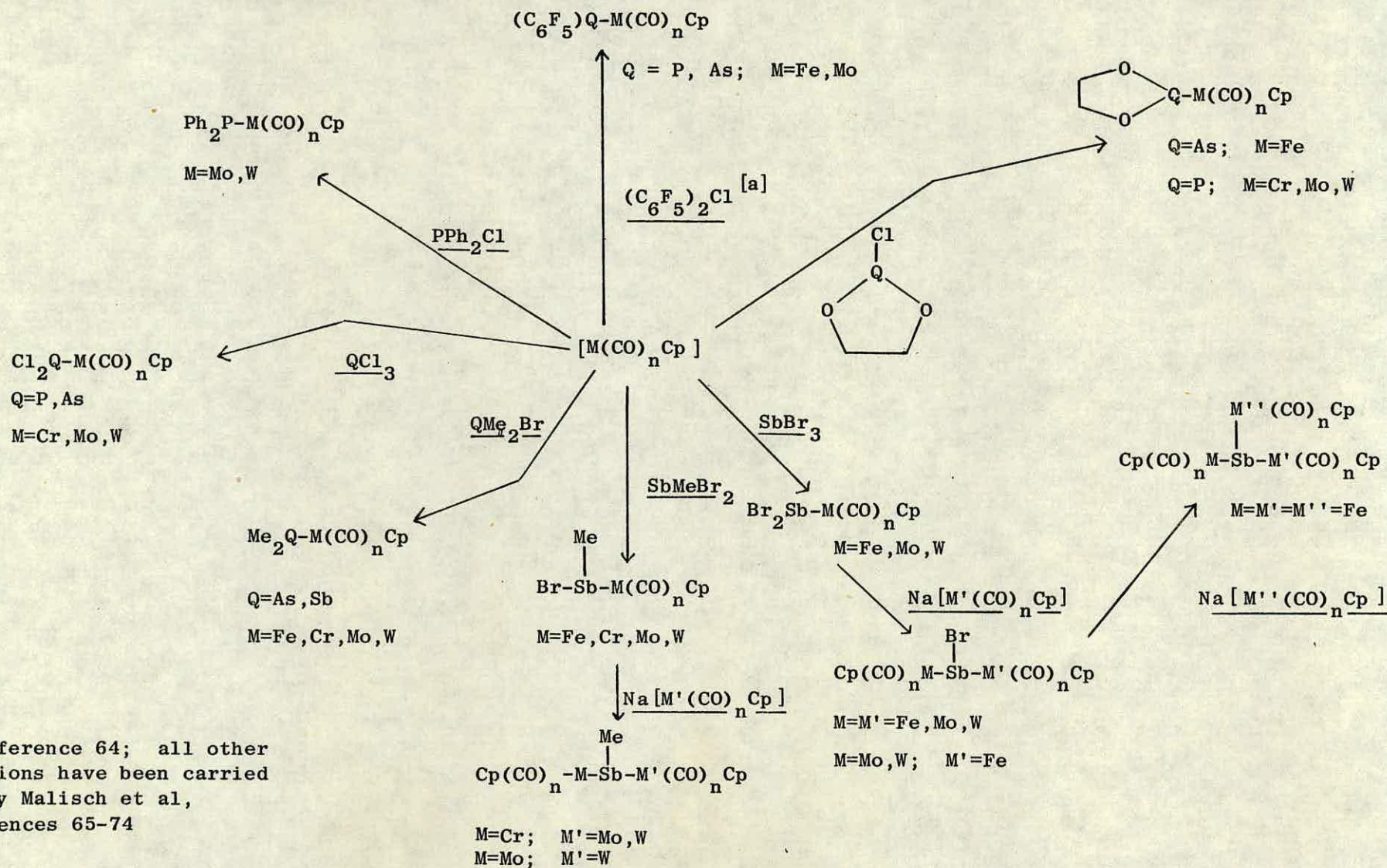
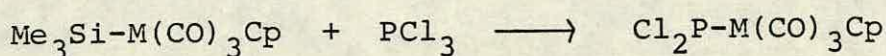


Figure 1.3.1 Syntheses of group VB compounds with metal substituents from the reactions of group VB halides with $\text{Na}[\text{M}(\text{CO})_n\text{Cp}]$ [$\text{M} = \text{Cr}, \text{Mo}, \text{W}$; $n=3$; $\text{M} = \text{Fe}$; $n=2$]



It is possible that this method has found less widespread use because^{of} the difficulty in synthesising anionic Group VB compounds compared with the relative ease of obtaining Group VB halides.

Malisch et al found that another convenient synthesis of the PCl_2 complexes (Figure 1.3.1) involved the elimination of trimethylsilylchloride⁽⁷²⁾ in the reaction of phosphorus trichloride with Group VIA metal silyl complexes.

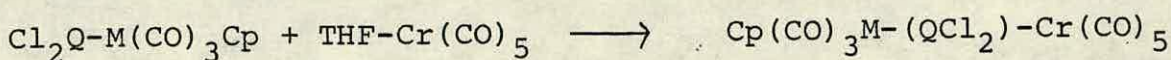
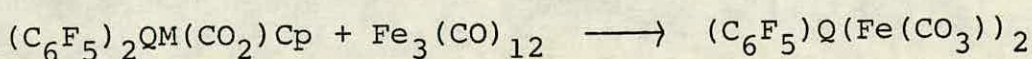


(M = Cr, Mo, W)

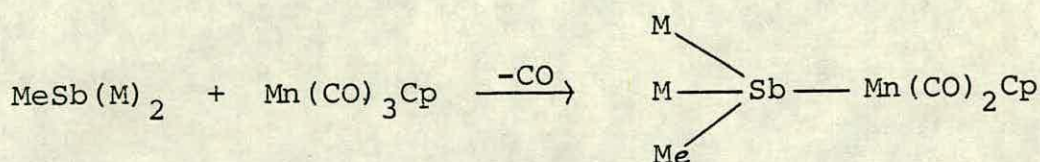
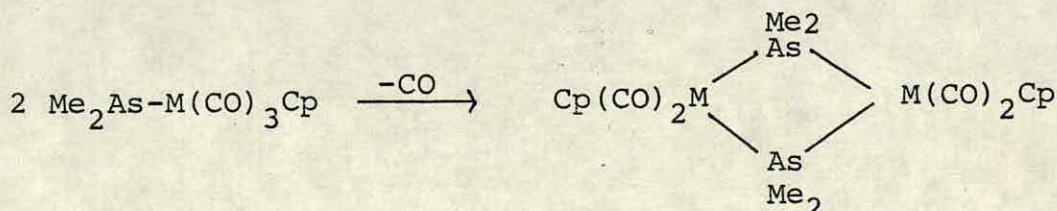
Much research has been carried out into the study of the reactivity of the Group VB compounds with metal substituents.

It has been found by many of the research groups involved in the syntheses of these compounds that the compounds react with other metal substrates^(61,63,64,67,71,76-78) in much the same way as 'normal' trivalent group VB ligands.

e.g.

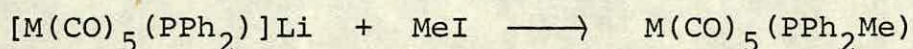


(Q = As, P; M = Cr, W)



(M = M' (CO)₃Cp; M' = Cr, Mo, W)

Treichel et al⁽⁶¹⁾ and Malisch et al^(71,74,78) also found that the compounds reacted readily with electrophilic reagents such as methyl iodide thus quaternising the Group VB centre.



(M = Cr, Mo, W)

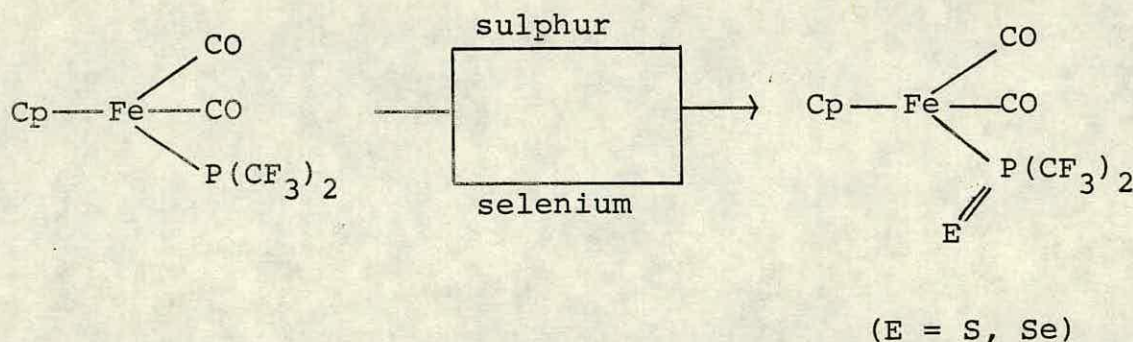


(Q = As, Sb; R = Me. Q = P; R = Ph.

R' = CH₃, CH₂COPh, SiMe₃, CH₂SiMe₃)

These results suggested that the Group VB centre has a high nucleophilic character in compounds of this type. This observation was not surprising for the diphenyl-phosphide compounds synthesised by Treichel where the negative charge was almost certainly localised on the phosphorus. The results were important in showing that in the other compounds the lone pair was localised at the Group VB centre.

Dobbie and Mason⁽⁵⁵⁾ did not report reactions of their compound with electrophilic reagents but they did carry out some work which went some way to proving that the metal-phosphorus bond of their product complex was highly polar with high electron density on the phosphorus. They observed that the phosphorus atom underwent unusually facile oxidation by elemental sulphur and selenium. (A finding which Malisch et al discovered was applicable to the M-PPh₂⁽⁷⁴⁾, -PCl₂⁽⁷²⁾ and -AsMe₂⁽⁷⁹⁾ compounds also).



They were also able to synthesise the analogous oxide by oxidation with nitrous oxide.

Studies of the carbonyl stretching frequencies (ν_{CO}) of both parent complex and products were made. These showed that ν_{CO} of the parent compound was significantly lower than those of the products. The higher ν_{CO} in the derivatives was caused by a decrease in backbonding to the coordinated carbonyl ligands as a result of increased backbonding to the phosphorus. Confirmation of this fact came from comparison of the X-ray crystal structures of the parent compound and the oxygen derivative⁽⁸⁰⁾. This showed that the Fe-P bond of the parent compound was some 7 pm longer than that of the oxygen derivative. These findings were deduced to be a result of a high polar character at the Fe-P bond in the parent compound with high electron density on the phosphorus and it was the fact that the phosphorus was highly electron rich which led to the ease of oxidation in order to relieve an unfavourable electronic environment.

It is worthy of note that the trivalent compounds of phosphorus with metal substituents tend to have electron withdrawing groups as the other substituents, presumably because the metal phosphorus bond is more polar than the bonds to the other Group VB elements and the high electron density has to be dissipated for the group to be stable. To support this observation Malisch et al observed that PCl_2 bridged species were far more thermally stable than the corresponding complexes with terminal ligands⁽⁷⁶⁾. In the bridged species the central bonding system is stabilised by mesomeric and inductive effects from the metal centres.

In general it can be said of trivalent Group VB compounds with metal substituents that the Group VB centre is electron rich with the lone pair localised on the Group VB centre.

CHAPTER 2

The Reactions of Hydrido- and Halo-Difluorophosphines

with $\text{IrY}(\text{CO})(\text{PEt}_3)_2$ [$\text{Y} = \text{Cl}^-$, Br^- or I^-]

2.1 Introduction

In the introductory chapter the two major modes of reaction of small covalent molecules with $\text{IrY(CO)(PEt}_3)_2$ were outlined.

The hydrido- and halo-difluorophosphines (PF_2X) have the potential to react by either:

(i) Forming donor adducts via the lone pair on the phosphorus,

or (ii) Oxidatively adding the P-X bond across iridium yielding six-coordinate iridium(III) complexes.

The major aim of the research was to form complexes containing terminal PF_2 groups, by the latter type of reaction.

The reactions were initially studied by ^{31}P , ^{19}F and ^1H n.m.r. The presence of those 100% I = $\frac{1}{2}$ nuclei in the reaction components meant that n.m.r. was the ideal technique for following the course of these reactions.

The n.m.r. data for the products obtained in the reactions described in this chapter are collected in Tables 2.1, 2.2 and 2.3.

2.2 The Reaction of HPF_2 with $\text{IrI(CO)(PEt}_3)_2$

This reaction was carried out in an n.m.r. tube. The ^{31}P , ^{19}F and ^1H n.m.r. spectra were recorded at various temperatures from 193 K to ambient temperature.

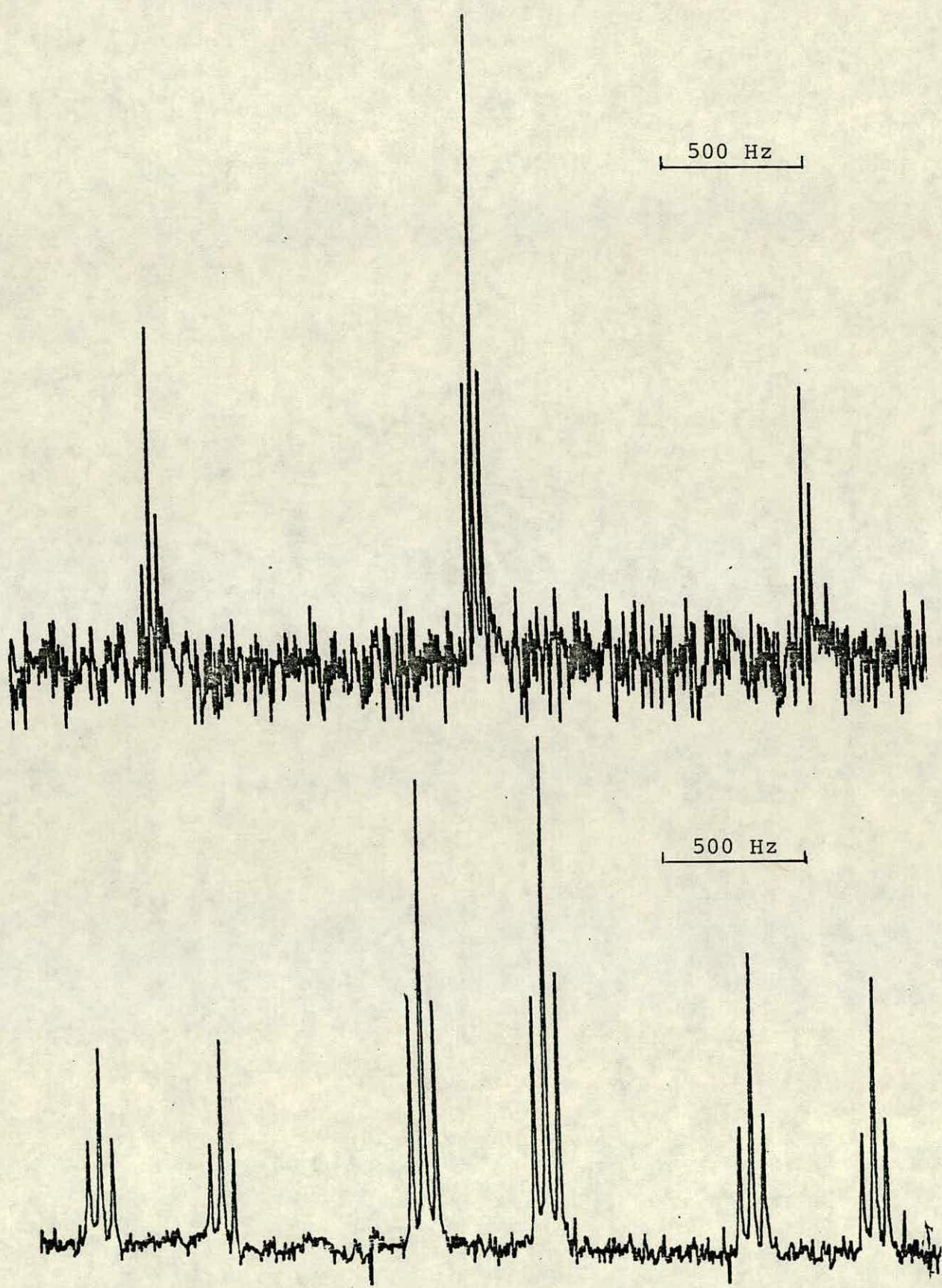
Reaction occurs at 193 K to yield one major product. The $^{31}\text{P}\{-^1\text{H}\}$ n.m.r. spectrum of this species consisted of two signals. A signal at relatively high frequency due to the HPF_2 phosphorus atom was split into a triplet of triplets. The large coupling was due to $^1J_{\text{PF}}$; the smaller coupling was deduced to be $^2J_{\text{PP}}$. The low frequency signal due to the PEt_3 phosphorus atoms was split into a doublet, the coupling constant being identical to the smaller J value in the PF_2 phosphorus resonance. The lines of the doublet were comparatively broad probably due to the presence of the unresolved $^3J_{\text{PF}}$. When ^1H coupling was retained the lines of the PEt_3 resonance broadened such that no couplings were resolved but the high frequency signal split into a further wide doublet, as shown in Figure 2.1, the magnitude of this coupling being ca. 400 Hz.

The ^{19}F n.m.r. spectrum consisted of one signal split into a doublet of doublets. The larger splitting was $^1J_{\text{PF}}$. The smaller coupling which had no equivalent in the ^{31}P n.m.r. spectrum was deduced to be derived from F-H coupling.

The ^1H n.m.r. spectrum consisted of very intense complex multiplets due to the ethyl protons and a much weaker signal at fairly high frequency (δH ca. 9 ppm). This resonance was split into a doublet of triplets. The doublet coupling (415 Hz) was the P-H coupling already mentioned. The triplet splitting (61 Hz) was the result of a coupling to the two fluorine atoms and was equal to the F-H splitting in the ^{19}F n.m.r. spectrum. At low frequency there were no signals that could be assigned to the presence of a metal hydride.

Figure 2.1

^{31}P n.m.r. spectrum of $\text{Ir}(\text{CO})(\text{PEt}_3)_2(\text{HPF}_2)\text{I}$
showing the HPF_2 resonance: above ^1H decoupled;
below ^1H coupled



From the data cited above a structure for the product was postulated. The magnitudes of J_{PH} and J_{FH} could only be accounted for if HPF_2 was present as a complete entity; this conclusion was confirmed by the failure to observe signals due to metal hydrides in the 1H n.m.r. spectrum. The pattern of the multiplets in the $^{31}P\{-^1H\}$ spectrum^{confirmed} that the HPF_2 moiety was bound to the $IrI(CO)(PEt_3)_2$ unit. Although no direct evidence for the presence of either I^- or CO was found, work on the analogous reactions of amino difluorophosphines (Appendix) showed that their loss was unlikely under the reaction conditions. This meant that the product was a complex of five-coordinated iridium. There were two possible configurations: square pyramidal and trigonal bipyramidal, although it was also possible that the complex was fluxional and existed as a rapid equilibrium between the two configurations. Within the two categories there were a number of possible isomers; examples are shown in Figure 2.2.



Figure 2.2

The criteria for defining these isomers were that HPF_2 was cis to both triethyl phosphine groups and that the triethylphosphine ligands were magnetically equivalent. It was impossible from the data available to speculate as to which would be the preferred isomer. Structural work on donor adducts of Vaska's compound^(81,82) has shown that either configuration was possible. The complex decomposed when the reaction mixture was warmed so no further characterisation was carried out.

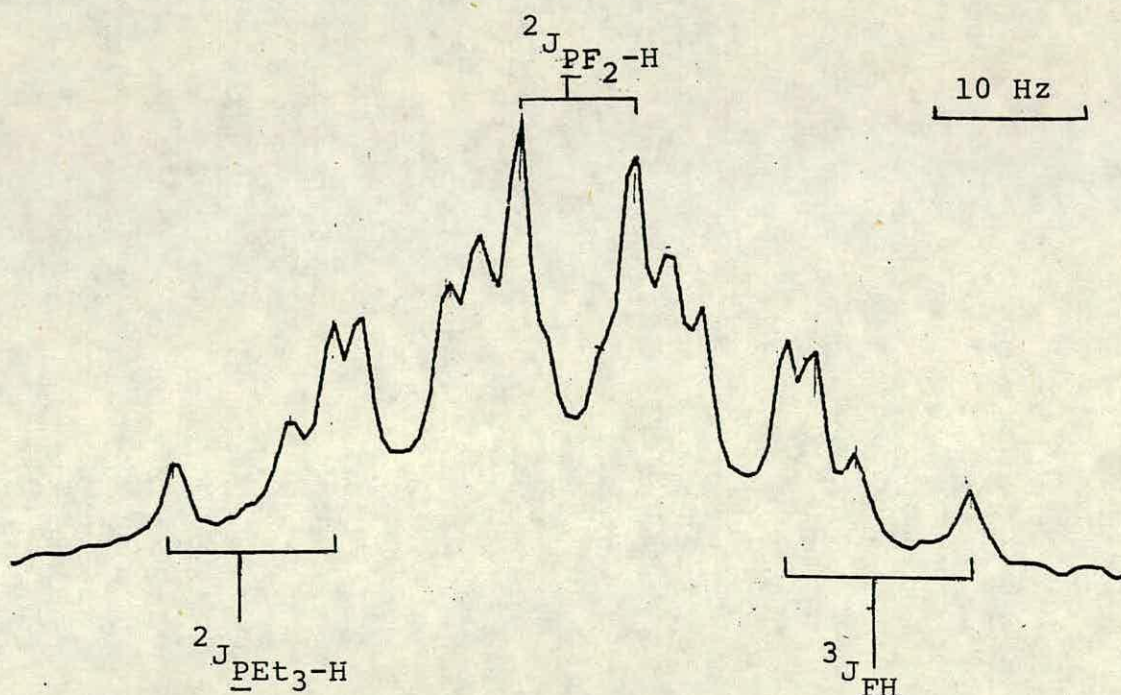
When the reaction mixture was warmed to ambient temperature a completely different species was formed.

In the $^{31}\text{P}\{-^1\text{H}\}$ n.m.r. spectrum two signals were again observed. The resonance due to the PF_2 phosphorus had shifted to very high frequency (376 ppm). The signal was split into a triplet of triplets as in the low temperature product but the magnitude of the couplings were markedly different. The PEt_3 resonance was shifted to slightly lower frequency and was split into a doublet of triplets. The doublet coupling was identical to the smaller triplet coupling of the PF_2 resonance and was assigned as $^2J_{\text{PP}'}$. The triplet coupling was found to be $^3J_{\text{PPF}}$. When ^1H coupling was retained the PF_2 resonance was again split by a further doublet coupling; however, the magnitude of the coupling in this case was of the order of 10 Hz. The PEt_3 resonance was split by a further doublet coupling of the order of 10 Hz on selectively decoupling the ethyl protons.

The ^{19}F n.m.r. spectrum consisted of a single resonance split into a doublet of triplets of doublets. The large doublet and the triplet couplings were assigned as $^1J_{\text{PF}}$ and $^3J_{\text{PF}}$ by comparison with the $^{31}\text{P}\{-^1\text{H}\}$ spectrum. The extra doublet coupling was deduced to be $^3J_{\text{HF}}$.

In the ^1H n.m.r. spectrum, besides the ethyl protons, a complex multiplet was observed at very low frequency (-15 ppm). The multiplet (Figure 2.3) was interpreted as a doublet of triplets of triplets due to the splittings $^2J_{\text{PF}_2-\text{H}}$, $^3J_{\text{FH}}$ and $^2J_{\text{PEt}_3-\text{H}}$ respectively.

Figure 2.3 ^1H n.m.r. spectrum of $\text{IrH}(\text{PF}_2)(\text{CO})(\text{PEt}_3)_2$ showing the hydride resonance



The chemical shift of this proton was characteristic for metal hydride trans to halogen^(34,83,84).

The interpretation of these results was that HPF_2 had oxidatively added across the Ir(I) complex to produce an Ir(III) complex containing a terminal PF_2 group. The reasons for this conclusion were:

(i) The PF_2 phosphorus resonance was at very high frequency. No previous examples of ^{31}P n.m.r. data for fully characterised terminal PF_2 groups were available for comparison but Malisch and co-workers found that the metal dichlorophosphanes that they had synthesised had very high ^{31}P chemical shifts⁽⁷²⁾.

(ii) The fact that a signal was observed in the ^1H n.m.r. due to the presence of a metal hydride implied that oxidative addition had taken place.

From the rest of the n.m.r. data the complete structure of the complex was deduced as that in Figure 2.4.

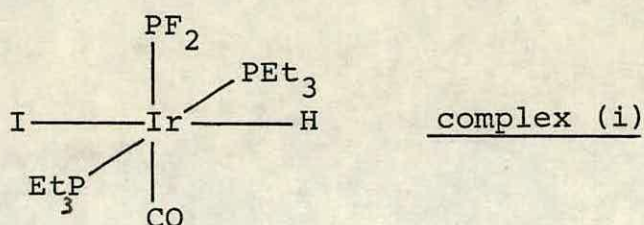


Figure 2.4

The fact that the hydride was cis to both the PF_2 group and the PEt_3 ligands was ascertained by the magnitudes of $^2J_{\text{PH}}$ (one would expect a trans $^2J_{\text{PH}}$ coupling to be of the order of 200 Hz). The hydride was placed as trans to iodide because of its proton chemical shift. Hydride trans to carbonyl would have a higher chemical shift (from -6 to -8 ppm) (33,34,83).

In the ^{31}P , ^{19}F and ^1H n.m.r. spectra, signals were observed for another species of interest. The n.m.r. data for this species are collected in Table 2.4.

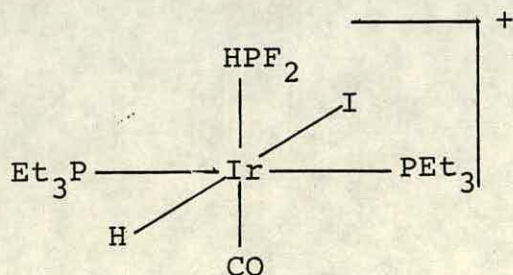
As in the ^{31}P n.m.r. of the species described above, the spectrum for this complex consisted of two signals. The splitting patterns of both signals (PF_2 and PEt_3) were qualitatively the same as those described above. The chemical shift of the PF_2 phosphorus was similar to that of the HPF_2 group in the five-coordinate complex described previously. On retaining ^1H coupling the signal due to the PEt_3 phosphorus broadened but that of the PF_2 phosphorus was split by a further two doublet couplings: the magnitudes of the two couplings were ca. 500 Hz and ca. 10 Hz.

The ^{19}F n.m.r. of this species consisted of a single resonance split into a doublet of doublets of triplets of doublets. The largest doublet coupling and the triplet coupling were assigned, by comparison with couplings in the ^{31}P n.m.r. spectrum, as $^1J_{\text{PF}}$ and $^3J_{\text{PF}}$ respectively. The two other doublet couplings were deduced to be $^2J_{\text{FH}}$ and $^3J_{\text{FH}}$ from the magnitudes of the couplings (ca. 60 Hz and 10 Hz respectively). Signals characteristic of the HPF_5^-

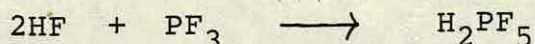
anion⁽⁸⁴⁾ (doublet of doublets of doublets at -56.4 ppm, and a doublet of quintets at -66.2 (curiously the trans $^2J_{\text{FH}}=0$)) were also detected in the ^{19}F n.m.r. spectrum.

Two signals besides those of the ethyl protons in the ^1H n.m.r. spectrum were assignable to protons in the iridium complex. A signal detected at high frequency (in the same region as the signal due to the HPF_2 proton in the five-coordinate iridium species) was split into a doublet ($^1J_{\text{PH}}$) of triplets ($^2J_{\text{FH}}$) of triplets ($^3J_{\text{PH}}$). At low frequency another complex multiplet, besides that of the hydride attached to the terminal PF_2 complex, was observed: the splitting pattern was qualitatively the same as that described for the hydride resonance of complex (i).

From these data this species had to contain both a metal hydride and coordinated HPF_2 (although no J_{HH} was resolved in the ^1H n.m.r. spectrum) bound to the $\text{IrI}(\text{CO})(\text{PEt}_3)_2$ unit. These groups had to be mutually cis because of the magnitudes of $^2J_{\text{PF}_2-\text{H}}$ and $^3J_{\text{FH}}$; they both had to be cis to the PEt_3 groups from the values of $^2J_{\text{PF}_2-\text{P}}$, $^3J_{\text{FP}}$ and $^2J_{\text{HP}}$. The chemical shift of the metal hydride placed it as being trans to the iodide. The resultant structure is shown below.



The resultant structure would be cationic. The counter ion was presumably the HPF_5^- whose presence was detected in the ^{19}F n.m.r. spectrum of the reaction mixture. How HPF_5^- was produced was a matter of some curiosity. Presumably some HPF_2 decomposed resulting in the production of quantities of HF and PF_3 which combined yielding H^+HPF_5^- .



The H^+HPF_5^- produced could then have reacted with complex (i) by protonating the PF_2 group to yield the Ir(III)-HPF_2 complex. The feasibility of this mechanism was supported by results described in Chapter 3.

There were signals in the n.m.r. spectra for other products which could not be identified by the nature of their n.m.r. signals and the complexes described above decomposed slowly at room temperature, for these reasons no attempt was made to isolate the species described above.

2.3 The Reaction of HPF_2 with $\text{IrBr(CO)(PEt}_3)_2$

This reaction was carried out in the same manner as 2.2.

The reaction followed the same course as 2.2 yielding similar products whose n.m.r. spectra were qualitatively the same as those described above; however, no signals were detected for any cationic Ir(III)-HPF_2 complex.

There was one major difference and that was the hydride chemical shift of the final product which occurred at -8.3 ppm in this case^(33,34,83). This implied that the hydride was trans to carbonyl in the final product. Hence the structure of the complex was that shown in Figure 2.5.

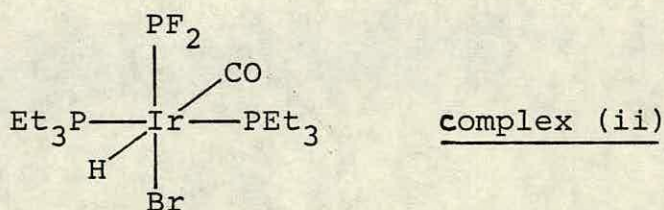


Figure 2.5

The complex shown above was not the only product and gradually decomposed at room temperature so no attempt was made to isolate the complex.

2.4 The Reaction of HPF_2 with $\text{IrCl}(\text{CO})(\text{PEt}_3)_2$

At low temperatures, traces of the five coordinate complex were present in the reaction media, judging by the n.m.r. spectra recorded. When warmed to room temperature there was no sign of the expected oxidative addition product. Unassignable signals made up the various n.m.r. spectra.

2.5 The Reactions of PF_2X with $\text{IrX}(\text{CO})(\text{PEt}_3)_2$ [X = Cl, Br or I]

In the case where X was Cl, at 193 K, $^{31}\text{P}\{-^1\text{H}\}$ and ^{19}F n.m.r. spectra consisted of signals with multiplet structures expected for a five-coordinate donor adduct. The n.m.r. parameters of the PF_2 group were those expected for a coordinated PF_2Cl ligand⁽⁵⁰⁾.

When the reaction mixture was warmed to room temperature, complete conversion to a terminal PF_2 complex occurred. The chemical shifts of the phosphorus and fluorine atoms of the PF_2 group were very similar to those of complexes (i) and (ii). (See Table 2.2).

The reaction in which X was Br yielded a very small concentration of the five-coordinate species at 193 K. When X was I, no signals were detectable for the corresponding five coordinate complex in the $^{31}\text{P}\{-^1\text{H}\}$ and ^{19}F n.m.r. spectra at 193 K; the only products at room temperature in both reactions were the six coordinate terminal PF_2 complexes.

These reactions all produced single products at room temperature. They were each isolated, and carbon and hydrogen analyses plus infra-red (i.r.) spectra were obtained for all three complexes. The analyses were consistent for $\text{Ir}(\text{PF}_2)(\text{CO})(\text{PEt}_3)_2\text{X}_2$ (see Experimental). Prominent in the I.R. spectra were bands at ca. 2040 cm^{-1} due to ν_{CO} ; the position of these bands implied that the products were Ir(III) complexes (ν_{CO} of Ir(I) is ca. 1960 cm^{-1}).

The n.m.r. parameters of the PF_2 groups (Table 2.2) were almost identical. This is as one would expect for complexes with terminal PF_2 groups; there is only slight dependence on the halogens present in the complex. One can see that there is a far greater difference in PF_2 n.m.r. parameters with change in X from the species formulated as five-coordinate iridium complexes. This supported the proposal that complexes containing terminal PF_2 ligands had been synthesised.

Unfortunately, no crystals of these complexes were obtained, so no direct confirmation of our proposals was forthcoming for these products. However, corroboration comes from some of the reactions described in Chapter 3 .

2.6 The Reactions of PF_2X with $\text{IrY}(\text{CO})(\text{PEt}_3)_2$

$[\text{X} \neq \text{Y} = \text{Cl, Br or I}]$

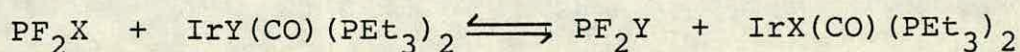
These reactions produced some interesting and useful results which followed two distinct reaction routes depending on the iridium starting material. Each class of reaction will be dealt with separately in the following subsections.

2.6.1 The Reactions of PF_2X with $\text{IrY}(\text{CO})(\text{PEt}_3)_2$

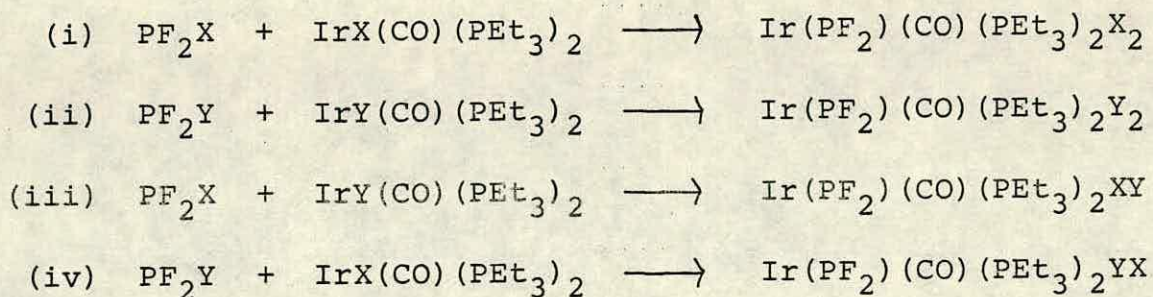
$[\text{X} = \text{Cl, Y} = \text{Br or I and } \text{X} \neq \text{Y} = \text{Br or I}]$

The reaction in which X was Cl and Y was Br yielded a five-coordinate complex at 193 K; in the other reaction of PF_2Cl like those of PF_2Br or PF_2I described later no such complexes were detected.

When these mixtures were warmed to room temperature, they all produced four products, each with a terminal PF_2 group, as a result of halogen exchange.



The four products were deduced to be a result of oxidative addition reactions involving all possible combinations of the above.



The relative abundances of the four products for three of the reactions are presented in Table 2.1 (it should be stressed that the values presented were not measured from integral plots of the n.m.r. signals relating to each species; they were measured from the heights of the ^{19}F n.m.r. signals of the species and so cannot be regarded as an accurate measure of the concentrations of the species; however, since the relaxation times of the fluorine nuclei are likely to be similar in all four complexes they provide a good rough measure of the relative concentrations of the four products).

Table 2.1

| X | Y | Relative abundance of products of the reactions ^a | | | |
|----|----|--|------|-------|------|
| | | (i) | (ii) | (iii) | (iv) |
| Cl | Br | 13 | 26 | 6 | 55 |
| Cl | I | 7 | 1 | 0 | 74 |
| Br | I | 21 | 21 | 8 | 50 |

^a see text for the relevant reaction pairing

2.6.2 The Reactions of PF_2X with $\text{IrY}(\text{CO})(\text{PEt}_3)_2$

[X = Br, I; Y = Cl]

These reactions followed the same course as those described in 2.5. No significant concentrations of the expected five-coordinated complexes were detected in the ^{31}P and ^{19}F n.m.r. spectra of the respective reaction systems at 193 K. The reactions at ambient temperature yielded single terminal PF_2 complexes.

The products of both reactions were isolated as off-white powders: i.r. spectra and C and H analyses were obtained; the analyses were correct for $\text{Ir}(\text{PF}_2)(\text{CO})(\text{PEt}_3)_2\text{ClY}$ (see Experimental).

The products of these reactions were also the major products of the reactions, described in 2.6.1, of PF_2Cl with $\text{IrY}(\text{CO})(\text{PEt}_3)_2$ (this observation was made by comparison of n.m.r. parameters).

Taking the two sets of results as a whole they indicated that the rates of formation of the six-coordinate Ir(III) complexes were highly dependent on the relative strengths of the P-X bonds. There appear to be two competing reactions: halogen exchange and oxidative addition. In reactions involving PF_2Br and PF_2I when X was Cl^- the rate of oxidative addition appears to be much faster than halogen exchange; hence there was no halogen exchange in the reactions described in 2.6.2. In the examples where PF_2Cl was allowed to react with $\text{IrY}(\text{CO})(\text{PEt}_3)_2$ [Y = Br or I], halogen exchange initially occurs more readily than oxidative addition, as is

shown by the high concentrations of products that resulted from the oxidative addition of PF_2Y to Ir(I) four-coordinate complexes in these reaction pairings. From these results the relative rates of reaction of the halodifluorophosphines would seem to be $\text{PF}_2\text{I} > \text{PF}_2\text{Br} \gg \text{PF}_2\text{Cl}$.

2.7 Discussion of N.m.r. Parameters

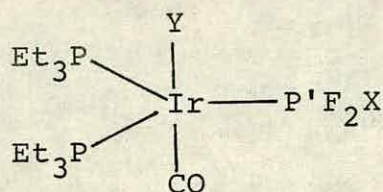
It was difficult to pick out any trends in the n.m.r. parameters of the five-coordinate complexes as so few of the possible products were detected.

It was apparent and understandable that the n.m.r. parameters of the PF_2X group varied considerably with X. However the n.m.r. parameters of different complexes with the same PF_2X group attached to the metal vary only slightly with the halogen bound to the iridium centre. The parameter which showed the most significant variation in such cases was the phosphorus chemical shift of the triethyl phosphine groups (δP). In the examples where HPF_2 was bound to iridium the values of δP for the two complexes follow the trend one would expect for such complexes. i.e. δP decreases with increase in size and/or decrease in electronegativity of the halogen attached to the iridium. (cf. δP 's of $\text{IrX(CO)(PEt}_3)_2$: X = Cl, $\delta\text{P} = 21$ ppm; X = Br, $\delta\text{P} = 17$ ppm; X = I, $\delta\text{P} = 13$ ppm). Surprisingly this trend was not observed in the examples with PF_2Cl bound to the iridium centre; one can only assume that this was due to differing configurational arrangements of ligands around the iridium. Unfortunately, from the little data available concerning these complexes there was no way of proving this. A fuller characterisation would have been possible if

Table 2.1

N.m.r. parameters for

[a]



| X | Y | $\delta\text{P/ppm}$ | $\delta\text{P' /ppm}$ | $\delta\text{F/ppm}$ | $^1\text{H}_{\text{PF}}/\text{Hz}$ | $^2\text{J}_{\text{PP}}/\text{Hz}$ | $^3\text{J}_{\text{PF}}/\text{Hz}$ |
|----|-------------------|----------------------|------------------------|----------------------|------------------------------------|------------------------------------|------------------------------------|
| H | Br ^[a] | -1.5 | 140 | -60.3 | 1112 | 41 | 4.8 |
| H | I ^[c] | -7.2 | 142 | -60.8 | 1105 | 38 | NR |
| Cl | Cl | -6.9 | 97 | 4.9 | 1333 | 42 | 9 |
| Cl | Br | 0.1 | 103 | 3.7 | 1332 | 44 | 8.8 |
| Br | Br | 0.3 | 110 | 6.3 | 1341 | 45 | NR |

[a] This is an arbitrary designation for the structure of the complexes

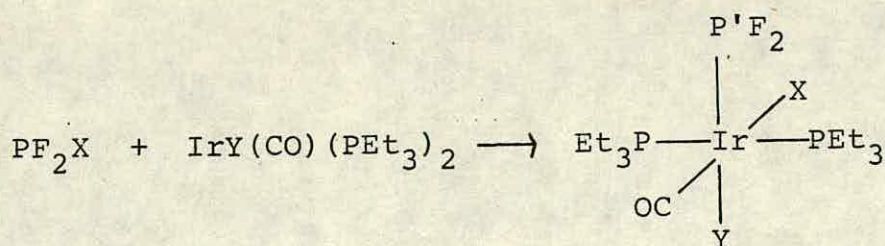
[b] $\delta\text{H} = 8.8 \text{ ppm}$; $^1\text{J}_{\text{PH}} = 416 \text{ Hz}$; $^2\text{J}_{\text{FH}} = 62 \text{ Hz}$; $^3\text{J}_{\text{PH}} = 6\text{Hz}$

[c] $\delta\text{H} = 8.7 \text{ ppm}$; $^1\text{J}_{\text{PH}} = 418 \text{ Hz}$; $^2\text{J}_{\text{FH}} = 62 \text{ Hz}$; $^3\text{J}_{\text{PH}} \text{ NR}$

NR = not resolved

The parameters were recorded in toluene at 203 K except for ^{13}C data which were recorded in benzene

Table 2.2 N.m.r. parameters for $\text{Ir}(\text{PF}_2)(\text{CO})(\text{PEt}_3)_2\text{XY}$ complexes



| Complex | X | Y | $\delta\text{P}/\text{ppm}$ | $\delta\text{P}'/\text{ppm}$ | $\delta\text{F}/\text{ppm}$ | $^1\text{J}_{\text{P}'\text{F}}/\text{Hz}$ | $^2\text{J}_{\text{PP}'}/\text{Hz}$ | $^3\text{J}_{\text{PF}}/\text{Hz}$ |
|----------|----|----|-----------------------------|------------------------------|-----------------------------|--|-------------------------------------|------------------------------------|
| (i) [a] | H | I | -10.8 | 367.7 | -61.5 | 1111 | 25.9 | 17.1 |
| (ii) [b] | H | Br | -5.4 | 380.8 | -62.4 | 1105 | 26.4 | 17.0 |
| (iii) | Cl | Cl | -9.3 | 364.8 | -68.3 | 1105 | 9.2 | 11.6 |
| (iv) | Br | Cl | -13.2 | 362.1 | -66.3 | 1111 | 8.6 | 11.6 |
| (v) | I | Cl | -18.7 | 359.5 | -65.0 | 1117 | 7.5 | 11.3 |
| (vi) | Br | Br | -18.1 | 363.1 | -64.7 | 1108 | 8.6 | 11.1 |
| (vii) | Cl | Br | <u>ca</u> 3.5 [c] | 365.6 | -66.7 | 1102 | 9.8 | 11.1 |
| (viii) | I | Br | -24.0 | 361.6 | -63.3 | 1113 | 7.4 | 10.9 |
| (ix) | Br | I | -25.6 | 366.7 | -62.4 | 1107 | 9.5 | 10.9 |
| (x) | I | I | -31.9 | 364.8 | -61.1 | 1112 | 8.3 | 10.6 |

[a] This complex does not have the configuration shown above (see section 2.2). $\delta\text{H} = -15.2$ ppm; $^2\text{J}_{\text{P}'\text{H}} = 7.5$ Hz; $^2\text{J}_{\text{PH}} = 10.0$ Hz; $^3\text{J}_{\text{FH}} = 11.5$ Hz

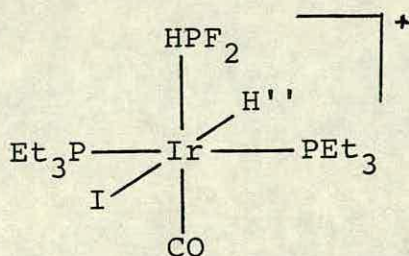
[b] $\delta\text{H} = -8.3$ ppm, $^2\text{J}_{\text{P}'\text{H}} = 9.9$ Hz; $^2\text{J}_{\text{PH}} = 16.0$ Hz; $^3\text{J}_{\text{PF}} = 11.4$ Hz

[c] This complex was one of the products in the reaction of PF_2Cl with $\text{IrI}(\text{CO})(\text{PEt}_3)_2$. Signals were observed for it in the PEt_3 region but they were intermingled with those of complex (iv) so the value of δP could only be approximated.

The parameters were recorded at room temperature in toluene

Table 2.3

N.m.r. parameters for



| $\delta P/\text{ppm}$ | $\delta P'/\text{ppm}$ | $\delta F/\text{ppm}$ | $\delta H/\text{ppm}$ | H''/ppm | $^1J_{PF}/\text{Hz}$ | $^1J_{PH}/\text{Hz}$ |
|-----------------------|------------------------|-------------------------|------------------------|----------------------|------------------------|----------------------|
| -26.0 | 122 | -58.5 | 8.4 | -9.0 | 1095 | 529 |
| $^2J_{FH}/\text{Hz}$ | $^2J_{PP'}/\text{Hz}$ | $^2J_{P'H''}/\text{Hz}$ | $^2J_{PH''}/\text{Hz}$ | $^3J_{PH}/\text{Hz}$ | $^3J_{FH''}/\text{Hz}$ | |
| 70.2 | 19.5 | 10 | NR | 4 | 9 | |

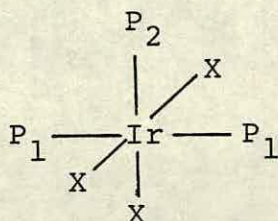
The parameters were recorded in toluene at room temperature

Table 2.4 N.m.r. parameters of some fluorophosphines

| Compound | $\delta P/\text{ppm}$ | $\delta F/\text{ppm}$ | $^1J_{PF}/\text{Hz}$ | reference |
|---------------------------|-----------------------|-----------------------|----------------------|-----------|
| PF_2I | 242 | -46 | 1340 | 85 |
| PF_2Br | 218 | -40 | 1388 | 85 |
| PF_2Cl | 176 | -37 | 1390 | 85 |
| PF_3 | 97 | -34 | 1401 | 86 |
| PF_2NMe_2 | 143 | -65 | 1197 | 85 |
| PF_2NH_2 | 130 | -58 | 1207 | 87 |
| PF_2OMe | 110 | -53 | 1278 | 17 |
| PF_2Me | 250 | -93 | 1157 | 17 |
| PF_2H | 223 | -116 | 1133 | |

Table 2.5

$^2J_{PP}$ values for some Ir(III) phosphine complexes^(88,89)



| P | X | $^2J_{P_1P_2}/\text{Hz}$ |
|---------------------|----|--------------------------|
| PEt ₃ | Cl | 16.5 |
| PEt ₃ | Br | 15.8 |
| PEt ₃ | I | 15.1 |
| PEt ₃ | H | 19 |
| PEt ₂ Ph | Cl | 15.8 |
| PEt ₂ Ph | Br | 15.6 |
| PEt ₂ Ph | I | 15.3 |
| PMe ₂ Ph | Cl | 16.5 |
| PMe ₂ Ph | Br | 15.7 |
| PMe ₂ Ph | I | 15.0 |

^{13}C enriched carbon monoxide had been incorporated into the iridium starting materials: the values of J_{PC} would have proved invaluable in deciding the relative positions of PF_2X and CO around the iridium.

It is also of general interest that the phosphorus chemical shifts of the PF_2X groups decrease sharply on coordinating to iridium. This observation is in keeping with that of Nixon and Schmutzler⁽⁹⁰⁾ who noted that in general the phosphorus chemical shift of a compound will decrease as its coordination number increases. It is worth bearing this fact in mind when one considers our assignment of the Ir(III) complexes.

It is doubtful that further useful information can be gleaned from the few examples of the five-coordinate complexes so we shall now consider the n.m.r. parameters of the six-coordinate Ir(III) complexes.

Taken as whole the values of some of the n.m.r. parameters are very interesting:

(i) The $^1J_{\text{PF}}$ values were very small in comparison to those observed for most three-coordinated phosphorus-fluorine compounds (cf. values in Tables 2.2 and 2.4).

(ii) The phosphorus chemical shifts of the PF_2 groups ($\delta\text{P}'$) were similarly high (cf. values in Tables 2.2 and 2.4).

(iii) The $^2J_{\text{PP}}$ values were for most of the complexes reported very low in comparison to those of previously reported six coordinate Ir(III) complexes (cf. values in Tables 2.2 and 2.5).

An examination of Table 2.4 provides the likely explanation for the low values of $^1J_{PF}$. If one compares $^1J_{PF}$ values of PF_3 , PF_2OMe , PF_2NR_2 and PF_2Me , or those of PF_3 , PF_2Cl , PF_2Br and PF_2I it is clear that the lowest values of $^1J_{PF}$ arise when the least electronegative substituent is bound to phosphorus (outside these groups $^1J_{PF}$ value of HPF_2 is also very low, hydride again being very electropositive). Iridium in the complexes in question has a very low electronegativity and coupled with this there is likely to be π back donation from iridium to phosphorus; therefore low $^1J_{PF}$ values would be expected for the $Ir-PF_2$ complexes when compared with general trends in difluorophosphine compounds. There is one other less plausible reason for the low values of $^1J_{PF}$ recorded for the terminal PF_2 groups; Rudolph and Parry⁽⁹¹⁾ suggested that the low value of $^1J_{PF}$ in HPF_2 might be a result of intramolecular hydrogen bonding between hydrogen and the fluorine atoms causing a disruption of the normal pyramidal arrangement of substituents around phosphorus and thus affecting the phosphorus fluorine bonding. If this postulation were correct then similar interactions may occur in the iridium complexes between iridium and the fluorine atoms, causing similar reductions of $^1J_{PF}$.

The high $\delta P'$ values are again almost certainly due to electron-releasing interactions from iridium. It can be seen from Table 2.4 that the highest values of $\delta P'$ are recorded for PF_2 compounds in which the other substituent has a low electronegativity; indeed studies have been made showing linear correlations between the values of δP , for a group of compounds



PF_2X , and the electronegativity of the group X⁽⁹²⁾ (low electronegativity being associated with higher values of $\delta\text{P}'$). The linear relationship was thought to apply only in compounds in which the degree of π back donation from X was low). The values are highest when hydride, an essentially releasing group, is bound to iridium; with hydride attached to iridium there would be more electron density available for donation to the PF_2 group than when the electronegative halide ligands are attached.

In comparing the values of $^2\text{J}_{\text{PP}}$ recorded in Table 2.2 to those in Table 2.5 one must consider the differences between the metal-phosphorus bonding to the terminal PF_2 groups and bonding to standard phosphine ligands. The value of $^2\text{J}_{\text{PP}}$ has been shown to be dependent, to a great extent, on the s electron density in the bonds⁽⁸⁸⁾. The donor-acceptor bonds in standard metal phosphine complexes has a high s character due to the high s character of the phosphorus lone pair - hence one observes relatively high $^2\text{J}_{\text{PP}}$ coupling constants. In the complexes described in this work, the metal can be regarded as a substituent of a phosphine; therefore the bonding would have considerably more p character than in a standard metal-phosphorus bond, thus resulting in comparatively low $^2\text{J}_{\text{PP}}$ values.

All the n.m.r. parameters of the complexes show, to a greater or lesser extent, a dependence on the halide/hydride bound to iridium.

Definite trends are observed in the n.m.r. parameters of complexes (iii) to (x); these will now be briefly discussed.

The δP values follow the trend observed for the five-coordinate HPF_2 -iridium complexes, i.e. the heavier, less electronegative, halogens giving rise to lower chemical shifts. The stereochemical position of the halide with respect to the CO or PF_2 groups has little bearing on the chemical shift (cf. δP of complexes (viii) and (ix)).

The magnitudes of δF follow a similar trend but in the opposite sense; these show an increase in chemical shift with an increase in size of the halogens bound to iridium.

The range of values of $\delta P'$ is very small but within it there are logical trends. Any attempt to draw these results together is dependent on the acceptance of the structural assignment shown above Table 2.2 (cis addition appears the most likely mode of reaction judging from reaction 2.2 and 2.3. The assignment was found to be correct for complex (iii) from X-ray crystal structures of some derivatives of the complex (see Chapter 3). One would intuitively expect, if both halide ligands were cis to the PF_2 group that the trend in the values of δP^1 would be similar to that for δP . This is clearly not the case if one compares the values of $\delta P'$ in complexes (iii) and (x). Thus considering the assignment to be correct, the observed trends show that for a given halogen trans to PF_2 there is a decrease in δP^1 with increasing size of halogen cis (cf. $\delta P'$ for complexes (iii), (iv) and (v)); for a given halogen

cis to the PF_2 group there is an increase in $\delta\text{P}'$ with increasing size of the trans halogen (cf $\delta\text{P}'$ of complexes (v), (vii) and (x)).

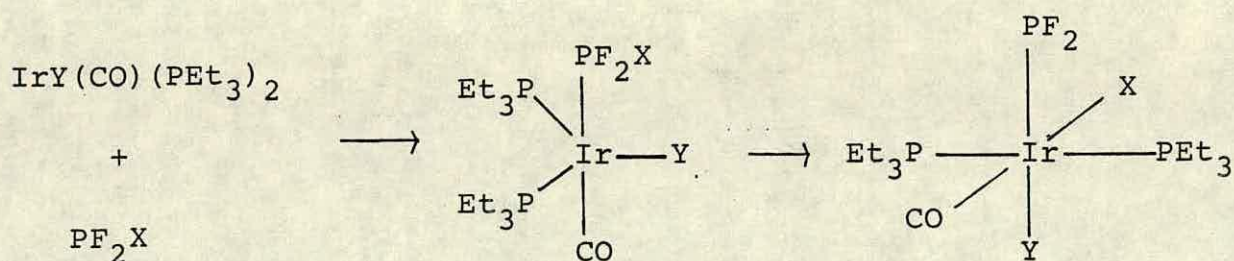
The observed trends for the values of $^1\text{J}_{\text{PF}'}$ were the converse of those for $\delta\text{P}'$.

The values of $^2\text{J}_{\text{PP}'}$ and $^3\text{J}_{\text{PF}}$ covered such small ranges that it was difficult to make conclusive comments concerning them.

Some of the n.m.r. parameters of complexes (i) and (ii) notably $\delta\text{P}'$, $^2\text{J}_{\text{PP}'}$ and $^3\text{J}_{\text{PF}}$ show marked differences to those of complexes (iii) to (x): presumably these are a result of the different electronic characteristics of the hydride ion compared to halide ions; hydride being an intrinsically electron donating group whereas halide ions are essentially electron withdrawing.

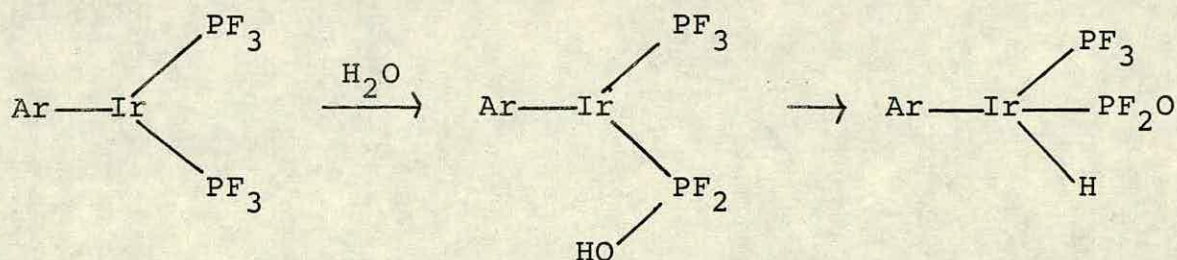
2.8 Conclusions

Our results have shown implicitly that terminal difluorophosphino complexes have been formed by oxidative addition of halo- or hydrido-difluorophosphines to carbonyl-halobistriethylphosphine iridium(I). In a few of the reactions, evidence for five-coordinate donor adducts has been obtained at low temperatures prior to the formation of the Ir(III) adducts.



Neither of these proposals has been proved by direct methods such as X-ray crystallography but it was believed that these interpretations provided the best explanation of the results obtained and both types of reaction were in keeping with the general chemistry of complexes of the type $\text{IrX(CO)(PR}_3)_2$. The proposals concerning the existence of terminal PF_2 groups were later confirmed by studying some reactions of the complexes (see Chapter 3).

Given that the proposals in this work, concerning the existence of terminal PF_2 groups bound to iridium is correct, the values of δF obtained for these complexes cast some doubt on the characterisation of the complex synthesised by King et al⁽⁴⁰⁾ (Section 1.1). Such a difference in chemical shifts ($\delta F = 4.1$ ppm compared with δF ca -65 ppm) would not be expected for different complexes containing the same group. Later results cited in this work would suggest that the complex in question contained a PF_2O group formed by the hydrolysis of a PF_3 group in the parent compound (a possible reaction mechanism is proposed below).



Ar = η_5 -pentamethylcyclopentadienyl.

King et al did report a band in the i.r. spectrum of the complex in the correct spectral region for a metal-hydride stretch but could not explain its presence as it did not concur with the assigned spectrum; however, it does support our proposed assignment of the structure.

CHAPTER 3

Reactions of $\text{Ir}(\text{PF}_2)(\text{CO})(\text{PEt}_3)_2\text{X}_2$

3.1 Reactions of $\text{Ir}(\text{PF}_2)(\text{CO})(\text{PEt}_3)_2\text{X}_2$ with Non-Metal Substrates

The reactions described in this chapter were carried out for two main reasons.

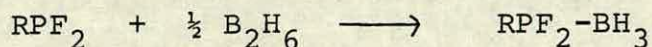
(i) To confirm that the complexes synthesised in the previous chapter contained terminal difluorophosphino groups.

(ii) To study the general chemistry of the terminal difluorophosphino grouping.

Most of the reactions were carried out using the $\text{Ir}(\text{PF}_2)(\text{CO})(\text{PEt}_3)_2\text{Cl}_2$ complex as it was the most convenient to synthesise. It was assumed that the presence of different halogens would make little difference to the chemistry of the grouping.

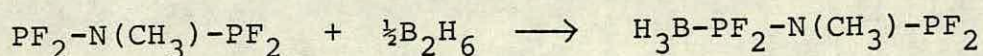
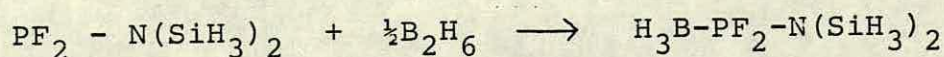
3.1.1 The Reaction of Diborane with $\text{Ir}(\text{PF}_2)(\text{CO})(\text{PEt}_3)_2\text{X}_2$ [X = Cl, I]

It is well known that diborane, being a Lewis acid, reacts with phosphines containing a free lone pair to form borane adducts. It has been found that diborane will react to form adducts with a number of different fluorophosphine compounds e.g. HPF_2 ⁽⁹²⁾ and cpd-PF_2 ⁽⁹³⁾ (cpd = cyclopentadiene).



R=H, cyclopentadiene.

Indeed it has been shown that in molecules containing difluorophosphino groups and other Lewis base-centres, adducts are formed preferentially with the difluorophosphine centre e.g. disilylaminodifluorophosphine and methylamino-bisdifluorophosphine⁽⁹⁵⁾.



(it is possible to achieve formation of adducts with the amino groups but a large excess of diborane is necessary).

The experiments described in this section were carried out in order to confirm that the complexes described in the previous chapter contained terminal PF_2 groups; from the reactions described above it was apparent that borane adducts should be formed if our structural assignment was correct.

In contrast to other reactions described in this chapter this reaction was studied for both the $\text{Ir}(\text{PF}_2)(\text{CO})(\text{PEt}_3)_2\text{I}_2$ and $\text{Ir}(\text{PF}_2)(\text{CO})(\text{PEt}_3)_2\text{Cl}_2$ complexes. There were no differences in the reactions of the two complexes. The reactions were carried out at room temperature in sealed n.m.r. tubes and ^{19}F and $^{31}\text{P}-\{^1\text{H}\}$ n.m.r. spectra were recorded. The n.m.r. data for the products are collected in Table 3.1.1.

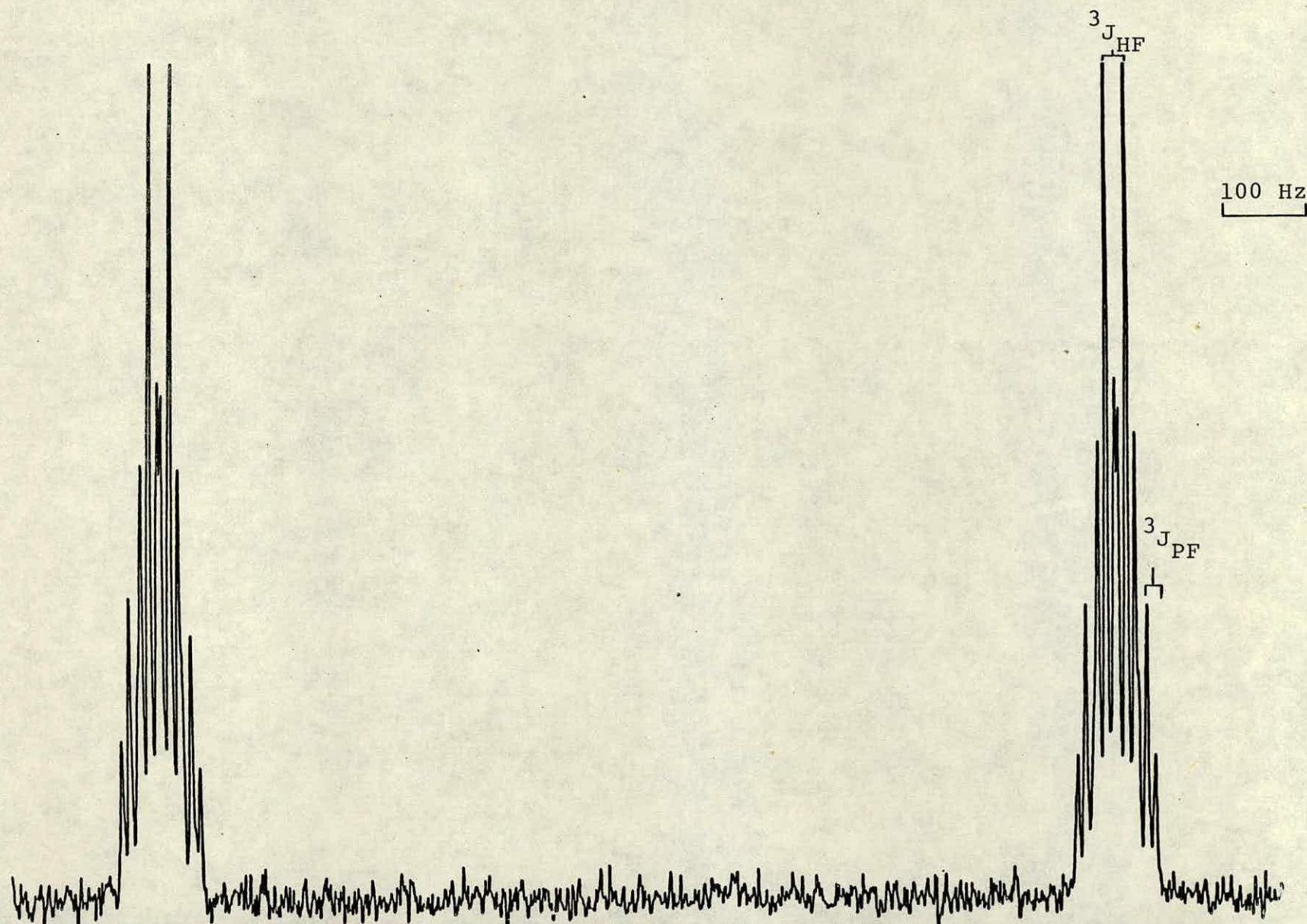
The $^{31}\text{P}-\{^1\text{H}\}$ n.m.r. of the products consisted of two signals, as did those of the starting materials. The signal to high frequency due to the PF_2 phosphorus differed in many respects from the equivalent signals in the iridium starting materials. The chemical shifts of the resonances were lower (δ_{P} ca. 250 ppm). Although the signals were split into a

triplet ($^1J_{PF}$) the lines constituting the signals were very broad (peak-width at half-height was ca. 100 Hz) such that no other couplings were resolved. The signals arising from the PEt_3 phosphorus nuclei were qualitatively the same as those of the iridium starting material except that the signal for the product of the $Ir(PF_2)(CO)(PEt_3)_2Cl_2$ reaction gave rise to a pseudoquartet splitting pattern because $^2J_{PP'}$ equalled $^3J_{PF}$.

The ^{19}F n.m.r. spectra of the products consisted of single resonances which were split into doublets (1:1) of triplets (1:2:1) of quartets (1:3:3:1) (Figure 3.1.1). The doublet and triplet couplings were $^1J_{PF}$ and $^3J_{PF}$ respectively. The quartet couplings which had no equivalents in the $^{31}P\{-^1H\}$ n.m.r. spectra were deduced to have been derived from coupling to three equivalent protons (no fluorine-boron couplings were apparent in the spectra).

The product of the reaction with $Ir(PF_2)(CO)(PEt_3)_2I_2$ was isolated as a pale-yellow microcrystalline solid. The C and H analyses obtained were consistent with the formulation $Ir(BH_3)(PF_2)(CO)(PEt_3)_2I_2$ (see Experimental). The i.r. spectrum contained bands not present in that of the starting material: at 2410 and 2345 cm^{-1} assigned as ν_{B-H} ; at 1060-1050 cm^{-1} ascribed to ν_{P-B} ; at 840-800 cm^{-1} due to ν_{P-F} (the ν_{P-F} of the starting materials were assumed to be in the region 780-700 cm^{-1} but as there were other skeletal bands of the complex in that region, they could not be assigned an actual value).

Figure 3.1.2 ^{19}F n.m.r. spectrum of $\text{Ir}(\text{PF}_2\text{BH}_3)(\text{CO})(\text{PEt}_3)_2\text{I}_2$



The conclusion to be drawn from these data was that stable borane adducts had been formed in the reactions. The decrease in phosphorus chemical shifts in going from starting materials to products was to be expected in going from a three-coordinate to four-coordinate phosphorus⁽⁹⁰⁾; the broadening of the lines of the said resonances was presumably due to unresolved coupling with the quadrupolar ¹⁰B and ¹¹B nuclei. The magnitudes of the J_{FH} couplings were of the order of those previously recorded for ³J_{FH} in fluorophosphine-borane adducts [³J_{FH} for R-PF₂: R=H, J = 26.5 Hz⁽⁹¹⁾; R = cpd⁽⁹³⁾, J = 22 Hz; R = N(SiH₃)₂, J = 16 Hz⁽⁹⁴⁾; R = N(CH₃)-PF₂, J = 16.8 Hz⁽⁹⁵⁾; R = C≡C-CH₃, J = 20.2 Hz⁽⁹⁶⁾]. The presence of ν_{B-H} and ν_{P-B} bands in the i.r. spectrum supported the postulate. The maintenance of the parent skeleton of the complexes i.e. Ir(CO)(PEt₃)₂X₂ was proved by the splitting patterns of the resonance arising from the PEt₃ phosphorus nuclei and the ¹⁹F nuclei, and the presence of ν_{CO} (ca 2060 cm⁻¹) in the i.r. spectrum.

This leads to only one conclusion relating to the iridium starting materials; that they do indeed contain terminal difluorophosphino groups.

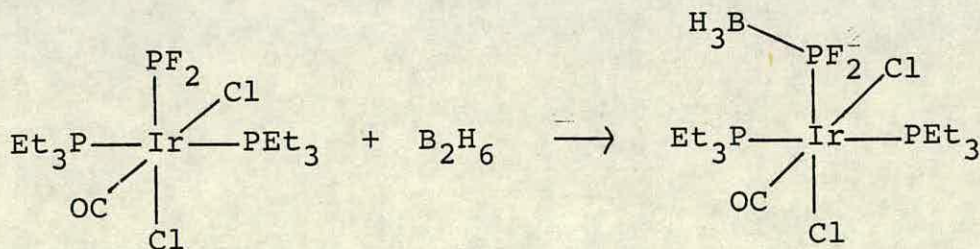
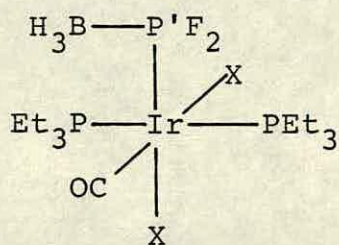


Table 3.1.1

N.m.r. parameters for



| X | $\delta\text{P/ppm}$ | $\delta\text{P' /ppm}$ | $\delta\text{F/ppm}$ | $^1\text{J}_{\text{P}'\text{F}}/\text{Hz}$ | $^2\text{J}_{\text{PP}'}/\text{Hz}$ | $^3\text{J}_{\text{PF}}/\text{Hz}$ | $^3\text{J}_{\text{FH}}/\text{Hz}$ |
|----|----------------------|------------------------|----------------------|--|-------------------------------------|------------------------------------|------------------------------------|
| Cl | -9.6 | 245 | -57.6 | 1108 | 8.4 | 8.4 | 22 |
| I | -35.8 | 250 | -46.9 | 1088 | 7.5 | 9.5 | 23 |

The parameters were recorded in toluene at room temperature

3.1.2 The Reaction of HCl with $\text{Ir}(\text{PF}_2)(\text{CO})(\text{PEt}_3)_2\text{Cl}_2$

The object of this experiment was to see if it was possible to protonate the PF_2 group and hence obtain further evidence for the existence of the iridium-terminal PF_2 complexes.

The reaction was followed by recording the ^{31}P and ^{19}F n.m.r. spectra at various temperatures from 193 K to ambient temperature. The n.m.r. parameters for the product complex of this reaction are presented in Table 3.1.2.

Reaction occurred at 193 K yielding a single species. The $^{31}\text{P}\{-^1\text{H}\}$ n.m.r. spectrum of this species was qualitatively the same as that of the iridium starting material except that couplings of a lower order than $^2\text{J}_{\text{PP}}$ were not resolved. On retaining ^1H coupling the signal due to the PF_2 phosphorus was split by a further doublet coupling (J_{PH} ca. 600 Hz).

The ^{19}F spectrum consisted of a doublet; the lines constituting the doublet were very broad (ca. 50 Hz).

On warming the reaction medium to 263 K the signals described above decrease in intensity. Complete decomposition of the complex described occurs at room temperature. Signals characteristic of PF_3 and PCl_3 were prominent in the ^{31}P n.m.r. of the reaction medium with a singlet in the region normally associated with PEt_3 bound to iridium(III) ($\delta_{\text{P}} = -2.2$ ppm). This signal was split by a further doublet coupling on selectively decoupling the ethyl protons.

Apart from signals arising from the ethyl protons, the ^1H n.m.r. spectrum of this species consisted of a triplet at very low frequency ($\delta_{\text{H}} = -17$ ppm, $^2J_{\text{PH}} = 5$ Hz).

The data obtained for the product observed at low temperature was of very poor quality; however the magnitude of J_{PH} recorded in the ^{31}P n.m.r. spectrum implied that a proton was directly bound to the unique phosphorus. Whether the proton had bound to phosphorus as a result of protonation of the lone pair on phosphorus or by oxidative addition of HCl across could not be established with any certainty from the results available. However, the similarity of the value of the parameter δP^1 (Table 3.1.2) to that of the Ir(III)-HPF_2^+ species described in Section 2.2 (Table 2.3) would suggest that the protonated species is the more likely, although other results described in this chapter show that the PF_2 group does undergo facile oxidative addition.

Other experiments might have been carried out to determine the mechanism of reaction: the reaction of $\text{Ir(PF}_2)(\text{PEt}_3)_2(\text{CO})\text{Cl}_2$ with another HX ($\text{X} = \text{Br}, \text{I}$) could have provided useful information, providing halogen exchange with the chloride substituents bound to iridium did not occur; if the reaction had been purely protonation of phosphorus then the values of the n.m.r. parameters would differ little from those of the reaction with HCl, as the only difference between the complexes would have been the counter ion; if oxidative addition had occurred then one would expect to observe significant differences in the values of δP^1 for the different complexes.

Another useful experiment would be to carry out the reaction in the presence of a large anion e.g. BPh_4^- or PF_6^- then it might be possible to trap out and characterise any cationic complex formed by the reaction.

The iridium complex detected for the reaction system at room temperature was characterised as $\text{Ir}(\text{CO})(\text{PEt}_3)_2\text{Cl}_2$ from its ^1H and ^{31}P n.m.r. spectra.

The overall reaction of HCl with $\text{Ir}(\text{PF}_2)(\text{CO})(\text{PEt}_3)_2$ is summarised below:

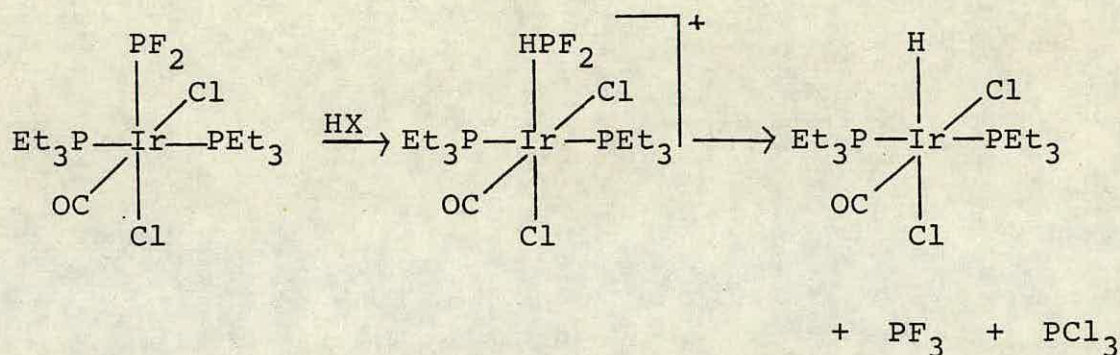
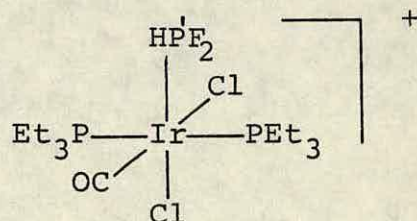


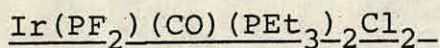
Table 3.1.2 N.m.r. Parameters for



| $\delta\text{P/ppm}$ | $\delta\text{P' /ppm}$ | $\delta\text{F/ppm}$ | $^1\text{J}_{\text{P',F}}/\text{Hz}$ | $^1\text{J}_{\text{P',H}}/\text{Hz}$ | $^2\text{J}_{\text{PP',}}/\text{Hz}$ |
|------------------------------------|------------------------------------|----------------------|--------------------------------------|--------------------------------------|--------------------------------------|
| -8.4 | 127 | -72.1 | 1124 | 647 | NR |
| $^2\text{J}_{\text{HF}}/\text{Hz}$ | $^3\text{J}_{\text{PF}}/\text{Hz}$ | | | | |
| NR | NR | | | | |

N.m.r. parameters were recorded in methylene chloride at 193 K.
NR = not resolved.

3.1.3 The Reactions of the Group VIB Elements with



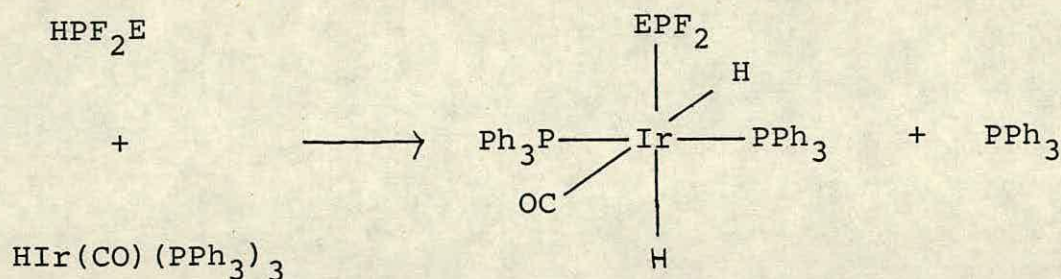
The object of these reactions was the oxidation of the PF_2 group to give corresponding difluorophosphonate, difluorothiophosphonate and difluoroselenophosphonate (PF_2E) complexes of iridium(III).

The ready oxidation of terminal Group VB centres on metals by Group VIB elements has already been outlined. Dobbie and Mason⁽⁵⁵⁾ found that terminal- $\text{P}(\text{CF}_3)_2$ groups underwent facile oxidation to the corresponding $-(\text{CF}_3)_2\text{PE}$ group. Similar results were reported by Malisch *et al* concerning the oxidation of terminal QR_2 groups^(72,74,79) [$\text{Q} = \text{P}$, $\text{R} = \text{Cl}$, Ph ; $\text{Q} = \text{As}$, $\text{R} = \text{Me}$].

Previous to this work there have been a number of reports on the synthesis of metal- PF_2E complexes.

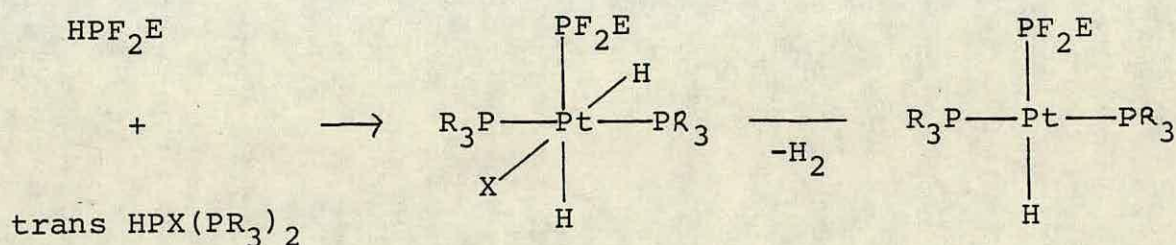
One synthesis has already been mentioned in the introductory chapter; the reaction of EPF_2Br [$\text{E} = \text{O}$, S] with Vaska's compound⁽³²⁾ (Figure 1.1.1) which proceeds via oxidative addition of the P-Br across iridium yielding $\text{Ir(III)-PF}_2\text{E}$ complexes.

The reactions of HPF_2E with the five-coordinate iridium complex $(\text{HIr}(\text{CO})(\text{PPh}_3)_3)$ give similar oxidative adducts although in this case addition is accompanied by elimination of phosphine⁽⁹⁷⁾:

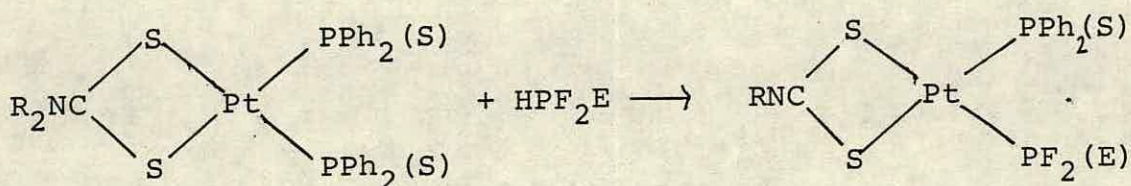
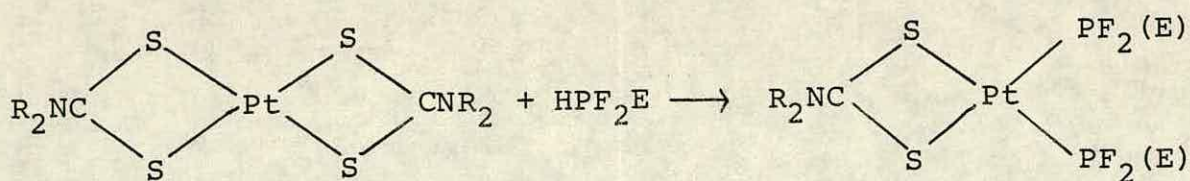


(E = O, S, Se)

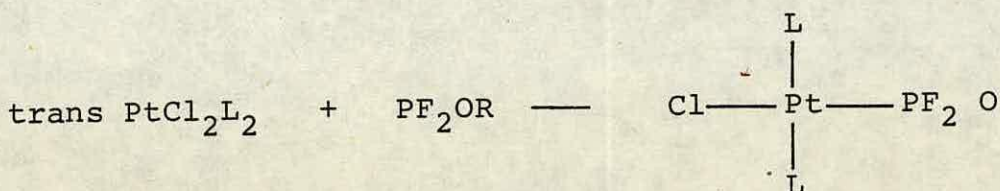
It is believed that an initial oxidative addition of the P-H bonds in $\text{HPF}_2(\text{E})$ [E = S, Se] across platinum are also involved in the reactions of HPF_2E with trans $\text{HPt}(\text{PR}_3)_2\text{X}$ [X = Cl, Br, I; R = Et, X = H; R = cyclohexyl] (97,98) however the oxidative adduct decomposes via reductive elimination of H_2 to yield four-coordinate platinum complexes.



Platinum dithiocarbamate complexes with $-\text{PF}_2\text{E}$ (E = O, S, Se) ligands have been synthesised, as above by reaction of HPF_2E , with platinum dithiocarbamate starting materials (99).



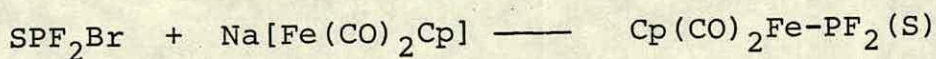
Grosse and Schmuzler succeeded in producing a series of platinum-PF₂O complexes by the reactions of alkoxy- and allyloxy-difluorophosphines with platinum phosphine complexes (100)



(L = PEt_nPh_{3-n}; n = 0-3)

Complexes of metals outwith the platinum group containing PF₂E ligands have also been reported but the methods of synthesis differ markedly from those described above.

The salt elimination reaction which has been described with respect to synthesis of M-QR₂ complexes (see section 1.3) has been used to attach a PF₂S group to iron⁽³²⁾.



The final example of synthetic routes to metal-PF₂E complexes is completely different from those described above. In all the previous examples the -PF₂E group has been introduced to the metal complex by reaction of a 'free' source of PF₂E; in this example the PF₂E (E = O) is introduced into the complex by modification of an already attached fluorophosphine ligand. Kruck et al⁽¹⁰¹⁾ found that metal-PF₂O complexes could be synthesised by reaction of base with coordinated trifluorophosphine ligands.



(M = Fe, n = 5; M = Ni, n = 4)

It was noted from a study of the above reactions that the metal bound PF₂E group is an essentially stable moiety and given that the oxidation reactions of the group VIB elements with Ir(PF₂)(CO)(PEt₃)₂Cl₂ were kinetically favourable it seemed likely that stable iridium-PF₂E complexes would be produced by the reactions.

The reactions of the Group VIB elements with Ir(PF₂)(CO)(PEt₃)₂Cl₂ were carried out at room temperature using the elements in their standard states, dioxygen (O₂), flowers of sulphur (S₈) and red selenium (Se).

The ¹⁹F and ³¹P-{¹H} n.m.r. spectra were recorded for the products of all three reactions and for the product of the reaction with Se a ⁷⁷Se-{¹H} n.m.r. spectrum was recorded. The n.m.r. parameters of the products are presented in Table 3.1.3.1.

The $^{31}\text{P}\{-^1\text{H}\}$ and ^{19}F n.m.r. spectra of all three products were qualitatively the same as that of the iridium starting material but the actual values of all parameters were markedly different from those of the starting material. Additionally the product of the reaction with Se had selenium satellites associated with the fluorine and phosphorus resonances of the PF_2 group (Figure 3.1.3.1) (selenium has 7.5% of the $I = \frac{1}{2}$ isotope, ^{77}Se , which gives rise to a further doublet coupling for 7.5% of a sample; selenium satellites are approximately 1/30th the height of the main signals); the $^{77}\text{Se}\{-^1\text{H}\}$ n.m.r. of the sample consisted of a signal split into a doublet (J_{PSe}) of triplets (J_{FSe}).

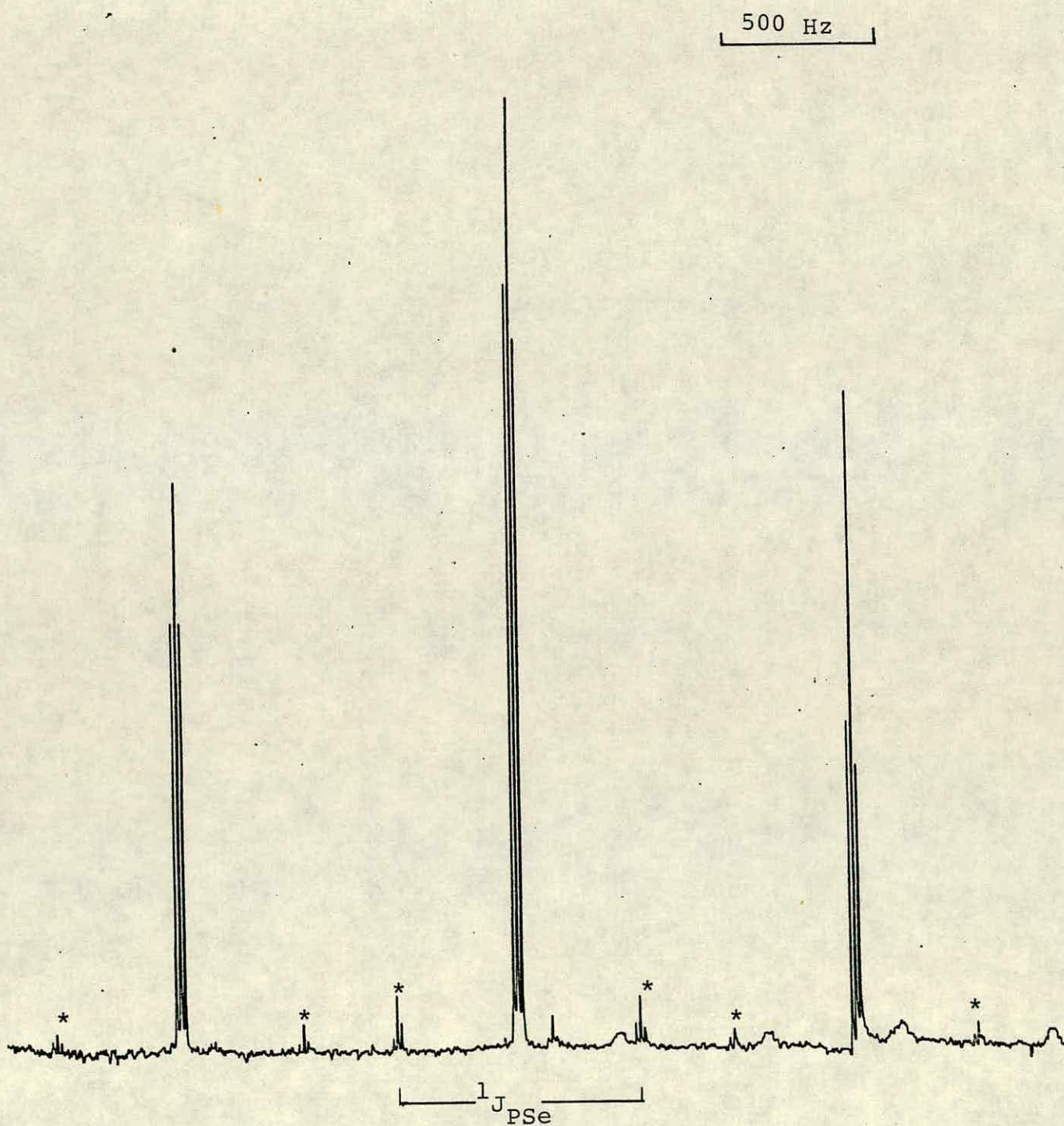
The products of the reactions were all obtained as air stable crystalline solids. Carbon and hydrogen analyses were correct for the formulation $\text{Ir}(\text{PF}_2\text{E})(\text{CO})(\text{PET}_3)_2\text{Cl}_2$ (see Experimental).

Infrared spectra of the products of the reactions of S_8 and Se were obtained; bands at ca. 2060 cm^{-1} and ca. 800 cm^{-1} were present in the spectra of both species and assigned as ν_{CO} and ν_{PF} respectively; bands at 820 and 670 cm^{-1} for the product of the reaction with S_8 , and 580 cm^{-1} for that of Se were assigned as $\nu_{\text{P-E}}$.

All the results suggested that $\text{Ir-PF}_2\text{E}$ complexes had been produced. The observed values of $\delta\text{P}'$ (Table 3.1.3.1) are typical of four-coordinate phosphorus V compounds (Tables 3.1.3.2 and 3.1.3.3). The values of δF and $^1J_{\text{PF}}$ are of the same order as those of previously reported metal

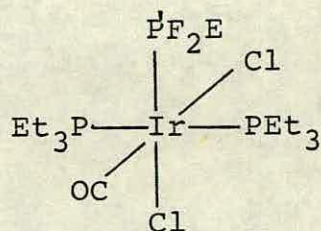
Figure 3.1.3.1 ^{31}P n.m.r. spectrum of $\text{Ir}(\text{PF}_2\text{Se})(\text{CO})(\text{PEt}_3)_2\text{Cl}_2$
showing PF_2 resonance

* are ^{77}Se satellites of the main signals



-PF₂E groups (Table 3.1.3.3). The observed J_{P'Se} and J_{FSe} can only be the result of selenium directly bound to the phosphorus of a PF₂Se group and the values were typical of metal bound PF₂Se ligand⁽⁹⁷⁻⁹⁹⁾.

Table 3.1.3.1 N.m.r. Parameters for



| E | $\delta P/\text{ppm}$ | $\delta P'/\text{ppm}$ | $\delta F/\text{ppm}$ | $^1J_{P'F}/\text{Hz}$ | $^2J_{P'P}/\text{Hz}$ | $^3J_{PF}/\text{Hz}$ |
|-------------------|-----------------------|------------------------|-----------------------|-----------------------|-----------------------|----------------------|
| O | - 9.0 | 7.4 | -12.7 | 1201 | 20.3 | 3.0 |
| S | -11.5 | 92.5 | - 2.3 | 1183 | 16.7 | 4.8 |
| Se ^[a] | -12.6 | 92.4 | - 2.5 | 1203 | 15.4 | 4.9 |

[a] $\delta_{\text{Se}} = 208.7$, $^1J_{P'Se} = 870$, $^2J_{FSe} = 83.6$

N.m.r. parameters recorded in toluene at room temperature.

An X-ray crystal structure of the product of the reaction with O₂ confirmed our proposal⁽¹⁰⁵⁾ (Figure 3.1.3.2). Structural parameters are collected in Table 3.1.3.4.

Figure 3.1.3.2 X-ray Crystal Structure of
 $\text{Ir}(\text{PF}_2\text{O})(\text{CO})(\text{PEt}_3)_2\text{Cl}_2$

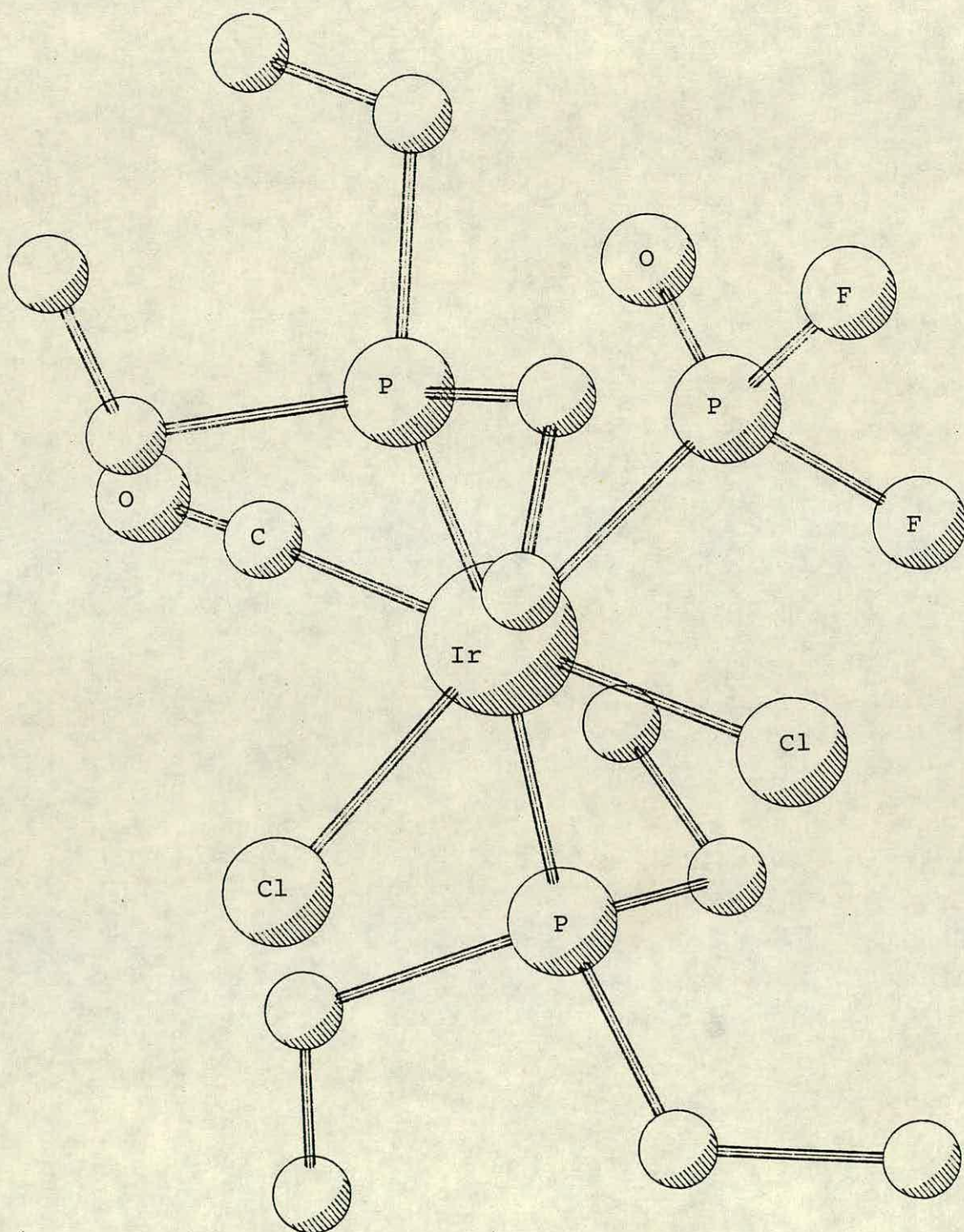


Table 3.1.3.2

N.m.r. parameters for some four-coordinate phosphorus V
fluorine compounds

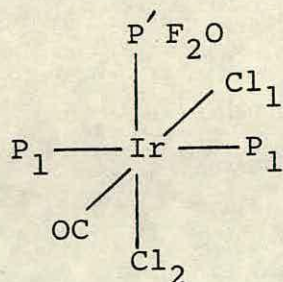
| Compound | $\delta P/\text{ppm}$ | $\delta F/\text{ppm}$ | $^1J_{PF}/\text{Hz}$ | Reference |
|---------------------------|-----------------------|-----------------------|----------------------|-----------|
| $\text{HPF}_2(\text{O})$ | -4.7 | -62.0 | 1121 | 102 |
| $\text{HPF}_2(\text{S})$ | 62.3 | -48.7 | 1153 | 102 |
| $\text{HPF}_2(\text{Se})$ | 74.2 | -37.0 | 1192 | 102 |
| OPF_3 | -35.5 | -94.3 | 1055 | 103 |
| SPF_3 | 32.4 | -51.3 | 1180 | 103 |
| OPF_2Cl | -14.8 | -48.1 | 1120 | 104 |
| SPF_2Cl | 50.0 | -15.9 | 1220 | 103 |
| SPF_2Br | 28.6 | - 2.3 | 1250 | 103 |

Table 3.1.3.3 N.m.r. parameters for some metal bound PF_2E groups

| Complex | $\delta\text{P}'/\text{ppm}$ | $\delta\text{F}/\text{ppm}$ | $^1\text{J}_{\text{P}'\text{F}}/\text{Hz}$ | reference |
|---|------------------------------|-----------------------------|--|-----------|
| $\text{ClPt}(\text{PEt}_2\text{Ph})(\text{P}'\text{F}_2\text{O})$ | 20.5 | -12.0 | 1175 | 100 |
| $\text{ClPt}(\text{PEt}_3)_2(\text{P}'\text{F}_2\text{O})$ | 23.8 | -15.8 | 1179 | 100 |
| $\text{ClPt}(\text{PEt}_3)_2(\text{P}'\text{F}_2\text{S})$ | 132.7 | -5.7 | 1162 | 98 |
| $\text{ClPt}(\text{PEt}_3)_2(\text{P}'\text{F}_2\text{Se})$ | 137.7 | -7.0 | 1181 | 98 |
| $\text{HPt}(\text{PEt}_3)_2(\text{P}'\text{F}_2\text{S})$ | 222 | -13.0 | 1210 | 98 |
| $\text{HPt}(\text{PEt}_3)_2(\text{P}'\text{F}_2\text{Se})$ | 235 | -16.0 | 1220 | 98 |
| $\text{HPt}(\text{PCy}_3)_2(\text{P}'\text{F}_2\text{O})$ | 126.2 | -11.2 | 1221 | 97 |
| $\text{HPt}(\text{PCy}_3)_2(\text{P}'\text{F}_2\text{S})$ | 224 | -8.4 | 1189 | 97 |
| $\text{HPt}(\text{PCy}_3)_2(\text{P}'\text{F}_2\text{Se})$ | 239 | -16.3 | 1189 | 97 |
| $\text{H}_3\text{Pt}(\text{PCy}_3)_2(\text{P}'\text{F}_2\text{O})$ | 114 | -4.1 | 1298 | 97 |
| $\text{H}_3\text{Pt}(\text{PCy}_3)_2(\text{P}'\text{F}_2\text{S})$ | 216 | 2.2 | 1199 | 97 |
| $\text{H}_2\text{Ir}(\text{PPh}_3)_2(\text{CO})(\text{P}'\text{F}_2\text{O})$ | 49.0 | -2.1 | 1225 | 97 |
| $\text{H}_2\text{Ir}(\text{PPh}_3)_2(\text{CO})(\text{P}'\text{F}_2\text{S})$ | 151.8 | 1.7 | 1187 | 97 |
| $\text{H}_2\text{Ir}(\text{PPh}_3)_2(\text{CO})(\text{P}'\text{F}_2\text{Se})$ | 159.5 | -5.2 | 1191 | 97 |
| $[\text{Et}_2\text{NCS}_2\text{Pt}(\text{PPh}_2(\text{SH}))(\text{P}'\text{F}_2\text{Se})]$ | 156.6 | -16.8 | 1220 | 99 |
| $[\text{iPrNCS}_2\text{Pt}(\text{PPh}_2(\text{S}))(\text{P}'\text{F}_2\text{Se})]$ | 165.2 | -21.8 | 1225 | 99 |
| $[\text{Fe}(\text{PF}_3)_4(\text{P}'\text{F}_2\text{O})]^-$ | 162.0 | -13.2 | 1250 | 101 |
| $[\text{Ni}(\text{PF}_3)_3(\text{PF}_2\text{O})]^-$ | 142.0 | -17.5 | 1250 | 101 |

Table 3.1.3.4

Structural Parameters for Ir(PF₂O)(CO)(PEt₃)₂Cl₂



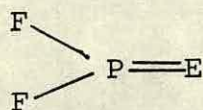
Selected Bond Lengths/pm

| | |
|--------------------|--------------|
| Ir-Cl ₁ | 236.9 |
| Ir-Cl ₂ | 241.6 |
| Ir-P ₁ | 240.2 |
| Ir-P' | 225.2 |
| Ir-C | 193.9 |
| P'-F | 156.2, 153.3 |
| P'-O | 144.6 |
| C-O | 100.5 |

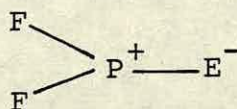
Selected Bond Angles

| | |
|-----------------------|--------------|
| F-P'-F | 96.2 |
| F-P'-O | 110.1, 109.0 |
| F-P'-Ir | 110.5, 108.6 |
| O-Ir-P' | 119.7 |
| P-Ir-P | 171.1 |
| Cl ₁ -Ir-C | 178.8 |

A point of discussion with such complexes is which of two possible representations is correct for the PF_2E grouping.



(A)



(B)

It is probably more correct to discuss to what extent either form is favoured.

There were three pieces of information from the data collected for the three complexes that gave evidence as to which was the better representation.

- (i) The values of $\nu_{\text{P-E}}$
- (ii) The value of $^1J_{\text{PSe}}$ for the PF_2Se complex
- (iii) The magnitude of the P-O bond length and the angles around phosphorus of the PF_2O group.

The values of $\nu_{\text{P-E}}$ that were recorded for the PF_2S and PF_2Se groups are well within the ranges one associates with double bonded phosphorus-sulphur or -selenium⁽¹⁸⁾

($\nu_{\text{P=S}}$ 515-862 cm^{-1} ; $\nu_{\text{P=Se}}$ 421-599 cm^{-1}). Two bands, one in the range 674-862 cm^{-1} and another in the range 515-725 cm^{-1} are typical of $\nu_{\text{P-S}}$ for a phosphorus-sulphur double bond (P=S)⁽¹⁸⁾ (It is thought that the two bands may be a result of Fermi resonance at the actual $\nu_{\text{P-S}}$). The fact that both products give rise to $\nu_{\text{P-E}}$ nearer the upper limit of the accepted ranges for P=S and P=Se , and both values of $\nu_{\text{P-E}}$ lie well outside

the ranges normally associated with P-S and P-Se⁽¹⁸⁾
($\nu_{\text{P-S}}$ 440-613 cm^{-1} ; $\nu_{\text{P-Se}}$ 439-477 cm^{-1}) implied that there was a high double bond character in the P-E bond and that the structure was more like representation (A).

The magnitude of $^1J_{\text{P-Se}}$ is accepted as a good guide to the degree of double bond character in the P-Se bond. The value recorded was well within the range normally associated with P=Se⁽¹⁰⁶⁾, although it lay just to the low side of the range, and was well outside the range normally associated with P-Se⁽¹⁰⁷⁾, thus supporting the proposal above concerning the most likely structure.

Comparison of the P-O bond length in the PF_2O complex (144.6 pm) with the equivalent values reported for other phosphorus-oxygen containing species showed that it was almost identical to that of OPF_3 (143.6 pm) and OPCl_3 (144.6 pm)⁽¹⁰⁸⁾; the P-O bonds in these compounds are generally accepted to be double bonds. The magnitude of P-O reported in this work is also found to be far shorter than accepted values for a P-O single bond, experimentally measured values for such a bond are generally in the region of 160 pm⁽¹⁰⁹⁾ and the theoretically predicted value is 171 pm⁽¹¹⁰⁾ (Schomaker-Stevenson rule). The value reported in this work is significantly shorter than that reported by Grosse et al for the equivalent distance in $\text{PtCl}(\text{PEt}_2\text{Ph})_2(\text{PF}_2\text{O})$ ⁽¹¹¹⁾ (P-O distance is 147.1 pm). This distance is probably greater in the platinum complex because of a higher degree of back donation to the PF_2O group in the platinum complex (Pt(II)), being more electron

rich than Ir(III), would have greater electron density available for back bonding) which would cause stabilisation of positive charge on phosphorus thus pushing the structure slightly towards form (B). This comparison was made in order to exemplify the effect greater double bond character has on the angles around phosphorus. The expected effect of a high double bond character on the groups around the central atom is that the double bonded group has a greater repulsive effect than singly bonded groups as a result of its greater lone pair character. Thus in the $M-PF_2O$ system one would expect the double bonded oxygen to repel the fluoride and metal groups such that the geometry around phosphorus is far from regular tetrahedral; the greater the double bond character the greater these effects would be. It would therefore be expected that the F-P-F angle, and M-P-F angles would be smaller in the iridium complex than in the platinum; this was found to be correct (see Table 3.1.3.4 for values in iridium complex. For $PtCl(PEt_2Ph)(PF_2O)$; F-P-F = 103° ; M-P-F = 110.3 and 114.4°). Conversely it would be expected that the angle M-P-O and the angles F-P-O would be greater in the iridium complex this again was found to be correct (see Table 3.1.3.4 for values in iridium complex. For $PtCl(PEt_2Ph)_2(PF_2O)$; M-P-O = 116° ; F-P-O = 103.1° and 109.4°). The angles around phosphorus may be affected by steric effects of bulky phosphine ligands on the metal but it was considered that the effects would be similar in both complexes. From the structural parameters

obtained relating to the geometry of the PF_2O group bound to iridium it was clear that the P-O bond had a very high double bond character thus confirming that the most likely structure is best represented by form (A).

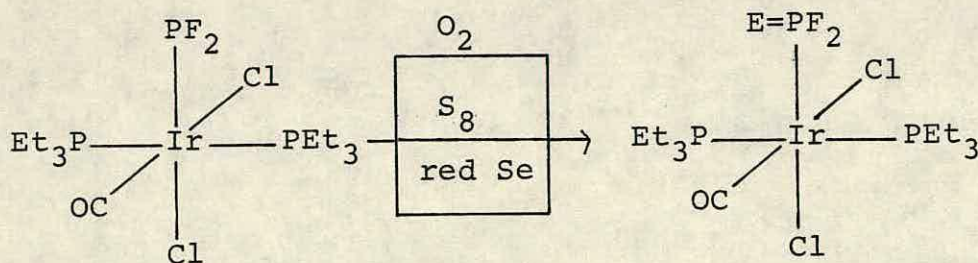
Further information from the X-ray crystal structure suggested that there was a fairly high degree of metal-to-phosphorus ($d \rightarrow d$) bonding between iridium and the PF_2O phosphorus; the iridium-phosphorus bond (Ir-P) for the PF_2O group was far shorter than that for the PEt_3 groups.

Evidence supporting this proposal was obtained from the i.r. spectra of the PF_2S and PF_2Se complexes; the values of ν_{CO} (ca. 2060 cm^{-1}) for these complexes was significantly greater than that of the iridium starting material and other values reported for six coordinate $\text{IrL}(\text{PEt}_3)_2(\text{CO})\text{XZ}$ complexes [$\text{X} = \text{Z} = \text{Cl}$, $\text{L} = \text{GeCl}_3$, SnCl_3 , AsCl_2 ⁽³⁵⁾, $\nu = 2040 \text{ cm}^{-1}$; $\text{X} = \text{H}$, $\text{Z} = \text{I}$, $\text{L} = \text{SiH}_2\text{Y}$ ⁽³³⁾; $\text{Y} = \text{OSiH}_2\text{Ir}$, $\nu = 1940 \text{ cm}^{-1}$; $\text{Y} = \text{N}(\text{SiH}_3)_2$, $\nu = 1980 \text{ cm}^{-1}$; $\text{Y} = \text{P}(\text{SiH}_2\text{Ir})_2$, $\nu = 1968 \text{ cm}^{-1}$]. This implied that there was less π back donation from metal to carbonyl; therefore, by inference there was greater back donation to phosphorus of the modified PF_2 group. The greater π back donation must arise due to a combination of two effects:

(i) The higher oxidation state of phosphorus which gives rise to a greater inductive electron withdrawing effect.

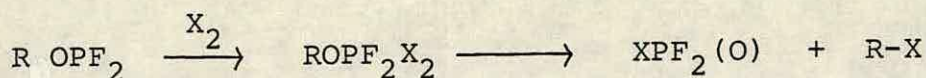
(ii) The higher oxidation state causes a contraction of phosphorus 3d orbitals thus making them more accessible for $d \rightarrow d$ back donation.

The results described in this section have shown that the terminal difluorophosphino groups undergo facile oxidation by the group VIB elements. This is in keeping with chemistry expected for phosphorus having a highly nucleophilic character.



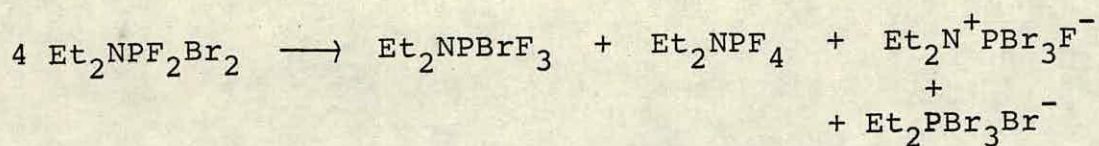
3.1.4 The Reaction of Dichlorine with $\text{Ir}(\text{PF}_2)(\text{CO})(\text{PET}_3)_2\text{Cl}_2$

The reaction of dichlorine (Cl_2) with PF_3 has already been described in the introductory chapter and it was mentioned that other fluorophosphines undergo similar reactions, e.g. dihalogens add oxidatively to difluorophosphites (X_2 , $\text{X} = \text{Cl}, \text{Br}$) to give the relevant phosphorane.



The phosphoranes produced by this reaction decompose by elimination of alkyl halide to the halodifluorophosphonates⁽¹⁴⁵⁾

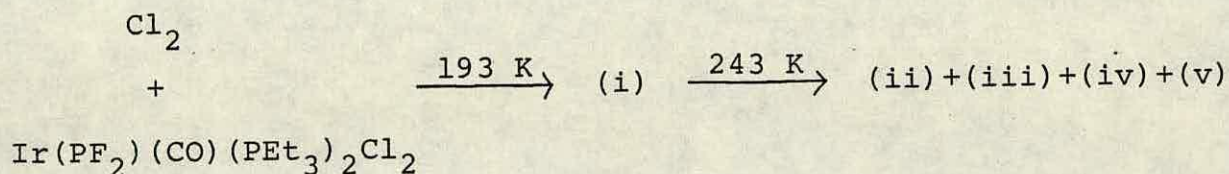
The oxidative addition products of the reactions of X_2 with aminodifluorophosphines also decompose at ambient temperatures, by intermolecular exchange of halides to give a complex mixture of species⁽¹⁸⁾:



The reaction of Cl_2 with $\text{Ir}(\text{PF}_2)(\text{CO})(\text{PEt}_3)_2\text{Cl}_2$ was carried out in order to observe if oxidative addition of Cl_2 across phosphorus of the terminal PF_2 group would take place.

The reaction was carried out in an n.m.r. tube and the n.m.r. spectra recorded at various temperatures from 193 K to ambient temperature. The n.m.r. parameters of the reaction products are collected in Table 3.1.4.1.

Reaction occurs at 193 K to yield a single product which subsequently decomposes at 243 K to give four other complexes.



At 243 K, the relative abundances of complexes (ii) and (iii) were very low compared with those of the other complexes, [(ii), (iv) and (v)], at 243 K; however on warming the reaction system to room temperature the relative abundance of complex (iii) increases.

The ^{31}P n.m.r. and ^{19}F n.m.r. spectra of complex (i) were qualitatively the same as those of the iridium starting material but values of the n.m.r. parameters were markedly different from those of the starting material. Hence complex (i) contained the grouping: $\text{Ir}(\text{PEt}_3)_2\text{PF}_2$, but the values of the n.m.r. parameters showed that reaction had occurred at the unique phosphorus.

The $^{31}\text{P}\{-^1\text{H}\}$ and ^{19}F n.m.r. spectra of complex (ii) and (iii) were qualitatively the same as those of the iridium starting material except that the ^{19}F n.m.r. signal for complex (ii) appeared to be split into a doublet ($^1\text{J}_{\text{PF}}$) of doublets. These data implied that complexes (ii) and (iii) also contained the $\text{Ir}(\text{PEt}_3)_2\text{PF}_2$ unit but were different from both starting material and complex (i).

The $^{31}\text{P}\{-^1\text{H}\}$ n.m.r. spectrum of complex (iv) also consisted of two signals. To high frequency a signal split into a quartet ($^1\text{J}_{\text{PF}}$) of triplets ($^2\text{J}_{\text{PP}}$) was observed. The PEt_3 resonance associated with this signal was split into a doublet, the lines of which were split further but no definite pattern could be assigned to them.

The ^{19}F n.m.r. spectrum of complex (iv) consisted of one signal split into a doublet ($^1\text{J}_{\text{PF}}$), the lines of which were very broad presumably because of unresolved $^3\text{J}_{\text{PF}}$ couplings.

The data collected for this species clearly implied that the complex contained the grouping $\text{Ir}(\text{PEt}_3)_2\text{PF}_3$ though the unique phosphorus could be four- or five-coordinate so long as the fifth substituent was not fluorine.

The $^{31}\text{P}\{-^1\text{H}\}$ n.m.r. spectrum of complex (v) consisted of two signals. The signal to high frequency was split into a doublet ($^1\text{J}_{\text{PF}}$) of triplets ($^2\text{J}_{\text{P},\text{P}}$). The PEt_3 resonance associated with this signal was split into a doublet ($^2\text{J}_{\text{P},\text{P}}$) of doublets ($^3\text{J}_{\text{PF}}$).

The ^{19}F n.m.r. spectrum of this species consisted of a doublet ($^1\text{J}_{\text{PF}}$) of triplets ($^3\text{J}_{\text{PF}}$).

The data collected for this species implied that it contained the grouping $\text{Ir}(\text{PEt}_3)_2\text{-(PFCl)}$ but is not a simple PFCl species.

There were two main possibilities to explain the structure of complex (i):

(a) that oxidative addition had taken place, followed by displacement of chloride from the unique phosphorus to give a cationic iridium(III) complex containing a coordinated PF_2Cl ligand,

(b) that oxidative addition of chlorine across phosphorus had taken place to yield a coordinated $\text{-PF}_2\text{Cl}_2$ group.

The n.m.r. parameters associated with the unique phosphorus ligand in complex (i) were of the order of those recorded previously for coordinated PF_2Cl ligands⁽⁵⁰⁾ (see Chapter 2, Table 2.1) and so it was considered that complex (i) might contain a coordinated PF_2Cl ligand, especially as the n.m.r. parameters of the grouping were not in good agreement with those of previously studied five-coordinate phosphorus-fluorine compounds (see Table 3.1.4.2);

however as the effect that a metal substituent would have had on the n.m.r. parameters of a phosphorane could not be predicted from previously recorded results, this argument was not particularly helpful.

The fact that three complexes containing modified PF_2 ligands were produced in the reaction system could not be explained by assuming the formation of different complexes containing coordinated PF_2Cl ligands and the n.m.r. parameters of the unique phosphorus group of complexes (ii) and (iii) were completely different from those expected for a coordinated PF_2Cl ligand. The presence of three different complexes could be rationalised if they each contained a PF_2Cl_2 group. Five-coordinate phosphorus (V) compounds generally have a trigonal-bipyramidal geometry and the molecules are often fluxional; if one assumes that stereochemically rigid structures are possible then one can propose three different isomers for the $(\text{Ir})\text{-PF}_2\text{Cl}_2$ [$(\text{Ir}) = \text{Ir}(\text{CO})(\text{PEt}_3)_2\text{Cl}_2$] complexes, shown in Figure 4.1.4.1.

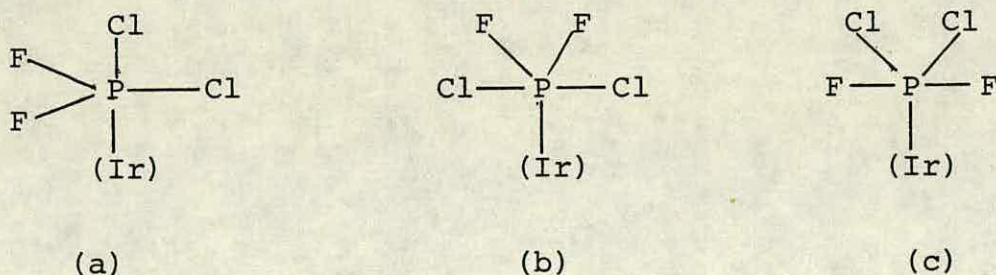


Figure 3.1.4.1 Isomers of $(\text{Ir})\text{-PF}_2\text{Cl}_2$

The most thermodynamically favoured complex would probably be that in which the fluorines are axial (c). Since complex (iii) appears to be the most stable of the $(\text{Ir})\text{-PF}_2\text{Cl}_2$ complexes it seems reasonable to suggest that complex (iii) has form (c), assuming the postulate that the complexes formed are metallo-phosphoranes. It is impossible to assign structures to the other complexes as there is so little information available.

Complex (iv) also has two possible forms: (a) a cationic complex containing a coordinated PF_3 ligand; (b) a neutral complex containing a $\text{-PF}_3\text{Cl}$ unit.

The n.m.r. parameters associated with the unique phosphorus fall within the ranges normally associated with coordinated PF_3 ligands^(17,46); however, as there are no equivalent data for PF_3Cl groupings bound to metals we cannot make real comparisons from n.m.r. data. The reactions of PF_3Cl_2 and HPF_4 with $\text{IrCl}(\text{CO})(\text{PEt}_3)_2$ have recently been studied⁽³⁵⁾. The main species formed by reaction of PF_3Cl_2 is complex (iv) of the reaction system reported here; in the reaction of HPF_4 there is oxidative addition of the P-H bond across iridium (a metal-hydride resonance with the expected splitting pattern was detected in the ^1H n.m.r. spectrum) but no product containing the $\text{Ir}(\text{PEt}_3)_2\text{-PF}_4$ unit was detected. Instead the product contains iridium bound to a unique phosphorus atom which also bears three F atoms;

the n.m.r. parameters of this group are very similar to those of complex (iv), and the fact that fluoride is not directly bound to iridium was proved by the n.m.r. spectra. Therefore the most likely conclusion to be drawn from these data is that PF_3 was coordinated to iridium.

It is difficult to make any concrete proposals concerning the nature of complex (v) as there are no previously recorded data for either of the possible groupings, i.e. a coordinated PFCl_2 or a metal- PFCl_3 grouping, at the unique phosphorus atom.

It would be difficult to prove directly any of the proposals put forward above; however, some experiments might be carried out to help to confirm or refute them.

Worthwhile information concerning complex (i), (ii) and (iii) might be obtained from the reaction of interhalogen compounds (ICl and BrCl) with the terminal $-\text{PF}_2$ complex; should these species add oxidatively across phosphorus to give phosphorus(V) species, the n.m.r. parameters of the products would be completely different from those recorded for complex (i); should a cationic species complex with a coordinated $-\text{PF}_2\text{Cl}$ ligand be formed then the n.m.r. parameters would be the same as those of complex (i). In these reactions however there might be a problem with halogen exchange at iridium, which would complicate the reaction system further. In that case it might be useful to carry out the reactions of Cl_2 and X-Cl ($\text{X} = \text{Br}, \text{I}$) with the mixed halide iridium- PF_2 complexes: $\text{Ir}(\text{PF}_2)(\text{CO})(\text{PET}_3)_2\text{ClX}$ (complexes (iv) and (v), chapter 2), and/or the complexes: $\text{Ir}(\text{PF}_2)(\text{CO})(\text{PET}_3)_2\text{X}_2$

(complexes (vi) and (x), chapter 2), in which the likelihood of halogen exchange would be lessened as the softer halides (I, Br) bound to iridium are less prone to exchange.

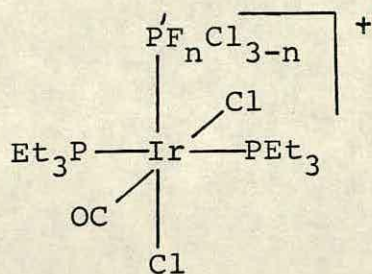
The reaction of Br_2 or I_2 (as well as the interhalogens) with $\text{Ir}(\text{PF}_2)(\text{CO})(\text{PEt}_3)_2\text{Cl}_2$ might prove indirectly the identity of complex (iv). The reaction should be allowed to follow the same course as that described in this section up to the point where the halogens redistribute and if a species with the same parameters as complex (iv) is detected then the characterisation of that complex postulated here would more than likely be correct. Again there may be a problem of halogen exchange at iridium in which case it might be better to study the reactions of X_2 ($\text{X} = \text{Cl}, \text{Br}, \text{I}$) with terminal- PF_2 complexes containing heavier halides.

The identity of complex (v) might be easier to prove. It will be shown in a later section that $\text{Ir}(\text{PFCl})(\text{CO})(\text{PEt}_3)_2\text{Cl}_2$ is produced by halogen exchange between the terminal- PF_2 group and PF_2Cl . It should be possible to synthesise this complex cleanly by reaction of PFCl_2 with $\text{IrCl}(\text{CO})(\text{PEt}_3)_2$. This complex should react with Cl_2 to give complex (v) which might then be isolated as a clean product to complete the characterisation.

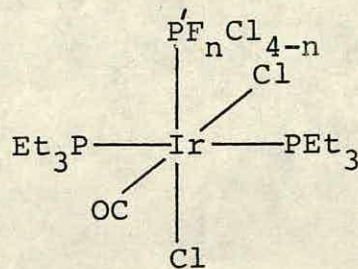
It is to be hoped that many of these suggested reactions will be carried out in future work thus shedding some light on the complicated transformations of the PF_2 grouping.

Table 3.1.4.1

N.m.r. Parameters for



or



| Complex | n | $\delta\text{P/ppm}$ | $\delta\text{P' /ppm}$ | $\delta\text{F/ppm}$ | $^1\text{J}_{\text{PF}}/\text{Hz}$ | $^2\text{J}_{\text{PP}}/\text{Hz}$ | $^3\text{J}_{\text{PF}}/\text{Hz}$ |
|-----------|---|----------------------|-------------------------|----------------------|------------------------------------|------------------------------------|------------------------------------|
| (i) [a] | 2 | -3.1 ✓ | 87.4 | -15.0 | 1276 | 16.1 16.2 | 4.3 |
| (ii) [b] | 2 | -6.9 | 47.9 42.6 | -15.5 | 1196 | 38.8 ca 39 | 3.6 |
| (iii) [b] | 2 | -7.5 | 17.4 12.1 | -13.0 | 1189 | 19.8 ✓ | 3.4 |
| (iv) [b] | 3 | -6.0 ✓ | 53.4 48.1 | -24.7 | 1297 | 18.3 18.2 | ca 2 |
| (v) [b] | 1 | -2.4 ✓ | 94.5 ✓ | -26.2 | 1229 | 14.3 14.8 | 9.1 ✓ |

The parameters were recorded in methylene chloride at:

[a] 203 K; [b] 223 K

Table 3.1.4.2

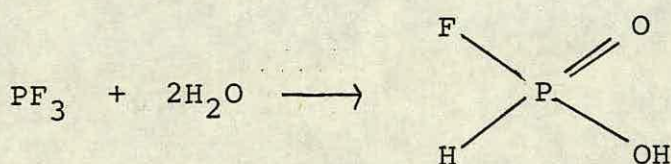
N.m.r. parameters for some five-coordinate phosphorus(V)-fluorine compounds

| Compound | $\delta P'/\text{ppm}$ | $\delta F/\text{Hz} [a]$ | $^1J_{PF}/\text{Hz} [a]$ | Reference |
|------------------|------------------------|--------------------------|--------------------------|-----------|
| PF_4Cl | 50 | -23 | 1030 | 112 |
| PF_3Cl_2 | 26 | -30 | 1048 | 112 |
| PF_2Cl_3 | 9 | -124 | 1045 | 113 |
| $EtS-PF_4$ | 34.2 | -42.1 | 1045 | 114 |
| $EtS(Me)-PF_3$ | -2.0 | +1.2, -75.2 | 925, 1062 | 114 |
| $Me_2N(Ph)-PF_3$ | -53.6 | -39.8, -68.0 | 821, 963 | 115 |
| $Me_2N(Me)-PF_3$ | -37.2 | -27.5, -67.6 | 804, 957 | 116 |
| $Et_2N(Ph)-PF_3$ | -52.5 | -43.5, -66.5 | 823, 966 | 116 |
| HPF_4 | 53.6 | +43.4 | 980 | 117 |
| H_2PF_3 | 24.1 | +46.2 | 877 | 117 |
| $(C_2F_5)PF_4$ | - | +55.8 | 1175 | 118 |
| $(C_2F_5)_2PF_3$ | - | +52.1 | 1245 | 118 |

[a] where two values are given the first refers to axial fluorines and the second to equatorial

3.1.5 The Reactions of H_2E with $Ir(PF_2)(CO)(PEt_3)_2Cl_2$ [E = O, S or Se]

The reactions described in this section were carried out to see if the PF_2 groups bound to iridium would undergo similar reactions to the hydrolysis of PF_3 ⁽¹¹⁹⁾ where phosphorus is oxidised and fluoride ions are displaced by hydroxyl groups.



No precedent was found for the reactions of H_2S and H_2Se with fluorophosphines so there was some doubt, as to whether there would be any reaction in these two examples.

The reactions were carried out in n.m.r. tubes and the ^{31}P , ^{19}F , 1H and ^{77}Se spectra recorded at room temperature. The n.m.r. data for the products are presented in Table 3.1.5.

The n.m.r. spectra of the main species formed in the reaction of H_2O with $Ir(PF_2)(CO)(PEt_3)_2Cl_2$ will be described prior to those of the H_2S and H_2Se reactions as they were slightly different from the others.

The $^{31}P\{^1H\}$ n.m.r. spectra of the reaction medium recorded immediately after warming to room temperature showed that reaction had occurred. The positions and splitting patterns of the signals arising from the major product were completely different from those of the iridium starting material. The spectrum consisted of two signals; that to high frequency

(δP ca. 47 ppm) was split into a doublet ($^1J_{PF}$) of triplets ($^2J_{PP}$); to low frequency (δP ca. -9 ppm) the PEt_3 resonance was split into a doublet ($^2J_{PP}$) of doublets ($^3J_{PF}$). The signal to high frequency was split by a further wide doublet coupling (J_{PH} ca. 500 Hz) on retaining 1H coupling.

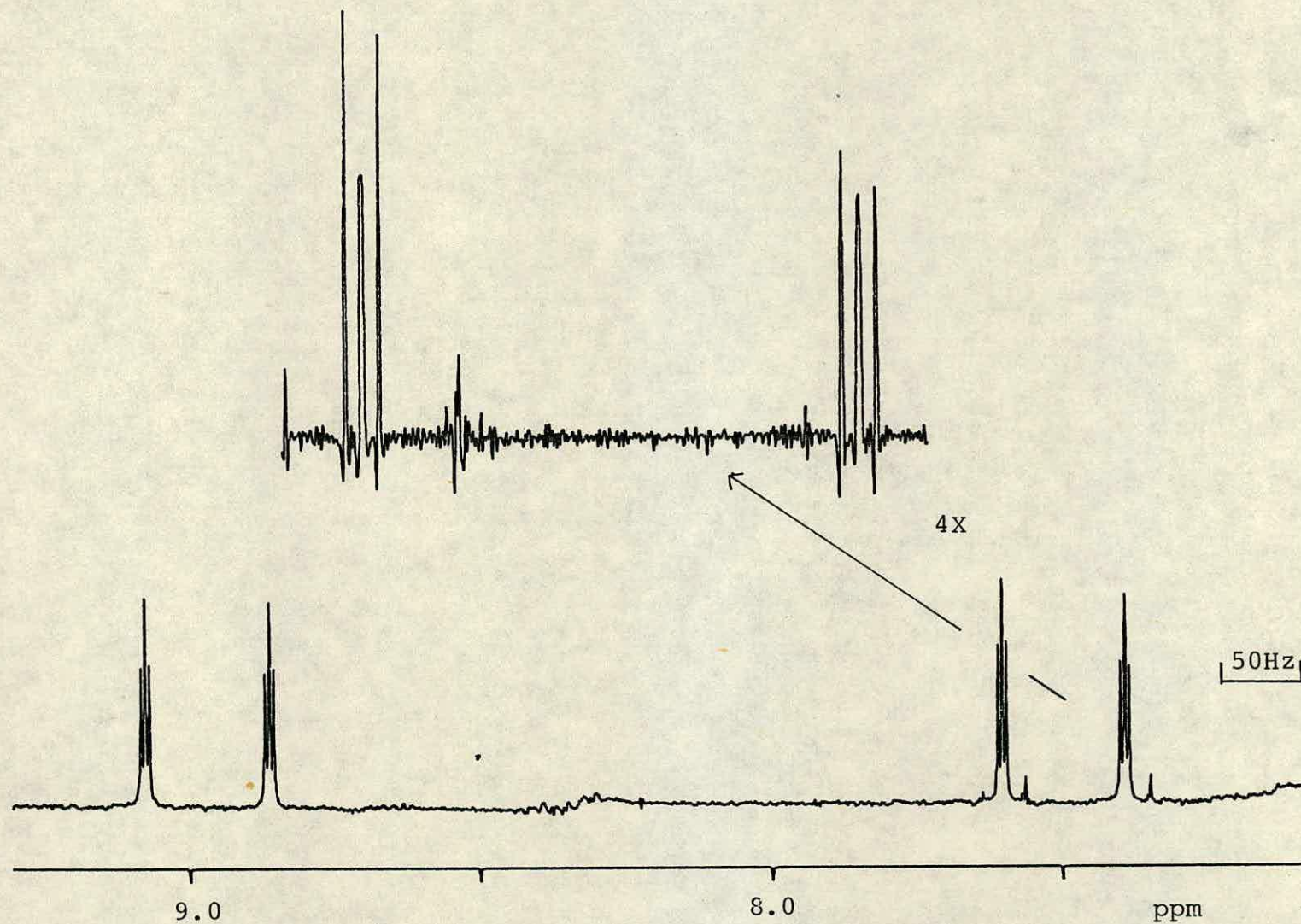
The ^{19}F n.m.r. spectrum of this species consisted of a doublet ($^1J_{PF}$) of doublets of triplets ($^3J_{PF}$). The smaller doublet coupling (J ca. 70 Hz) which had no equivalent in the ^{31}P n.m.r. spectra was deduced to be derived from an F-H coupling.

The 1H n.m.r. spectrum consisted of signals arising from protons of the ethyl groups and a resonance to high frequency (δH ca. 8 ppm) split into a doublet (J_{PH}) of doublets (J_{FH}) of triplets. When line narrowing of the spectrum was carried out the apparent triplet pattern showed some signs of resolution into a doublet of doublets (Figure 3.1.5.1).

From the splitting patterns of the signals in the n.m.r. spectra it was apparent that reaction had occurred at what was the phosphorus of the PF_2 group of the iridium starting material to give a species in which both a proton and a single fluorine atom were bound to phosphorus; the observed J_{PH} and J_{FH} could only be explained by having the proton directly bound to phosphorus. The low phosphorus chemical shift value suggested that a phosphorus V species had been formed. The most likely interpretation of these facts was that the PF_2 group had been converted to an $HPF(O)$ group.

Figure 3.1.5.1 ^1H n.m.r. spectrum of $\text{Ir}(\text{HPF}(\text{O}))(\text{CO})(\text{PEt}_3)_2\text{Cl}_2$ showing $\text{HPF}(\text{O})$ resonance.

The expansion shown is line narrowed



The reactions of H_2S and H_2Se did not progress as quickly as that of H_2O . The reaction of H_2S was very slow at room temperature; as a result the reaction system was maintained at 313 K to accelerate the process. The reaction of H_2Se reached completion with respect to iridium starting material after ca. 2 hours at room temperature.

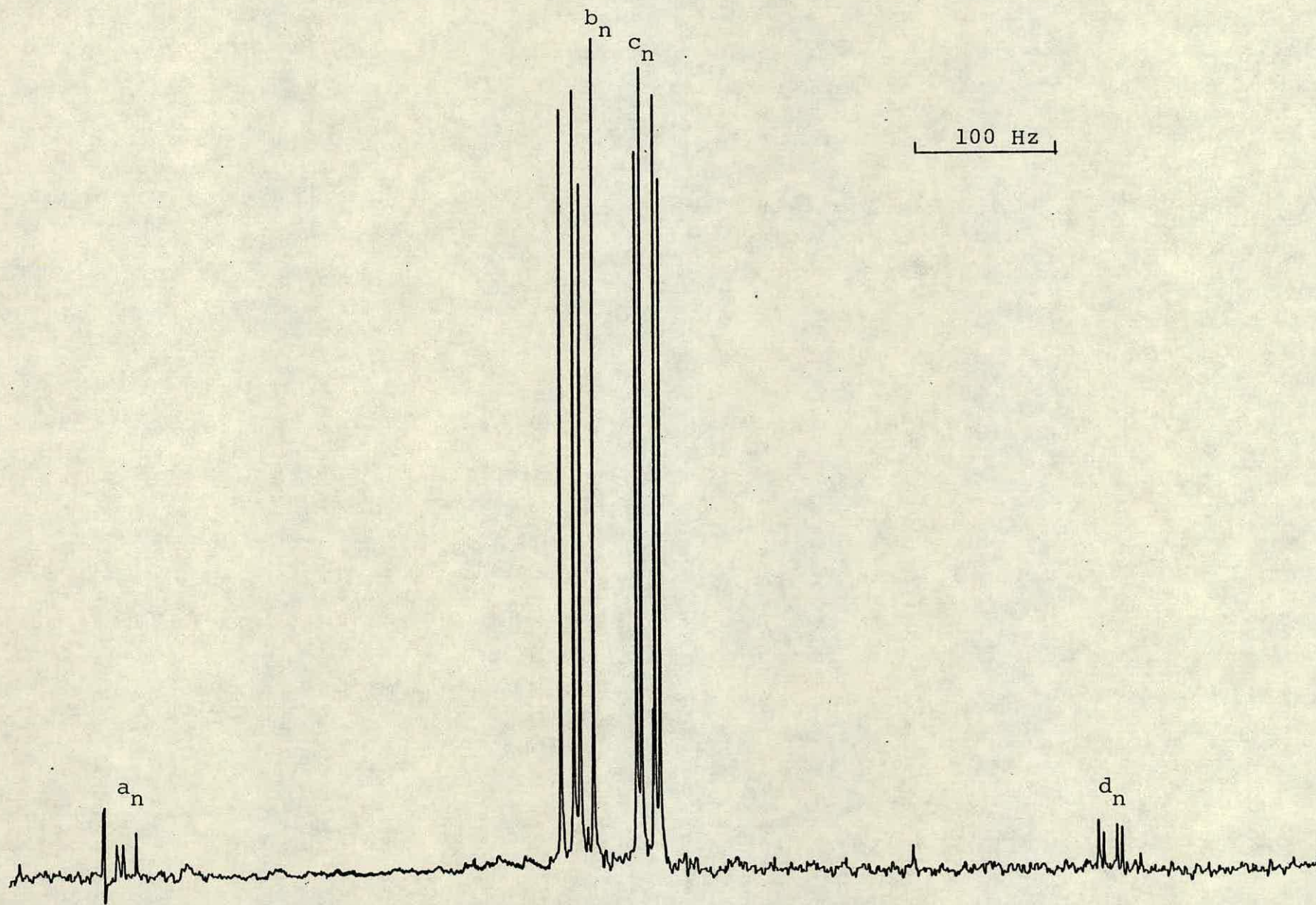
The n.m.r. spectra of the main products of both reactions were qualitatively the same.

The $^{31}\text{P}\{-^1\text{H}\}$ n.m.r. spectra of the main products of both reactions consisted of two signals. The signals to high frequency were split into doublets ($^1\text{J}_{\text{PF}}$) of triplets ($^2\text{J}_{\text{PP}}$) and as for the main product of the reaction of H_2O these signals were split by further wide doublet couplings (J_{PH} ca. 500 Hz) on retaining ^1H coupling. The splitting patterns for the signals due to the PEt_3 phosphorus nuclei were more complex. The resonances were split into what was identified as the pattern for the AB signals of an ABMX spin system (Figure 3.1.5.2), i.e. some factor had given rise to magnetically non equivalent PEt_3 groups. The non equivalence gives rise to an AB quartet (a_n, b_n, c_n, d_n) which is split by further doublet couplings due to $\text{M}=\text{P}$ and $\text{X}=\text{F}$ (The high frequency signal of the ^{31}P n.m.r. spectrum should have been split into a doublet ($^1\text{J}_{\text{PF}}$) of doublets ($^2\text{J}_{\text{PA}'}^{\text{P}}$) of doublets ($^2\text{J}_{\text{PB}'}^{\text{P}}$) because of this, but calculated values of $^2\text{J}_{\text{PA}'}^{\text{P}}$ and $^2\text{J}_{\text{PB}'}^{\text{P}}$ were very similar in both systems, resulting in pseudo triplet splittings).

The ^{19}F n.m.r. spectra of the main products in both reaction systems consisted of a doublet ($^1\text{J}_{\text{PF}}$) of doublets (J_{FH}) of

Figure 3.1.5

$^{31}\text{P}\{-^1\text{H}\}$ n.m.r. spectrum of $\text{Ir}(\text{HPF}(\xi))(\text{CO})(\text{PEt}_3)_2\text{Cl}_2$ showing the PEt_3 resonances. a_n, b_n, c_n, d_n ($n = 1-4$) represent the AB quartet of an ABMX spin system



doublets ($^3J_{FP_A}$) (calculations for $^3J_{PF}$ showed that $^3J_{P_B}$ was <1Hz in both examples and was therefore not resolved).

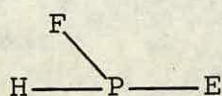
The 1H n.m.r. spectra of the main products of both reaction systems consisted of signals due to ethyl protons and at high frequency (δH ca. 8 ppm) a signal split into a doublet ($^1J_{PH}$) of doublets (J_{FH}) of doublets ($^3J_{PH}$) (the values of $^3J_{P_A/P_B-H}$ could not be calculated from the ^{31}P n.m.r. spectra but presumably one of the $^3J_{PH}$ values was <1 Hz and was therefore not resolved).

A $^{77}Se\{-^1H\}$ spectrum of the H_2Se reaction system was recorded. To high frequency (δSe ca. 160 ppm) a signal split into a doublet of doublets was observed; the couplings were deduced to be derived from $^1J_{P'Se}$ and $^2J_{FSe}$ respectively (see Table 3.1.5).

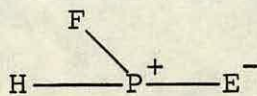
From these results it seemed apparent that the same conversion of the PF_2 group had taken place in these two reactions as had taken place in the reaction of H_2O . The major difference between the n.m.r. spectra of the product on reaction with H_2O and those of the reactions with H_2S and H_2Se was the fact that the latter gave rise to second order spectra whereas the former appeared to give rise to approximately first order n.m.r. spectra. The $^{77}Se\{-^1H\}$ spectrum could only be interpreted by Se being directly bound to phosphorus therefore the group bound to iridium is in fact $HPF(Se)$; by inference the major products of all three reactions were $HPF(E)$ [$E = O, S, Se$].

The fact that there were three different substituents bound to phosphorus implied that it was chiral. The magnetic inequivalence of the PEt_3 groups arises from the asymmetry of the groups; any orientation of the HPF(E) group would result in the magnetic environments of the two PEt_3 groups being different. It should be noted that in the complex containing the HPF(O) unit the PEt_3 groups are practically equivalent; the only sign of inequivalence was the doublet couplings which are almost resolved by line narrowing in the ^1H n.m.r. spectrum.

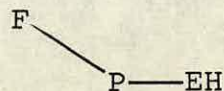
As with the PF_2E groups bound to iridium described in section 3.1.3 the HPF(E) groups may be one of a number of different forms.



A



B



C

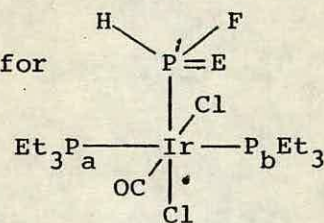
We have less information to decide which is the most favoured structure than with the PF_2E groups. There is the value of J_{PSe} , although slightly low to assume that the P-Se bond was completely double bonded⁽¹⁰⁶⁾ it was somewhat higher than the value expected for a P-Se single bond⁽¹⁰⁷⁾ suggesting that the HPF(Se) group existed largely in form A. Nothing definite could be said about the HPF(S) group but as the magnitudes of most of the n.m.r. parameters of this group were in close agreement with those of the HPF(Se) group it was

assumed that the arrangement of the HPF(S) group was also largely form A. The observation that the PEt_3 groups in the complex containing the HPF(O) group did not give rise to an AB pattern suggested that the above argument did not follow for this example. Given that the PEt_3 groups in this complex were to all intents and purposes magnetically equivalent, the HPF(O) group must be practically symmetric. For this to be the case the oxygen must be similar electronically as well as with respect to size to the fluorine atom, this could only be the case if there was a relatively higher tendency towards form B. (Since the J_{PH} couplings for all three complexes were large, implying $^1J_{\text{PH}}$, and the signals of the ^1H resonance were sharp it was apparent that tautomer C was an unlikely possibility).

It is interesting that the P-O bond in the HPF(O) group seems to have a relatively high P^+-O^- character whereas that in the PF_2O group was strongly double bonded. The only possible explanation for this is that the electropositive hydrogen stabilises the positive charge on phosphorus resulting in a greater preference for form B. The observed $^1J_{\text{PSe}}$ for the HPF(Se) group is significantly smaller than that for the PF_2E group suggesting that the P-Se bond of the HPF(Se) group is similarly less strongly double bonded than that of the PF_2Se group. We have no data for the HPF(S) group to make a similar comparison to those above but by inference it is likely to be the same as O and Se.

Table 3.1.5

N.m.r. parameters for



| E | $\delta P_a/\text{ppm}$ | $\delta P_b/\text{ppm}$ | $\delta P'/\text{ppm}$ | $\delta F/\text{ppm}$ | $\delta H/\text{ppm}$ | $^1J_{P',F}/\text{Hz}$ | $^1J_{P',H}/\text{Hz}$ | $^2J_{P_aP_b}/\text{Hz}^*$ |
|-------------------|-------------------------|-------------------------|------------------------|-----------------------|-----------------------|------------------------|------------------------|----------------------------|
| O | -8.8 | | 46.9 | -42.2 | 8.2 | 1004 | 530 | - |
| S | -9.0 | -16.6 | 79.6 | -73.7 | 8.4 | 1001 | 507 | 321.2 |
| Se ^[a] | -10.0 | -18.5 | 82.2 | -93.5 | 8.0 | 1011 | 492 | 322.3 |

| E | $^2J_{P_aP'}/\text{Hz}^*$ | $^2J_{P_bP'}/\text{Hz}^*$ | $^2J_{HF}/\text{Hz}$ | $^3J_{P_aF}/\text{Hz}^*$ | $^3J_{P_bF}/\text{Hz}^*$ | $^3J_{P_aH}/\text{Hz}$ | $^3J_{P_bH}/\text{Hz}$ |
|-------------------|---------------------------|---------------------------|----------------------|--------------------------|--------------------------|------------------------|------------------------|
| O | 15.2 | | 76.6 | 5.4 | | 2.8 | |
| S | 14 | 12 | 75.1 | 12 | <1 | 7.1 ^[b] | NR |
| Se ^[a] | 14 | 11 | 72.9 | 11 | <1 | 6.9 ^[b] | NR |

[a] $\delta\text{Se} = 161.9$; $^1J_{P\text{Se}} = 735$; $^2J_{F\text{Se}} = 25$

[b] We were unable to deduce if the resolved $^3J_{PH}$ was $^3J_{P_aH}$ or $^3J_{P_bH}$; so the designations

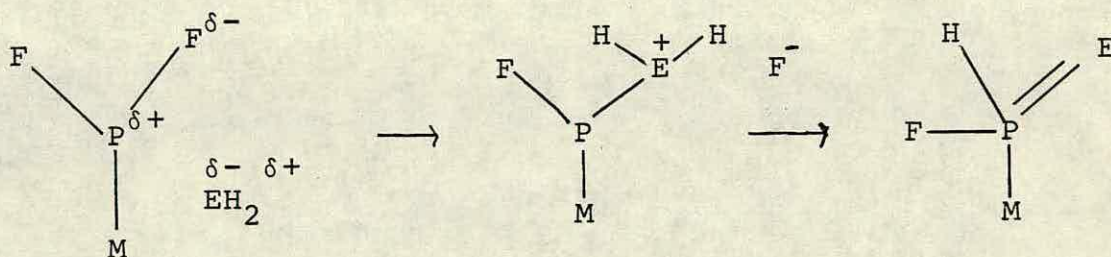
* is arbitrary

The values of these parameters were calculated by carrying out standard solutions for AB patterns for each line of the multiplets (a_n, b_n, c_n, d_n ; Figure 3.2.5.2) consisting of the ABMX pattern; couplings being calculated after positions of the actual AB patterns had been determined.

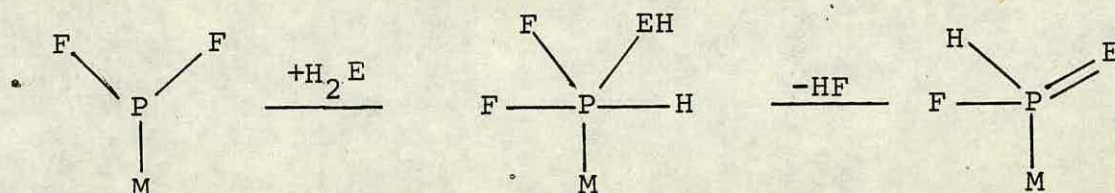
N.m.r. spectra were recorded in toluene at room temperature

Two mechanisms are possible for these reactions:

(i) Initial nucleophilic substitution of fluoride by the H_2E followed by rearrangement of the bound H_2E group.



(ii) Oxidative addition across phosphorus by an E-H bond of the H_2E compound followed by loss of HF.



No conclusive information pertaining to the mechanism of reaction was deduced from the results collected. However, the oxidative addition mechanism seemed more likely for the reactions of H_2S and H_2Se ; given that results of the reactions already described have shown that the phosphorus has a relatively high nucleophilic character and undergoes facile oxidation by the Group VIB elements, and possibly chlorine, coupled with the fact that the Group VIB centres do not have a highly nucleophilic character, makes the possibility of nucleophilic substitution unlikely. The likelihood of initial nucleophilic attack would be greater for the reaction

with H_2O as the oxygen has a relatively high nucleophilic character but overall, the chemistry of the terminal PF_2 group discussed in the previous sections would suggest that the oxidative addition mechanism was the more likely.

3.1.6 The Reaction of Excess PF_2Cl with $\text{Ir}(\text{PF}_2)(\text{CO})(\text{PEt}_3)_2\text{Cl}_2$

An excess of PF_2Cl was accidentally incorporated into an n.m.r. tube reaction between PF_2Cl and $\text{IrCl}(\text{CO})(\text{PEt}_3)_2$; the reaction medium was left at room temperature for some days after which time it was clear that conversion of the terminal PF_2 ligand was occurring.

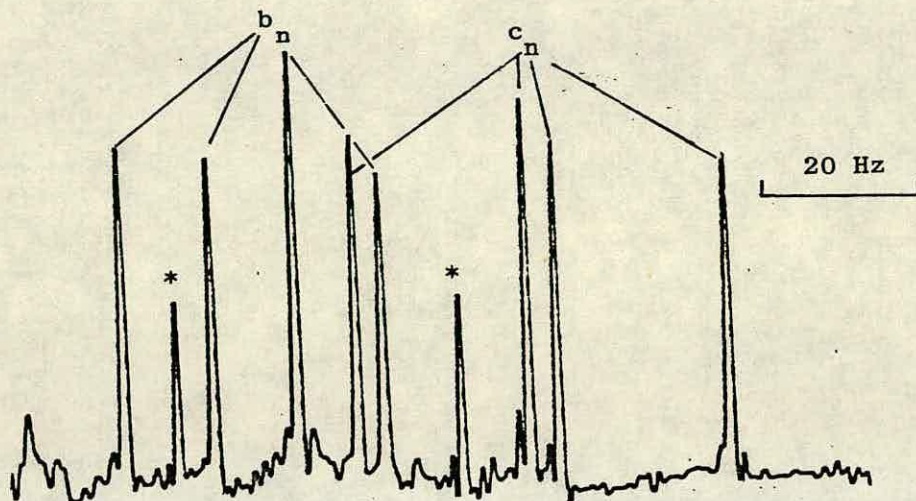
The n.m.r. parameters of the species produced are collected in Table 2.1.6.

The n.m.r. spectra of the reaction media were recorded after a period of two days at room temperature. After this period the n.m.r. consisted mainly of signals arising from the complex $\text{Ir}(\text{PF}_2)(\text{CO})(\text{PEt}_3)_2\text{Cl}_2$; however there were also relatively weak signals arising from another species.

The $^{31}\text{P}\{^1\text{H}\}$ n.m.r. of this species consisted of two signals. To high frequency (ca. 330 ppm) there was a resonance split into a doublet ($^1J_{\text{PF}}$) of doublets ($^2J_{\text{PP}}$) of doublets ($^2J_{\text{PP}}$). The signals to low frequency in the spectral region associated with PEt_3 bound to iridium when recorded on low field n.m.r. (60 MHz) consisted of what appeared to be a complex series of doublets (Figure 3.1.6.1); when recorded on a high field n.m.r. instrument the signals were shown to be the AB part of an ABMX pattern. (The Δ_{AB} between the signals A

and B was so small in comparison to J_{AB} , that it was impossible to detect the outer lines of the AB quartet in the low field n.m.r.).

Figure 3.1.6.2 $^{31}\text{P}\{-^1\text{H}\}$ n.m.r. of $\text{Ir}(\text{PFCl})(\text{CO})(\text{PEt}_3)_2\text{Cl}_2$ showing the central signals (b_n, c_n) of the AB quartet arising from the PEt_3 groups.



* are the signals arising from the PEt_3 groups of $\text{Ir}(\text{PFCl}_2)(\text{CO})(\text{PEt}_3)_2\text{Cl}_2$

The ^{19}F n.m.r. of this species was a single resonance at very low frequency, split into a doublet ($^1J_{\text{PF}}$) of pseudo triplets ($^3J_{\text{PAF}}$ was found to ca. equal $^3J_{\text{PBF}}$).

On leaving the reaction medium at room temperature for two weeks no signals arising from $\text{Ir}(\text{PF}_2)(\text{CO})(\text{PEt}_3)_2\text{Cl}_2$ or those described above were detected. The n.m.r. spectra consisted of signals arising from PF_3 and $\text{Ir}(\text{PFCl}_2)(\text{CO})(\text{PEt}_3)_2\text{Cl}_2$ (described in Chapter 4).

The structure of the species formed after ca. two days reaction was determined from the n.m.r. data recorded. The fact that the signal to high frequency in the ^{31}P n.m.r. spectrum was split only by a doublet from $^1J_{\text{P}'\text{F}}$ implied that

only a single fluorine was bound to phosphorus this was supported by the nature of the splitting of the PEt_3 resonances. The high chemical shift of the unique phosphorus implied that phosphorus was trivalent and bound to iridium. The ABMX splitting pattern of the PEt_3 resonance implied that the unique phosphorus was chiral. Given these constraints the complex formed is almost certainly $\text{Ir}(\text{PFCl})(\text{CO})(\text{PEt}_3)_2\text{Cl}_2$ produced by substitution of fluorine on the terminal PF_2 group by chlorine from PF_2Cl .

The results from the n.m.r. spectra of the reaction medium after 2 weeks imply that further substitution of fluorine on the terminal phosphorus-fluorine groups yields the final products $\text{Ir}(\text{PCL}_2)(\text{CO})(\text{PEt}_3)_2\text{Cl}_2$ (see Figure 3.1.6.2).

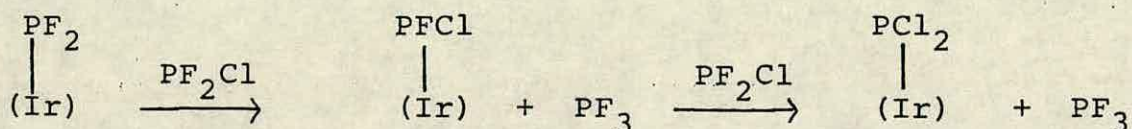
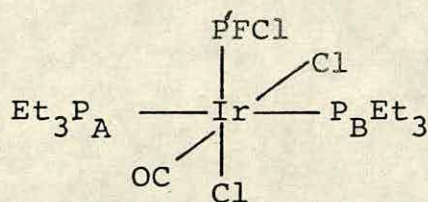


Figure 3.1.6.2

The $\text{Ir}(\text{PFCl})(\text{CO})(\text{PEt}_3)_2\text{Cl}_2$ complex was not isolated and so no further characterisation was possible. Proof of our characterisation might be obtained if the reaction PFCl_2 with $\text{IrCl}(\text{CO})(\text{PEt}_3)_2$ was carried out; it would seem PFCl_2 would add oxidatively across iridium yielding the $(\text{Ir})\text{-PFCl}$ complex.

Table 3.1.6.2 N.m.r. parameters for



| $\delta P_a^*/\text{ppm}$ | $\delta P_B^*/\text{ppm}$ | $\delta P'/\text{ppm}$ | $\delta F/\text{ppm}$ | $^1J_{PF}/\text{Hz}$ | $^2J_{P_AP_B}^*/\text{Hz}$ | $^2J_{P_AP'}^*/\text{Hz}$ |
|---------------------------|---------------------------|------------------------|-----------------------|----------------------|----------------------------|---------------------------|
| -6.8 | -10.6 | 345.2 | -106.1 | 1121 | 309 | 4 |

| $^2J_{P_BP'}^*/\text{Hz}$ | $^3J_{P_AF}/\text{Hz}$ |
|---------------------------|------------------------|
| 31 | 22 |

* see Table 3.1.5

The parameters were recorded in methylene chloride at room temperature.

3.2 The Reactions of $\text{Ir}(\text{PF}_2)(\text{CO})(\text{PEt}_3)_2\text{Cl}_2$ with Transition Metal Substrates

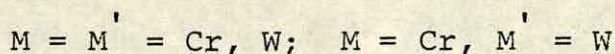
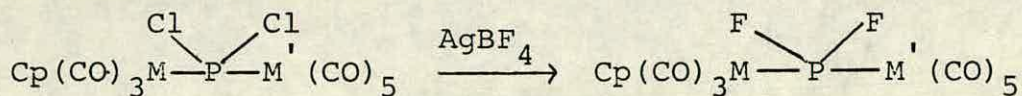
3.2.1 Introduction

The object of these reactions was to synthesise mixed metal PF_2 bridged species using the terminal PF_2 complexes as the basis of the PF_2 bridge.

Few metal complexes with PF_2 bridging ligands have been previously reported in the literature. But within the few examples reported, complexes with mono- and bis- PF_2 bridging ligands have been synthesised.

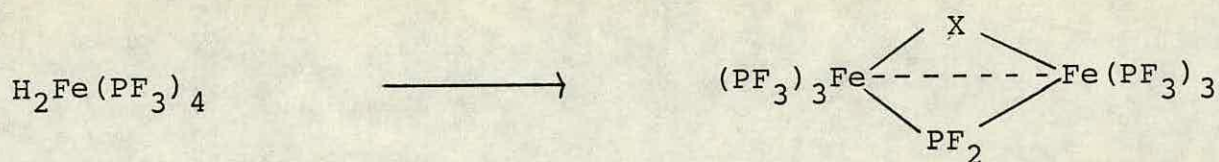
Two complexes with single PF_2 bridging ligands have already been described in the introductory chapter in the section relating reactions of PF_2X ($\text{X} = \text{Cl}, \text{Br}, \text{I}, \text{H}$) with transition metal substrates; these are $[\text{Cl}_2\text{Et}_3\text{PPt}-\mu(\text{PF}_2)-\text{Pt}(\text{PEt}_3)_2\text{Cl}]^-$ (48) and $(\text{CO})_4\text{Mn}-\mu(\text{PF}_2)-\mu(\text{I})-\text{Mn}(\text{CO})_4$ (49).

Another example of a transition metal complex with a single PF_2 bridge was reported by Malisch and Panster⁽⁷⁶⁾ who were able to synthesise such a complex by fluorination of complexes with single PCl_2 bridges (the synthesis of these complexes was described in Section 1.3).



It was noted that the central bridging system in these complexes was very stable; the $\text{Cp}(\text{CO})_3\text{M-PF}_2$ group could not be displaced by either strongly basic phosphines or thermal treatment.

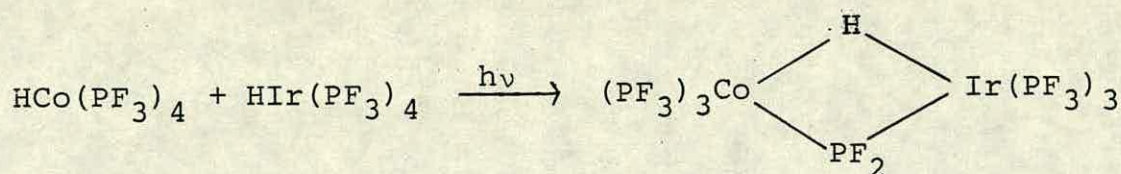
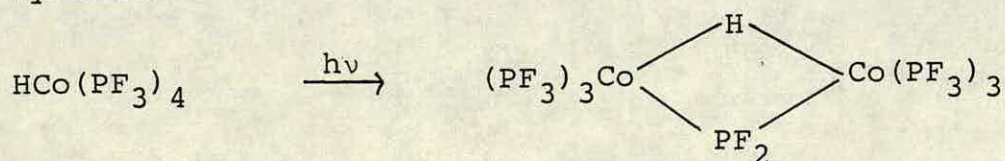
Kruck and Kobelt⁽¹²⁰⁾ reported the synthesis of iron complexes similar to the manganese complex already described, in that the complexes contained a single PF_2 bridge ligand plus one other bridging ligand (I or SET). The method of synthesis was completely different from that reported for the manganese species; iodine and ethane thiol were reacted with dihydridotetrakis trifluorophosphine iron(II) thus modifying one of the PF_3 ligands and displacing hydride groups.



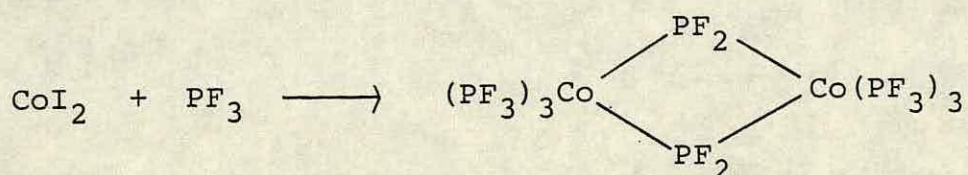
X = I or SET

Neither complex was very stable and both were characterised by mass spectral evidence.

Kruck et al⁽¹²¹⁾ have also reported the synthesis of complexes with a single PF_2 bridging ligand plus a bridging hydride.

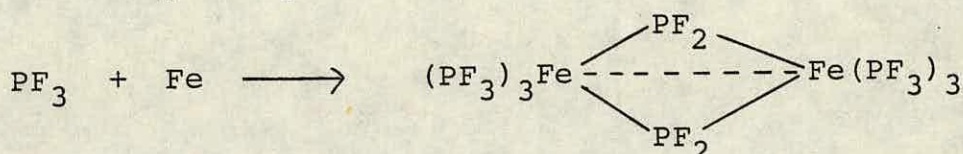


One might regard complexes containing bis PF_2 bridging ligands as analogous to these complexes: few complexes containing two bridging PF_2 groups have been synthesised. Kruck and Lang⁽¹²²⁾ reported the first synthesis of such a complex; they discovered that the direct reaction of cobalt iodide with PF_3 at high temperature and pressure yielded a binuclear cobalt complex with two PF_2 bridging ligands.

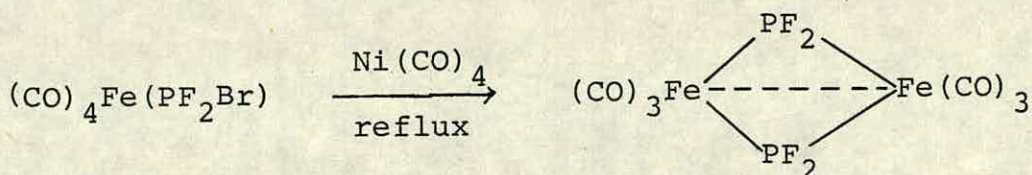


Mass spectral results showed that the central bridging system of this complex was very stable, with a relatively high intensity peak at $m/e = 256$ for the fragment $[\text{Co}(\text{PF}_2)_2\text{Co}]^+$.

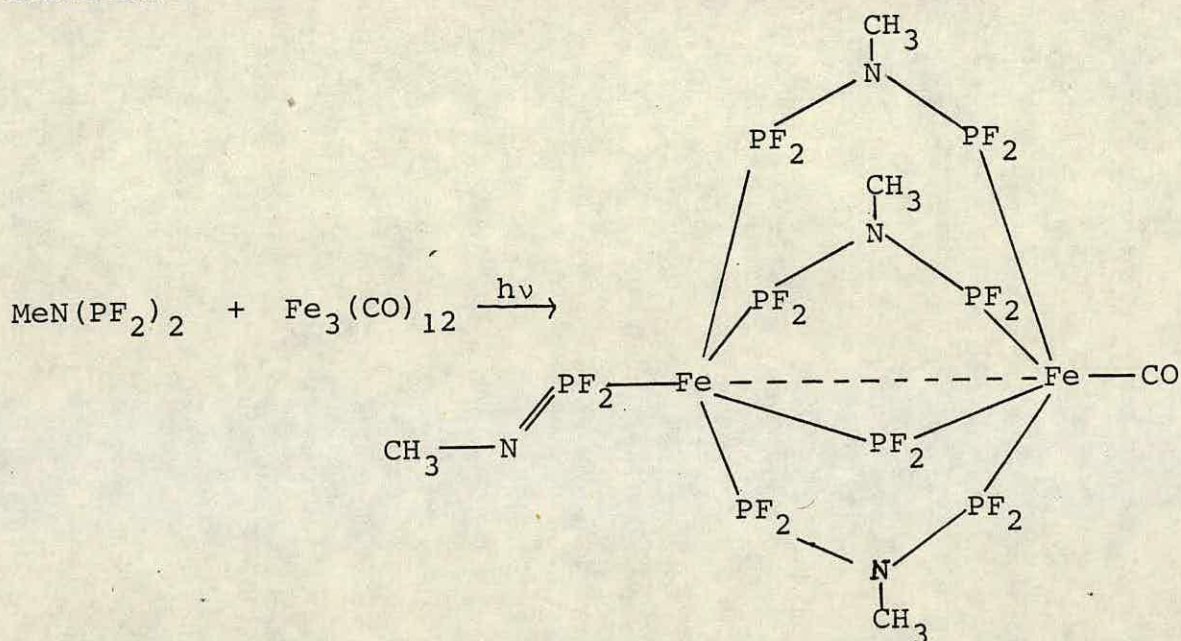
Timms⁽¹²³⁾ was able to synthesise the iron analogue of this complex by the reaction of iron atoms with PF_3 .



The analogue of this complex containing CO groups in the place of PF_3 was synthesised by a completely different method. Douglas and Ruff⁽¹²⁴⁾ reported the reaction of iron complexes with coordinated PF_2Br ligands in the presence of $\text{Ni}(\text{CO})_4$ yielded the binuclear iron PF_2 -bridged complex



King et al reported that the photochemically induced reaction of methyl amino bis(difluorophosphine) $[\text{CH}_3\text{N}(\text{PF}_2)_2]$ with $\text{Fe}_3(\text{CO})_{12}$ ⁽¹²⁵⁾ yielded a binuclear iron complex with only a single PF_2 bridging ligand but containing also three bridging $\text{CH}_3\text{N}(\text{PF}_2)_2$ ligands. The characterisation of this extraordinary complex was proved by an X-ray crystal structure.

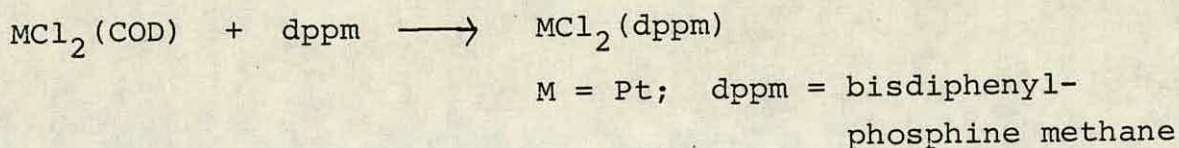
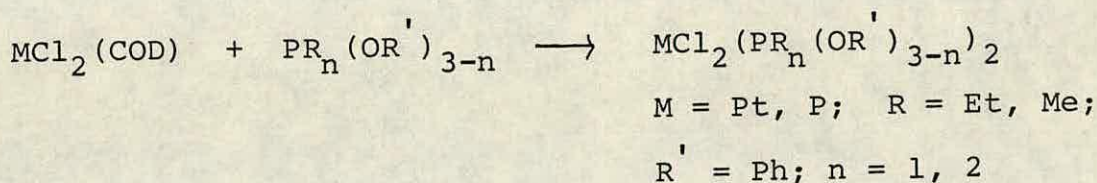
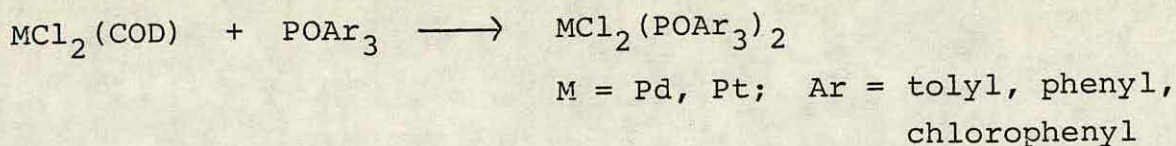


The few previously reported examples of metal complexes with PF_2 bridging groups indicated that PF_2 was a good bridging ligand. The central bonding system of complexes containing these groups have on the whole been very stable.

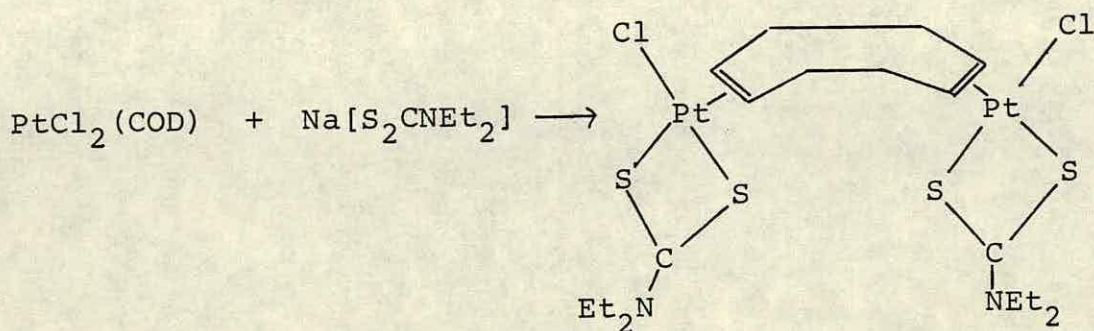
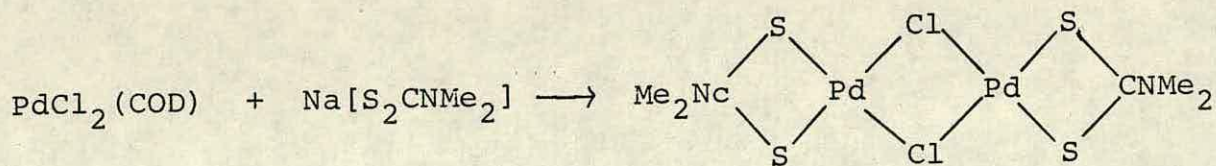
3.2.2 The Reactions of $\text{Ir}(\text{PF}_2)(\text{CO})(\text{PEt}_3)_2\text{Cl}_2$ with $\text{MCl}_2(\text{COD})$
[M = Pt, Pd; COD = 1,5-cyclo-octadiene]

It has been shown in the introductory chapter that fluorophosphines displace metal bound olefin ligands to yield metal fluorophosphine complexes. It was hoped that the reactions of the iridium PF_2 complexes with $\text{MCl}_2(\text{COD})$ would follow such a course, yielding complexes containing a bridging PF_2 ligand.

In the reactions $\text{MCl}_2(\text{COD})$ with phosphites⁽¹²⁶⁾, phosponites⁽¹²⁷⁾ and phosphines⁽¹²⁸⁾ COD has been displaced yielding MCl_2L_2 [$\text{L} = \text{POAr}_3, \text{PR}_n(\text{OR})_{3-n}, n = 1, 2; \text{PR}_3$].



Reactions of $\text{MCl}_2(\text{COD})$ with dithiocarbamate salts have followed a different course⁽¹²⁹⁾; with displacement of both chloride and COD occurring. In these reactions $\text{PtCl}_2(\text{COD})$ yields different final products from $\text{PdCl}_2(\text{COD})$.



It is probable that the elimination of Cl^- in these reactions is driven by NaCl salt formation and for that reason was unlikely to happen in the reactions of $\text{MCl}_2(\text{COD})$ with the iridium $-\text{PF}_2$ complexes.

The reactions of both $\text{PdCl}_2(\text{COD})$ and $\text{PtCl}_2(\text{COD})$ were carried out at room temperature but with different periods of reaction.

Phosphorus-31 and ^{19}F n.m.r. spectra of the residue of reaction involving $\text{PdCl}_2(\text{COD})$ showed that reaction had taken place (no signals were observed for iridium starting material). The n.m.r. spectra showed that a number of metal PF_2 species had formed in the reaction. Identification of these species could not be made from their n.m.r. spectra and the different species could not be separated from one another to obtain any further characterisations.

The ^{31}P and ^{19}F n.m.r. spectra of the residue of reaction from that involving $\text{PtCl}_2(\text{COD})$ showed that reaction yielded only one product. The n.m.r. data for this species are collected in Table 3.2.2.1.

The ^{31}P n.m.r. spectrum of this species consisted of two signals. To high frequency (see Figure 3.2.2.1) (δP ca. 177 ppm) a signal split into a triplet ($^1\text{J}_{\text{PF}}$) the lines of which were further split as is shown by the expansion of the central triplet in Figure 3.2.2.1. The complex centrosymmetric splitting of the resonance made it clear that the n.m.r. spectrum of this species was not first order. It can be seen in Figure 3.2.2.1 that associated with the central ' PF_2 ' triplet were platinum satellites (Pt has 33% $I = \frac{1}{2}$ nucleus ^{195}Pt); the intensities of the Pt satellites relative to the main peaks are ca 1:4. To low frequency the signal arising from the PEt_3 groups was split into a complex multiplet (Figure 3.2.2.2) which again was obviously not first order.

The ^{19}F n.m.r. of this species consisted of one signal split by an apparent doublet coupling (" $^1\text{J}_{\text{PF}}$ ") the lines of the doublet were very broad; shoulders were apparent on the lines and they were arranged symmetrically across the centre of the splitting pattern (see Figure 3.2.2.3). The main peaks of the resonance again had Pt satellites associated with them (intensity of satellite to main signal was again 1:4).

Figure 3.2.2.1 $^{31}\text{P}\{-^1\text{H}\}$ n.m.r. of $[(\text{Ir})\text{-PF}_2]_2\text{PtCl}_2$

* are ^{195}Pt satellites of signals A, B and C

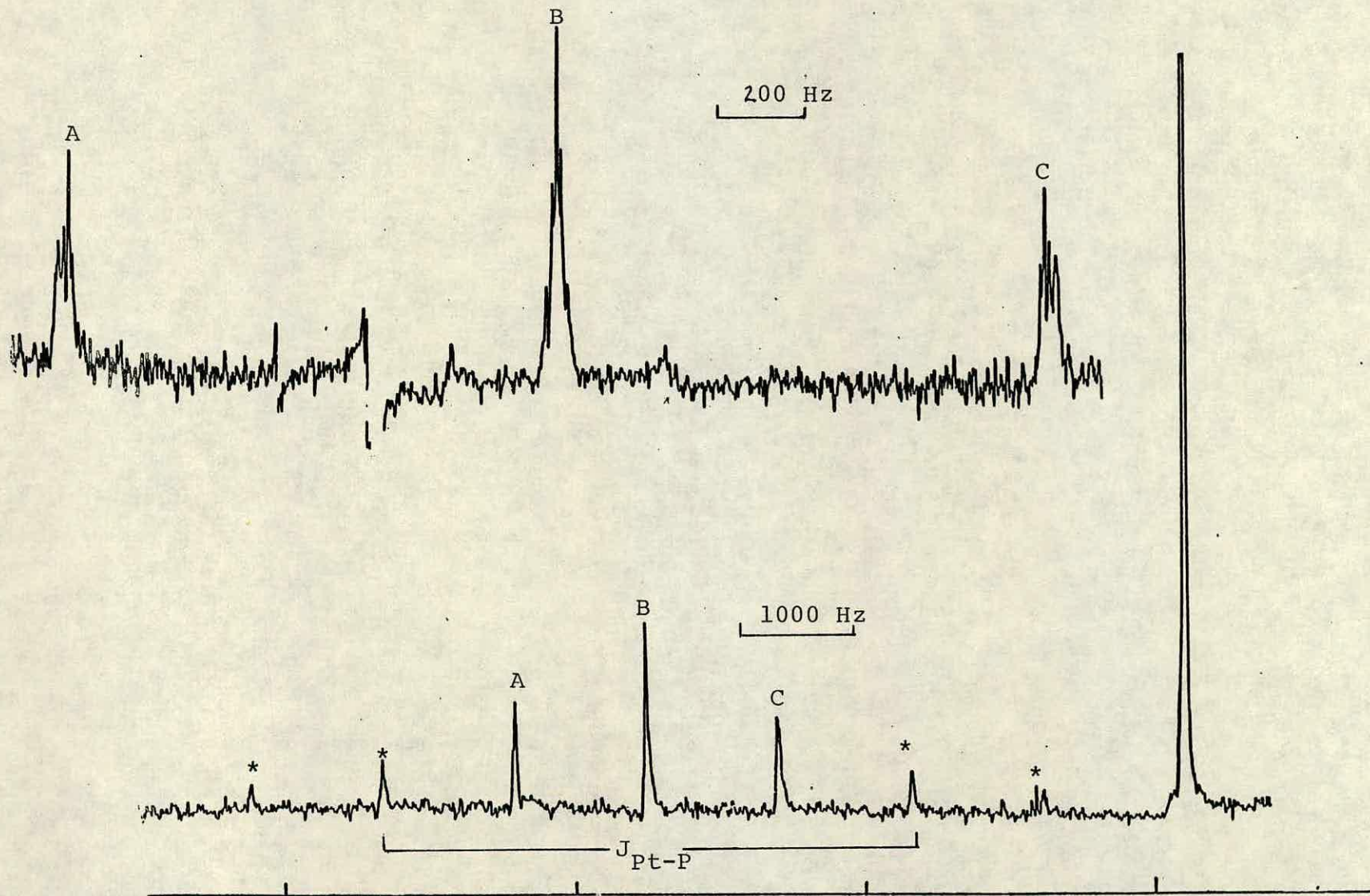
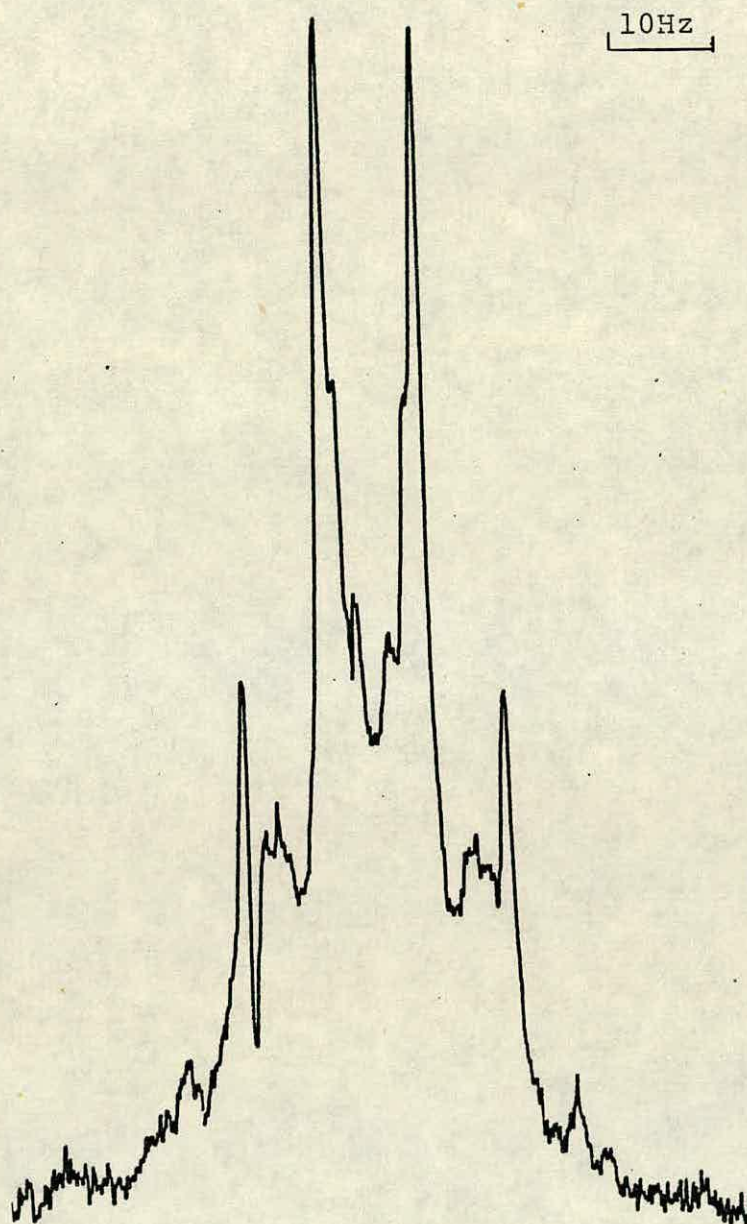
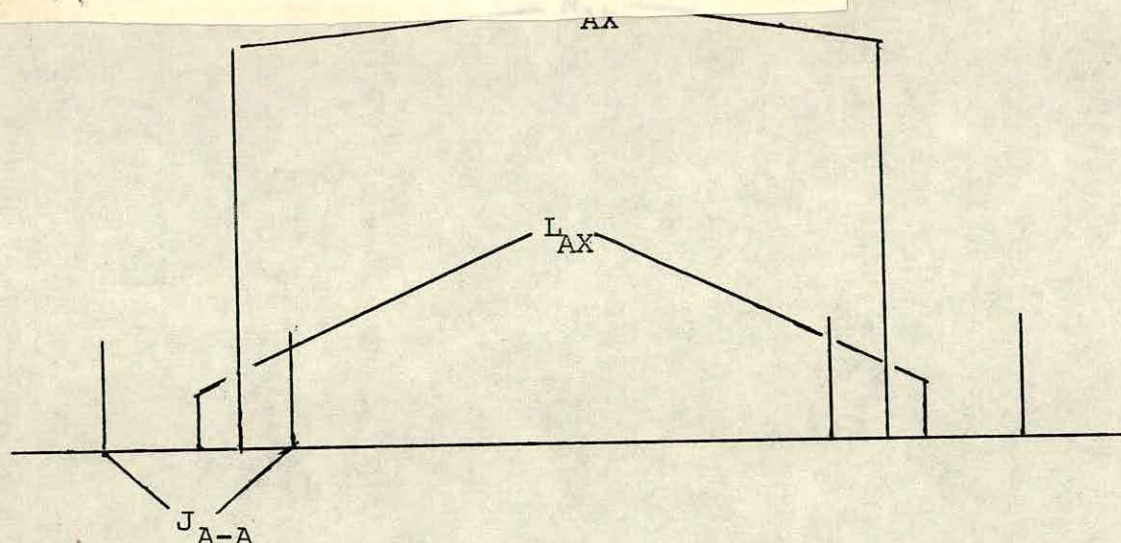


Figure 3.2.2.2 $^{31}\text{P}\{-^1\text{H}\}$ n.m.r. of $[(\text{Ir})\text{-PF}_2]_2\text{PtCl}_2$ showing the PEt_3 resonance, $[(\text{Ir}) = \text{Ir}(\text{CO})(\text{PEt}_3)_2\text{Cl}_2]$



The order of pages 115 to 117 inc. should be 116, 117, 115.

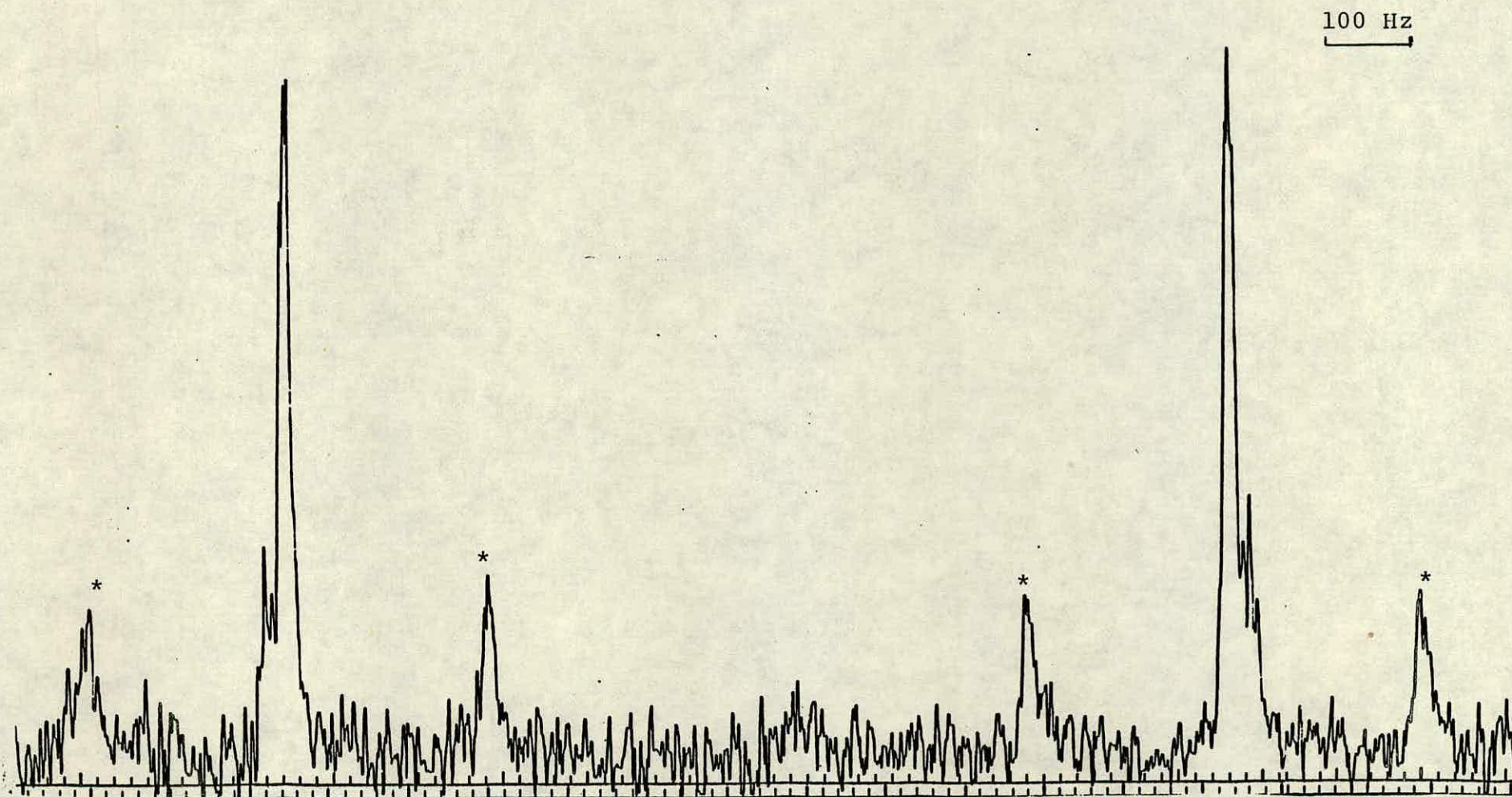


The main peaks which are split by $N_{AX} = |J_{AX} + J_{AX'}|$ represent half the total intensity of the splitting pattern; L_{AX} , which is the splitting between the centres of each half of the splitting pattern, $= |J_{AX} - J_{AX'}|$, the splitting between the outer lines of each half of the splitting pattern is equivalent to J_{AA} . The pattern obtained for the ^{19}F n.m.r. spectrum of the product complex could not definitely be assigned as that of an $[\text{AX}_2]_2$ spin system; however if one considers that the PF_2 groups are mutually cis then one would expect J_{AA} to be fairly small (ca 20-40 Hz), within such a range one would have to include all the peaks of the $[\text{AX}_2]_2$ spin system, with additional splittings from the PEt_3 groups adding to the complication, then it is not surprising that the expected splitting pattern was not obvious. The approximate width of the main peaks of the ^{19}F spectrum provided a very rough measure of $^2J_{\text{P},\text{P}'} = \text{ca. } 20 \text{ Hz}$.

An X-ray crystal structure of the product was obtained to confirm the structural assignment (See Figure 3.2.2.4) structural parameters are presented in Table 3.2.2.2.

Figure 3.2.2.3 ^{19}F n.m.r. spectrum of $[(\text{Ir})\text{-PF}_2]_2\text{PtCl}_2$, $[(\text{Ir}) = \text{Ir}(\text{CO})(\text{PEt}_3)_2\text{Cl}_2]$

* are ^{195}Pt satellites of the main signals



The product of the reaction was isolated as a white crystalline solid. Carbon and hydrogen analysis figures were correct for $\text{Ir}_2(\text{PEt}_3)_4(\text{PF}_2)_2(\text{CO})_2\text{Cl}_4 \cdot \text{PtCl}_2$ (see Experimental). The i.r. spectrum had assignable bands at: 2060 cm^{-1} (ν_{CO}); 790 and 845 cm^{-1} ($\nu_{\text{P-F}}$).

From the data presented above it was possible to determine a possible structure for the complex. The magnitude of $J_{\text{Pt-P}}$ (ca. 3300 Hz) although low for a fluorophosphine directly bound to Pt (for: $\text{PtCl}_2(\text{PF}_3)_2$, $^1J_{\text{Pt-P}} = 6478 \text{ Hz}^{(130)}$; $\text{PtCl}_2(\text{PF}_2\text{Cl})_2$, $^1J_{\text{Pt-P}} = 5996 \text{ Hz}^{(50)}$; $\text{PtCl}_2(\text{PF}_2\text{NMe}_2)_2$, $^1J_{\text{Pt-P}} = 5722 \text{ Hz}^{(50)}$), could only be explained by phosphorus being directly bound to platinum; the value of J_{PtF} was of the order of those previously recorded for $^3J_{\text{Pt-F}}$ (for: $\text{PtCl}_2(\text{PF}_3)_2$ $^{(130)}$; $^3J_{\text{Pt-F}} = 629 \text{ Hz}$; $\text{PtCl}_2(\text{PF}_2\text{Cl})_2$ $^{(50)}$; $^3J_{\text{Pt-F}} = 536 \text{ Hz}$; $\text{PtCl}_2(\text{PF}_2\text{NMe}_2)_2$; $^3J_{\text{Pt-F}} = 595 \text{ Hz}^{(50)}$). These data along with the analytical data implied that platinum had two $\text{Ir}(\text{PF}_2)(\text{CO})(\text{PEt}_3)_2\text{Cl}_2$ units directly bound through phosphorus, plus two chlorides. The ^{19}F n.m.r. data suggested that the two PF_2 groups were mutually cis; the complex should give rise to an $[\text{AX}_2]_2$ second order spin system for the PF_2 groups $^{(131)}$ (the X nuclei couple to the adjacent A nucleus differently from the non adjacent A nucleus thus giving rise to complex splitting of the signals arising from such a system). A schematic representation showing the major peaks of the X n.m.r. spectrum of such a splitting pattern is shown below (n.b. all these peaks are further split in the correct form of splitting pattern).

Figure 3.2.2.4 X-Ray crystal structure of $[(\text{Ir})\text{-PF}_2]_2\text{PtCl}_2$, $[(\text{Ir}) = \text{Ir}(\text{CO})(\text{PEt}_3)_2\text{Cl}_2]$

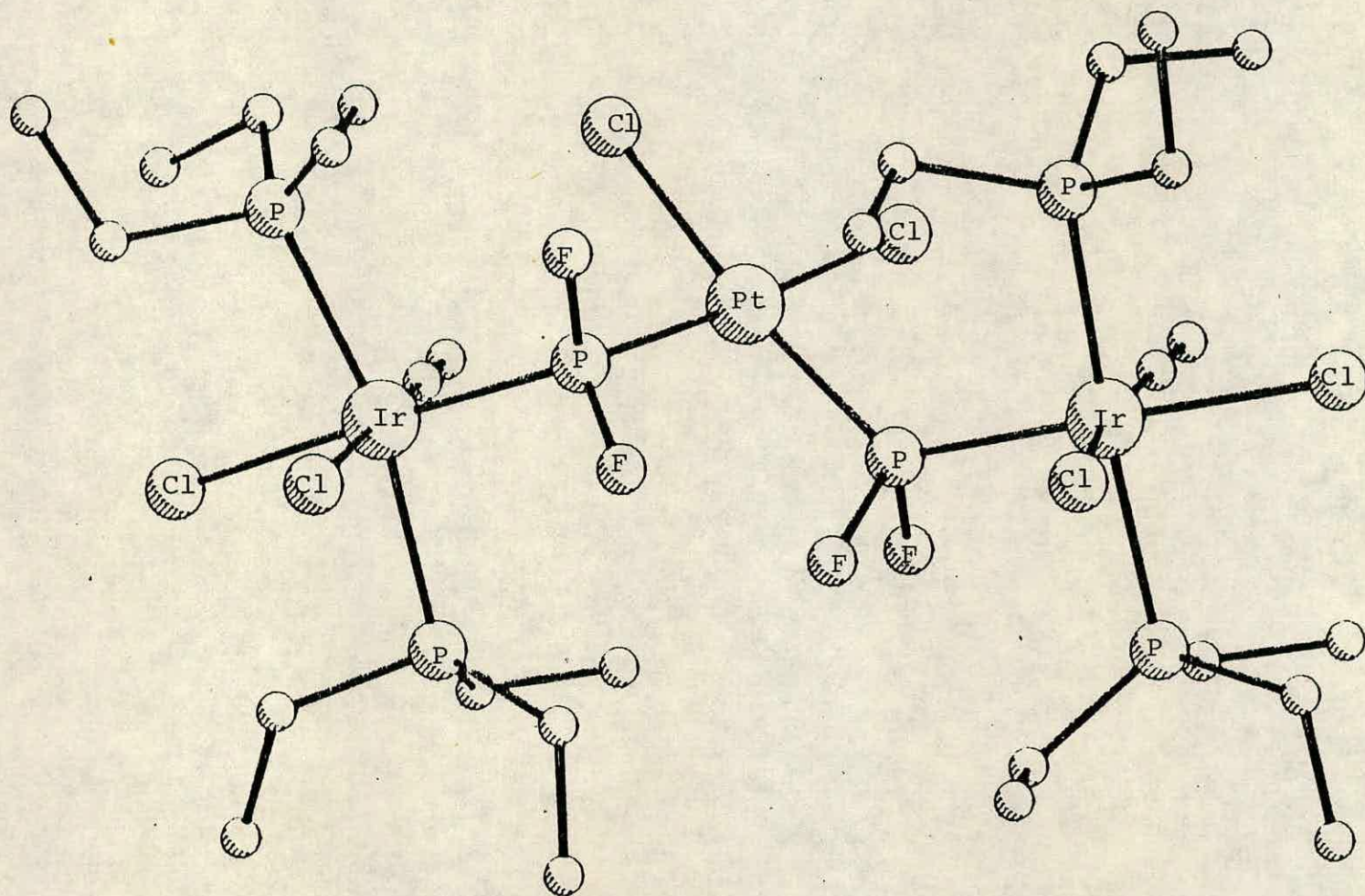
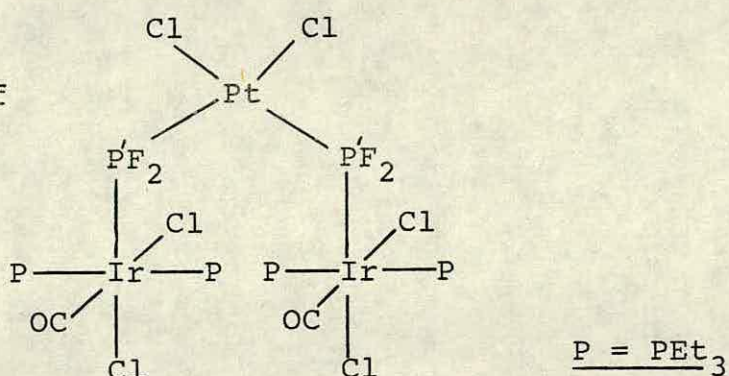


Table 3.2.2.1

N.m.r. parameters of



| $\delta P/\text{ppm}$ | $\delta P'/\text{ppm}$ | $\delta F/\text{ppm}$ | $^1J_{\text{PtP}}/\text{Hz}$ | $^1J_{\text{P}'\text{F}}^{[a]}/\text{Hz}$ | $^2J_{\text{PtF}}/\text{Hz}$ |
|-----------------------|------------------------|-----------------------|------------------------------|---|------------------------------|
| -11.2 | 177.2 | -32.7 | 3360 | 1111 | 472 |

| $^2J_{\text{PP}}^{[b]}/\text{Hz}$ | $^3J_{\text{PF}}/\text{Hz}$ |
|-----------------------------------|-----------------------------|
| 9.4 | NO |

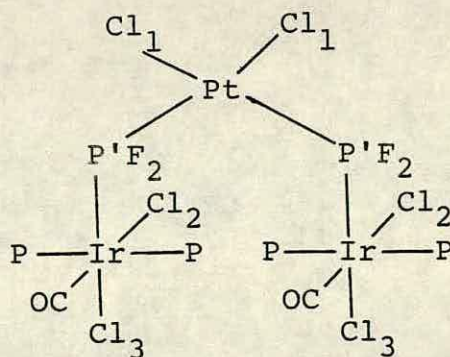
[a] This represents the splitting between the most intense peaks of the ^{19}F spectrum, so it is more correct to refer to the splitting as N_{PF}

[b] This was the value of the splitting between the two most intense peaks of the PEt_3 resonance. Due to the complex nature of the splitting pattern for that signal it was impossible to assign values to coupling constants

The parameters were recorded in methylene chloride at room temperature

Table 3.2.2.2

Some structural parameters for



Bond Lengths/pm

| | |
|--------------------|----------------------------|
| Ir-P | 242.3, 241.4, 245.6, 243.1 |
| Ir-P' | 228.9, 229.6 |
| Ir-Cl ₂ | 234.5, 235.0 |
| Ir-Cl ₃ | 245.9, 245.6 |
| Ir-C | 192 |
| Pt-Cl ₁ | 233.4, 236.3 |
| Pt-P' | 224.3, 221.4 |
| P-F | 151.7, 150.5, 153.1, (162) |

Bond Angles/Degrees

| | |
|-----------------------|----------------------------|
| Ir-P'-Pt | 120.4, 126.7 |
| P-Ir-P | 166.9, 169.3 |
| Cl ₂ -Ir-C | 173.6, 176.5 |
| P'-Pt-P' | 101.9 |
| Cl-Pt-Cl | 90.1 |
| Cl-Pt-P' | 83.5, 84.7 |
| F-P'-F | 99.1, 94.9 |
| F-P'-Pt | 106.4, 111.6, 107.6, 108.5 |

Table 3.2.2.3

Some bond lengths of square planar Pt(II) complexes

| Complex | Distances/pm | | Reference |
|--|--------------------|--------------|-----------|
| $\begin{array}{c} \text{P}_1\text{Et}_3 \\ \\ \text{SF}_2\text{P}_2 - \text{Pt} - \text{Cl} \\ \\ \text{P}_1\text{Et}_3 \end{array}$ | Pt-P ₁ | 233.8 | 98 |
| | Pt-P | 221.3 | |
| | Pt-Cl | 236.8 | |
| $\begin{array}{c} \text{PF}_3 \\ \\ \text{Cl}_1 - \text{Pt} - \text{P}_1\text{Et}_3 \\ \\ \text{Cl}_2 \end{array}$ | Pt-P ₁ | 227.2 | 132 |
| | Pt-P ₂ | 214.1 | |
| | Pt-Cl ₁ | 235.7 | |
| | Pt-Cl ₂ | 230.5 | |
| $\begin{array}{c} \text{PEt}_2\text{Ph} \\ \\ \text{OF}_2\text{P}_2 - \text{Pt} - \text{Cl} \\ \\ \text{PEt}_2\text{Ph} \end{array}$ | Pt-P ₁ | 233.8 | 111 |
| | Pt-P ₂ | 219.9 | |
| | Pt-Cl | 236.6 | |
| $\begin{array}{c} \text{CO} \\ \\ \text{Cl}_1 - \text{Pt} - \text{PEt}_3 \\ \\ \text{Cl}_2 \end{array}$ | Pt-P | 226.5 | 133 |
| | Pt-Cl ₁ | 236.8 | |
| | Pt-Cl ₂ | 229.6 | |
| $\begin{array}{c} \text{CO} \\ \\ \text{Cl}_1 - \text{Pt} - \text{PPh}_3 \\ \\ \text{Cl}_2 \end{array}$ | Pt-P | 228.2 | 134 |
| | Pt-Cl ₁ | 234.3 | |
| | Pt-Cl ₂ | 227.6 | |
| $\begin{array}{c} \text{P}(\text{C}_6\text{F}_5)_2\text{Me}_2 \\ \\ \text{Cl}_1 - \text{Pt} - \text{P}(\text{C}_6\text{F}_5)_2\text{Me}_2 \\ \\ \text{Cl}_2 \end{array}$ | Pt-P | 224.0, 223.1 | 135 |
| | Pt-Cl | 235.5, 233.2 | |

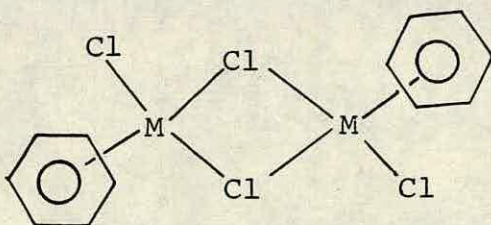
It was of interest to compare the structural parameters of the ligands around platinum in this complex with those of some other square-planar platinum complexes; some data for these complexes are presented in Table 3.2.2.3.

It can be seen that the mean Pt-P bond length (222.8) reported in this work is significantly longer than those from platinum to the strong π acids PF_3 and PF_2O but markedly shorter than those to alkyl or aryl phosphines, suggesting that there is only moderate back donation from platinum to phosphorus in the Ir- PF_2 -Pt bridge. This is probably the main reason why the value of $^1J_{\text{Pt-P}}$ is low in comparison with those recorded previously for platinum-fluorophosphine complexes. It should perhaps be noted at this point that considerable back donation from iridium to phosphorus is implied by the high value of ν_{CO} in comparison to that of the iridium starting material.

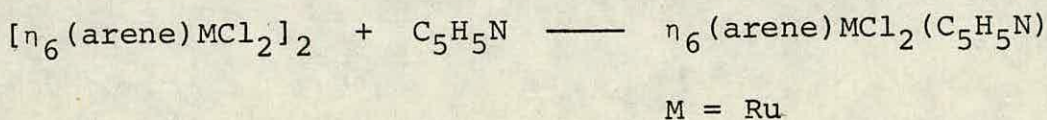
The trans influence of the PF_2 groups can also be compared with those of other ligands by comparing Pt-Cl bond lengths. The mean Pt-Cl bond length (234.8) reported in this work is approximately the same as that trans to PPh_3 and is considerably longer than those trans to the low trans influence ligands PF_3 and CO, suggesting a moderately high trans influence for the PF_2 -(Ir) groups.

3.2.3 The Reactions of $\text{Ir}(\text{PF}_2)(\text{CO})(\text{PEt}_3)_2\text{Cl}_2$ with $[\eta_6(\text{arene})\text{MCl}_2]_2$ [M = Ru, Os; arene = benzene or paracycene]

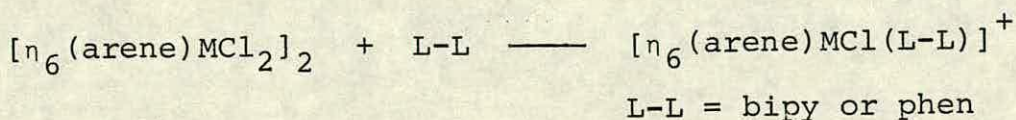
The structure of the complexes $[\eta_6(\text{arene})\text{MCl}_2]_2$ is shown below.



It has been found that complexes of this type readily react with nucleophiles with breakdown of the central bridging system to give monomeric complexes^(136,137) as exemplified below.



It has also been shown that anionic monomeric complexes are formed in the reactions of the chloro-bridged complexes with some bidentate ligands such as 2,2'-bipyridyl and 1,10-phenanthroline⁽¹³⁸⁾. In these reactions not only is the bridging system broken but a chloride ion is also displaced.



It was hoped that reaction of $\text{Ir}(\text{PF}_2)(\text{CO})(\text{PEt}_3)_2\text{Cl}_2$ with these binuclear complexes would result in breakdown of the dichloro bridges by incorporation of the $\text{PF}_2\text{-(Ir)}$ unit.

The reactions of $\text{Ir}(\text{PF}_2)(\text{CO})(\text{PEt}_3)_2\text{Cl}_2$ with $[\eta_6(\text{C}_6\text{H}_6)\text{RuCl}_2]_2$ and $[\eta_6(\text{p-cymene})\text{MCl}_2]_2$ [$\text{M} = \text{Ru}, \text{Os}$; $\text{p-cymene} = \text{p-isopropyl toluene}$] were carried out at room temperature and the resultant products of reaction were studied. The product of the reaction with $[\eta_6(\text{C}_6\text{H}_6)\text{RuCl}_2]_2$ was less well characterised than those of the other two reactions as it was less stable and less soluble than those of the other reactions.

The reactions produced single products. The ^{31}P and ^{19}F n.m.r. spectra of the products were qualitatively the same as those of the iridium starting material except that the signal arising from the PEt_3 groups was split into a pseudo quartet because $^2J_{\text{PP}} \approx ^3J_{\text{PF}}$. The n.m.r. parameters of the products are presented in Table 3.2.3.1. The actual values of the n.m.r. parameters, in particular the phosphorus and fluorine chemical shifts, were noticeably different from those of the iridium starting material.

Carbon and hydrogen analyses for the products of the reactions with $[\eta_6(\text{p-cymene})\text{MCl}_2]_2$ were correct for $\text{Cl}_2(\text{PEt}_3)_2(\text{CO})\text{Ir-PF}_2\text{-MCl}_2(\text{p-cymene})$. Infrared spectra of the products had bands at ca. 2065 (ν_{CO}) and 800 ($\nu_{\text{P-F}}$).

A mass spectrum of the product from the reaction of $[(p\text{-cymene})\text{OsCl}_2]_2$ was recorded (see Figure 3.2.3.1). The molecular ion peak is at m/e 992, the correct value for $[\text{Cl}_2(\text{PEt}_3)_2(\text{CO})\text{Ir-PF}_2\text{-OsCl}_2\text{-(p-cymene)}]^+ = (\text{A})$. Some fragments of the breakdown were identified: m/e 973 = A-F, m/e 957, = (A)-Cl; m/e 858 = (A) - p-cymene; m/e 561 = $\text{Ir}(\text{PF}_2)(\text{CO})(\text{PEt}_3)_2\text{Cl}$. (The peaks at m/e 733 and 453 can only be explained if one assumes that molecular rearrangement has taken place in the spectrometer; the m/e values are consistent with $[\text{IrOs}(\text{CO})(\text{PEt}_3)(p\text{-cymene})\text{Cl}_2]^+$ and $[\text{IrOsCl}_2]^+$ respectively. Presumably the fragments have Cl bridges between iridium and osmium).

All data cited above supported the postulate that complexes containing PF_2 bridging ligands had been formed. The n.m.r. spectra of the complexes were consistent with the presence of a quaternary phosphorus fluorine grouping, in that the phosphorus chemical shifts were lower than that of the starting material. All analytical data and in particular the mass spectral data supported the theoretical molecular formulae of the products.

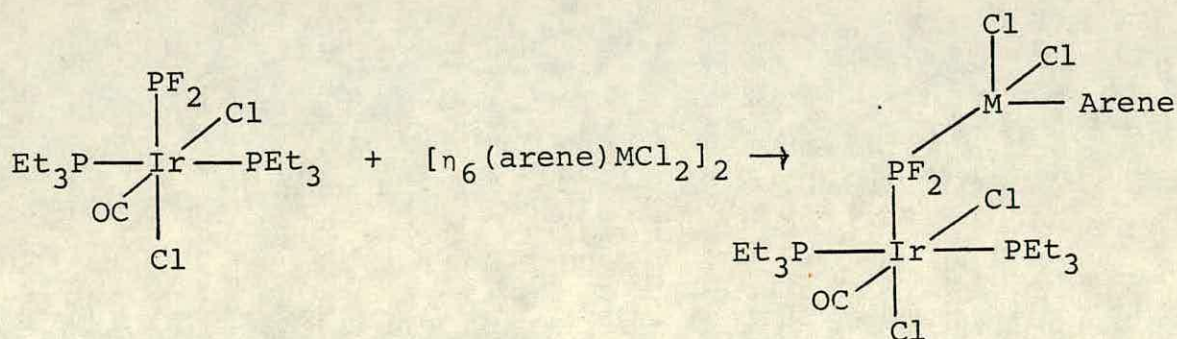


Figure 3.2.3.1 Mass spectrum of $\text{Cl}_2(\text{PEt}_3)_2(\text{CO})\text{Ir-PF}_2^-$
 OsCl_2 (p-cymene)

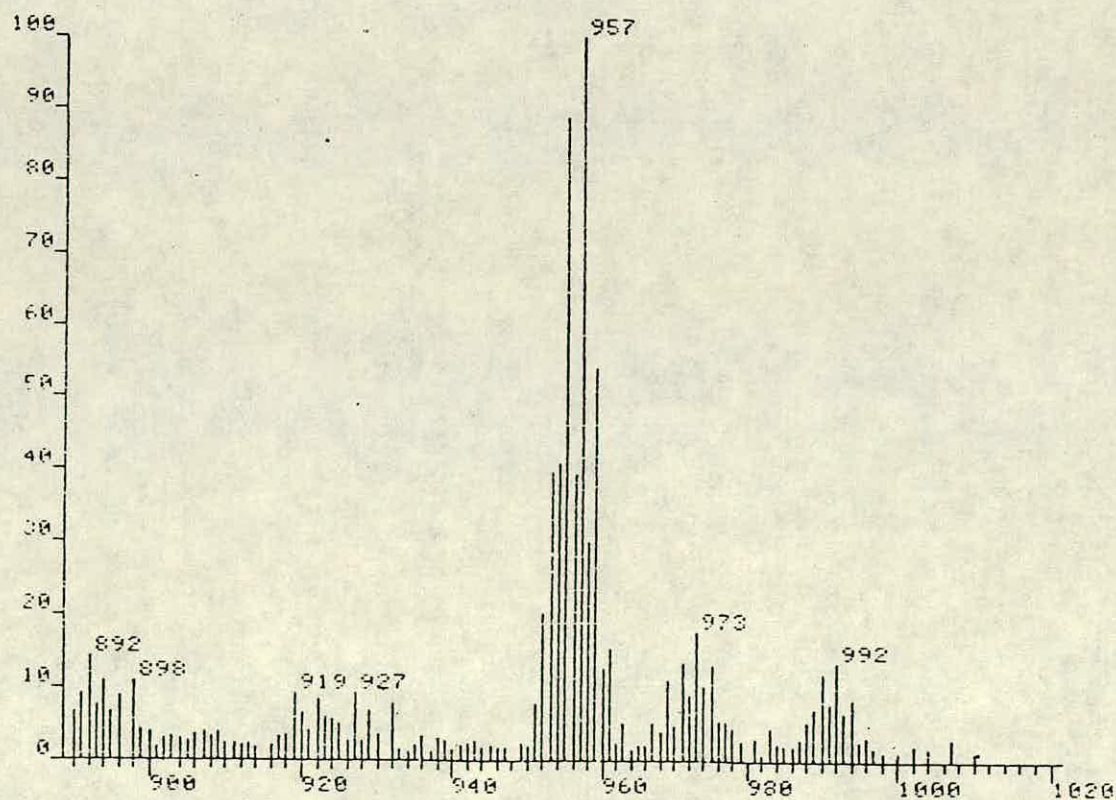
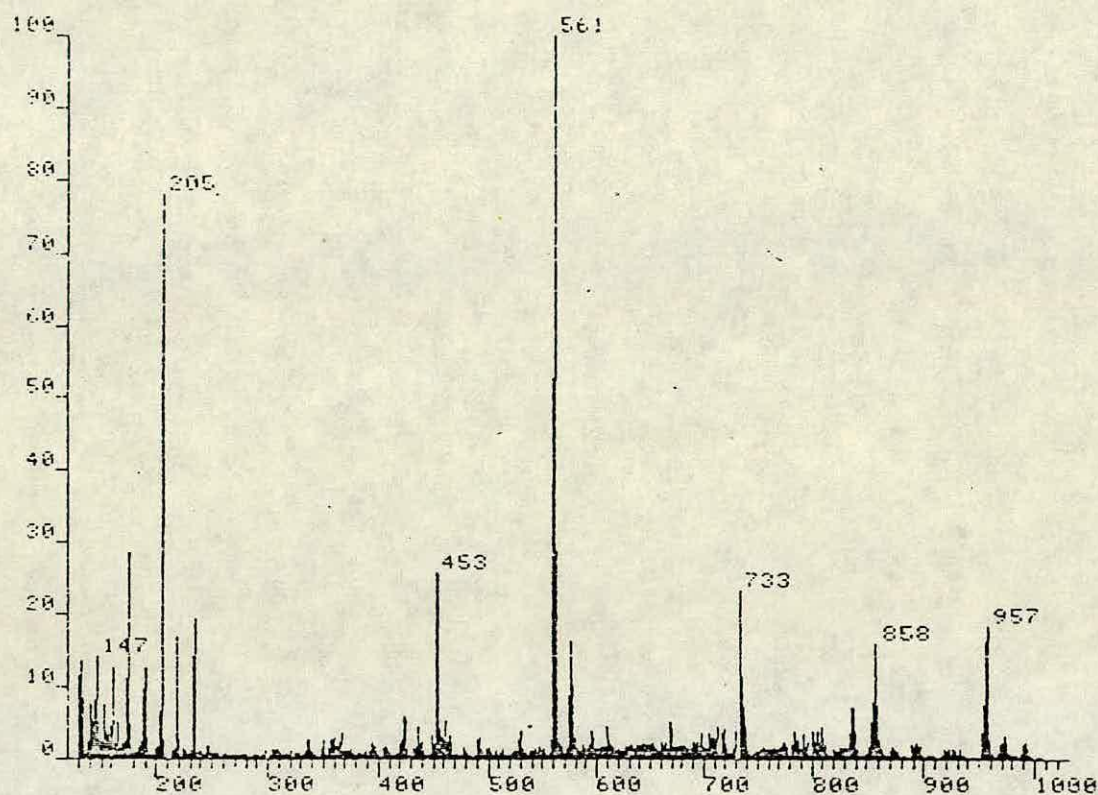
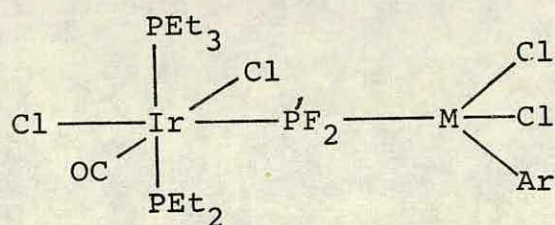


Table 3.2.3.1

N.m.r. parameters for



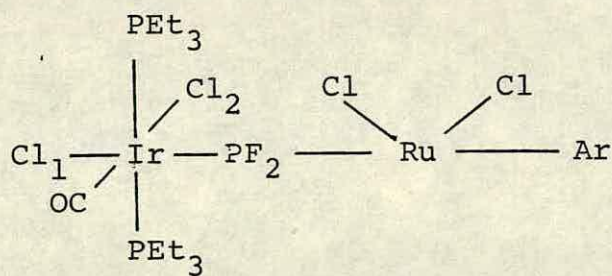
| M | Ar | $\delta P/\text{ppm}$ | $\delta P'/\text{ppm}$ | $\delta F/\text{ppm}$ | $^1J_{PF}/\text{Hz}$ | $^2J_{PP}/\text{Hz}$ | $^3J_{PF}/\text{Hz}$ |
|----|-----------------|-----------------------|------------------------|-----------------------|----------------------|----------------------|----------------------|
| Ru | benzene | -14 | 250.8 | NO | 1112 | 8 | NO |
| Ru | <u>p</u> cymene | -13.8 | 252.6 | -21.7 | 1109 | 7.6 | 7.6 |
| Os | <u>p</u> cymene | -13.9 | 192.9 | -25.1 | 1075 | 8.3 | 8.3 |

N.m.r. parameters were recorded in nitromethane at room temperature

NO: not observed

Table 3.2.3.2

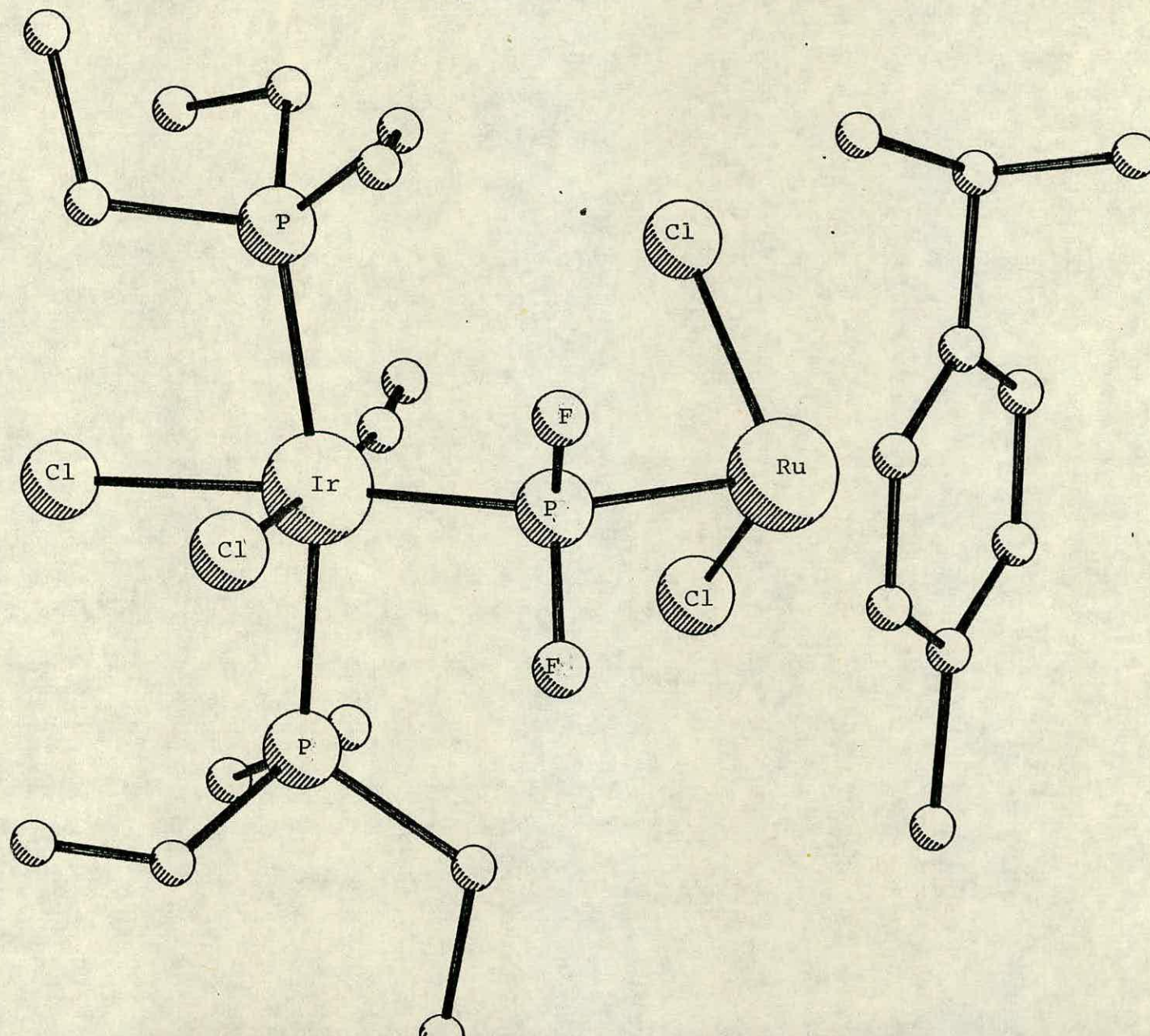
Some bond lengths for



| Bond | Bond Length/pm | Bond | Bond Length/pm |
|--------------------|----------------|-------|----------------|
| Ir-P | 242 | Ru-Cl | 240 |
| Ir-P' | 228 | Ru-P | 228 |
| Ir-Cl ₁ | 246 | | |
| Ir-Cl ₂ | 238 | | |
| Ir-C | 185 | | |
| P-F | 159 | | |

Figure 3.2.2.2

X-ray crystal structure of $\text{Cl}_2(\text{PEt}_3)_2(\text{CO})\text{Ir}-\text{PF}_2-\text{RuCl}_2-$
(p-cymene)



An X-ray crystal structure of the derivative synthesised from [p-cymene RuCl₂]₂ confirmed this proposal, (see Figure 3.2.3.2). Structural parameters for the complex are presented in Table 3.2.3.2 (unfortunately no data relating to bond angles of the complex had been obtained at the time of writing). One cannot comment on the structural parameters of this complex at this time as the structure has not been fully refined.

3.3 General Discussion of Experimental Data Relating to the Derivatives of $\text{Ir}(\text{PF}_2)(\text{CO})(\text{PEt}_3)_2\text{Cl}_2$

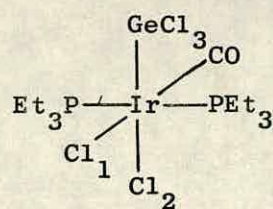
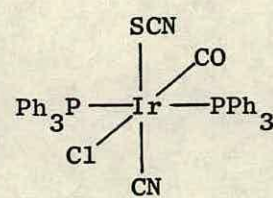
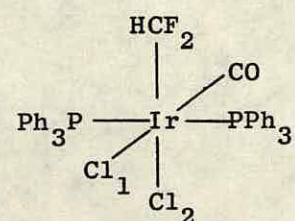
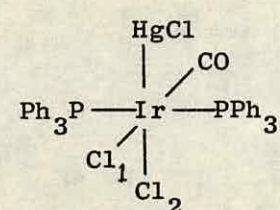
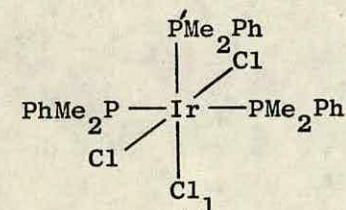
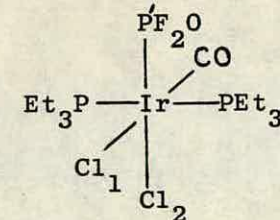
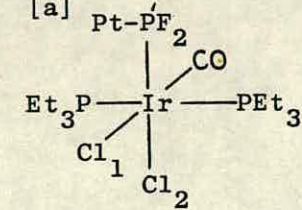
3.3.1 X-ray Crystal Structure Data

Comments concerning the structural parameters of the modified PF_2 groups have already been discussed in Sections 3.1.3 and 3.2.2. In this section we will present a brief discussion of the parameters relating more to the iridium metal centre. Table 3.3.1 presents some X-ray crystal structure data for comparison.

From Table 3.3.1, it was noted that the values of Ir-Cl bond lengths obtained in this work, for Cl trans to CO, were fairly typical of those previously reported in the literature. It has been stated that the degree of π bonding from metal to ligand dictates the trans influence of that ligand⁽¹⁴⁴⁾; a high degree of π back bonding causes a shortening of the bond of the trans ligand to metal, hence M-Cl bonds trans to CO are typically very short. Therefore by comparing the length of M-Cl bond trans to phosphorus we can gain some knowledge of the back bonding from metal to phosphorus. From these results it is clear that the ligand with the lowest trans influence is the PF_2O group. It is also clear that the trans influence of the $(\text{PF}_2\text{-Pt})$ group is comparatively high; it is probable that there is back bonding to the PF_2 group in this complex from both platinum and iridium.

The Ir-C distances of the complexes have not been discussed, even though they would be of interest, as the positions of carbon were badly defined in the structures described in this work.

Table 3.3.1 Some X-ray Crystal Structure Data of some Six-Coordinate Ir(III) Complexes

| Complex | Bond Lengths/pm | reference |
|---|---|-----------|
|  | Ir-P 240.6 Ir-Cl ₁ 235.4 Ir-Cl ₂ 245.7 | 139 |
|  | Ir-P 241.8 Ir-Cl 237 | 140 |
|  | Ir-P 242.9, 241.2 IrCl ₁ 237.5 Ir-Cl ₂ 247.5 | 141 |
|  | Ir-P 238.7, 237.8 Ir-Cl ₁ 240.1 Ir-Cl ₂ 245.3 | 142 |
|  | Ir-P 236.3 Ir-P' 227.7 Ir-Cl 236.1 Ir-Cl ₁ 242.9 | 143 |
|  | Ir-P 240.2 Ir-P' 225.2 Ir-Cl ₁ 236.9 Ir-Cl ₂ 241.6 | this work |
| [a]  | Ir-P ^[b] 243.1 Ir-P' ^[b] 229.2 Ir-Cl ₁ ^[b] 234.8 Ir-Cl ₂ ^[b] 245.8 | this work |

[a] see section 3.2.3 for complete description of complex

[b] these values are the mean of all such bond lengths in the structure

3.3.2 Nuclear Magnetic Resonance Data

It was noted that an increase in the coordination number of phosphorus of the PF_2 group resulted in a decrease in $\delta\text{P}'$ and an increase in δF (with the exception of the $\text{HPF}(\text{E})$ groups which cannot be compared with the other complexes as one fluoride has been substituted).

The lowest phosphorus chemical shifts were recorded for those complexes in which the phosphorus was in oxidation state (V), (PF_2E , $\text{HPF}(\text{E})$). The phosphorus chemical shifts of the PF_2E and $\text{HPF}(\text{E})$ groups differ little, which is a little surprising as one would expect a proton to have a different shielding effect from fluorine. The fluorine chemical shifts of the PF_2E and $\text{HPF}(\text{E})$ do differ greatly; the fluorine resonances of the $\text{HPF}(\text{E})$ groups arise at far lower frequency to those of the PF_2E group and show a far greater dependence on E; the shielding of fluorine increases with increasing size of the group VIB element. It is difficult to explain why there should be such a marked and regular variation in the case of the $\text{HPF}(\text{E})$ groups whereas the δF values of the PF_2E groups cover such a small range and if there is a trend in these values then the shielding of fluorine decreases with increasing size of E, which is also the trend observed for other $\text{X-PF}_2\text{E}$ compounds (see Table 3.1.3.2).

The values of $\delta P'$ and δF for the $(Ir)-PF_2E$ ($E = O, S$) are in agreement with those expected for XPF_2E for which it has been shown that $\delta P'$ increases and δF decreases as the electronegativity of X decreases⁽⁹²⁾.

It is difficult to make such comments concerning the other derivatives of the $Ir-PF_2$ complexes that have been produced as there are no data for comparison.

3.3.3 Infra Red Data

The main general points of note in the infra red spectra of the derivatives of the terminal PF_2 group were that ν_{CO} of the derivatives was always higher than that of the starting material as were the values of ν_{P-F} .

3.4 Conclusions and Some Suggestions for Further Work

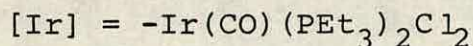
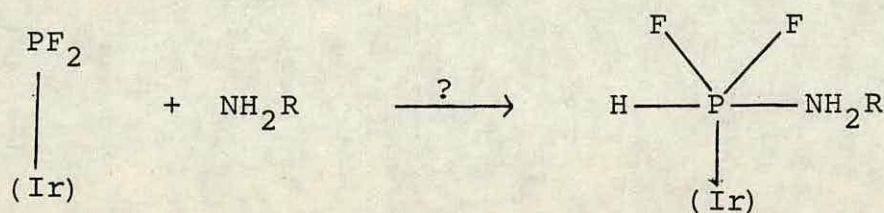
In this chapter we have presented results which proved our proposal from Chapter 2 concerning the formation of complexes containing terminal $-PF_2$ groups. The formation of borane adducts and mixed metal bridges could not be explained otherwise.

In general the reaction systems studied have shown that the phosphorus of the PF_2 group has a highly nucleophilic character. This is indicated by its reaction with the electrophilic reagents, B_2H_6 , and transition metal substrates, and the ease of oxidative addition of the Group VIB elements and the Group VIB hydrides.

There are a number of reactions that might be studied to get a more complete picture of the chemistry of the terminal-PF₂ moiety:

(i) Reactions with further electrophillic reagents such as MeI and Me₃SiI to see how general is the quaternisation of the PF₂ group.

(ii) It has been shown in Section I.1 that ammonia and primary amines oxidatively add across phosphorus of fluoro-phosphine compounds to yield five coordinate phosphorus(V) compounds; similar reactions might be possible for the terminal PF₂ groups.



R = H, alkyl

(iii) It might also be possible to expand the range of mixed-metal-PF₂ bridged compounds by reaction of the iridium-PF₂ complexes with further transition metal substrates, e.g. (THF)Cr(CO)₅, Fe₂CO₉, [Et₂NCS₂PdCl]₂, [M η₅-(pentamethylcyclopentadienyl)Cl₂]₂, [M = Ir, Rh].

CHAPTER 4

Synthesis and some Reactions of Iridium and Rhodium
Complexes Containing Terminal Dichlorophosphino Groups

4.1 Synthesis

The high reactivity of P-X bonds towards oxidative addition across $\text{IrX}(\text{CO})(\text{PEt}_3)_2$ was apparent from the results presented in Chapter 2. It was therefore considered possible that phosphorus trichloride (PCl_3) would add oxidatively a P-Cl bond across iridium in $\text{IrCl}(\text{CO})(\text{PEt}_3)_2$ with the hoped for formation of terminal- PCl_2 grouping.

The only previously reported example of a metal complex with a terminal- PCl_2 group was that synthesised by Malisch and Alsmann⁽⁷²⁾ and described in section (1.3).

The reactions of PCl_3 with both $\text{IrCl}(\text{CO})(\text{PEt}_3)_2$ and $\text{RhCl}(\text{CO})(\text{PEt}_3)_2$ were studied; both reactions were found to yield similar products. The reactions were carried out initially in n.m.r. tubes and the $^{31}\text{P}\{^1\text{H}\}$ n.m.r. spectra of the products of both reaction systems recorded at various temperatures. As well as these, the ^{13}C spectrum of the product of the reaction of PCl_3 with $\text{IrCl}(\text{CO})(\text{PEt}_3)_2$ was recorded at room temperature. The n.m.r. parameters of the products of both reactions are presented in Table 4.1.1.

In both reactions there was no sign of any reaction below 243 K. At 243 K species are produced which are temperature stable up to at least ambient temperature. The $^{31}\text{P}\{^1\text{H}\}$ n.m.r. spectra of the products of both reactions were qualitatively the same except that the signals arising from the product of the reaction with $\text{RhCl}(\text{CO})(\text{PEt}_3)_2$ were further split because the isotope of rhodium with nuclear spin $\frac{1}{2}$, ^{103}Rh , is present in 100% natural abundance. The $^{31}\text{P}\{^1\text{H}\}$ n.m.r. spectrum of the product of the reaction PCl_3 with $\text{IrCl}(\text{CO})(\text{PEt}_3)_2$ consisted of two signals: the signal to high

frequency (δP ca. 300 p.p.m.) was split into a triplet ($^2J_{P,P}$); that to low frequency, arising from the PEt_3 groups was split into a doublet with the same coupling ($^2J_{P,P}$). The $^{31}P\{^1H\}$ n.m.r. spectrum of the product from the reaction of PCl_3 with $RhCl(CO)(PEt_3)_2$ was qualitatively the same except that the two signals were split by further doublet splittings as a result of couplings to ^{103}Rh .

The $^{13}C\{^1H\}$ n.m.r. spectrum consisted of signals arising from carbon nuclei of the PEt_3 groups at low frequency and a signal at high frequency ($\delta C = 160$ p.p.m.) due to the carbon of the CO ligand which was split into a triplet ($^2J_{C-PEt_3}$) ($J_{P,-C}$ was not resolved).

The products of both reactions were isolated: the iridium complex as a white powder, the rhodium complex as a yellow-orange powder. Carbon and hydrogen analyses of the products were correct for $M(PCl_2)(CO)(PEt_3)_2Cl_2$. An infra-red spectrum of the product of the reaction with $IrCl(CO)(PEt_3)_2$ contained bands at: 2043 cm^{-1} (ν_{CO}) and 562 cm^{-1} ($? \nu_{P-Cl}$). A mass spectrum of the same complex (Fig. 4.1) gave a molecular ion peak at $m/e = 629$ which is correct for $[Ir(PCl_2)(CO)(PEt_3)_2Cl_2]^+$ = (A) (The isotopic splitting pattern of the fragment was consistent with the expected pattern). There were other fragments that could be assigned structures: m/e 593 (base peak) = (A)-Cl; m/e 558 = A-2Cl; m/e 529 \approx A- PCl_2 + H $[IrH(CO)(PEt_3)_2Cl_2]$; m/e 492 = $IrCl(CO)(PEt_3)_2$; m/e 465 $IrCl(PEt_3)_2$.

Taking the data obtained as a whole it was apparent that oxidative addition across iridium had taken place in the reaction systems. The ^{31}P n.m.r. chemical shifts of the PEt_3 groups were characteristic of M(III) complexes; ν_{CO} was also in

Figure 4.1 Mass spectrum of $\text{Ir}(\text{PCl}_2)(\text{CO})(\text{PEt}_3)_2\text{Cl}_2$

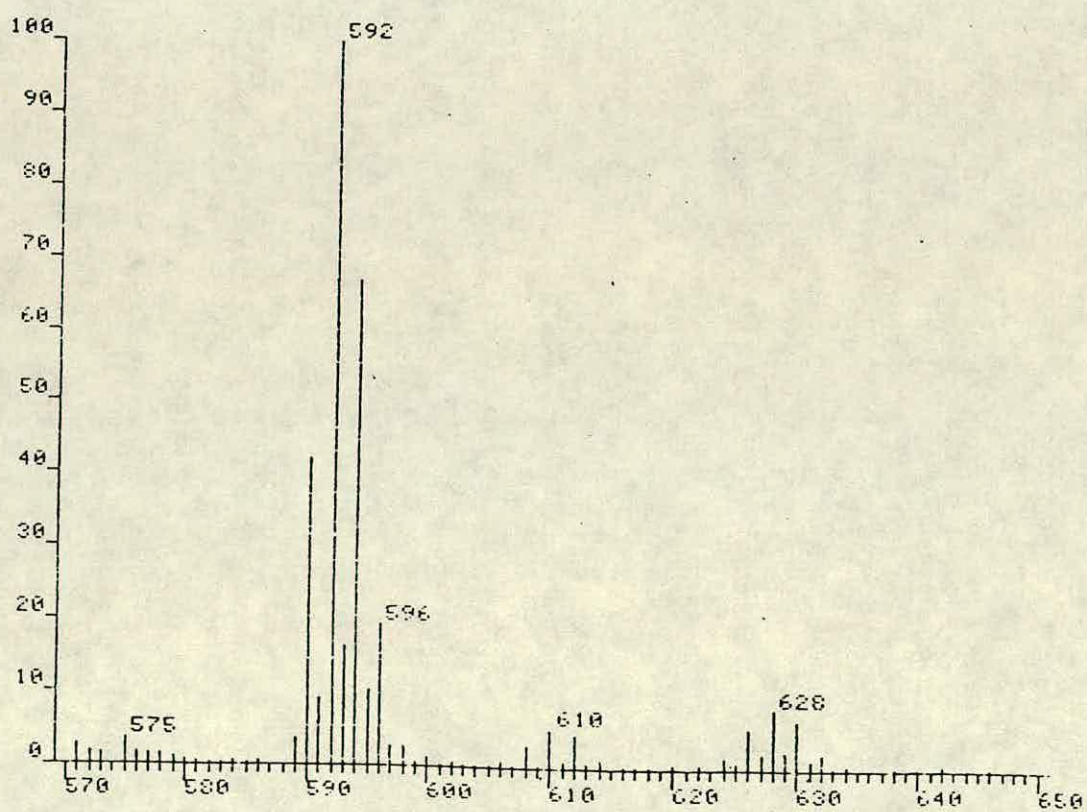
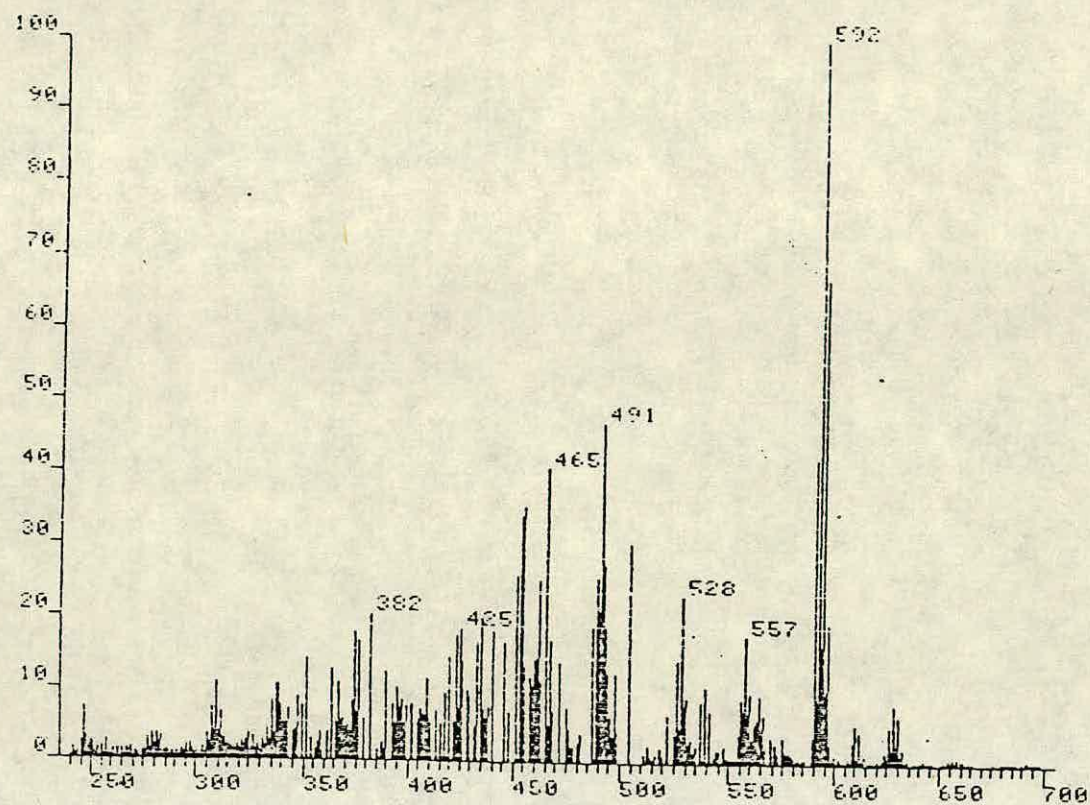
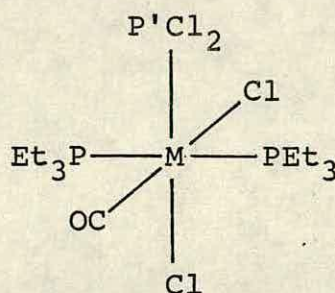


TABLE 4.1.1

N.m.r. parameters for



| M | $\delta P/p.p.m.$ | $\delta P^1/p.p.m.$ | $^1J_{PP}/Hz$ | $^1J_{P-Rh}/Hz$ | $^1J_{P'-Rh}/Hz$ |
|-------------------|-------------------|---------------------|---------------|-----------------|------------------|
| Rh | 19.2 | 339.1 | 32.1 | 79.5 | 24.2 |
| Ir ^(a) | -9.2 | 304.0 | 34 | - | - |

(a) $\delta CO = 162.7$ p.p.m.; $^1J_{C-\underline{P}Et_3} = 7$ Hz ; $^2J_{C-P'}$ NR.

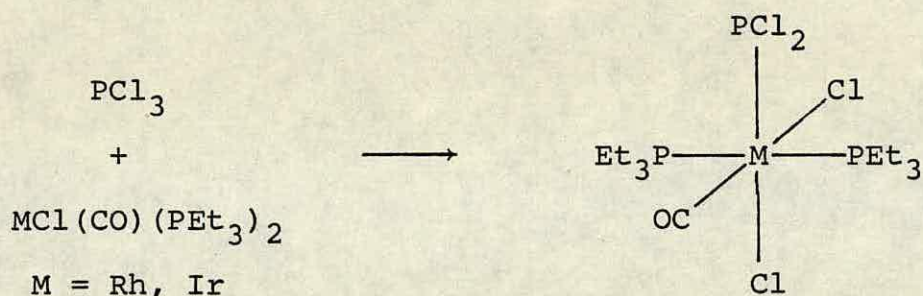
* Sample for ^{13}C n.m.r. was kindly supplied by Mr. N.J. Pilkington
Parameters were recorded in methylene chloride at room temperature
except for ^{13}C data which were recorded in benzene.

TABLE 4.1.2

N.m.r. parameters for $PCl_2-M(CO)_3Cp^{(72)}$

| M | $\delta P/p.p.m.$ |
|----|-------------------|
| Cr | 421 |
| Mo | 394 |
| W | 362 |

the spectral region typical for an Ir(III) complex;
 $^1J_{\text{PEt}_3\text{-Rh}}$ was characteristic of a Rh(III) complex^(38,39),
 (see Table 5.4). The high chemical shifts of the other
 phosphorus nuclei were of the order of those cited by Malisch
 and Alsmann for $\text{Cl}_2\text{P-M}(\text{CO})_3(\text{cp})$ ⁽⁷²⁾, (see Table 4.1.2);
 implying that the reaction systems described above had
 produced iridium and rhodium complexes with terminal- PCl_2
 groups. The lack of an observed $^2J_{\text{P-C}}$ meant that the unique
 phosphorus was cis to CO in the iridium complex, one would
 expect a trans $^2J_{\text{P-C}}$ to be an order of magnitude higher.

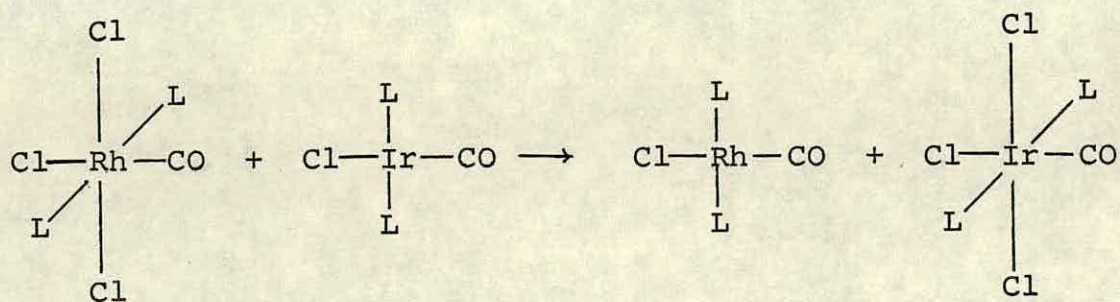


4.2 Some Reactions of $\text{M}(\text{PCl}_2)(\text{CO})(\text{PEt}_3)_2\text{Cl}_2$ [M = Rh, Ir]

The above heading is slightly misleading as very few
 reactions of the rhodium complex have been carried out
 because of lack of time.

4.2.1 The Reaction of $\text{Rh}(\text{PCl}_2)(\text{CO})(\text{PEt}_3)_2\text{Cl}_2$ with $\text{IrCl}(\text{CO})(\text{PEt}_3)_2$

It has been reported in the literature that complexes of
 the type $\text{RhCl}_3(\text{CO})\text{L}_2$ react with $\text{IrCl}(\text{CO})\text{L}_2$ [L = PMePh_2 , PEt_2Ph]
 to give $\text{RhCl}(\text{CO})\text{L}_2$ and $\text{IrCl}_3(\text{CO})\text{L}_2$.⁽¹⁴⁶⁾



The reaction described in this section was carried out to see if it would follow a similar course.

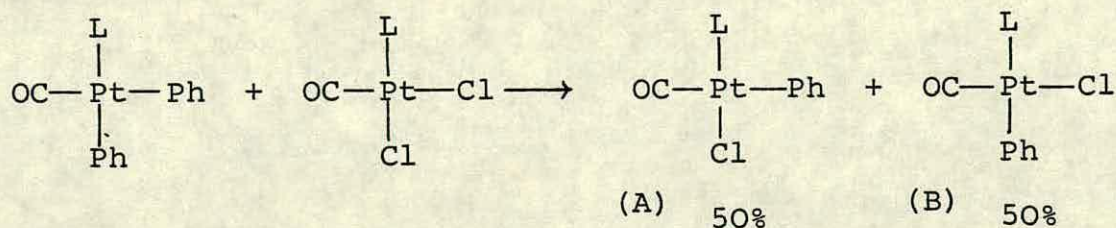
The reaction was carried out in an n.m.r. tube at room temperature and the ^{31}P n.m.r. spectrum of the reaction medium recorded.

The ^{31}P n.m.r. spectrum of the reaction system recorded immediately after warming to room temperature consisted of the signals characteristic of $\text{Ir}(\text{P}(\text{Cl})_2)(\text{CO})(\text{P}(\text{Et})_3)_2\text{Cl}_2$ (see Section 4.1) and $\text{RhCl}(\text{CO})(\text{P}(\text{Et})_3)_2$ [doublet at $\delta\text{P} = 23.7$ p.p.m.; $^1\text{J}_{\text{P-Rh}} = 116$ Hz] ⁽¹⁴⁷⁾.

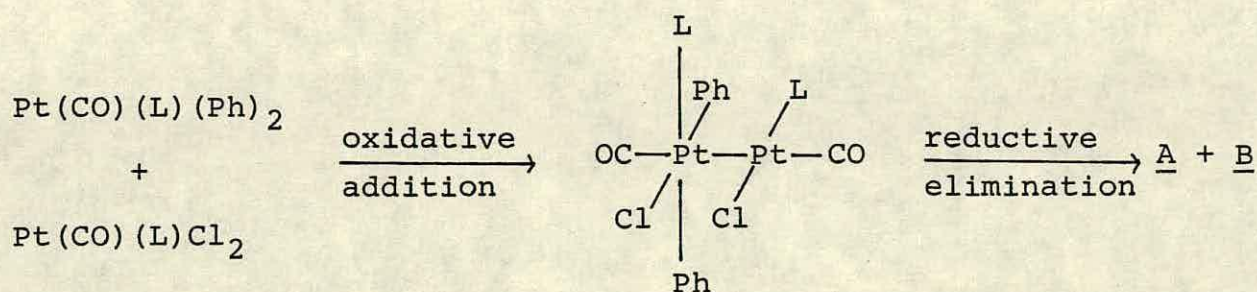
It was obvious from ^{the} n.m.r. spectrum that reaction analogous to that observed for $\text{RhCl}_3(\text{CO})(\text{P}(\text{Et})_3)_2$ had taken place.

The mechanism proposed for the previously reported oxidative addition-reductive elimination reaction was an inner-sphere double electron transfer via a dichloro-bridged species, although no evidence was put forward in the paper to support this postulate.

The possibility of a different reaction mechanism is provided by the proposed mechanism of ligand exchange for the reaction of $\text{Pt}(\text{CO})(\text{L})\text{Cl}_2$ with $\text{Pt}(\text{CO})(\text{L})(\text{Ph})_2$ ⁽¹⁴⁸⁾.

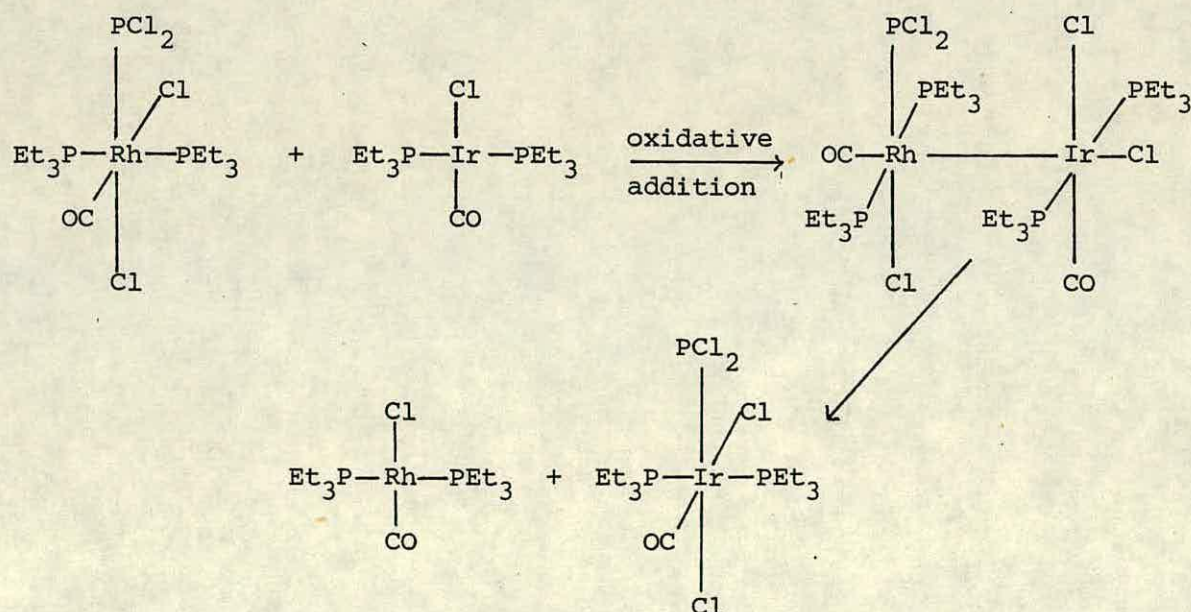


In order to explain the distribution of exchange-products Cross proposed an oxidative addition of a Pt-Cl bond across platinum of the platinum-phenyl complex which is followed by rapid reductive elimination to give the two Pt(CO)(L)(Ph)Cl isomers.



There was no concrete evidence for the intermediate species but this proposed mechanism best explained the experimental results.

If the above proposals are correct then a similar mechanism could be involved in the reaction described here: with initial oxidative addition of a Rh-Cl across iridium and subsequent reductive elimination of the six-coordinate iridium-PCl₂ complex:



The other possibility is that there is dissociation of PCl₃ from the rhodium followed by a rapid oxidative addition of PCl₃ to the iridium complex.

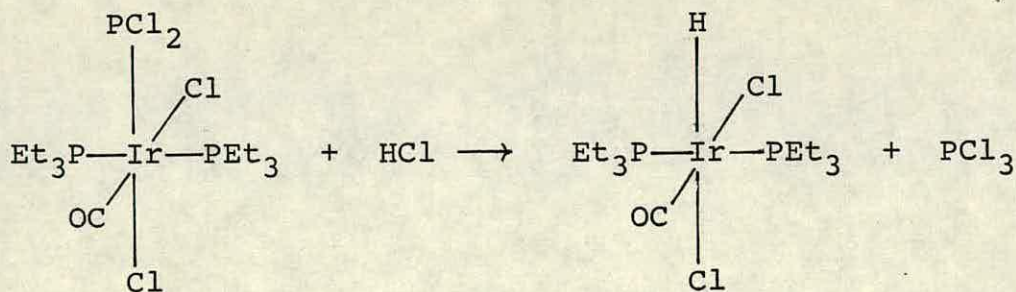
None of the data collected for this reaction system shed any light on the possible mechanism of reaction. It might, however, have been possible to observe reaction intermediates if the system had been studied to low temperatures and these may have provided an indication of the reaction mechanism.

4.2.2 ^{of} The Reaction of HCl with $\text{Ir}(\text{PCl}_2)(\text{CO})(\text{PEt}_3)_2\text{Cl}_2$

This reaction was carried out to see if it would be similar to that of HCl with $\text{Ir}(\text{PF}_2)(\text{CO})(\text{PEt}_3)_2\text{Cl}_2$.

The reaction was studied in an n.m.r. tube and the ^{31}P n.m.r. spectra recorded at various temperatures.

In the ^{31}P n.m.r. spectra of the reaction system no signs of any products of reaction could be detected in the temperature range 193 K to 253 K. At 263 K, signals characteristic of PCl_3 (singlet at $\delta\text{P} = 218$ p.p.m.) and $\text{IrH}(\text{CO})(\text{PEt}_3)_2\text{Cl}_2$ (see Section 3.3) (singlet at $\delta\text{P} = -2.1$ p.p.m.) were detected. At ambient temperature complete conversion of $\text{Ir}(\text{PCl}_2)(\text{CO})(\text{PEt}_3)_2\text{Cl}_2$ to PCl_3 and $\text{IrH}(\text{CO})(\text{PEt}_3)_2\text{Cl}_2$ was observed



4.2.3 The Reactions of Group VIB Elements with $\text{Ir}(\text{PCl}_2)(\text{CO})(\text{PEt}_3)_2\text{Cl}_2$

The object of these reactions was the oxidation of the PCl_2 group to give the corresponding dichlorophosphonate, dichlorothiophosphonate and dichloroselenophosphonate iridium complexes.

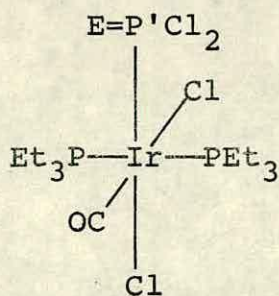
It has already been mentioned that Malisch and Alsmann were able to produce dichloro-thio and selenophosphonate complexes by elemental oxidation of the tungsten and chromium dichlorophosphane compounds⁽⁷²⁾.

The reactions were carried out in the same manner as the equivalent reactions of the Ir-PF_2 complexes; however, because the reactions were carried out towards the end of this research project, full characterisations of the products were not obtained, the only results obtained were ^{31}P n.m.r. data which are presented in Table 4.2.1.

The $^{31}\text{P}\{^1\text{H}\}$ n.m.r. spectra of all three products were qualitatively the same as those of the starting material. The phosphorus chemical shifts of what was the PCl_2 phosphorus were at very low frequency, in the region one would associate with a phosphorus (V) species; the magnitude of the difference in chemical shifts for this resonance in the starting material and product complexes were of the same order as those observed by Malisch and Alsmann⁽⁷²⁾ cf Tables 4.1.2 and 4.2.2.2 [$\Delta\delta\text{P} = \delta\text{P}'$ starting material - $\delta\text{P}'$ product ≈ 250 p.p.m.] in going from $[\text{M}]-\text{PCl}_2$ to $[\text{M}]-\text{PCl}_2\text{E}$ [$\text{M} = \text{M}'(\text{CO})_3\text{Cp}$; $\text{M}' = \text{Cr}, \text{W}$; $\text{E} = \text{S}, \text{Se}$]. Associated with this resonance for the product of reaction with Se were selenium satellites ($J_{\text{P-Se}} = 774 \text{ Hz}$).

TABLE 4.2.3.1

N.m.r. parameters for



| E | $\delta P/\text{p.p.m.}$ | $\delta P'/\text{p.p.m.}$ | $^2J_{PP'}/\text{Hz}$ | $^1J_{P'-Se}/\text{Hz}$ |
|----|--------------------------|---------------------------|-----------------------|-------------------------|
| O | -2.5 | 36.5 | 21.7 | - |
| S | -10.7 | 44.2 | 13.7 | - |
| Se | -11.6 | 19.2 | 12.4 | 774.1 |

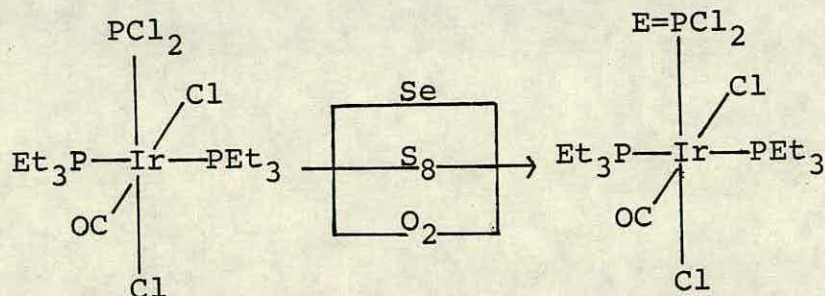
Parameters were recorded in chloroform at room temperature.

TABLE 4.2.3.2

N.m.r. parameters for $\text{EPCl}_2 - \text{M}(\text{CO})_3\text{Cp}^{(72)}$

| E | M | $\delta P/\text{p.p.m.}$ |
|----|----|--------------------------|
| S | Cr | 196 |
| S | W | 89 |
| Se | W | 62 |

The small amount of data obtained on these products implied that oxidation of phosphorus by the group (VIB) elements had taken place in the reactions. Observation of J_{P-Se} gave good support to this postulate for the reaction with Se and by inference the products of reactions with O_2 and S_8 would be similar



4.2.4 The Reactions of $\text{Ir}(\text{PCl}_2)(\text{CO})(\text{PEt}_3)_2\text{Cl}_2$ with H_2E ($\text{E} = \text{O}, \text{S}, \text{Se}$)

The three reactions described in this section proved to be in some ways very different from one another and so will be described separately.

4.2.4.1 The Reaction of $\text{Ir}(\text{PCl}_2)(\text{CO})(\text{PEt}_3)_2\text{Cl}_2$ with H_2Se

This reaction was carried out in a n.m.r. tube and the ^{31}P , ^1H and $^{77}\text{Se}\{^1\text{H}\}$ n.m.r. spectra of the products recorded. The molar ratio of H_2Se to $\text{Ir}(\text{PCl}_2)(\text{CO})(\text{PEt}_3)_2\text{Cl}_2$ used was 2:1.

The reaction system was observed to produce three different products, sequentially. Reaction occurred at room temperature. On standing for ca. 15 mins complex (a) was produced; after ca. 2 hrs complexes (b) and (c) were produced; after 12 hrs, complete conversion to complex (c) was attained.

To preserve complexes (a) and (b) whilst recording their n.m.r. spectra, the reaction systems were cooled to 223 K. N.m.r. data for the products are presented in Table 4.2.3.1.

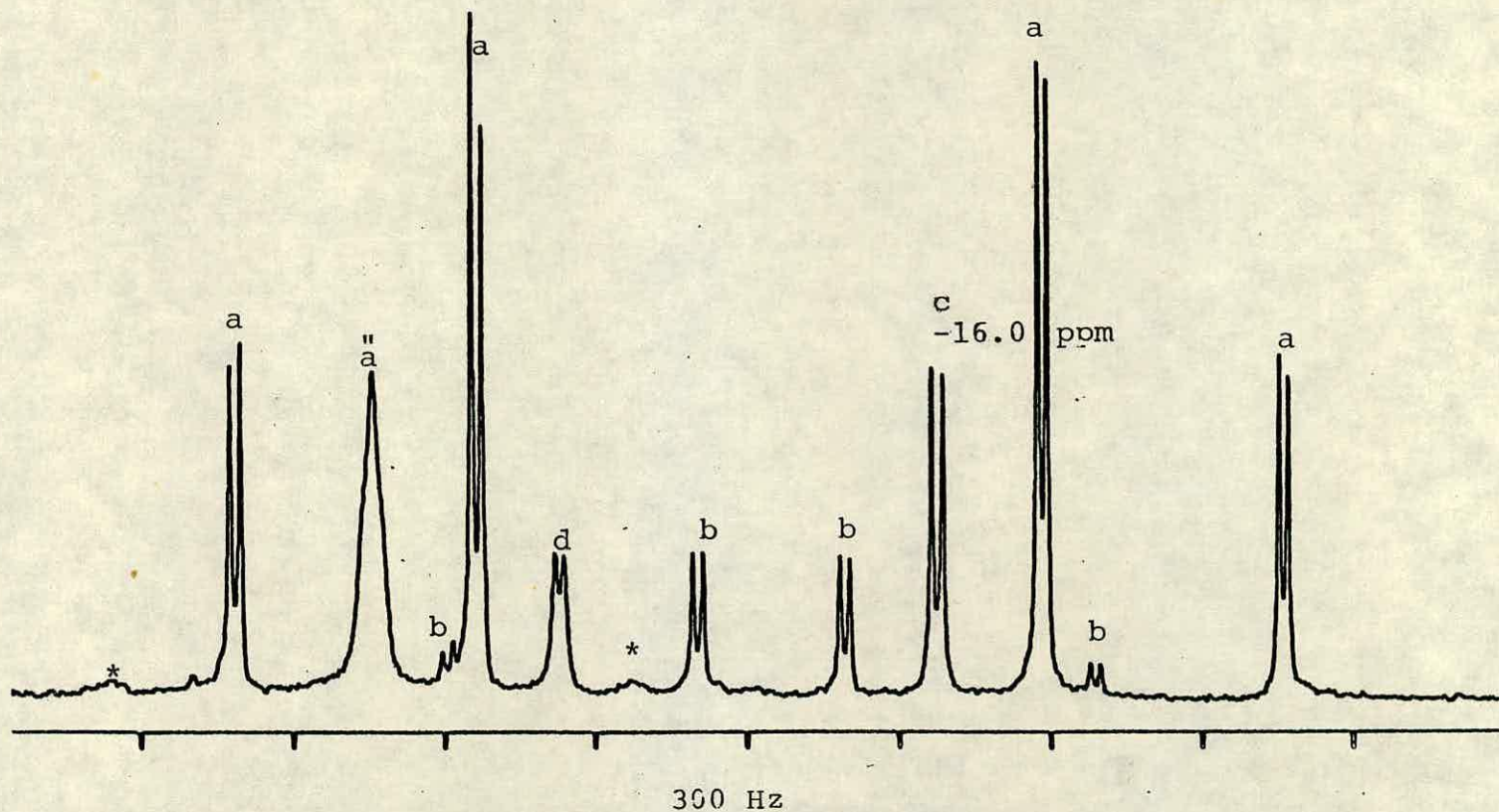
The $^{31}\text{P}\{^1\text{H}\}$ n.m.r. spectrum of complex (a) consisted of two signals, each in the same spectral region. The signal associated with the PET_3 phosphorus nuclei was split into an ABX pattern. The other signal was split by a further wide doublet coupling on removal of ^1H decoupling (J_{PH} ca. 480 Hz). Also associated with the signal were selenium satellites [see Fig. 4.2.4.1 which shows the $^{31}\text{P}\{^1\text{H}\}$ n.m.r. spectrum of the reaction system with both signals for complex (a), and the signals for the PET_3 phosphorus nuclei of complexes (b) and (c)]. The triplet coupling of signal a is not resolved in the spectrum shown which was recorded on the 360 MHz spectrometer but is resolved in the spectrum recorded on the 60 MHz instrument.

The ^1H n.m.r. spectrum of this species consisted of signals arising from the ethyl protons of the PET_3 groups and a signal at high frequency ($\delta\text{H} = 7.4$ p.p.m.) split into a doublet ($^1J_{\text{P},\text{H}}$) of doublets ($^3J_{\text{PH}}$) (presumably one of the $^3J_{\text{PH}}$ couplings is not resolved).

The $^{77}\text{Se}\{^1\text{H}\}$ n.m.r. spectrum consisted of one signal at high frequency split into a doublet.

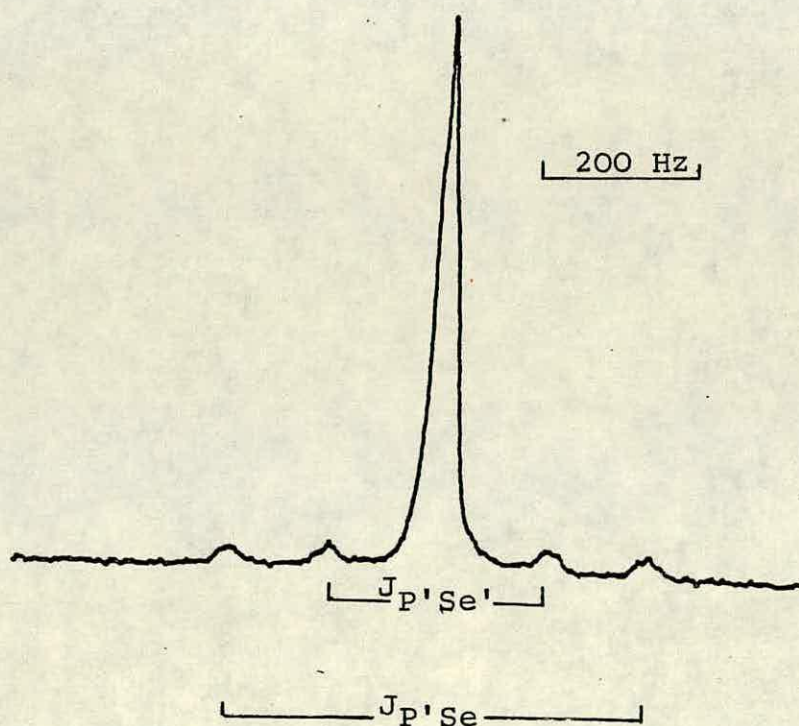
It could be ascertained from the n.m.r. spectra that complex (a) contained the (P)-Ir(PET_3)₂ unit and that directly bound to the unique phosphorus were a proton and one selenium atom.

Figure 4.2.2.1 $^{31}\text{P}\{-^1\text{H}\}$ n.m.r. spectrum of the reaction of H_2Se with $\text{Ir}(\text{PCl}_2)(\text{CO})(\text{PEt}_3)_2\text{Cl}_2$ showing: (a) the PEt_3 resonances of $(\text{Ir})-(\text{HPCl}(\text{Se}))$, (a'') the signal arising from the $(\text{HPCl}(\text{Se}))$ group, (b) the PEt_3 resonances of $(\text{Ir})-\text{HPSe}(\text{SeH})$, (c) the PEt_3 resonance of $(\text{Ir})-(\text{PH}_2\text{Se})$, (d) the PEt_3 resonance of $(\text{Ir})-(\text{PCl}_2)$
 * are the ^{77}Se satellites of (a''). $[(\text{Ir}) = -\text{Ir}(\text{CO})(\text{PEt}_3)_2\text{Cl}_2]$



The n.m.r. spectra of complex (b) were qualitatively the same as those of complex (a) except that the signal arising from the unique phosphorus nucleus which was at very low frequency (δP ca. -60 p.p.m.) had associated with it two sets of selenium satellites ($J_{P-Se} = 596$ and 317 Hz). (see Fig. 4.2.2.2).

Figure 4.2.2.2 $^{31}P\{^1H\}$ n.m.r. spectrum of $Ir(HP'Se(Se'H))(CO)(PEt_3)_2$ showing the $HP'Se(Se'H)$ resonance.



It was curious that in the ^{77}Se n.m.r. spectrum only one signal was detected for this species, for which $J_{\text{P-Se}}$ was the same as the wider J_{PSe} in the ^{31}P spectrum; no reason for the absence of one signal was found.

From the n.m.r. spectra of complex (b) it was apparent that the complex contained the $(\text{P})\text{-Ir}(\text{PEt}_3)_2$ unit but that further reaction had occurred at the unique phosphorus atom to give a species with a proton and two different selenium atoms bound to phosphorus. It was apparent that the two selenium atoms were different as the PEt_3 resonance was split by an ABX splitting pattern which meant that the unique phosphorus was chiral and that two J_{PSe} couplings were apparent in the ^{31}P n.m.r. spectrum.

The ^1H n.m.r. of complex (c) consisted of a doublet of triplets, besides signals arising from the PEt_3 groups.

The ^{31}P n.m.r. spectrum differed to some extent from those of (a) and (b). The signal arising from the PEt_3 phosphorus nuclei was split into a doublet ($^2J_{\text{PP}}$). The signal arising from the unique phosphorus nucleus was at very low frequency and was very broad; associated with the signal was one set of selenium satellites. The main signal did resolve into a triplet on line narrowing the spectrum. This resonance was split by a further wide triplet coupling when ^1H coupling was retained (J_{PH} ca. 400 Hz).

It was clear from the n.m.r. data that this species also contained the $(\text{P})\text{-Ir}(\text{PEt}_3)_2$ unit but further reaction had occurred at the unique phosphorus atom to produce a species in which two protons and one selenium atom were bound to phosphorus.

Complex (c) was isolated and C and H analyses were obtained that were consistent with the formulation $\text{Ir}(\text{PH}_2\text{Se})(\text{CO})(\text{PEt}_3)_2\text{Cl}_2$ (see experimental). The i.r. spectrum of this species was recorded, assignable bands were detected at: $2340\text{--}2280\text{ cm}^{-1}$ ($\nu_{\text{P-H}}$); 2043 cm^{-1} (ν_{CO}); 480 cm^{-1} ($\nu_{\text{P-Se}}$).

From the data obtained relating to this reaction system we can follow the reaction pathway. It was apparent that species (c) contained a $\text{-PH}_2\text{Se}$ group. The n.m.r. spectra for complex (b) showed that a proton and two different selenium atoms were directly bound to the unique phosphorus; from the magnitudes of the observed $J_{\text{P-Se}}$ it was apparent that one selenium was doubly bonded to phosphorus ($J_{\text{P}'\text{Se}} = 596\text{ Hz}$)⁽¹⁰⁶⁾ and the other was singly bonded to phosphorus ($J_{\text{P}'-\text{Se}'} = 317\text{ Hz}$)⁽¹⁰⁷⁾; the only possible grouping that could fit the data was -HPSe(SeH) , although there was no evidence for a proton directly bound to selenium; the phosphorus was not split by a further doublet coupling due to this proton and no signal in the ^1H n.m.r. spectrum could be definitely assigned to this proton. The assumption to be drawn from these observations was that the proton was exchanging rapidly (in the n.m.r. time scale) onto and off selenium, though the exchange would have to preserve the distinction between the two selenium nuclei, in the n.m.r. time scale. The data obtained from complex (a) were similar to those of complex (b); as in (b) it was noted from the ABX spin system of the PEt_3 resonance that the unique phosphorus was chiral; the observed J_{PSe} was well within the range associated with phosphorus-selenium double bonds⁽¹⁰⁶⁾ and so it was apparent that only one selenium atom was directly bound to the unique phosphorus, (with the other known group attached

to phosphorus being a proton) it meant that (a) contained the grouping - HPX(Se). Although we have no direct evidence for X, it must be Cl.

The overall reaction scheme is shown below in Figure 4.2.4.3.

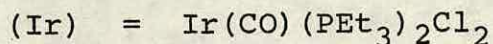
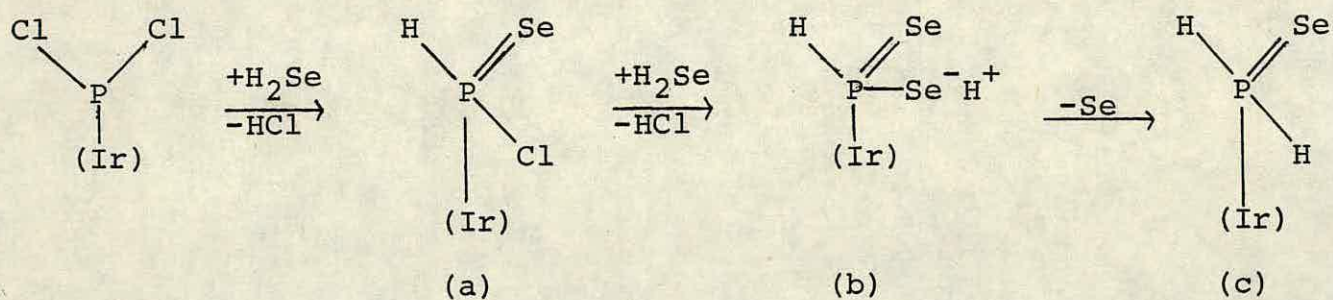
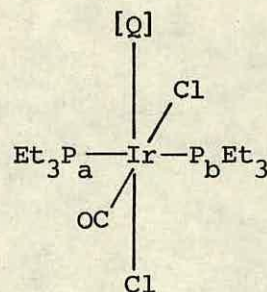


Fig. 4.2.4.3 Reaction of H_2Se with $\text{Ir}(\text{PCl}_2)(\text{CO})(\text{PEt}_3)_2\text{Cl}_2$

The loss of selenium in the final stage of the reaction is supported by the observation that a copious red precipitate drops out of solution during reaction.

TABLE 4.2.4.1

N.m.r. parameters for



| complex | [Q] | δP_a /p.p.m. | δP_b /p.p.m. | $\delta P'$ /p.p.m. | δH /p.p.m. | $^1J_{P'H}$ /Hz | $^2J_{P'P}$ /Hz | $^3J_{P_aH}$ /Hz* |
|---------|------------------------------------|----------------------|----------------------|---------------------|--------------------|-----------------|-----------------|-------------------|
| (a) | HPCl(Se) ^[a] | -9.1 | -16.1 | -9.1 | 7.4 | 482 | 13 | 9.8 |
| (b) | HP'Se(Se'H) ^[b] | -11.1 | -14.1 | -60.1 | 7.4 | 437 | 14 | 11.6 |
| (c) | P'H ₂ Se ^[c] | -14.2 | | -105 | 4.2 | 405 | 14 | 6.4 |

[a] $^2J_{P_aP_b} = 318.7$ Hz; $\delta Se = 245$ p.p.m.; $^1J_{P-Se} = 687$ Hz. Parameters recorded in toluene at 223 K.

[b] $^2J_{P_aP_b} = 329$ Hz; $\delta Se = 32.2$ p.p.m. $\delta Se'$ not observed; $^1J_{P'-Se} = 596$ Hz; $^1J_{P'-Se'} = 317$ Hz.

Parameters recorded in toluene at 223 K.

[c] δSe not observed; $^1J_{P'-Se} = 534$ Hz. Parameters recorded in toluene at room temperature.

* This is an arbitrary designation for the only $^3J_{PH}$ resolved in the 1H n.m.r. spectrum and the label P_a' only applies to complexes (a) and (b).

4.2.4.2 The Reaction of $\text{Ir}(\text{PCl}_2)(\text{CO})(\text{PET}_3)_2\text{Cl}_2$ with H_2S

The reaction of H_2S with $\text{Ir}(\text{PCl}_2)(\text{CO})(\text{PET}_3)_2\text{Cl}_2$ was carried out in an n.m.r. tube; the molar ratio of H_2S to $\text{Ir}(\text{PCl}_2)(\text{CO})(\text{PET}_3)_2\text{Cl}_2$ used was 2:1. The ^{31}P n.m.r. spectra recorded at room temperature after ca. 1 hr. showed little trace of any product and so the reaction medium was maintained at ca. 323 K for 12 hrs; after this period the reaction had gone to completion, with respect to iridium starting material, yielding a single product. The n.m.r. parameters of this species are presented in Table 4.2.4.2.

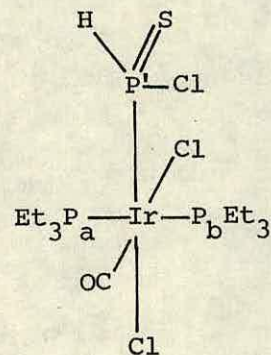
The ^{31}P and ^1H n.m.r. spectra of this species were qualitatively the same as those of complexes (a) and (b) described in the previous section.

The product was isolated. The C and H analysis figures obtained (see experimental) were consistent with the required values for $(\text{Ir})-(\text{H-PCl}(\text{S}))$ or $(\text{Ir})-(\text{HPS}(\text{SH}))$ [$(\text{Ir}) = \text{Ir}(\text{CO})(\text{PET}_3)_2\text{Cl}_2$] and so S and Cl analyses were obtained and these were more consistent with the former of the two possible complexes. The i.r. spectrum of the complex was recorded and assignable bands were detected at: 2300 cm^{-1} ($\nu_{\text{P-H}}$); 2045 cm^{-1} (ν_{CO}); 640 cm^{-1} ($\nu_{\text{P-S}}$) (there may have been another band assignable to $\nu_{\text{P-S}}$ at 760 cm^{-1} but as there were other skeletal bands for the complex in this region a definite assignment could not be made).

From the data obtained a probable assignment of the structure of the complex could be made. The splitting patterns of the n.m.r. spectra implied that the complex contained the $\text{Ir}(\text{PET}_3)_2-(\text{PH})$ unit. The ABX spin system implied that the unique phosphorus was chiral; one of the substituents bound

TABLE 4.2.4.2

N.m.r. parameters for

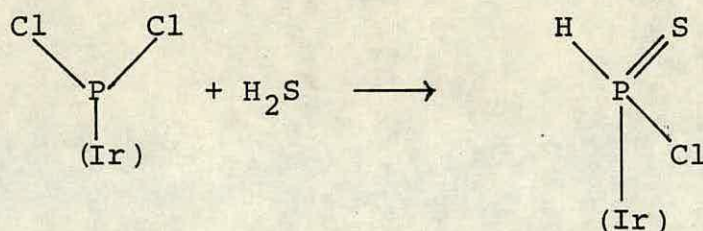


| δP_a /p.p.m. | δP_b /p.p.m. | $\delta P'$ /p.p.m. | δH /p.p.m. | $^1J_{P'H}$ /Hz | $^2J_{P_aP_b}$ /Hz | $^2J_{P'P}$ /Hz | $^3J_{P_aH}$ /Hz | $^3J_{P_bH}$ /Hz |
|----------------------|----------------------|---------------------|--------------------|-----------------|--------------------|-----------------|------------------|------------------|
| -11.2 | -15.4 | 19.4 | 8.0 | 4.89 | 327.0 | 13.7 | 4 | 9 |

Parameters were recorded in toluene at room temperature.

to phosphorus was identified as probably sulphur, from the presence of the band in the i.r. spectrum assigned as $\nu_{\text{P-S}}$; the position of this band implied that phosphorus was doubly bonded to sulphur. The analytical data implied that the other substituent on phosphorus was chlorine. The species formed is analogous to the complex formed on reaction of H_2S with the $(\text{Ir})\text{-PF}_2$ complex and complex (a) in the reaction of H_2Se with $(\text{Ir})\text{-PCl}_2$.

No further reaction was observed if the period of reaction was extended and so the complete reaction is:



4.2.4.3 The Reaction of $\text{Ir}(\text{PCl}_2)(\text{CO})(\text{PEt}_3)_2\text{Cl}_2$ with H_2O

The reaction of H_2O with $\text{Ir}(\text{PCl}_2)(\text{CO})(\text{PEt}_3)_2\text{Cl}_2$ was initially carried out in an n.m.r. tube at room temperature. The stoichiometry of the reaction was unknown, as the amount of water used was not measured. The reaction reached completion with respect to iridium starting material after ca. 4 hrs, yielding a single product.

The $^{31}\text{P}\{^1\text{H}\}$ n.m.r. spectrum consisted of two signals. The signal to high frequency (δP ca. 40 p.p.m.) was split into a triplet ($^2J_{\text{PP}}$); the signal was split by a further wide doublet coupling (J_{PH} ca. 500 Hz) on retaining ^1H coupling. The signal to low frequency was split into a doublet ($^2J_{\text{PP}}$).

The ^1H n.m.r. spectrum consisted of signals arising from the ethyl protons and a resonance at high frequency (δH ca. 8 p.p.m.) split into a doublet ($^1\text{J}_{\text{PH}}$) of triplets ($^3\text{J}_{\text{PH}}$).

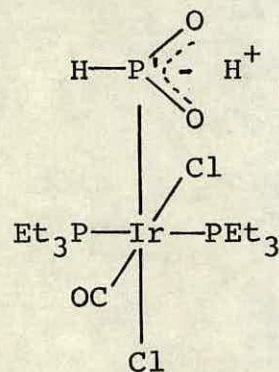
These observations implied that a phosphorus (V) species with hydrogen directly bound to phosphorus had been formed.

The product was isolated as a crystalline white solid. The C and H analysis figures (see experimental) were not consistent with either $(\text{Ir})-\text{HPO}(\text{OH})$ or $(\text{Ir})-\text{HPCl}(\text{O})$ they were, however, consistent with $(\text{Ir})-\text{HPO}(\text{OH})(\text{H}_3\text{O}^+\text{Cl}^-)$. The i.r. spectrum had assignable bands at: 2298 cm^{-1} ($\nu_{\text{P-H}}$); 2045 cm^{-1} (ν_{CO}) no bands in the spectrum could be definitely assigned to $\nu_{\text{P-O}}$. Crystals suitable for an X-ray structural analysis were obtained. Data were collected for a crystal but it was found that the data did not relate to any of the common crystallographic space groups and so the X-ray crystal structure for the complex was not obtained.

From the other data obtained for the complex its likely structure was determined. The fact that the n.m.r. spectra of the complex were completely first order implied that the reaction at the PCl_2 group had not produced a chiral phosphorus centre so the possibility of a $-\text{HPCl}(\text{O})$ group could be eliminated. The chemical shift of the phosphorus at which reaction had occurred was in the range associated with P(V) species which implied a P=O in the grouping and since we require the group to have a plane of symmetry the other group bound phosphorus must be OH. The resultant group is therefore a metal bound hypophosphite $[\text{HPO}_2\text{H}]$. Such species are known and the n.m.r. data obtained in this work is in good agreement with those of $\text{PtCl}(\text{HP}'\text{O}_2\text{H})(\text{PEt}_3)_2$

TABLE 4.2.3.3

N.m.r. parameters for [a]

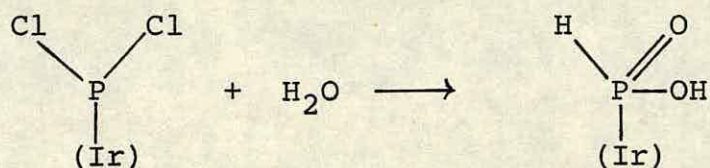


| $\delta P/\text{p.p.m.}$ | $\delta P'/\text{p.p.m.}$ | $\delta H/\text{p.p.m.}$ | $^1J_{P'H}/\text{Hz}$ | $^2J_{PP'}/\text{Hz}$ | $^3J_{PH}/\text{Hz}$ |
|--------------------------|---------------------------|--------------------------|-----------------------|-----------------------|----------------------|
| -9.0 | 39.2 | 8.1 | 503 | 15 | 2.6 |

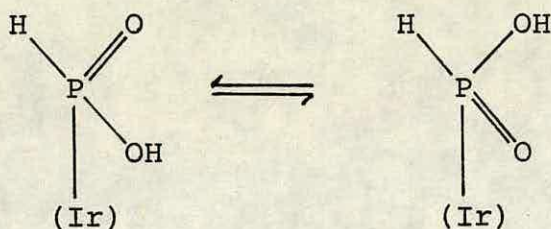
[a] These are the n.m.r. parameters for the isolated complex. The n.m.r. parameters of complex in the presence of H₂O were slightly different.

The parameters were recorded in methylene chloride at room temperature.

[$\delta P' = 51.5$ p.p.m.; $^1J_{PH} = 461$ Hz] which has been synthesised by reaction of hypophosphorus acid and $HPtCl(PEt_3)_2$ ⁽¹⁴⁹⁾.



The fact that the n.m.r. signals of the complex have first order splitting patterns implies that the hypophosphite group is in equilibrium between two tautomers whilst in solution



It is also worthy of note that the n.m.r. parameters associated with the above complex are very similar to those of the complex containing the $HPF(O)$ group (see Table 3.1.5) which is isoelectronic with the hypophosphite group.

4.2.3.4 Summary

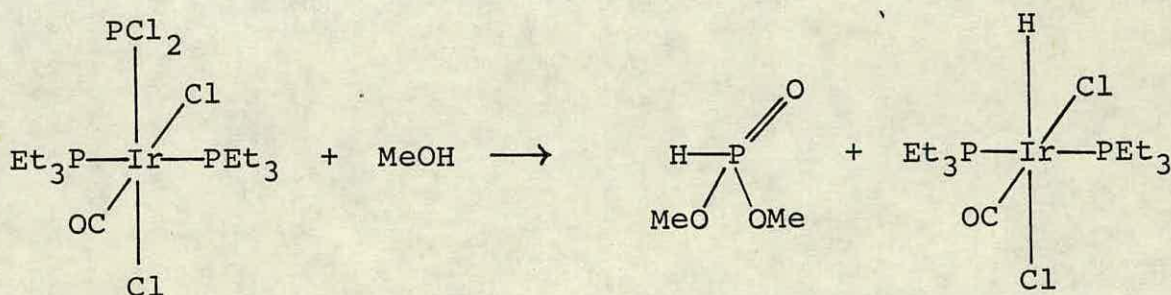
The reactions of H_2E with the terminal PCl_2 group are similar to those with the terminal PF_2 complex in that both yield hypophosphite derivatives. The major differences concern the reactions of H_2O and H_2Se in their reactions with terminal- PF_2 and $-PCl_2$ groups. In the latter case two chlorides are displaced by group VIB substituents whereas in the former only one fluoride substituent was replaced; presumably this is partly due to the weaker P-Cl bond, when compared with the P-F, being easier to break.

4.2.5 The Reaction of Methanol with $\text{Ir}(\text{PCl}_2)_2(\text{CO})(\text{PEt}_3)_2\text{Cl}_2$

It was hoped that in this reaction methoxide would replace the chlorides bound to phosphorus of the $-\text{PCl}_2$ group to form a terminal- $\text{P}(\text{OMe})_2$ group.

The reaction was studied in a n.m.r. tube with ^{31}P spectra being recorded at room temperature.

After ca. 15 mins at room temperature two signals were detected in the ^{31}P n.m.r. spectrum. The first signal was characteristic of dimethylphosphite $\text{HP}(\text{OMe})_2(\text{O})$ (a singlet at $\delta\text{P} = 10.5$ p.p.m. which split into a doublet ($^1\text{J}_{\text{PH}} = 709$ Hz) of septets ($^3\text{J}_{\text{PH}} = 12$ Hz) when ^1H coupling was retained). The second signal was characteristic of $\text{IrH}(\text{CO})(\text{PEt}_3)_2\text{Cl}_2$ (see 3.2.2). It was, therefore, apparent that cleavage of the metal-phosphorus bond and methanolysis of the unique phosphorus had taken place.



4.2.6 The Reaction of Dichlorine with $\text{Ir}(\text{PCl}_3)(\text{CO})(\text{PEt}_3)_2\text{Cl}_2$

This reaction was carried out in the hope that Cl_2 would add oxidatively across phosphorus to yield a $-\text{PCl}_4$ group bound to iridium.

The reaction was initially carried out in an n.m.r. tube and the ^{31}P n.m.r. spectra of the reaction system were studied at temperatures ranging from 213 K to room temperature.

At 213 K a dense white precipitate formed. The $^{31}\text{P}\{^1\text{H}\}$ n.m.r. spectrum of the solution showed signals for two products (complexes (i) and (ii)). At 213 K the relative intensity of the n.m.r. signals showed that complex (i) was the more abundant species in solution; however, as the temperature was raised the relative abundance of complex (ii) increased until at room temperature the more abundant species was complex (ii). The phosphorus-31-n.m.r. spectrum of the precipitate isolated from the reaction medium showed that it was complex (ii). N.m.r. parameters of both complexes are presented in Table 4.2.4.

The $^{31}\text{P}\{^1\text{H}\}$ n.m.r. spectra of both products were qualitatively the same as that of the iridium starting material; this implied that the $\text{Ir}(\text{PEt}_3)_2\text{-(P)}$ unit had been retained but the values of the n.m.r. parameters showed that reaction had occurred at what was the phosphorus of the -PCl_2 group.

A sample of the precipitate isolated from the reaction was submitted for C and H analyses; the values obtained were consistent with the molecular formula $\text{Ir}(\text{PCl}_4)(\text{CO})(\text{PEt}_3)_2\text{Cl}_2$ (see experimental).

A sample was also submitted for Cl analysis and the value obtained was consistent with the formula $\text{Ir}(\text{PCl}_2)(\text{CO})(\text{PEt}_3)_2\text{Cl}_2$ or $\text{Ir}(\text{OPCl}_2)(\text{CO})(\text{PEt}_3)_2\text{Cl}_2$; it was considered that, since this sample was not analysed immediately after submission, gradual loss of Cl_2 had occurred over a long period. The solution to this problem would be to carry out Cl analysis immediately after isolation of the product but due to lack of time this was not done. The i.r. spectrum showed bands assignable at: 2065 cm^{-1} for ν_{CO} ;

545 and 530 cm^{-1} for $\nu_{\text{P-Cl}}$. The complex was found to be essentially non-conducting in air the value of this result is doubtful as it was later found that the complex decomposed in air to give $\text{Ir}(\text{OPCl}_2)(\text{CO})(\text{PEt}_3)_2\text{Cl}_2$.

From the data obtained there were two plausible explanations for the complexes formed:

a) Complexes (i) and (ii) were two different isomers of the complex $\text{Ir}(\text{PCl}_4)(\text{CO})(\text{PEt}_3)_2\text{Cl}_2$ (see Fig. 4.2.4)



Fig. 4.2.4

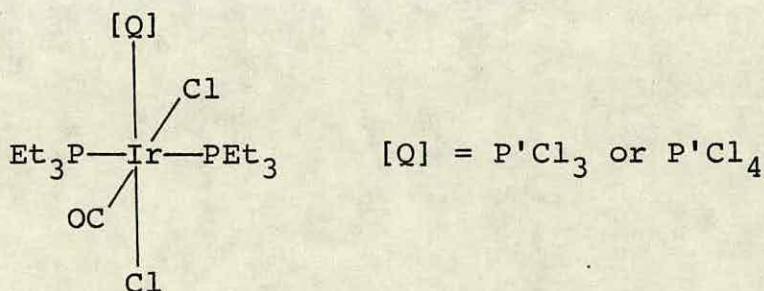
b) That one of the complexes was $[\text{Ir}(\text{PCl}_3)(\text{CO})(\text{PEt}_3)_2\text{Cl}_2]^+\text{Cl}^-$ and the other, one of the isomers shown above.

From the value of $\delta\text{P}'$ it was possible that complex (i) contained a coordinated PCl_3 ligand as it was similar to those recorded for the species: $\text{PtCl}_2(\text{P}'\text{Cl}_3)_2$, $\delta\text{P}' = 111.5\text{ p.p.m.}$; $\text{PtCl}_2(\text{P}'\text{Cl}_3)(\text{PF}_3)$, $\delta\text{P}' = 107.5\text{ p.p.m.}$; $[\text{PtCl}_2(\text{P}'\text{Cl}_3)_2]_2$, $\delta\text{P}' = 71.50\text{ p.p.m.}$; but since we have no comparable data for metal bound PCl_4 groups this comparison is not very helpful. The value of $\delta\text{P}'$ for complex (ii) was very much in the range associated with phosphorus (V) species (see Table 3.1.5.2), implying that this compound may well have been one of the possible isomers shown above. There is much work to be done before complete characterisation of these complexes are possible: good chloride analysis of the isolable complex is essential to prove the molecular formula; a conductivity

measurement in air-free conditions is also necessary; mass spectral information could prove helpful but as loss of chlorine seems to occur fairly readily it may be impossible to observe molecular ion peaks; other reactions might be tried to prove indirectly the mode of reaction, namely the reactions of interhalogen compounds ICl and Br-Cl with $\text{Ir}(\text{PCl}_2)(\text{CO})(\text{PEt}_3)_2\text{Cl}_2$ since from differences or similarities in the n.m.r. parameters of products from these reactions with those of complexes (i) and (ii) it should be possible to determine if the complexes are cationic with coordinated PCl_3 ligand or neutral with $-\text{PXCl}_3$ groups attached, providing no halogen exchange at iridium takes place. Of course, a better confirmation of the structure would be an X-ray crystal structure.

TABLE 4.2.4

N.m.r. parameters for



| Complex | $\delta\text{P}'/\text{p.p.m.}$ | $\delta\text{P}'/\text{p.p.m.}$ | $^2\text{J}_{\text{P-P}'}/\text{Hz}$ |
|---------|---------------------------------|---------------------------------|--------------------------------------|
| (i) | -3.3 | 65.9 | 14.2 |
| (ii) | -8.6 | 7.3 | 17.7 |

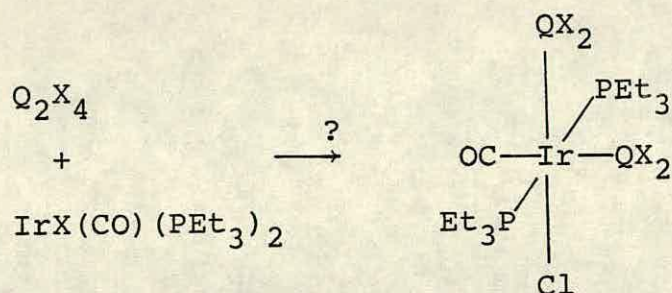
Parameters were recorded in chloroform at room temperature.

4.3 Conclusions and some Suggestions for Further Work

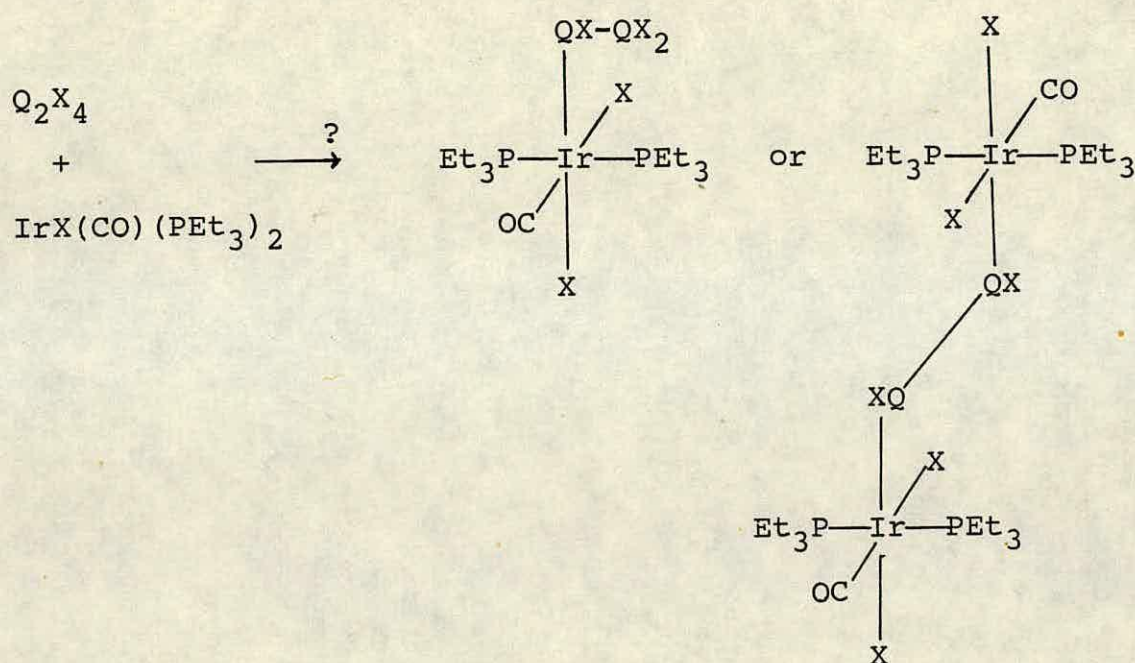
In this chapter we have described the synthesis and some reactions of iridium and rhodium complexes containing terminal dichlorophosphino groups.

The successful syntheses of these compounds and the analogous iridium- PF_2 complexes have shown that certain phosphorus-halogen bonds are activated towards oxidative addition across $\text{IrX}(\text{CO})(\text{PEt}_3)_2$. These results have since stimulated a research project into the reactivity of other main group halides towards oxidative addition across iridium (some of the reactions carried out in the project are mentioned in section 1.1)⁽³⁵⁾. There are a vast number of reactions which could be carried out in this area of chemistry; for instance, it would be interesting to study the reactions of halides of the heavier group VB elements, antimony and bismuth; it has been shown in section 1.3 that these elements may form trivalent compounds with more than one metallic substituent; therefore it might be possible for the halides to undergo more than one oxidative addition reaction at the same group VB centre. It would also be interesting to study the reaction of the group VB tetrahalides Q_2X_4 ($\text{Q} = \text{P}, \text{X} = \text{Cl}, \text{I}; \text{Q} = \text{As}, \text{X} = \text{I}$) with $\text{IrX}(\text{CO})(\text{PEt}_3)_2$, these compounds would appear to have two potential modes of reaction:

i) oxidative addition of the Q-Q bond across iridium



ii) oxidative addition of Q-X bonds across iridium



The reactions of the -PCl₂ grouping described in this chapter can really be regarded as only preliminary studies into its reactivity. The reactions studied have shown that the -PCl₂ grouping has a reasonably high nucleophilic character as it undergoes oxidative addition of all of the group VIB elements, H₂E and probably Cl₂. There are, however, many other reactions of the -PCl₂ groups which would be potentially very interesting:

i) The reduction of the -PCl_2 group to give a metal- PH_2 species by reagents such as $\text{Li(AlH}_4\text{)}$ or $\text{Na(BH}_4\text{)}$ might be possible.

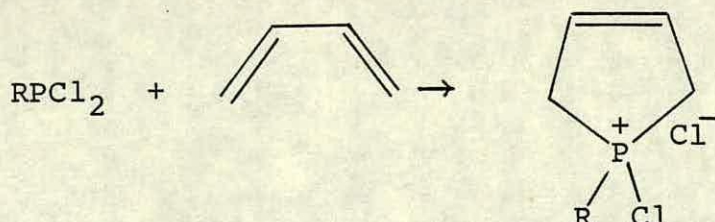
ii) Alkyl phosphines are produced by the reaction of PCl_3 with grignard reagents or metal alkyls such as Li^+Me^- and so it might be possible to form metal- PR_2 groups by such a reaction with the $(\text{Ir})\text{-PCl}_2$ complex, although this grouping might not be electronically favourable as it has already been noted in section 1.3 that the other substituents on terminal phosphorus ligands tend to be electron withdrawing.

iii) The reaction of secondary amines with PCl_3 results in displacement of one of the chlorides by formation of the relevant ammonium chloride to give amino dichloro phosphines; it would be interesting to see if the metal- PCl_2 would undergo similar reactions.

iv) It would be of interest to see if reaction with other alcohols besides methanol would result in the formation terminal- P-OR_2 groups.

v) Attempts should be made to synthesise mixed metal- PCl_2 bridged compounds starting from the terminal- PCl_2 complexes.

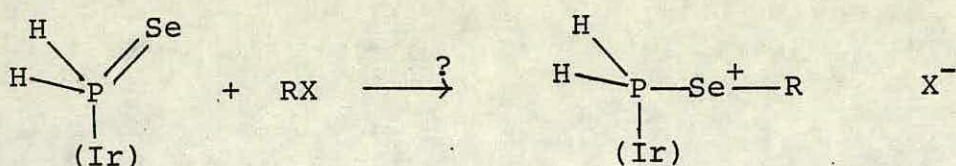
vi) Another potentially interesting reaction of the PCl_2 group is that with conjugated dienes alkyl dichloro phosphines react with conjugated dienes to give heterocyclic compounds. (18)



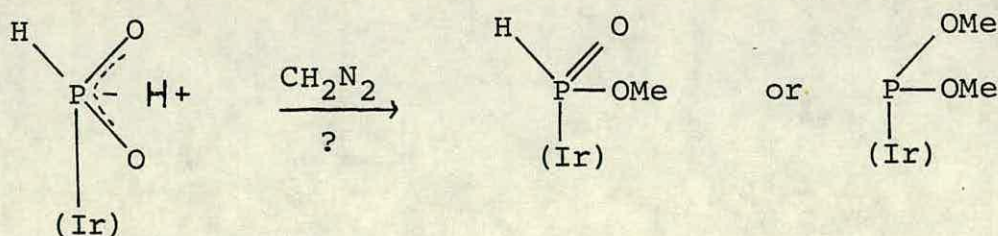
and it would be of interest to see if the metal- PCl_2 group would undergo similar reactions.

Many reactions might also be carried out on some of the derivatives of the metal- PCl_2 described in this chapter:

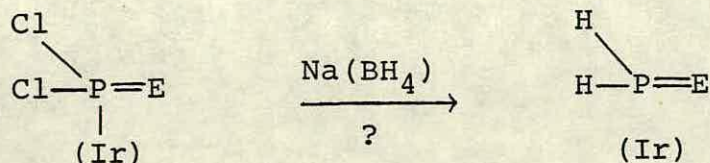
a) The relatively low value of $^1J_{\text{P-Se}}$ for the $[\text{Ir}]\text{-PH}_2\text{Se}$ compound described in 4.2.2a implies that the phosphorus-selenium bond was a fairly low double bond (cf. $(\text{Ir})\text{-PF}_2\text{Se}$) character which must mean that the bond is highly polar ($\text{P}^{\delta+}\text{-Se}^{\delta-}$) it might then be possible to react selenium with electrophiles such as activated alkyl halides (MeI), trimethylsilyl halides HX , and metal substrates e.g. $\text{PtCl}_2(\text{COD})$, $(\text{THF})\text{Cr}(\text{CO})_5$.



b) Diazomethane ($\text{CH}_2\text{-N}_2$) is an excellent methylating agent for compounds with acidic protons such as in alcohols, therefore it might be possible to methylate the hydroxyl groups of the iridium-hypophosphite group.

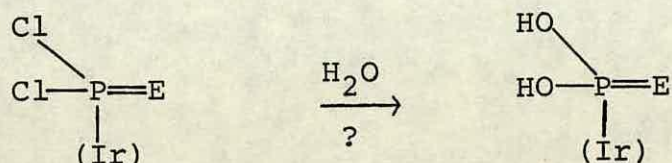


c) The hydrogenation of the P-Cl bonds in the PCl_2E ($\text{E} = \text{O}, \text{S}, \text{Se}$) might be possible by their reaction with reducing agents such as $\text{Li}(\text{AlH}_4)$ or $\text{Na}(\text{BH}_4)$ to form the novel $(\text{Ir})\text{-PH}_2\text{E}$ complexes.



Although there may be difficulties here with reduction of the P-E bond.

d) The hydrolysis of the same P-Cl bonds might also be possible by reaction with water or base to yield metal bound $(\text{HO})_2\text{P-E}$ groups.



The above suggestions for further work might only touch on the chemistry of the compounds described in this chapter but they do give an idea of the potentially rich chemistry of the various groups.

CHAPTER 5

The Reactions of Halodifluorophosphines with $\text{RhY(CO)(PEt}_3)_2$

[Y = Cl, Br or I]

5.1 Introduction

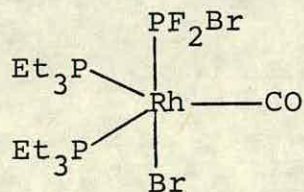
As already mentioned in the introductory chapter the complexes $\text{RhY}(\text{CO})(\text{PEt}_3)_2$ undergo reactions analogous to those of the equivalent iridium complexes; however, the stability of $\text{Rh}(\text{III})$ adducts formed by oxidative addition to the above is normally lower and is heavily dependent on the ligands attached to the rhodium centre. It has been shown in the previous chapter that the $\text{Rh}(\text{III})\text{-PCl}_2$ complex produced in the reaction of PCl_3 with $\text{RhCl}(\text{CO})(\text{PEt}_3)_2$ is stable at room temperature; it was hoped that the reactions of PF_2X with $\text{RhY}(\text{CO})(\text{PEt}_3)_2$ would yield similarly stable $\text{Rh}(\text{III})\text{-PF}_2$ complexes.

The reactions were carried out in n.m.r. tubes and the ^{31}P and ^{19}F n.m.r. spectra recorded at various temperatures ranging from 193 K to ca. 298 K. Although ^{103}Rh is another 100% $I = \frac{1}{2}$ isotope, no ^{103}Rh n.m.r. spectra were obtained; however, the presence of this isotope in product complexes gave rise to further splittings of ^{31}P and ^{19}F resonances of ligands bound to the rhodium centre.

The n.m.r. data for the product complexes are collected in Tables 5.1, 5.2 and 5.3.

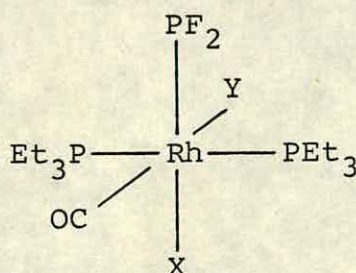
5.2 The Reactions of PF_2X with $\text{RhY}(\text{CO})(\text{PEt}_3)_2$ $[\text{X} = \text{Y} = \text{Br or I}]$

At 193 K, PF_2Br reacted with $\text{RhBr}(\text{CO})(\text{PEt}_3)_2$ yielding a species whose ^{31}P and ^{19}F n.m.r. spectra were qualitatively the same as those described for the iridium- PF_2X complexes apart from the additional doublet splittings due to coupling to ^{103}Rh . The chemical shift of the PF_2 grouping (Table 4.1) was as expected for a coordinated PF_2X ligand; likewise $^1\text{J}_{\text{PF}}$ was similar to that of coordinated PF_2Br in the five-coordinate iridium- PF_2Br complex, and $^1\text{J}_{\text{P}'\text{Rh}}$ was very high (ca. 200 Hz) as one would expect for a fluorophosphine group coordinated to a rhodium centre (e.g. $\text{RhH}(\text{PF}_3)(\text{PPh}_3)_3$; $\text{J}_{\text{P}'-\text{Rh}} = 254 \text{ Hz}$)⁽¹⁵⁰⁾. The value of δ_{PEt_3} was high relative to that of the starting material suggesting that the product was a rhodium(I) complex. Curiously the value of $^1\text{J}_{\text{PEt}_3-\text{Rh}}$ was in the range one normally associates with phosphines bound to rhodium(III) [$^1\text{J}_{\text{PRh}}$ for $\text{Rh}(\text{I})$ complexes are typically in the range 100-140 Hz, see Table 5.4]. The most likely formulation for this species is that of a five-coordinate rhodium(I) complex containing a coordinated PF_2Br ligand; one of the possible isomers for the complex is shown below:

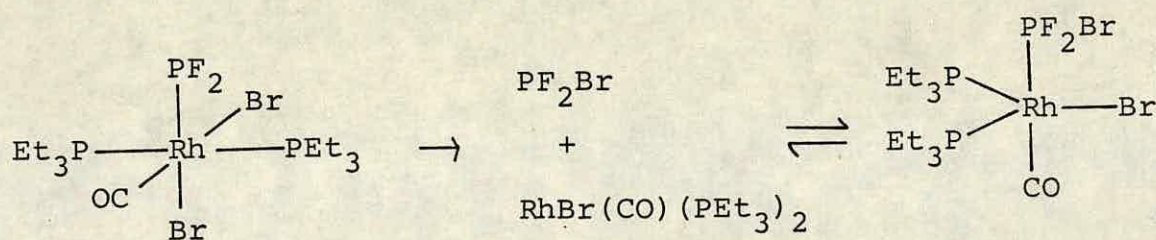


At 213 K this species rearranged irreversibly to give a single complex stable to 273 K whose n.m.r. spectra were different from those of the initial product. The reaction between PF_2I and $\text{RhI}(\text{CO})(\text{PEt}_3)_2$ gave no detectable signals that could be assigned to a derivative of five coordinate $\text{Rh}(\text{I})$; the sole product was clearly analogous to the rearranged product of the bromide system and it was stable up to 273 K.

The ^{31}P and ^{19}F n.m.r. spectra for both of these species were qualitatively the same as those described for the $(\text{Ir})\text{-PF}_2$ complexes, apart from additional doublet splittings of the signals due to coupling to ^{103}Rh . The chemical shifts of the PF_2 phosphorus atoms occurred at very high frequency (Table 5.2). The chemical shifts of the PEt_3 phosphorus nuclei were to low frequency of those of the rhodium starting materials, implying that the products were rhodium(III) complexes; this postulate was supported by the magnitudes of $^1\text{J}_{\text{PEt}_3\text{-Rh}}$ which fell in range normally expected for $\text{Rh}(\text{III})$ complexes (see Table 5.4). These results implied that the reactions of PF_2X with $\text{RhX}(\text{CO})(\text{PEt}_3)_2$ at 213 K had resulted in the formation of rhodium(III) complexes containing terminal- PF_2 groups. A possible structure is shown below.

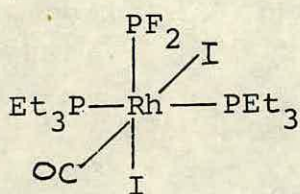


On leaving the reaction media at room temperature the above complexes gradually decomposed: the n.m.r. spectra of the reaction media in the PF_2Br system contained signals in the same spectral regions as those assigned to the five-coordinate species described previously; though no $^1\text{J}_{\text{PF}_2-\text{Rh}}$ or $^2\text{J}_{\text{PP}}$ couplings were resolved in the spectra, the phosphorus chemical shift of the PF_2 group was lower than that of free PF_2Br and δ_{PEt_3} was higher than that of $\text{RhBr}(\text{CO})(\text{PEt}_3)_2$. These results suggested that free PF_2Br was exchanging with PF_2Br on the complex $\text{RhBr}(\text{CO})(\text{PEt}_3)_2(\text{PF}_2\text{Br})$.

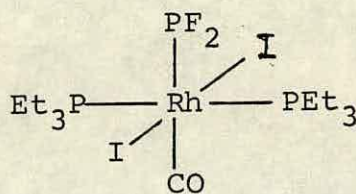


The reaction involving PF_2I does not seem to follow the same decomposition route. Two species become relatively more abundant on leaving the reaction mixture standing at room temperature. The first gave rise to no ^{19}F n.m.r. signals; the $^{31}\text{P}-\{^1\text{H}\}$ n.m.r. spectrum consisted of a single resonance split into a doublet ($\delta\text{P} = -5$ ppm; $^1\text{J}_{\text{PEt}_3-\text{Rh}} = 74$ Hz). This product was most likely to be $\text{RhI}_3(\text{CO})(\text{PEt}_3)_2$ judging from the very low chemical shift (see Table 5.4) ($\text{J}_{\text{P-Rh}}$ confirmed it to be a Rh(III) complex [see Table 5.4]). The n.m.r. spectra of the other species (complex (iii), Table 5.2) were qualitatively the same as those of the $(\text{Rh})-\text{PF}_2$ complexes already discussed.

The chemical shift of the PF_2 phosphorus atom of this species was almost identical to that of the $(\text{Rh})\text{-PF}_2$ complex already discussed for this reaction system (complex (ii), Table 5.2); however, there were marked differences between the remaining n.m.r. parameters of the two complexes, and in particular in δF , $\delta\text{P}_{\text{-Et}_3}$, $^1\text{J}_{\text{PF}}$, $^2\text{J}_{\text{PP}}$ and $^3\text{J}_{\text{PF}}$. Intuitively, one would not expect to observe such differences if complexes (ii) and (iii) were merely isomers of the same species e.g. (A) and (B) below.



(A)

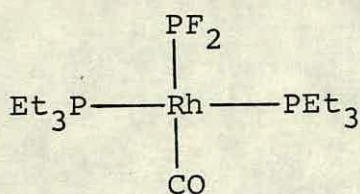


(B)

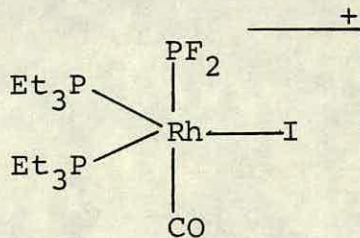
Although it can be seen from Table 5.4 that there are marked differences in δP and $^1\text{J}_{\text{P-Rh}}$ for phosphines trans to halide and those mutually trans in the complexes RhCl_3PR_3 .

We have no concrete evidence as to the formulation of complex (iii) but the magnitudes of $^1\text{J}_{\text{PF}_2\text{-Rh}}$ and $^2\text{J}_{\text{P'P}}$ might provide some indication of the form which complex (iii) takes. The relatively high values of these parameters for complex (iii) were presumably due to a higher degree of s character of the Rh-P bond in this complex. This might be the result of an overall positive charge or a change of coordination around the metal to a four- or five-coordinate species (hybridisation in transition metal complexes can be regarded as the following: four-coordinate square planar

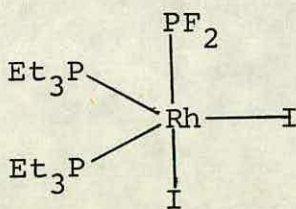
sp^2d ; five-coordinate trigonal bipyramidal sp^3d ; six-coordinate octahedral sp^3d^2 , so the relative s character of a hybrid is greatest in square planar complexes). Possible formulations for complexes which fit the n.m.r. data and are of a lower coordination number than complex (ii) are shown below.



(C)



(D)



(E)

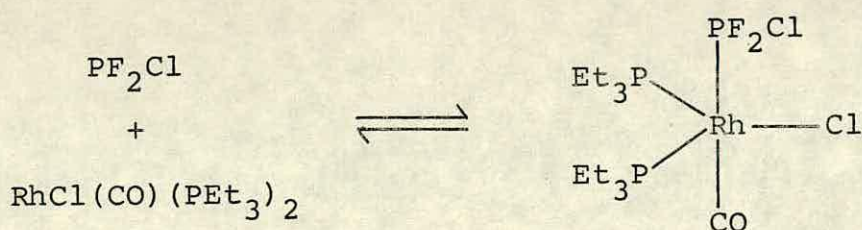
The observation that $RhI_3(CO)(PEt_3)_2$ is probably produced would seem to suggest that either complex (C) or (D) are the more likely formulations since they would be produced by loss of I^- from complex (ii). The magnitude of J_{PEt_3-Rh} for complex (iii) is intermediate between that of a four-coordinate $Rh(I)$ species and a six-coordinate $Rh(III)$ species; therefore the most likely structure is the five-coordinate species (D).

None of the species described in this section was isolated from the reaction mixtures because of the decomposition which occurred at room temperature so no absolute confirmation of the structures postulated were obtained.

5.3 The Reaction of PF_2Cl with $\text{RhCl}(\text{CO})(\text{PEt}_3)_2$

This reaction was followed in the same manner as those described in the previous section.

At 193 K the ^{31}P and ^{19}F n.m.r. spectra consisted of signals with the splitting patterns one would have expected for a five-coordinate rhodium- PF_2Cl complex, although no coupling constant of a lower order than $^2J_{\text{PP}}$ was resolved. On increasing the temperature to 293 K, the lines constituting the splitting patterns broaden such that the only resolvable couplings were $^1J_{\text{PF}}$ and $^2J_{\text{PEt}_3-\text{Rh}}$; however, the signals due to the PF_2Cl group and those of the PEt_3 ligands were centred on approximately the same positions as those at 193 K. This situation remained up to 243 K. On recooling the reaction mixture to 193 K without allowing further reaction to take place, ^{31}P and ^{19}F n.m.r. spectra identical to the original spectra were collected. These data could only be explained by proposing that at 193 K the resultant product is a PF_2Cl donor adduct, which dissociates reversibly and fairly fast on the n.m.r. time scale when the temperature of the reaction system is increased above 193 K i.e. the formation of the donor adduct was a temperature-dependent equilibrium.

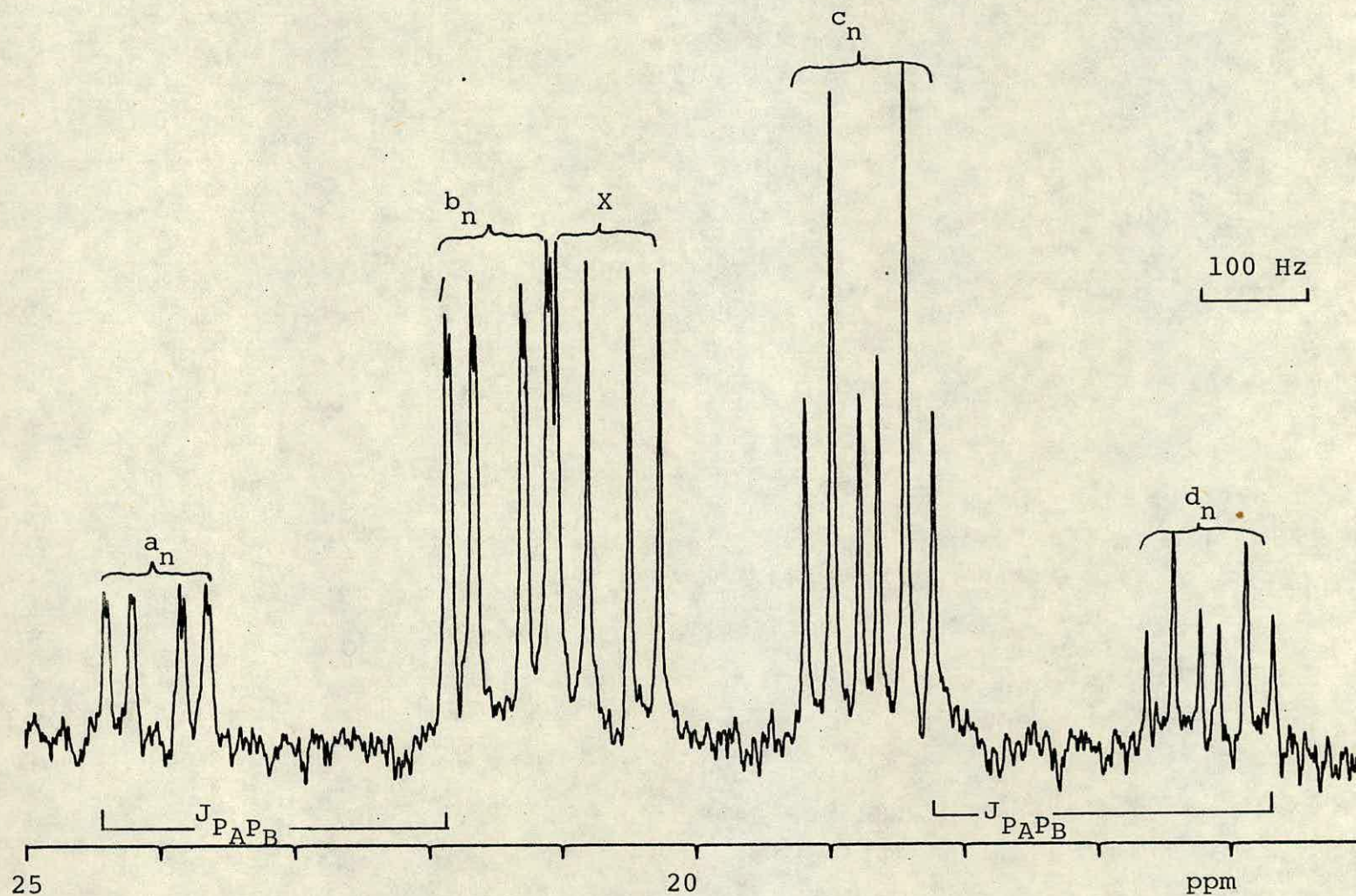


At temperatures above 243 K, the ^{31}P and ^{19}F n.m.r. showed that a number of new species had been produced.

Firstly the ^{19}F n.m.r. contained signals in the region associated with a terminal PF_2 attached to a rhodium centre. The signals were very weak, however, and no corresponding signals for the PF_2 phosphorus atom were detected in the $^{31}\text{P}\{-^1\text{H}\}$ n.m.r. spectrum; it was apparent that there were only trace amounts of a terminal PF_2 complex present in the reaction medium.

The second species to be described was present in far greater abundance. The ^{31}P nmr spectrum of this species consisted of two signals whose splitting patterns were qualitatively the same as those described for the complex $\text{Ir}(\text{PFCl})(\text{CO})\text{---}(\text{PEt}_3)_2\text{Cl}_2$ described in Section 3.1.6 apart from the presence of Rh-P couplings which resulted in further doublet splittings for both sets of signals. Therefore this results in an ABHXY spin system and so the AB quartet expected for the PEt_3 resonances is split by three different doublet couplings (see Figure 5.1).

Figure 5.1 $^{31}\text{P}\{-^1\text{H}\}$ n.m.r. spectrum of the reaction system; $\text{PF}_2\text{Cl} + \text{RhCl}(\text{CO})(\text{PEt}_3)_2$
 a_n, b_n, c_n, d_n , represent the PEt_3 resonances for $\text{Rh}(\text{PFCl})(\text{CO})(\text{PEt}_3)_2\text{Cl}_2$.
 X represents the PEt_3 resonance of $\text{Ir}(\text{PCl}_2)(\text{CO})(\text{PEt}_3)_2\text{Cl}_2$



The ^{19}F n.m.r. spectrum of this species was also qualitatively the same as that obtained for $\text{Ir}(\text{PFCl})(\text{CO})-(\text{PEt}_3)_2\text{Cl}_2$ with further doublet couplings resulting from $^3\text{J}_{\text{RhF}}$.

In the ^{31}P n.m.r. spectrum, signals arising from the $\text{Rh}(\text{PCl}_2)(\text{CO})(\text{PEt}_3)_2\text{Cl}_2$ complex were also detected (see Chapter 4). Further signals, arising from free PF_3 exchanging with PF_3 in the complex $\text{RhCl}(\text{CO})(\text{PEt}_3)_2(\text{PF}_3)$ were also detected; these consisted of a quartet ($^1\text{J}_{\text{PF}}$) at relatively high frequency and a doublet ($^1\text{J}_{\text{PEt}_3-\text{Rh}}$) occurring in the same spectral region as the PEt_3 resonances in the five-coordinate $(\text{Rh})-\text{PF}_2\text{X}$ species. The lines making up both sets of signals were so broad that no couplings of a lower order than $^1\text{J}_{\text{PF}}$ and $^1\text{J}_{\text{PEt}_3-\text{Rh}}$ were resolved. (The values of the n.m.r. parameters were not those of either free PF_3 or $\text{RhCl}(\text{CO})(\text{PEt}_3)_2$).

On allowing the reaction medium to stand at room temperature for an hour or two, the only signals detected in the n.m.r. spectra were those arising from the $\text{Rh}(\text{PCl}_2)(\text{CO})(\text{PEt}_3)_2\text{Cl}_2$ complex and those of PF_3 exchanging onto and off the $\text{RhCl}(\text{CO})(\text{PEt}_3)_2$.

It was apparent that rhodium complexes in the reaction medium were enhancing the rate of halogen interchange between PF_2Cl molecules.

There are two possible pathways for this 'catalytic' process:

(1) A rhodium complex containing a terminal PF_2 ligand is formed by oxidative addition of the P-Cl bond across rhodium. The $-\text{PF}_2$ group of this complex quickly reacts with a further PF_2Cl molecule yielding PF_3 and the $(\text{Rh})-\text{PFCl}$ complex. The $(\text{Rh})-\text{PFCl}$ complex appeared to have greater stability than the $-\text{PF}_2$ complex as it was detected in far greater quantities. However ultimately the $(\text{Rh})-\text{PFCl}$ rearranges on reaction with further PF_2Cl to give the $(\text{Rh})-\text{PCl}_2$ complex. This scheme is summarised in Figure 5.2.

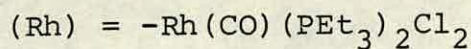
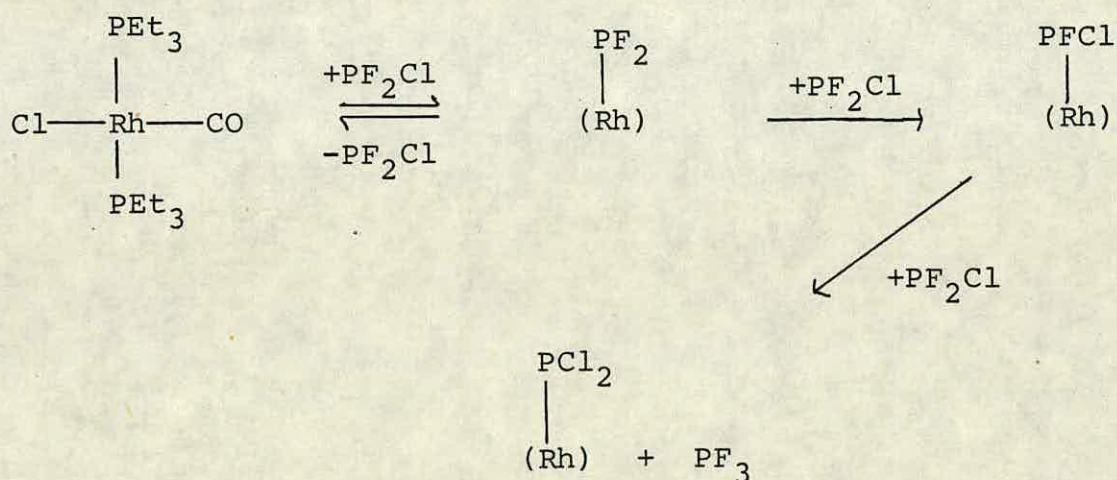
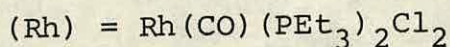
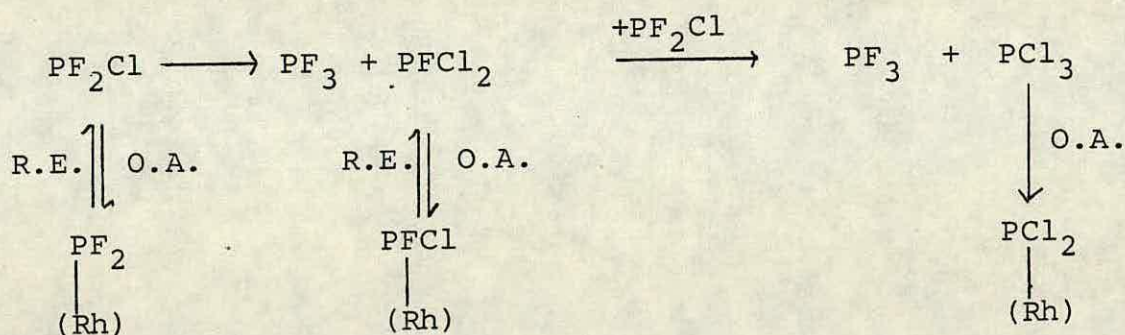
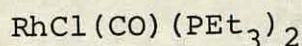


Figure 5.2

(2) The disproportionation of PF_2Cl (and PFCl_2) is catalysed by rhodium complexes in the reaction medium, producing PF_3 , PFCl_2 and PCl_3 . The disproportionation reactions for PF_2Cl and PFCl_2 presumably compete with oxidative addition across rhodium, with the stability of the respective Rh(III) adducts determining the relative abundance of the respective adducts. As the temperature of the reaction system is raised the reaction pathway would tend towards the most thermodynamically stable products, i.e. PF_3 and $(\text{Rh})\text{-PCl}_2$ complex. A representation of this reaction pathway is shown in Figure 5.3.



O.A. = oxidative addition of $\text{PF}_n\text{X}_{3-n}$ ($n = 1-3$) to



R.E. = reductive elimination of $\text{PF}_n\text{X}_{3-n}$

Figure 5.3

From the data obtained, the most likely pathway for the disproportionation pathway could not be ascertained; indeed, it may have been combination of both.

5.4 Discussion of N.M.R. Parameters

There is little that can be said about the parameters of the five-coordinate species that was not said about the equivalent iridium complexes. As in the iridium complexes the $\delta P'$ values are lower than those of the PF_2X starting materials and they also show significant variation with X.

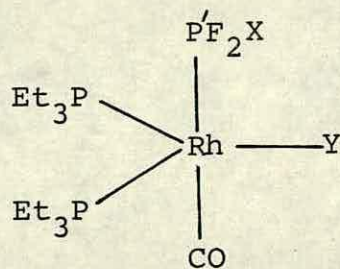
Probably the most interesting points of note are the magnitudes of the Rh-P coupling constants. First $^1J_{P^{Rh}}$; the two values obtained in this work are fairly typical for fluorophosphine ligands bound to rhodium^(97,150). These values are far higher than those of alkyl or aryl phosphines bound to rhodium, this is mainly because of the greater s character of the lone pair in fluorophosphines compared with alkyl phosphines which is due to a high s character in the metal-phosphorus bond.

Secondly $^1J_{PRh}$; the magnitudes of these parameters are in the range one normally associates with six-coordinate Rh(III) complexes (see Table 5.3). This may be due to the unusually high s character of the Rh- PF_2X bond causing a proportionate decrease in s character of the Rh- PEt_3 bonds.

These arguments are probably over simplistic for describing what is certainly a complicated bonding arrangement around rhodium, but as it is generally accepted that the

Table 5.1

N.m.r. data for



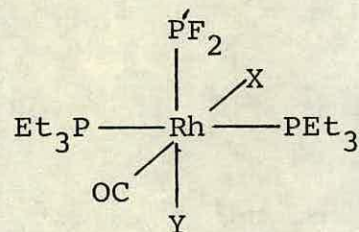
| X | Y | $\delta P/\text{ppm}$ | $\delta P'/\text{ppm}$ | $\delta F/\text{ppm}$ | $^1J_{P'F}/\text{Hz}$ | $^1J_{PRh}/\text{Hz}$ |
|----|----|------------------------|------------------------|-----------------------|-------------------------|-----------------------|
| Br | Br | 32.1 | 156 | 2.3 | 1362 | 83 |
| Cl | Cl | 35.0 | 146 | -0.1 | 1362 | 74 |
| | | $^1J_{P'Rh}/\text{Hz}$ | $^2J_{PP'}/\text{Hz}$ | $^3J_{PF}/\text{Hz}$ | $^3J_{FRh'P}/\text{Hz}$ | |
| | | 226 | 63 | 10 | NR | |
| | | 250 | 42 | NR | NR | |

The parameters were recorded in toluene at 193 K

NR = not resolved

Table 5.2

N.m.r. data for



| Complex | X | Y | $\delta P/\text{ppm}$ | $\delta P'/\text{ppm}$ | $\delta F/\text{ppm}$ | $^1J_{P'F}/\text{Hz}$ | $^1J_{PRh}/\text{Hz}$ | $^1J_{P'Rh}/\text{Hz}$ | $^2J_{PP}/\text{Hz}$ | $^3J_{PF}/\text{Hz}$ |
|---------|-----|----|-----------------------|------------------------|-----------------------|-----------------------|-----------------------|------------------------|----------------------|----------------------|
| (i) | Br | Br | 12.6 | 388.0 | -54.7 | 1153 | 85 | 27 | 6.8 | 15.9 |
| (ii) | I | I | 3.4 | 395.4 | -52.9 | 1155 | 86.9 | 25 | 7.3 | 15.4 |
| (iii) | [a] | | 16.1 | 394.8 | -4.3 | 1288 | 94.7 | 56 | 24.4 | 24.4 |

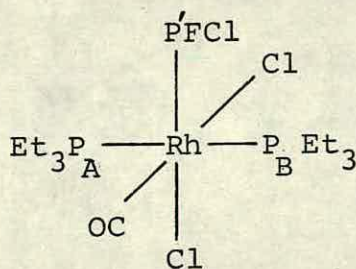
[a] This complex does not have the structure shown above, see text (5.2)

$$^3J_{FRh} = 6, 5, 5$$

The parameters were recorded in toluene at room temperature.

Table 5.3

N.m.r. parameters for



| $\delta P_A^*/\text{ppm}$ | $\delta P_B^*/\text{ppm}$ | $\delta P'/\text{ppm}$ | $\delta F/\text{ppm}$ | $^1J_{PF}/\text{Hz}$ | $^1J_{P_A Rh}^*/\text{Hz}$ |
|---------------------------|---------------------------|------------------------|-----------------------|----------------------|----------------------------|
| 22.4 | 17.7 | 369.8 | -100.3 | 1195 | 82 |

| $^1J_{P_B Rh}^*/\text{Hz}$ | $^1J_{P' Rh}/\text{Hz}$ | $^2J_{P_A P_B}^*/\text{Hz}$ | $^2J_{P' P_B}^*/\text{Hz}$ |
|----------------------------|-------------------------|-----------------------------|----------------------------|
| 80 | 26 | 372.2 | 3 |

* The magnitudes of the parameters were calculated by carrying out standard solutions of AB patterns⁽¹⁶⁵⁾ for each line of the multiplets (a,b,c,d) of ABMX pattern (see Figure 5.1). The values cited above are those obtained from the high field n.m.r. spectrum; there were minimal differences in the values calculated for the low field n.m.r. spectrum.

The parameters were recorded in toluene at 233 K.

Table 5.4 N.m.r. parameters for some rhodium-complexes containing alkyl-phosphine ligands

| Complex | $\delta P^{[a]}$ /ppm | $^1J_{PRh}^{[a]}$ /Hz | Ref. |
|-------------------------------------|-----------------------|-----------------------|------|
| $RhCl(PPh_3)_3$ | 48.0, 31.5 | 189, 142 | 151 |
| $RhBr(PPh_3)_3$ | 46.8, 29.8 | 192, 141 | 151 |
| $RhI(PPh_3)_3$ | 43.2, 27.1 | 194, 139 | 151 |
| $RhCl(CO)(PPh_3)_2^{[b]}$ | 29.1 | 124 | 151 |
| $RhCl(CO)(PEt_3)_2^{[b]}$ | 23.7 | 116 | 147 |
| $RhI(CO)(PEt_3)_2^{[b]}$ | 19.9 | 114.4 | 39 |
| $RhCl_3(PPh_3)_3^{[c]}$ | 15.1, -0.5 | 113, 84 | 151 |
| $RhCl_3(PEt_3)_3^{[c]}$ | 20.0, 4.3 | 112, 83.8 | 152 |
| $RhCl_3(CO)(PEt_3)_2^{[b]}$ | 19.3 | 72 | 146 |
| $RhHCl(SiH_2Cl)(CO)(PEt_3)_2^{[b]}$ | 26.8 | 87.8 | 38 |
| $RhH((SiH_2I)(CO)(PEt_3)_2^{[b]}$ | 17.3 | 85.0 | 38 |
| $RhHCl_2(CO)(PEt_3)_2^{[b]}$ | 26.7 | 80.6 | 39 |
| $RhHI_2(CO)(PEt_3)_2^{[b]}$ | 13.7 | 80.6 | 39 |

[a] where two values are given the first refers to phosphine trans to halide and the second for mutually trans phosphines

[b] phosphines are mutually trans

[c] the values given are for the mer-isomers of these complexes

influence on one-bond coupling constants is the degree of s character in that bond, the arguments seem plausible for explaining the observed results.

An examination of the n.m.r. parameters of the rhodium(III)-PF₂ complexes is also hampered by the small number of complexes available for comparison. It is worth noting that they do share certain points of interest with their iridium counterparts. These are very high $\delta P'$ values, relatively low $^1J_{PF}$ values, relatively high $^3J_{PF}$ values and proportionately low $^2J_{PP'}$ values. The explanations for these observations in the rhodium systems can be regarded as the same as those put forward for the iridium systems.

The postulation made in chapter 2 that the M-PF₂ bond in the iridium complexes lacked s character, manifesting this in the relatively low $^2J_{PP'}$ values, is supported by the fact that the $^1J_{RhP'}$ coupling constants are unusually low [this is true for all the Rh(PF_{2-n}Cl_n) (n = 0, 1, 2) complexes] and can only be explained by assuming a high degree of p character in the rhodium-phosphorus bonding.

The values of δP_{Et_3} for the six-coordinate -PF₂ complexes follow the expected trend, i.e. the higher value is observed when smaller and more electronegative halogens are bound to rhodium.

It is, however, impossible to decide if the trends in values of $\delta P'$ and $^1J_{PF}$ are dependent on the same factors as those described for the (Ir)-PF₂ complexes [(Ir) = -Ir(CO)(PEt₃)₂XY] as so few examples of (Rh)-PF₂ complexes [(Rh) = Rh(CO)(PEt₃)₂X₂] were synthesised.

There is an interesting trend in values of $\delta P'$ for the group of compounds (Rh)-PF_{2-n}Cl_n [(Rh) = -Rh(CO)(PEt₃)₂-Cl₂ (n = 0, 1, 2) if one assumes that $\delta P'$ when n = 0 would be in the region of 390 ppm (this seems reasonable in the light of the values of $\delta P'$ for the complexes in Table 5.2); there is a steady decrease in values of $\delta P'$ from n = 0 to n = 2. This trend must be the result of the lesser electronegativity of chlorine, compared to fluorine, resulting in a diminishing of the electron withdrawal from the phosphorus atom giving rise to greater shielding of the phosphorus nucleus.

5.5 Conclusions

The results described in this chapter have shown that the reactions of PF₂X with RhY(CO)(PEt₃)₂ are similar in many ways to those described for the reactions involving the analogous iridium systems: the reactions have again yielded complexes containing terminal PF₂ groups and in two of the cases described signals have been detected in the ³¹P and ¹⁹F n.m.r. spectra assignable to five-coordinate complexes. The various Rh(III) products do show considerable differences

in their stability compared with the equivalent iridium complexes. The complex $\text{Rh}(\text{PF}_2)(\text{CO})(\text{PEt}_3)_2\text{Cl}_2$ appears to be the least stable of the complexes $\text{Rh}(\text{PF}_2)(\text{CO})(\text{PEt}_3)_2\text{X}_2$; ^{19}F n.m.r. signals for this species in the spectrum of the reaction system involving PF_2Cl and $\text{RhCl}(\text{CO})(\text{PEt}_3)_2$ show that it is produced only in trace amounts. The equivalent complex formed in the reaction of PF_2Br with $\text{RhBr}(\text{CO})(\text{PEt}_3)_2$ is formed quantitatively at 213 K but when the reaction system is warmed to ambient temperature it reverts to starting materials, this type of decomposition has been observed for some Rh(III)-silyl complexes (see 1.1). The complex $\text{Rh}(\text{PF}_2)(\text{CO})(\text{PEt}_3)_2\text{I}_2$ formed quantitatively in the reaction of PF_2I with $\text{RhI}(\text{CO})(\text{PEt}_3)_2$, at 193 K, rearranges at ambient temperature to produce what is probably a five-coordinate rhodium complex containing a terminal- PF_2 ligand.

The reaction of PF_2Cl with $\text{RhCl}(\text{CO})(\text{PEt}_3)_2$ was of interest in that rhodium complexes in the reaction medium seemed to 'catalyse' the disproportionation of PF_2Cl , this is shown by the rapid production of PF_3 , $(\text{Rh})\text{-PFCl}$ complex and $(\text{Rh})\text{-PCl}_2$ complex at temperatures above 243 K.

Unfortunately, due to the complex mixture of products formed from the reaction pairings, at room temperature, none of the complexes described in this chapter were isolated. However low temperature isolation techniques could be successful in isolating clean products from the reactions involving PF_2Br and PF_2I since in the temperature range 203 K to 243 K only the terminal- PF_2 complexes were detected in significant quantities.

CHAPTER 6

EXPERIMENTAL

6.1 Vacuum Line Techniques

All volatile compounds were handled on a pyrex vacuum line of conventional design⁽¹⁵³⁾. The vacuum line was built up from detachable sections; apiezon N and L greases were used on taps and ground glass joints respectively. Detachable reaction ampules were in most cases fitted with Rotaflo and Sovirel greaseless taps. High vacuum necessary for handling compounds without decomposition by air and moisture was maintained by a mercury diffusion pump assisted by a rotary oil pump. The pressures of the materials inside the apparatus were measured using a spiral gauge with a mirror, employed as a null point instrument with a lamp and scale. Pressure of non condensable gases in the line was checked by a Pirani gauge. The line was calibrated for volume using a molecular weight bulb; accurate volumes for individual sections combined with pressure readings allowed rapid calculation of the amount of volatile materials present so that quantities of volatiles could be measured to an accuracy of $\pm 2\%$.

6.2 Handling of Air Sensitive Solids

Air sensitive solids were prepared and handled on a Schlenk vacuum-and-nitrogen line. High purity nitrogen (B.O.C. white spot nitrogen specified less than 0.5% H_2O and O_2) was passed through columns of NaOH pellets and activated charcoal before being admitted to the line. Preparations were carried out in pyrex reaction vessels

with tapped side arms to allow for evacuation, evaporation of solvents and addition of nitrogen. Reactions were agitated with teflon coated stirrer bars.

Highly air sensitive compounds were handled in V.A.C. model HE-493 glove box with a V.A.C. Model HE-493 Dri-train to remove contaminants. High purity nitrogen was fed directly from a cylinder into the body of the box and then continually circulated through the Dri-train to remove contaminants. The pressure was maintained marginally above atmospheric pressure by means of a Pedatrol attachment supplied by V.A.C. California, U.S.A.

6.3 Instruments

Phosphorus-31-n.m.r. spectra were recorded using Jeol FX60Q, Varian Associates XL100 and Bruker WH360 spectrometers. A deuterated solvent was employed as lock; variable temperature facilities were provided by all three spectrometers; chemical shifts were measured as positive to high frequency of 85% H_3PO_4 .

Fluorine-19-n.m.r. spectra were recorded using a Varian Instruments XL100; chemical shifts were measured as positive to high frequency of CFCl_3 .

Hydrogen-1-n.m.r. spectra were recorded using the Bruker WH360 spectrometer; chemical shifts were measured as positive to high frequency of T.M.S.

Selenium-77-n.m.r. spectra were recorded on the Bruker WH360 spectrometer; chemical shifts were measured as positive to high frequency of Me_2Se .

Infra-red spectra were recorded using Perkin Elmer 457 and 577 double beam spectrometers ($250\text{--}4000\text{ cm}^{-1}$). Gas phase spectra were recorded on these spectrometers using a gas cell fitted with KBr plates.

Analyses for carbon, hydrogen and nitrogen were carried out using a Perkin Elmer 240 elemental analyser. Analyses for chlorine and sulphur were carried out at Butterworth Laboratories Ltd., Teddington, Middlesex.

Mass Spectra were run on a Kratos-80RF spectrometer which utilised fast atom bombardment ionisation and not standard electron beam ionisation.

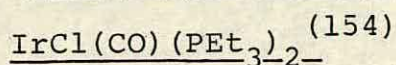
6.4 Reactions in Sealed N.m.r. Tubes

Reactions of this type were used extensively in this project for reaction systems in which a volatile compound was reacted with a metal complex.

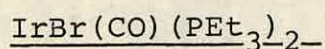
In a typical reaction 0.1 mmole of metal complex was weighed into a n.m.r. tube with a B10 cone extension. The tube was then evacuated and ca. 3 cm of the appropriate solvent condensed into the tube. The complex was then dissolved. Following this the relevant amount of volatile reactant was condensed into the tube and the tube was sealed and then stored at liquid nitrogen temperature until it was time to examine the reaction system.

6.5 Experimental Relating to Reactions Described in
Chapter 2

6.5.1 Synthesis of Metal-Complex Starting Materials



In a typical preparation, 0.45 g of $[\text{IrCl}(\text{C}_8\text{H}_{14})_2]_2$ (C_8H_{14} = cyclooctene) was stirred under nitrogen in 5 ml of degassed acetone. At room temperature, CO was slowly bubbled through the slurry for 4-5 minutes during which time it turned dark blue. To this solution was added a solution of 0.3 ml triethylphosphine in 5 ml acetone. The mixture was stirred vigorously until the solution was a straw yellow colour. Any solids were Schlenk-filtered off; solvent was then evaporated from the filtrate and the product maintained at 80°C for 90 minutes under vacuum. The product was sublimed at 120°C under vacuum to yield yellow crystals which were air sensitive but could be handled for short periods in air.



$\text{IrCl}(\text{CO})(\text{PEt}_3)_2$ was dissolved in degassed acetone and to this was added a 500% excess of dried LiBr. The resulting slurry was stirred for 45 minutes at room temperature. The solvent was evaporated off and sublimation of the product yielded yellow crystals of $\text{IrBr}(\text{CO})(\text{PEt}_3)_2$ which was air sensitive and had to be handled using Schlenk techniques.

IrI(CO)(PEt₃)₂

The procedure used was as for IrBr(CO)(PEt₃)₂ except that only a 100% XS of NaI was used and the slurry was stirred for only 15 minutes. IrI(CO)(PEt₃)₂ is particularly air sensitive and had to be handled in the glove box.

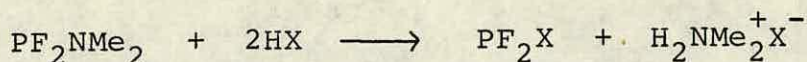
[IrCl(C₈H₁₄)₂]₂

This was prepared using standard literature method⁽¹⁵⁵⁾ by refluxing IrCl₃(H₂O)₃ with isopropanol, cyclooctene and water.

6.5.2 Preparation of Gaseous Starting Materials

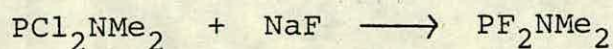
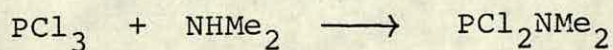
Halodifluorophosphines

PF₂X (X = Cl, Br, I) were prepared using standard literature methods⁽¹⁵⁶⁾ by reaction of dimethylamino-difluorophosphine with the appropriate hydrogen halide.



Dimethylaminodifluorophosphine

PF₂NMe₂ was prepared using standard literature methods⁽¹⁵⁶⁾ by reaction of PCl₂NMe₂ with NaF. PCl₂NMe₂ was prepared by reaction of PCl₃ with dimethylamine.

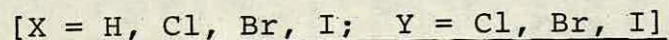


Hydridodifluorophosphine

HPF₂ was prepared using standard literature methods⁽¹⁵⁷⁾ by reaction of PF₂I and HI in the presence of mercury.

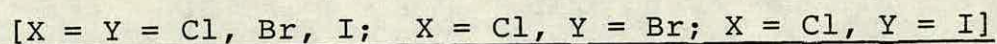


6.5.3 The Reactions of PF₂X with IrY(CO)(PEt₃)₂



These reactions were carried out and studied in sealed n.m.r. tubes. The standard procedure for setting up such an experiment is described in section 6.4.

6.5.4 The Isolation of Ir(PF₂)₂(CO)(PEt₃)₂XY



These complexes were the clean products of the respective reaction pairings of PF₂X and IrY(CO)(PEt₃)₂. In a typical isolation, the sealed n.m.r. tubes in which the reaction system was studied was opened under nitrogen and the contents tipped into a Schlenk tube with washing by the appropriate solvent. The Schlenk tube was then connected to the Schlenk line and all volatiles pumped off. The resulting gum was triturated with degassed petrol-ether (40°-60°) to yield powdery solids (N.B. for isolation of solid material it was essential that pure starting materials were used; other wise intractable gums were produced). Analysis figures and infra-red spectral data of the solids are presented in Tables 6.5.1 and 6.5.2 respectively.

Table 6.5.1 Analysis figures for $\text{Ir}(\text{PF}_2)(\text{CO})(\text{PEt}_3)_2\text{XY}$

| Complex | Found | | Required | |
|--|-------|-----|----------|-----|
| | %C | %H | %C | %H |
| $\text{Ir}(\text{PF}_2)(\text{CO})(\text{PEt}_2)\text{Cl}_2$ | 26.2 | 5.2 | 26.2 | 5.1 |
| $\text{Ir}(\text{PF}_2)(\text{CO})(\text{PEt}_3)_2\text{Br}_2$ | 23.0 | 4.6 | 22.8 | 4.4 |
| $\text{Ir}(\text{PF}_2)(\text{CO})(\text{PEt}_3)_2\text{I}_2$ | 20.3 | 4.0 | 20.0 | 3.9 |
| $\text{Ir}(\text{PF}_2)(\text{CO})(\text{PEt}_3)_2\text{ClBr}$ | 24.6 | 4.6 | 24.4 | 4.7 |
| $\text{Ir}(\text{PF}_2)(\text{CO})(\text{PEt}_3)_2\text{ClI}$ | 22.6 | 4.3 | 22.7 | 4.4 |

Table 6.5.2 Infra-red spectral data for $\text{Ir}(\text{PF}_2)(\text{CO})(\text{PEt}_3)_2\text{XY}$

| | |
|--|---|
| $\text{Ir}(\text{PF}_2)(\text{CO})(\text{PEt}_3)_2\text{Cl}_2$ | 2042vs, 1260m, 1200m, 1035vs, 760vsb, 732vs, 625w, 575s, 420m, 388m, 310m. |
| $\text{Ir}(\text{PF}_2)(\text{CO})(\text{PEt}_3)_2\text{Br}_2$ | 2042vs, 1261m, 1200s, 1035s, 760s, 745m, 560m, 440m, 380w. |
| $\text{Ir}(\text{PF}_2)(\text{CO})(\text{PEt}_3)_2\text{I}_2$ | 2040vs, 1260m, 1200m, 1034s, 740m, 720s, 550m, 540m, 480w. |
| $\text{Ir}(\text{PF}_2)(\text{CO})(\text{PEt}_3)_2\text{BrCl}$ | 2042vs, 1255m, 1240w, 1198w, 1035s, 770m, 745s, 715s, 620w, 570m, 430w, 420m, 380m, 315w. |
| $\text{Ir}(\text{PF}_2)(\text{CO})(\text{PEt}_3)_2\text{ICl}$ | 2040vs, 1260m, 1200m, 1034s, 750s, 730m, 615w, 570m, 560w, 530m, 430bw, 380w, 305w. |

Abbreviations: vs = very strong; s = strong; m = medium;
w = weak; b = broad

Data was obtained from nujol mulls and KBr discs

6.6 Experimental Relating to Reactions Described in Chapter 3

All volatile reagents used in the reaction systems described in Chapter 3 were synthesised using standard literature methods and the reactions used for the syntheses are summarised in Table 6.6.1.

Table 6.6.1

| <u>Reagent</u> | <u>Method</u> | <u>Reference</u> |
|----------------|---------------------------|------------------|
| B_2H_6 [a] | $KBH_4 + H_3PO_4$ | 158 |
| HCl | $HCl(aq) + H_2SO_2(conc)$ | 159 |
| H_2S [b] | $FeS + H_2SO_4$ | 159 |
| H_2Se [b] | $Al_2Se_3 + H_2SO_4$ | 159 |

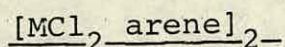
[a] Kindly supplied by Dr. G.M. Hunter

[b] Kindly supplied by Mr. P.G. Page

6.6.2 Synthesis of Transition Metal Reagents

$PtCl_2(COD)$

$PtCl_2(COD)$ was synthesised using standard literature methods⁽¹⁶⁰⁾ by reaction of tetrachloroplatinate and cyclooctadiene in ethanol.



$[RuCl_2(\text{benzene})]_2$ was synthesised using standard literature methods⁽¹³⁷⁾ by reacting $RuCl_3 \cdot x(H_2O)$ with 1,3-cyclohexadiene. $[MCl_2(p\text{-cymene})]_2$ ($M = Os, Ru$)⁽¹³⁷⁾ were similarly synthesised by reacting $MCl_3 \cdot x(H_2O)$ with α -phallandrene (5-isopropyl,2-methylcyclohexadiene). These complexes were kindly supplied by Mr. D.A. Tocher.

6.6.3 Reactions of $Ir(PF_2)(CO)(PEt_3)_2X_2$ with Volatile Compounds

$Ir(PF_2)(CO)(PEt_3)_2X_2$ was synthesised in the n.m.r. tube in which the reaction system would be studied ($IrX(CO)(PEt_3)_2$) was weighed into a n.m.r. tube with extension; the tube was then evacuated; sufficient solvent to dissolve the complex was condensed into the tube followed by the appropriate PF_2X . The mixture was then warmed to room temperature and allowed to stand for ca 5 minutes after which time all volatiles were pumped off). With the $Ir(PF_2)(CO)(PEt_3)_2X_2$ in the n.m.r. tube the procedure for setting up a reaction in a sealed n.m.r. tube was then followed (see Section 6.4).

The above procedure was utilised for the reactions of $Ir(PF_2)(CO)(PEt_3)_2X_2$ with B_2H_6 and $Ir(PF_2)(CO)(PEt_3)_2Cl_2$ with Cl_2 , HCl , H_2S and H_2Se .

6.6.4 The Isolation of $Ir(PF_2BH_3)(CO)(PEt_3)_2I_2$

The n.m.r. tube in which the reaction was studied was opened under nitrogen and the contents of the tube emptied into a Schlenk tube with careful washing with dry degassed

toluene. The Schlenk tube was then attached to a Schlenk line and all volatiles pumped off yielding a gum which gave a pale yellow powder on trituration with degassed petrol-ether (40° - 60°). Analytical and i.r. spectral data for $\text{Ir}(\text{PF}_2\text{BH}_3)(\text{CO})(\text{PEt}_3)_2\text{I}_2$ are presented in Tables 6.6.1 and 6.6.2 respectively.

6.6.5 The Reaction of $\text{Ir}(\text{PF}_2)(\text{CO})(\text{PEt}_3)_2\text{Cl}_2$ with Sulphur

$\text{Ir}(\text{PF}_2)(\text{CO})(\text{PEt}_2)\text{Cl}_2$ (0.060 g; 0.1 m mole) was dissolved in a mixture of dry toluene and CS_2 (50%:50%) (5 ml). To the solution was added flowers of sulphur (0.004 g; 0.12 mmole). The resulting slurry was stirred for 15 hours at room temperature, under nitrogen. After this time the solvents were pumped off; following this a further 2 ml of toluene was added to the residue. Residual S_8 was filtered off. The filtrate was concentrated by evaporation of solvent and microcrystalline off-white solid was precipitated out on addition of petrol ether (40° - 60°).

Analytical and i.r. spectral data for the product $\text{Ir}(\text{PF}_2\text{S})(\text{CO})(\text{PEt}_3)_2\text{Cl}_2$ are presented in Tables 6.6.1 and 6.6.2 respectively.

6.6.6 The Reaction of $\text{Ir}(\text{PF}_2)(\text{CO})(\text{PEt}_3)_2\text{Cl}_2$ with Selenium

The procedure followed was as in 6.6.5 using red selenium in place of flowers of sulphur.

Analytical and i.r. spectral data for the pale-yellow micro-crystalline solid $\text{Ir}(\text{PF}_2\text{Se})(\text{CO})(\text{PEt}_3)_2\text{Cl}_2$ are presented in Tables 6.6.1 and 6.6.2 respectively.

6.6.7 The Reaction of $\text{Ir}(\text{PF}_2)(\text{CO})(\text{PET}_3)_2\text{Cl}_2$ with Oxygen

A sample of $\text{Ir}(\text{PF}_2)(\text{CO})(\text{PET}_3)_2\text{Cl}_2$ was dissolved in methylene chloride and left in an open vessel for 1 week. Crystals of $\text{Ir}(\text{PF}_2\text{O})(\text{CO})(\text{PET}_3)_2\text{Cl}_2$ were obtained after dissolving the solid in the minimum of CH_2Cl_2 , adding sufficient petrol-ether ($40^\circ\text{--}60^\circ$) to cause cloudiness and allowing the solvent to evaporate gradually.

6.6.8 The Reaction of $\text{Ir}(\text{PF}_2)(\text{CO})(\text{PET}_3)_2\text{Cl}_2$ with H_2O

$\text{Ir}(\text{PF}_2)(\text{CO})(\text{PET}_3)_2\text{Cl}_2$ was made in situ as in 6.6.3. Once all volatiles had been pumped off, the n.m.r. tube was removed from the line and 0.05 ml H_2O introduced quickly into the tube by means of a syringe. The tube was replaced onto the line and re-evacuated then the standard procedure for setting up a reaction in a sealed n.m.r. tube was applied.

6.6.9 The Reaction of $\text{PdCl}_2(\text{COD})$ with $\text{Ir}(\text{PF}_2)(\text{CO})(\text{PET}_3)_2\text{Cl}_2$

$\text{PdCl}_2(\text{COD})$ (0.03 g; 0.1 mmole) was added to a solution of $\text{Ir}(\text{PF}_2)(\text{CO})(\text{PET}_3)_2\text{Cl}_2$ (0.12 g; 0.2 mmole) in CH_2Cl_2 (3 ml). The slurry was stirred for 20 minutes. The resultant yellow powder was filtered off and washed with CH_2Cl_2 and petrol-ether ($40^\circ\text{--}60^\circ$), then dried under high vacuum.

The resultant solid was shown to be a mixture of complexes, which could not be isolated pure.

6.6.10 The Reaction of $\text{PtCl}_2(\text{COD})$ with $\text{Ir}(\text{PF}_2)(\text{CO})(\text{PEt}_3)_2\text{Cl}_2$ -

$\text{PtCl}_2(\text{COD})$ (0.04 g; 0.1 mmole) was added to a solution of $\text{Ir}(\text{PF}_2)(\text{CO})(\text{PEt}_3)_2$ (0.11 g; 0.18 mmole) in CH_2Cl_2 . The resulting solution was shaken for ca. 5 minutes, after which time all volatiles were pumped off. The residue was redissolved and the resulting solution filtered. The solvent was evaporated off from the filtrate and the residue (white powder) was maintained at 70°C for 3 hours under vacuum to remove the residual free COD. The white solid was crystallised by evaporating a CH_2Cl_2 /diethyl ether solution of the solid *to dryness*.

Analytical and i.r. spectral data for the product $[(\text{Cl}_2(\text{PEt}_3)_2(\text{CO})(\text{PF}_2)\text{Ir})_2\text{PtCl}_2]$ are presented in Table 6.6.1 and 6.6.2 respectively.

6.6.11 The Reactions of $[\text{MCl}_2(\text{arene})]_2$ with $\text{Ir}(\text{PF}_2)(\text{CO})-(\text{PEt}_3)_2\text{Cl}_2$ -

The same procedure was used for all three reactions of $[\text{MCl}_2(\text{arene})]_2$ [$\text{M} = \text{Ru}$; arene = benzene, p-cymene; $\text{M} = \text{Os}$; arene = p-cymene)]. In a typical reaction $[\text{MCl}_2(\text{arene})]_2$ (0.1 mmole) was added to a solution of $\text{Ir}(\text{PF}_2)(\text{CO})(\text{PEt}_3)_2\text{Cl}_2$ (0.2 mmole) in dry degassed toluene. The resultant slurries were stirred for ca. 18 hours to yield an orange-red precipitate when $\text{M} = \text{Ru}$ and a bright-yellow precipitate when $\text{M} = \text{Os}$. The solids were filtered under nitrogen and then washed with degassed toluene and petrol-ether (40°O - 60°O). The complexes $\text{Cl}_2(\text{PEt}_3)_2(\text{CO})\text{Ir}-\text{PF}_2-\text{MCl}_2(\text{p-cymene})$ were recrystallised from nitromethane.

Table 6.6.1 Analytical data for complexes synthesised
and isolated from the reactions described in
Chapter 3

| Complex | Found | | Required | |
|--|-------|-----|----------|-----|
| | %C | %H | %C | %H |
| $\text{Ir}(\text{PF}_2\text{BH}_3)(\text{CO})(\text{PEt}_3)_2\text{I}_2$ | 20.3 | 4.1 | 19.7 | 4.2 |
| $\text{Ir}(\text{PF}_2\text{S})(\text{CO})(\text{PEt}_3)_2\text{Cl}_2$ | 25.1 | 4.8 | 25.1 | 4.8 |
| $\text{Ir}(\text{PF}_2\text{Se})(\text{CO})(\text{PEt}_3)_2\text{Cl}_2$ ^[a] | 26.8 | 4.9 | 23.1 | 4.4 |
| $(\text{Cl}_2(\text{PEt}_3)_2(\text{CO})\text{Ir}-\mu\text{-PF}_2)_2\text{PtCl}_2$ | 21.7 | 4.1 | 21.4 | 4.1 |
| $\text{Cl}_2(\text{PEt}_3)_2(\text{CO})\text{Ir-PF}_2\text{-RuCl}_2(\text{p-cymene})$ | 30.4 | 5.0 | 30.6 | 4.9 |
| $\text{Cl}_2(\text{PEt}_3)_2(\text{CO})\text{Ir-PF}_2\text{-OsCl}_2(\text{p-cymene})$ | 27.9 | 4.6 | 27.8 | 4.4 |

[a] Sample was not completely dry. Figures are acceptable if one assumes that the sample is contaminated by 3/4 mole toluene per mole of complex; requires %C = 26.9; %H = 4.7

Table 6.6.2 Infra-red spectral data for complexes synthesised and isolated from reactions described in Chapter 2.

| | |
|--|---|
| $\text{Ir}(\text{PF}_2\text{BH}_3)(\text{CO})(\text{PEt}_3)_2\text{I}_2$ | 2410m, 2393m, 2345m, 2065vs, 2055vs, 1260m, 1240w, 1120m, 1055s, 1035vs, 840s, 820s, 805vs, 780s, 740s, 708s, 620m, 542m, 528m, 420m, 380m. |
| $\text{Ir}(\text{PF}_2\text{S})(\text{CO})(\text{PEt}_3)_2\text{Cl}_2$ | 2060s, 1260m, 1238w, 1030s, 820s, 800vs, 760s, 740s, 730s, 716s, 680s, 620w, 560m, 549m, 505w, 453m, 410w, 395w, 380m, 320w, 300vw, 280m. |
| $\text{Ir}(\text{PF}_2\text{Se})(\text{CO})(\text{PEt}_3)_2\text{Cl}_2$ | 2063s, 1244w, 1240w, 1215w, 1030s, 810s, 759s, 740s, 730s, 620w, 580s, 560m, 540m, 500w, 433w, 410w, 385w, 322w, 300w, 280m. |
| $(\text{Cl}_2(\text{PEt}_3)_2(\text{CO})\text{Ir}-\mu\text{-PF}_2)_2\text{PtCl}_2$ | 2045vs, 2005w, 1258m, 1080bw, 1025s, 840s, 785s, 755s, 715s, 555m, 535m, 465s, 405w, 380w, 315w, 295w, 275w. |
| $\text{Cl}_2(\text{PEt}_3)_2(\text{CO})\text{Ir-PF}_2\text{-RuCl}_2\text{-}(\eta_6\text{-benzene})$ | 2055vs, 1265w, 1250w, 1150m, 1035s, 820m, 810s, 800s, 778s, 750m, 722s, 555s, 475m, 455m, 430w, 305w, 275w. |
| $\text{Cl}_2(\text{PEt}_3)_2(\text{CO})\text{Ir-PF}_2\text{-RuCl}_2\text{-}(\eta_6\text{-p-cymene})$ | 2063vs, 1270w, 1034s, 800s, 765s, 755sh, 722s, 550m, 465m, 320w, 300w, 260w, 249w. |
| $\text{Cl}_2(\text{PEt}_3)_2(\text{CO})\text{Ir-PF}_2\text{-OsCl}_2\text{-}(\eta_6\text{-p-cymene})$ | 2063vs, 1325w, 1267m, 1158w, 1115w, 1090w, 1035s, 910w, 878w, 802vs, 768vs, 725vs, 692w, 620w, 555s, 500m, 473s, 445sh, 418w, 341w, 320w, 310w, 265w. |

Abbreviations: vs=very strong; s=strong; m=medium; w=weak;
b=broad; sh=shoulder

Data were obtained from nujol mulls of the solids on CsI plates

Analytical data for $\text{Cl}_2(\text{PEt}_3)_2(\text{CO})\text{Ir-PF}_2\text{-MCl}_2$ (p-cymene) are presented in Table 6.6.1. Infra-red spectral data for all three product complexes are presented in Table 6.6.2.

6.7 Experimental Related to the Reactions Described in Chapter 4

6.7.1 The Synthesis of $\text{M}(\text{PCl}_2)(\text{CO})(\text{PEt}_3)_2\text{Cl}_2$ [M = Ir, Rh]

In a typical reaction a drop of PCl_3 was added to a solution of $\text{MCl}(\text{CO})(\text{PEt}_3)_2$ (0.2 mmole) in degassed toluene. In the synthesis of $\text{Ir}(\text{PCl}_2)(\text{CO})(\text{PEt}_3)_2\text{Cl}_2$ the solution immediately became colourless on addition of PCl_3 ; in that of $\text{Rh}(\text{PCl}_2)(\text{CO})(\text{PEt}_3)_2\text{Cl}_2$ there was no apparent colour change. The solvent and the excess of PCl_3 were then pumped off, the residue was then dissolved in the minimum amount of toluene and microcrystalline solids precipitated out by adding petrol-ether ($40^\circ\text{-}60^\circ$).

Analytical data for $\text{M}(\text{PCl}_2)(\text{CO})(\text{PEt}_3)_2\text{Cl}$ are presented in Table 6.7.1. Infra-red spectral data for $\text{Ir}(\text{PCl}_2)(\text{CO})-(\text{PEt}_3)_2\text{Cl}_2$ are presented in Table 6.7.2.

6.7.2 The Reaction of $\text{Rh}(\text{PCl}_2)(\text{CO})(\text{PEt}_3)_2\text{Cl}_2$ with $\text{IrCl}(\text{CO})(\text{PEt}_3)_2$

$\text{Rh}(\text{PCl}_2)(\text{CO})(\text{PEt}_3)_2\text{Cl}_2$ (0.05 g; 0.09 mmole) and $\text{IrCl}(\text{CO})(\text{PEt}_3)_2$ (0.05 g; 0.1 mmole) were each weighed into a n.m.r. tube, the standard procedure for setting up a reaction in a sealed n.m.r. tube was then carried out (see Section 6.4).

6.7.3 Reactions of $\text{Ir}(\text{PCl}_2)(\text{CO})(\text{PEt}_3)_2\text{Cl}_2$ with volatile Reagents

The standard procedure for setting up a reaction in an n.m.r. tube was applied for the reactions of $\text{Ir}(\text{PCl}_2)(\text{CO})(\text{PEt}_3)_2\text{Cl}_2$ with HCl , H_2S , H_2Se , MeOH and Cl_2 (see Section 6.4).

6.7.4 The Reactions of $\text{Ir}(\text{PCl}_2)(\text{CO})(\text{PEt}_3)_2\text{Cl}_2$ with Sulphur and Selenium

The procedures for both these reactions were exactly the same. The group VIB elements (S_8 , red Se) (0.1 mmole) were added to solutions of $\text{Ir}(\text{PCl}_2)(\text{CO})(\text{PEt}_3)_2\text{Cl}_2$ (0.06g; 0.1 mmole) in $\text{CHCl}_3/\text{CS}_2$ (50%:50%) mixed solvent. The reactions were stirred for 15 hours under nitrogen after which time all volatiles were pumped off. The residues were washed with CHCl_3 and any excess of S_8 or Se filtered off. The volume of filtrate was reduced and powders precipitated out of solution on addition of petrol-ether ($40^\circ\text{--}60^\circ$).

6.7.5 The Reaction of $\text{Ir}(\text{PCl}_2)(\text{CO})(\text{PEt}_3)_2\text{Cl}_2$ with Oxygen

A solution of $\text{Ir}(\text{PCl}_2)(\text{CO})(\text{PEt}_3)_2\text{Cl}_2$ (0.06 g; 0.1 mmole) in toluene (3 ml) was stirred under an atmosphere of air for ca. 2 weeks. The solvent was pumped off and subsequently the residue was dissolved in the minimum amount of CHCl_3 . A white solid was precipitated out in poor yield on adding petrol-ether ($40^\circ\text{--}60^\circ$) to the solution.

6.7.6 The Reaction of $\text{Ir}(\text{PCl}_2)(\text{CO})(\text{PEt}_3)_2\text{Cl}_2$ with H_2O

$\text{Ir}(\text{PCl}_2)(\text{CO})(\text{PEt}_3)_2$ (0.06 g; 0.1 mmole) was weighed into a n.m.r. tube. Then 0.05 ml of H_2O was introduced into the tube by means of a syringe. The tube was evacuated and then the H_2O washed down the sides of the tube on addition of solvent (CD_2Cl_2). The tube was then sealed using the standard technique.

6.7.7 The Isolation of $\text{Ir}(\text{PH}_2\text{Se})(\text{CO})(\text{PEt}_3)_2\text{Cl}_2$

The n.m.r. tube in which the reaction of H_2Se with $\text{Ir}(\text{PCl}_2)(\text{CO})(\text{PEt}_3)_2\text{Cl}_2$ was studied was opened under nitrogen and the contents washed into a Schlenk tube. The contents of the tube consisted of two layers, the upper-layer being a yellow solution and the lower an orange oil. The upper solution was drawn off the oil using a pasteur pipette and transferred to another Schlenk tube; the oil was washed twice with 1 ml aliquots of dry degassed toluene, and the washings were transferred to the Schlenk tube containing the original solution. The volatiles from the solution were pumped off. The residue was then dissolved in the minimum of CH_2Cl_2 and a pale yellow solid was precipitated out on addition of petrol-ether ($40^\circ\text{--}60^\circ$).

Analytical and i.r. spectral data for $\text{Ir}(\text{PH}_2\text{Se})(\text{CO})-(\text{PEt}_3)_2\text{Cl}_2$ are presented in Tables 6.7.1 and 6.7.2 respectively.

6.7.8 The Isolation of $\text{Ir}(\text{HPCl}(\text{S}))(\text{CO})(\text{PEt}_3)_2\text{Cl}_2$

The n.m.r. tube in which the reaction of H_2S and $\text{Ir}(\text{PCl}_2)(\text{CO})(\text{PEt}_3)_2\text{Cl}_2$ was studied was opened under nitrogen and the contents transferred into a Schlenk tube with careful washing with dry toluene. After attaching the Schlenk tube to the Schlenk line all volatiles were pumped off and the residue was triturated with petrol-ether (40° - 60°) to yield a cream coloured powder.

Analytical and i.r. spectral data for $\text{Ir}(\text{HPCl}(\text{S}))(\text{CO})-(\text{PEt}_3)_2\text{Cl}_2$ are presented in Tables 6.7.1 and 6.7.2 respectively.

6.7.9 The Isolation of $\text{Ir}(\text{HPO}_2\text{H})(\text{CO})(\text{PEt}_3)_2\text{Cl}_2$

The n.m.r. tube in which the reaction was studied was opened and the contents transferred to a Schlenk tube with careful washing with toluene. All volatiles were pumped off (the residue was maintained under vacuum for 4 hours to ensure that most of the excess of H_2O had been removed). A white solid was obtained on trituration with a petrol-ether/diethylether mixture. Crystals of the complex were obtained on allowing the solvent from a concentrated solution of $\text{Ir}(\text{HPO}_2\text{H})(\text{CO})(\text{PEt}_3)_2\text{Cl}_2 [\text{H}_3\text{O}^+\text{Cl}^-]$ in CHCl_3 /petrol-ether to evaporate slowly.

Analytical and i.r. spectral data for $\text{Ir}(\text{HPO}_2\text{H})(\text{CO})-(\text{PEt}_3)_2\text{Cl}_2 [\text{H}_3\text{O}^+\text{Cl}^-]$ are presented in Tables 6.7.1 and 6.7.2 respectively.

Table 6.7.1 Analytical Data for complexes synthesised
and isolated from the reactions described in
Chapter 4

| Complex | Found | | Required | |
|---|-------|-----|----------|-----|
| | %C | %H | %C | %H |
| $\text{Ir}(\text{PCl}_2)(\text{CO})(\text{PEt}_3)_2\text{Cl}_2$ | 24.6 | 4.7 | 24.8 | 4.8 |
| $\text{Rh}(\text{PCl}_2)(\text{CO})(\text{PEt}_3)_2\text{Cl}_2$ | 28.7 | 5.6 | 28.9 | 5.6 |
| $\text{Ir}(\text{PH}_2\text{Se})(\text{CO})(\text{PEt}_3)_2\text{Cl}_2$ | 24.4 | 4.8 | 24.4 | 5.0 |
| $\text{Ir}(\text{PHCl}(\text{S}))(\text{CO})(\text{PEt}_3)_2\text{Cl}_2$ ^[a] | 24.8 | 5.0 | 25.0 | 5.1 |
| $\text{Ir}(\text{HPO}_2\text{H})(\text{CO})(\text{PEt}_3)_2\text{Cl}_2$ $[\text{H}_3\text{O}^+\text{Cl}^-]$ | 24.7 | 5.4 | 24.1 | 5.4 |
| $\text{Ir}(\text{PCl}_4)(\text{CO})(\text{PEt}_3)_2\text{Cl}_2$ | 22.0 | 4.2 | 22.3 | 4.3 |

[a] %Cl Found = 18.3, Required = 16.9;

%S Found = 6.1, Required = 5.1

Table 6.7.2

Infra-red spectral data for complexes synthesised and isolated from the reactions described in Chapter 4.

| | |
|---|---|
| $\text{Ir}(\text{PCl}_2)(\text{CO})(\text{PEt}_3)_2\text{Cl}_2$ | 2045vs, 1255m, 1235w, 1090m, 1030s, 935s, 925s, 900s, 770m, 740s, 710m, 670w, 615m, 575s, 515w, 478w, 495m, 480m, 411w, 375w, 320m, 305w, 280wsh, 270m, 230w. |
| $\text{Ir}(\text{PH}_2\text{Se})(\text{CO})(\text{PEt}_3)_2\text{Cl}_2$ [a] | 2340w, 2320w, 2290w, 2055vs, 1260m, 1105m, 1070s, 885s, 765s, 740s, 710w, 550m, 480m, 380w, 310w. |
| $\text{Ir}(\text{PHCl}(\text{S}))(\text{CO})(\text{PEt}_3)_2\text{Cl}_2$ | 2390w, 2050vs, 1260m, 1240m, 1030s, 925m, 885m, 758s, 740s, 730s, 710m, 645s, 565m, 510w, 460s, 430sh, 390w, 350w, 320w, 305vw. |
| $\text{Ir}(\text{HPO}_2\text{H})(\text{CO})(\text{PEt}_3)_2\text{Cl}_2$ $[\text{H}_3\text{O}^+\text{Cl}^-]$ | 3160bw, 2720w, 2680w, 2280w, 2050vs, 1300w, 1260m, 1165w, 1150w, 1097m, 1054w, 1032s, 988w, 935s, 925s, 900s, 850bsh, 770s, 740s, 720m, 710s, 670w, 620w, 565s, 512m, 442m, 428m, 380m, 320m, 300w, 280wsh, 265m. |
| ' $\text{Ir}(\text{PCl}_4)(\text{CO})(\text{PEt}_3)_2\text{Cl}_2$ ' | 2060vs, 1295w, 1257m, 1245m, 1210w, 1150w, 1050m, 1030m, 998w, 950bw, 855w, 760m, 715s, 570m, 555m, 530m, 490w, 330m, 310m |

Abbreviations: v = very, s = strong, m = medium, w = weak,
b = broad, sh = shoulder

6.7.10 The Isolation of $\text{Ir}(\text{PCl}_4)(\text{CO})(\text{PEt}_3)_2\text{Cl}_2$ "
of Cl_2 and $\text{Ir}(\text{PCl}_2)(\text{CO})(\text{PEt}_3)_2\text{Cl}_2$

The n.m.r. tube in which the reaction was studied was opened under nitrogen. The contents of the tube were then transferred to a Schlenk tube and the solid in the n.m.r. tube was carefully washed into the Schlenk tube with degassed CHCl_3 . A little petrol-ether ($40^\circ\text{--}60^\circ$) was added to the suspension and the solid allowed to settle to the bottom of the Schlenk tube after which the solvent was drawn off using a Pasteur pipette. The solid was washed with a further portion of CHCl_3 /petrol-ether with solvents being drawn off after allowing the solid to settle. The solid was dried under high vacuum for 5 hours.

Analytical and i.r. spectral data for $\text{Ir}(\text{PCl}_4)(\text{CO})(\text{PEt}_3)_2\text{Cl}_2$ are presented in Tables 6.7.1 and 6.7.2 respectively.

6.8 Experimental Related to the Reactions Described in Chapter 5

6.8.1 Preparation of $\text{RhX}(\text{CO})(\text{PEt}_3)_2$ [$\text{X} = \text{Cl}, \text{Br}, \text{I}$]

$\text{RhCl}(\text{CO})(\text{PEt}_3)_2$

$\text{RhCl}(\text{CO})(\text{PEt}_3)_2$ was prepared using standard literature methods⁽¹⁶¹⁾ by refluxing $\text{RhCl}_3 \cdot 3\text{H}_2\text{O}$ in KOH , H_2O , MeOH and ethanol. The complex was purified by subliming under high vacuum at 110°C .

RhBr(CO)(PEt₃)₂

A solution of RhCl(CO)(PEt₃)₂ (0.3 g; 0.67 mmole) in acetone (5 ml) was stirred with a 300% excess of LiBr for 1 hour. The solvent was then pumped off. The product was collected as yellow needles by sublimation of the residue at 110°C.

RhI(CO)(PEt₃)₂

The procedure used was as for RhBr(CO)(PEt₃)₂ except that only a 100% excess of NaI was used and the slurry was stirred for only 15 minutes.

6.8.2 The Reactions of PF₂X with RhX(CO)(PEt₃)₂

These reactions were carried out and studied in sealed n.m.r. tubes. The standard procedure for setting up such an experiment is described in section 6.4.

APPENDIX I

Reactions of some Aminodifluorophosphines

with $\text{IrX(CO)(PEt}_3)_2$ [X =, Cl, Br, I]

AI.1 Introduction

There is a vast number of reported reactions of amino-difluorophosphines (PF_2NR_2) with metal complexes^(17,42). In general, it has been found that they react in a similar manner to PF_3 (see 1.2).

There have been no previous reports of reactions of PF_2NR_2 with Vaska's type complexes; in fact there are few reports of reactions of any fluorophosphine compounds with this type of complex. Grosse and Schmutzler have reported the reaction $\text{PF}_2\text{OC}_3\text{H}_5$ with Vaska's compound⁽¹⁶²⁾. They were unable to characterise fully the products formed by the reaction but two different complexes were produced depending on the mole ratio of fluorophosphine to Vaska's compound; the two species were formulated as $[\text{C}_3\text{H}_5\text{PPh}_3]_2^+[\text{IrCl}(\text{CO})(\text{PF}_2\text{O})_2]^{2-}$ and $[\text{C}_3\text{H}_5\text{-PPh}_3]_2^+[\text{Ir}(\text{PF}_2\text{O})_3(\text{PF}_2\text{OC}_3\text{H}_5)]^{2-}$.

In this work the reactions of $\text{PF}_2\text{NRR}'$ [$\text{R} = \text{R}' = \text{H}, \text{Me}; \text{R} = \text{H}, \text{R}' = \text{Me}$] with $\text{IrX}(\text{CO})(\text{PEt}_3)_2$ [$\text{X} = \text{Cl}, \text{Br}, \text{I}$] were studied. Phosphorus-31 and fluorine 19-n.m.r. were used to characterise species and the n.m.r. data for the different types of products are presented in Tables AI.1, AI.2 and AI.3.

AI.2 The Reaction of PF_2NMe_2 with $\text{IrX}(\text{CO})(\text{PEt}_3)_2$ [$\text{X} = \text{Cl}, \text{Br}, \text{I}$]

These reactions were studied in sealed n.m.r. tubes using a 1:1 molar ratio of reactants with toluene as solvent.

Reaction occurs at 193 K in all three cases. Each reaction gives rise to only one product.

At 193 K, the $^{31}\text{P}\{-^1\text{H}\}$ n.m.r. spectra of all three products were qualitatively the same as those already described for $\text{Ir}(\text{PF}_2\text{X})(\text{CO})(\text{PEt}_3)_2\text{Y}$. The high frequency resonance arising from the PF_2 phosphorus nucleus broadened for the complexes formed in the reaction of PF_2NMe_2 with $\text{IrX}(\text{CO})(\text{PEt}_3)_2$ [$\text{X} = \text{Cl}, \text{I}$] when ^1H coupling was retained; however the equivalent signal for the complex formed from reaction of PF_2NMe_2 with $\text{IrBr}(\text{CO})(\text{PEt}_3)_2$ was split by a further septet coupling, presumably as a result of coupling with the protons of the $-\text{NMe}_2$ group.

The ^{19}F n.m.r. spectra of all three complexes consisted of single resonances split by a wide doublet ($^1\text{J}_{\text{PF}}$). The lines of the signals were very broad, presumably because of unresolved F-H and F-P couplings.

On warming the reaction systems to ambient temperature, the lines of the $^{31}\text{P}\{-^1\text{H}\}$ n.m.r. spectra of the complexes formed from reaction of PF_2NMe_2 with $\text{IrX}(\text{CO})(\text{PEt}_3)_2$ [$\text{X} = \text{Cl}, \text{Br}$] broadened so that the $^2\text{J}_{\text{PP}}$ couplings were not resolved. On recooling to 243 K the couplings were again resolved. Similar effects are not observed for the complex formed in the reaction of PF_2NMe_2 and $\text{IrI}(\text{CO})(\text{PEt}_3)_2$.

The product of the reaction of PF_2NMe_2 with $\text{IrI}(\text{CO})(\text{PEt}_3)_2$ was isolated. The C, H and N analysis figures were consistent with the formulation $\text{IrI}(\text{CO})(\text{PEt}_3)_2(\text{PF}_2\text{NMe}_2)$ (see Table A.1.4). The i.r. spectrum had assignable bands at 1927 cm^{-1} (ν_{CO}); 810 cm^{-1} ($\nu_{\text{P-F}}$).

The data collected suggested that five-coordinate $\text{Ir}(\text{I})$ complexes had been formed in all three reaction systems. The values of the n.m.r. data for the PF_2 group (see Table A.1) fell within ranges associated with PF_2NMe_2 ligands coordinated to metals^(17,46). The fact that the NMe_2 group was still attached to phosphorus was implied by the observed coupling of the PF_2 phosphorus to protons. The observed (ν_{CO}) meant that the complex formed in the reaction involving $\text{IrI}(\text{CO})(\text{PEt}_3)_2$ was centred around $\text{Ir}(\text{I})$; by inference, those formed in the reactions involving $\text{IrX}(\text{CO})(\text{PEt}_3)_2$ would be similar. No direct evidence of X^- bound to iridium was obtained but it was considered that the high solubility of the complexes formed in non-polar solvents (toluene) meant that they were neutral. Therefore the complexes would be isomers of that shown below.

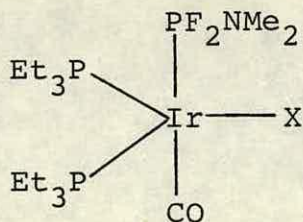
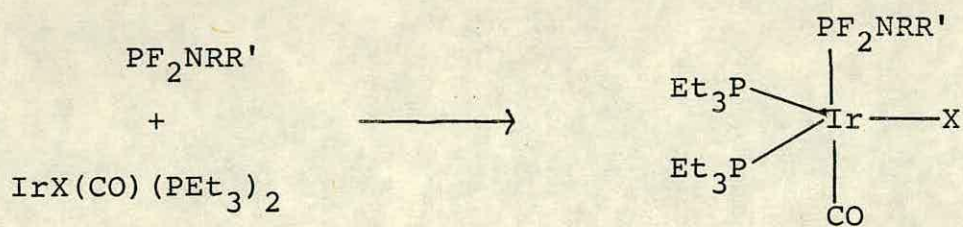
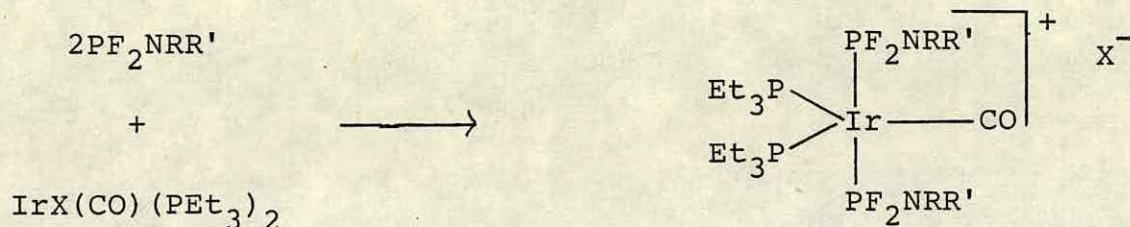


Figure A.1 Summary of Reactions of $\text{PF}_2\text{NRR}'$ with $\text{IrX}(\text{CO})(\text{PEt}_3)_2$



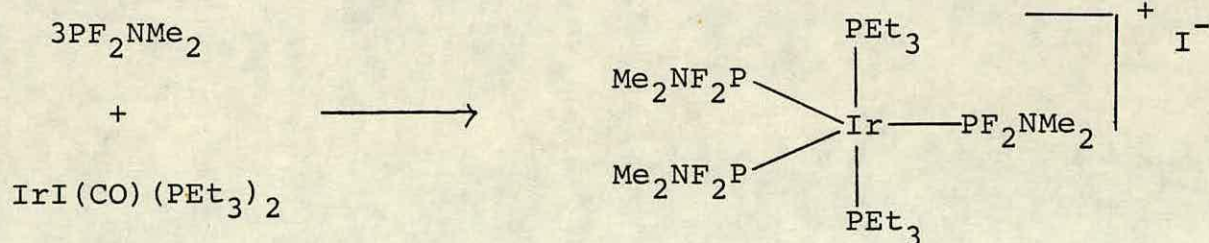
Complexes A(i) - A(v)

- A(i) $\text{X}=\text{Cl}$, $\text{R}=\text{R}'=\text{Me}$;
 A(ii), $\text{X}=\text{Br}$, $\text{R}=\text{R}'=\text{Me}$;
 A(iii), $\text{X}=\text{I}$, $\text{R}=\text{R}'=\text{Me}$;
 A(iv), $\text{X}=\text{I}$, $\text{R}=\text{H}$, $\text{R}'=\text{Me}$;
 A(v), $\text{X}=\text{I}$, $\text{R}=\text{R}'=\text{H}$



Complexes A(vi) - A(viii)

- A(vi), $\text{X}=\text{Cl}$, $\text{R}=\text{R}'=\text{Me}$;
 A(vii), $\text{X}=\text{Cl}$, $\text{R}=\text{H}$, $\text{R}'=\text{Me}$;
 A(viii), $\text{X}=\text{Cl}, \text{Br}, \text{I}$, $\text{R}=\text{R}'=\text{H}$



Complex A(ix)

The broadening of the ^{31}P n.m.r. signals for complexes A(i) and A(ii) (see Figure A.1) at room temperature, was presumably due to free PF_2NMe_2 exchanging with PF_2NMe_2 bound to iridium. One can only presume that no such effect is observed for complex A(iii) (see Figure A.1) because of stronger metal-phosphorus back-bonding in the complex containing the least electronegative halide.

AI.3 The Reaction of PF_2NHMe with $\text{IrI}(\text{CO})(\text{PEt}_3)_2$

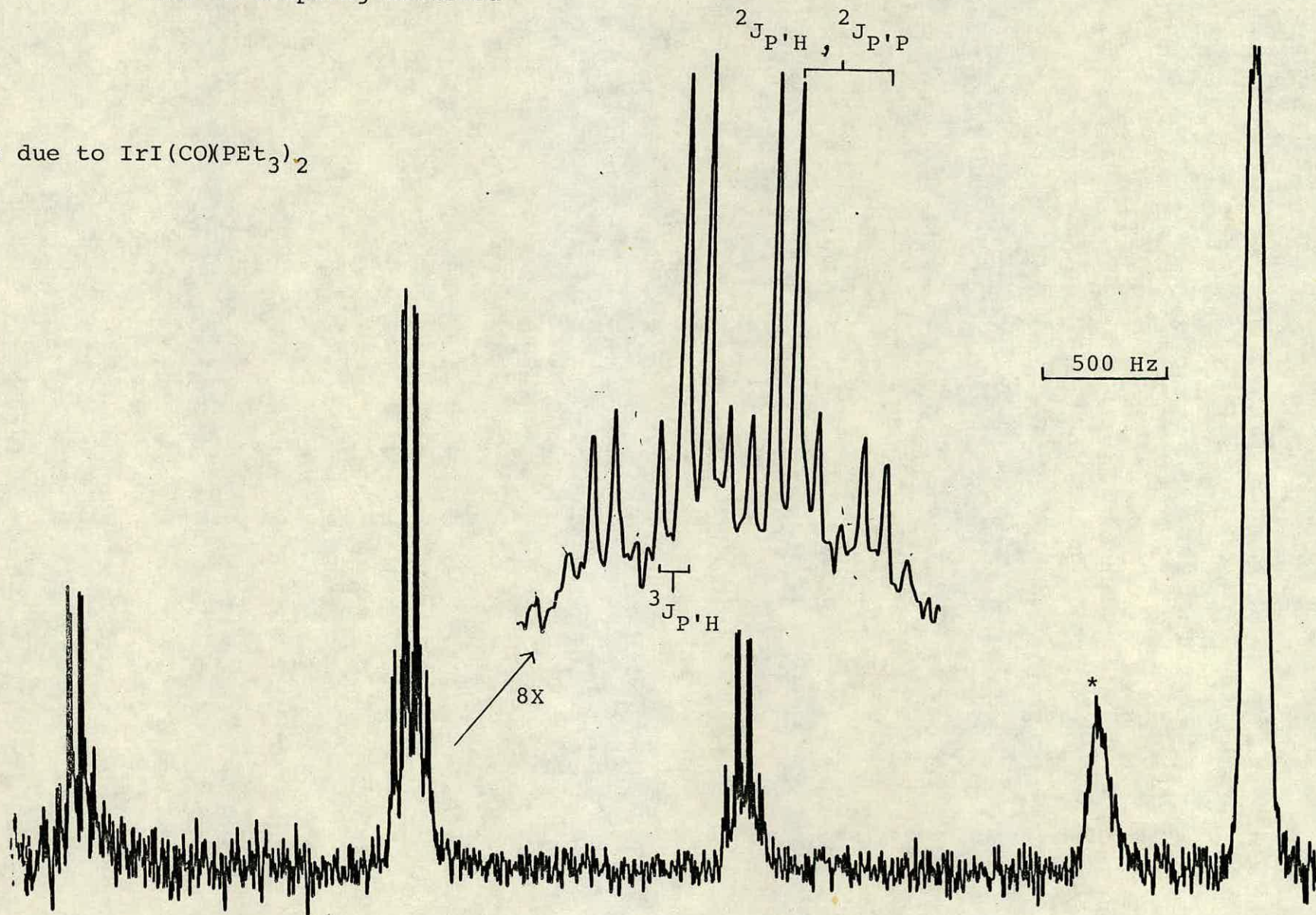
This reaction was carried out in the same manner as those described in AI.2.

At 203 K, a species is formed which is temperature-stable up to room temperature. The $^{31}\text{P}\{-^1\text{H}\}$ n.m.r. spectra for this species are qualitatively the same as those described for complexes A(i)-A(iii). The PF_2 phosphorus resonance was split further when ^1H coupling was retained. The resulting splitting pattern for the resonance (see Figure A.2) was a triplet ($^1J_{\text{PF}}$) of pseudo quartets (this pattern arises because $^2J_{\text{PP}} = ^2J_{\text{PH}}$) of quartets ($^3J_{\text{PH}}$) (see Figure A.2).

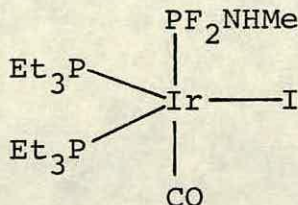
The ^{19}F n.m.r. spectrum consisted of a single resonance split by a wide doublet coupling ($^1J_{\text{PF}}$), the lines of which were split further. An exact interpretation of the splittings could not be made because the resolution was very poor; it was thought that ^1H decoupling would have helped the characterisation of the pattern but at the time the experiment was studied this facility was not available.

Figure A.2 ^{31}P n.m.r. spectrum of $\text{IrI}(\text{CO})(\text{PEt}_3)_2(\text{PF}_2\text{NHMe})$
with ^1H coupling retained

* is due to $\text{IrI}(\text{CO})(\text{PEt}_3)_2$



From the n.m.r. data collected (see Table A.1) it was apparent that the complex formed (A(iv) of Figure A.1) was completely analagous to complexes A(i)-A(iii).



Complex A(iv)

AI.4 The Reaction of PF_2NHMe with $\text{IrCl}(\text{CO})(\text{PEt}_3)_2$

This reaction was initially studied in the same manner as those described in AI.2 and AI.3. At 203 K, a white precipitate dropped out of solution and from the $^{31}\text{P}\{-^1\text{H}\}$ n.m.r. spectrum recorded it was apparent that the only species in solution was $\text{IrCl}(\text{CO})(\text{PEt}_3)_2$. On warming the reaction system to ambient temperature the spectrum did not alter from that described above. The precipitate was isolated and found to dissolve in chloroform.

The n.m.r. spectra of the species formed were completely different from those described in AI.2 and AI.3 for complexes A(i)-A(iv).

The ^{31}P n.m.r. spectrum of this species consisted of two signals. That to high frequency ($\delta\text{P} = 108$ ppm) was split into a complex second order pattern (see Figure A.3). The signal to low frequency, arising from the PEt_3 groups, was split into a triplet (deduced to be $^2\text{J}_{\text{PP}}$) of quintets ($^3\text{J}_{\text{PF}}$).

Figure A.3 $^{31}\text{P}\{-^1\text{H}\}$ n.m.r. spectrum of $[\text{Ir}(\text{PF}_2\text{NHMe})_2(\text{PEt}_3)_2(\text{CO})]\text{Cl}$
showing the PF_2NHMe resonance

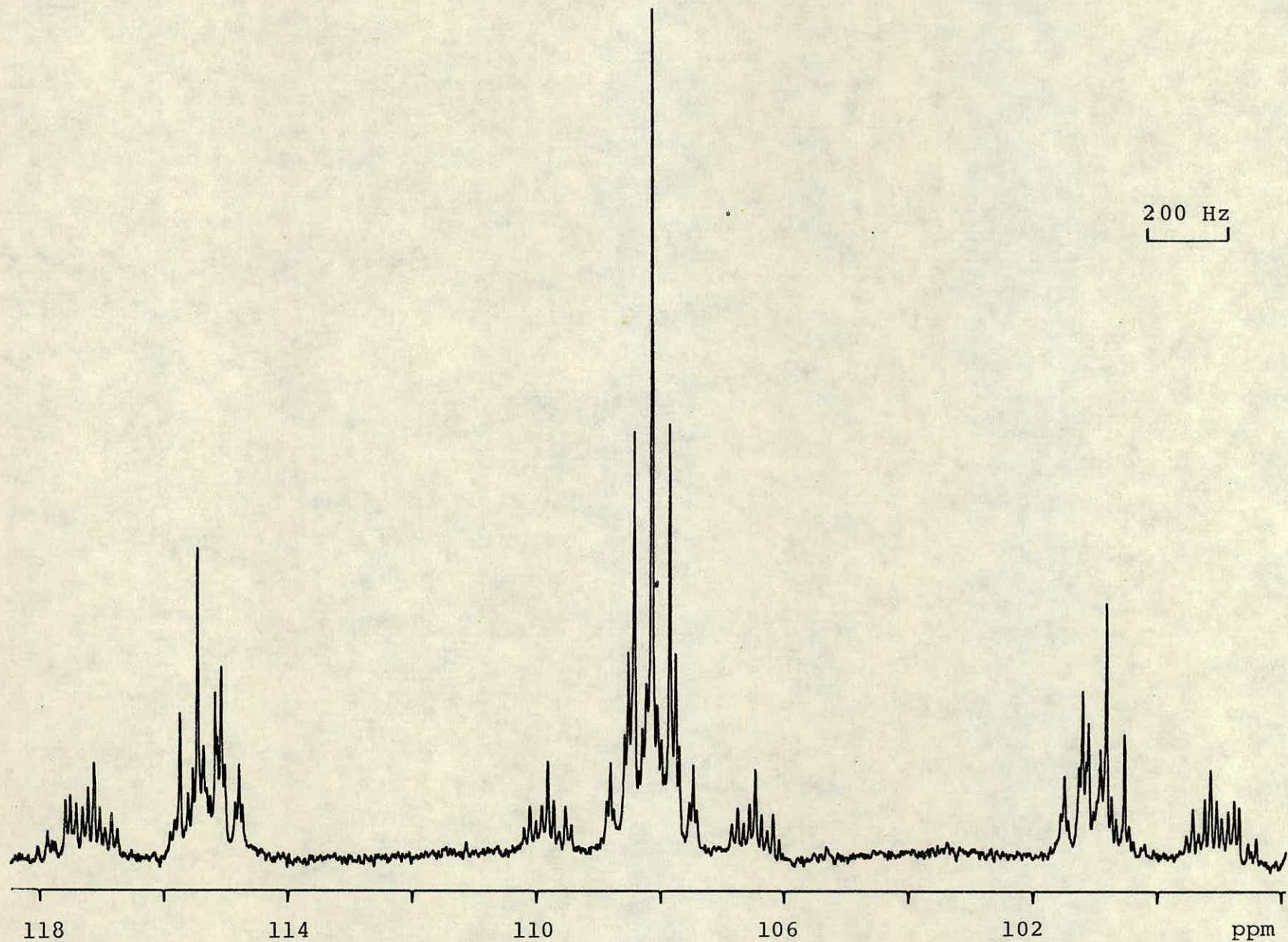
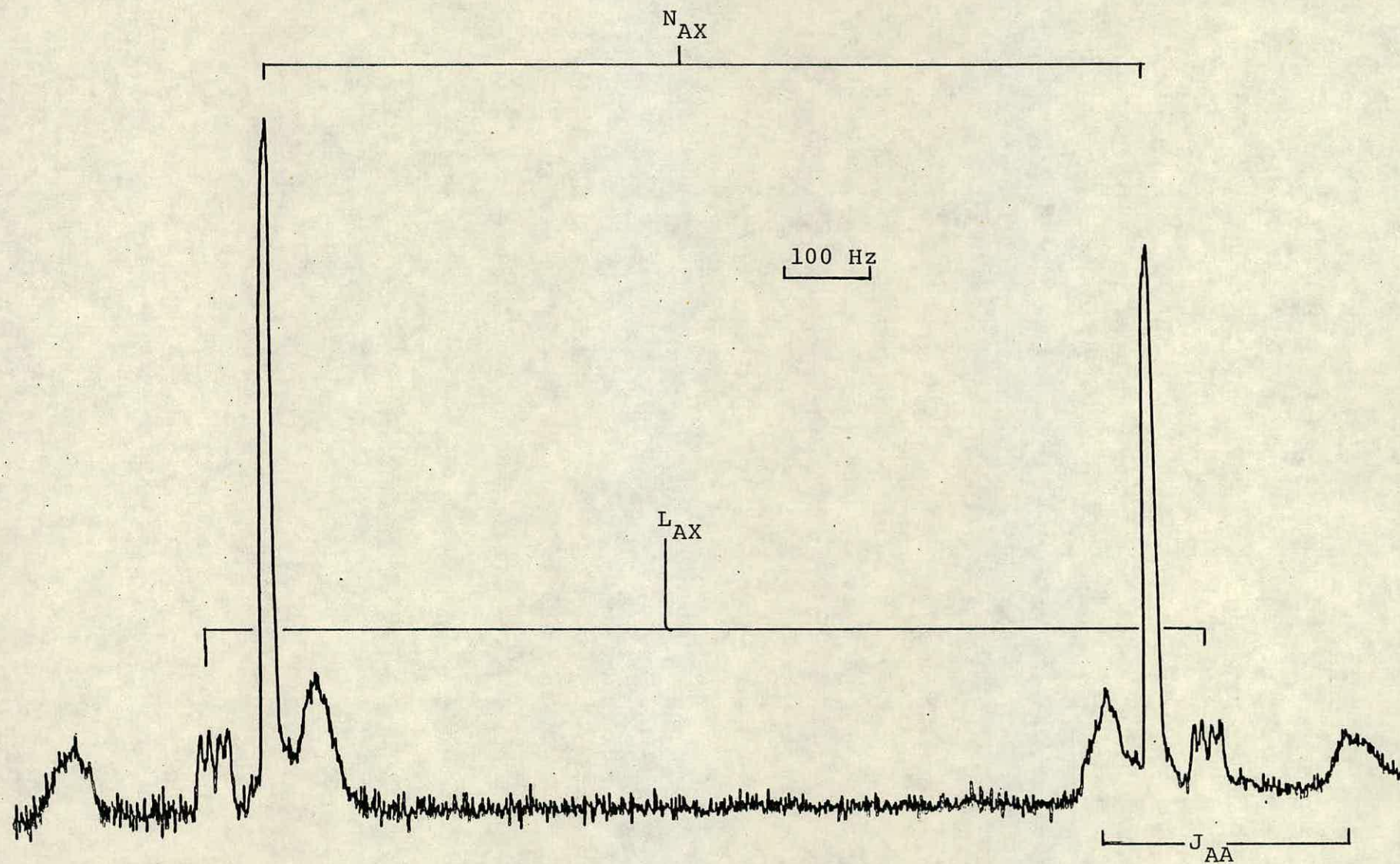


Figure A.4

^{19}F n.m.r. spectrum of $[\text{Ir}(\text{PF}_2\text{NHMe})_2(\text{PEt}_3)_2(\text{CO})]^+\text{Cl}^-$

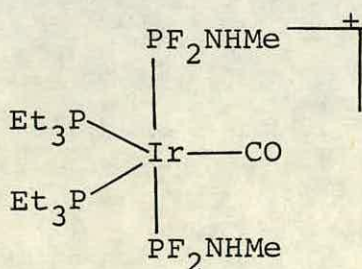


Both signals broadened so that no couplings were resolved when ^1H coupling was retained.

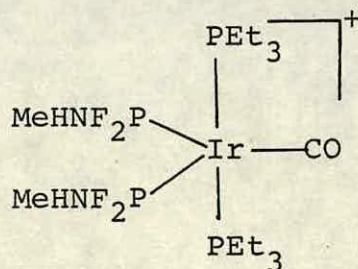
The ^{19}F n.m.r. spectrum consisted of a single resonance split into a complex second order pattern (see Figure A.4) which was consistent with the expected pattern for the X resonance of an $[\text{AX}_2]_2$ spin system⁽¹³¹⁾ (see 2.2).

Carbon, hydrogen and nitrogen analysis figures were obtained for the complex which were consistent with the formulation $[\text{Ir}(\text{PF}_2\text{NHMe})_2(\text{PEt}_3)_2(\text{CO})]^+\text{Cl}^-$. The i.r. spectrum of the complex contained assignable bands at: 3112 cm^{-1} ($\nu_{\text{N-H}}$); 1963 cm^{-1} (ν_{CO}).

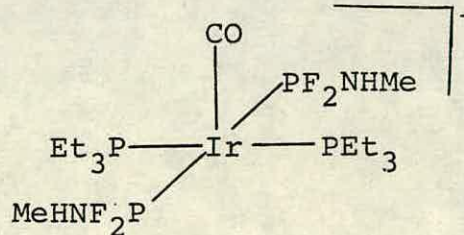
The complex was found to be conducting in nitromethane. It was apparent from the data collected that a cationic five-coordinate Ir(I) complex had been formed with two PF_2NHMe ligands, two PEt_3 ligands and a CO ligand bound to iridium. (Since the complex was conducting in solution it seemed likely that Cl^- had been displaced from the iridium centre). The most likely formulation for the product was therefore $[\text{Ir}(\text{PF}_2\text{NHMe})_2(\text{PEt}_3)_2(\text{CO})]^+\text{Cl}^-$. There are three possible isomers for this complex if one assumes that the PF_2NHMe groups are magnetically equivalent with respect to the PEt_3 groups.



(A)



(B)



(C)

From the ^{19}F n.m.r. spectrum it was possible to determine $^2J_{\text{P,P'}}$ (the coupling between the two PF_2NHMe phosphorus atoms) (see 2.2) as 293 Hz which meant that the two PF_2NHMe groups must have been mutually trans and the product (complex A(vii)) was (A) or (C). From the data available it was not possible to decide which of the two was correct.

AI.5 The Reaction of PF_2NH_2 with $\text{IrX}(\text{CO})(\text{PEt}_3)_2$ [X = Cl, Br]

These reactions were initially studied in the same manner as those described in AI.2 and AI.3.

At 203 K, a white solid precipitated from solution; from the $^{31}\text{P}\{-^1\text{H}\}$ n.m.r. spectra of the reaction media it was apparent that the only species in solution were $\text{IrX}(\text{CO})(\text{PEt}_3)_2$. On warming the reaction system to ambient temperature it did not alter from that described above. The precipitates were isolated and found to dissolve in methylene chloride.

The n.m.r. spectra of the products from both reactions were found to be identical, as were the values of their n.m.r. parameters (complex A(viii), Table A.1.2). The n.m.r. spectra of the products were qualitatively the same as those described for A(vii).

Carbon, hydrogen and nitrogen analysis figures were obtained for the complex which were reasonably consistent with the formulation $[\text{Ir}(\text{PF}_2\text{NH}_2)_2(\text{PEt}_3)_2\text{CO}]^+\text{Cl}^-$.

The i.r. spectrum showed ν_{CO} at 1951 cm^{-1} .

The complex was also found to be conducting in nitromethane.

All the data obtained relating to the reactions described in this section implied that complexes of the same type as A(vii) had been formed. Support for this formulation came from the observation that the n.m.r. parameters of the products from both reactions were identical as one would expect for complexes whose only difference in structure was their counterion. (The complex produced was A(viii) of Figure A.1).

AI.6 The Reaction of PF_2NH_2 with $\text{IrI}(\text{CO})(\text{PEt}_3)_2$

This reaction was studied in the same manner as those described in AI.2 and AI.3.

At 203 K, reaction takes place producing a product whose ^{31}P and ^{19}F n.m.r. spectra were qualitatively the same as those of complexes A(i)-A(iv). The species formed was temperature stable up to ambient temperature.

From the n.m.r. spectra it was apparent that the complex $\text{Ir I}(\text{CO})(\text{PEt}_3)_2(\text{PF}_2\text{NH}_2)$ (complex A(v), Figure A.1) had probably been produced.

The reaction was studied a second time; this time the reaction medium was warmed rapidly to ambient temperature and a white solid was precipitated from the toluene solution. The white solid was isolated and found to dissolve in methylene chloride. Its $^{31}\text{P}\{-^1\text{H}\}$ n.m.r. spectrum was recorded and found to be identical to that of complex A(viii) which implied that $[\text{Ir}(\text{PF}_2\text{NH}_2)_2(\text{PEt}_3)_2\text{CO}]\text{I}$ had presumably been produced.

AI.7 The Reaction of PF_2NMe_2 with $\text{IrCl}(\text{CO})(\text{PEt}_3)_2$

This reaction was repeated, this time using a 2:1 molar ratio of reactants in the hope that a complex containing two PF_2NMe_2 groups would be formed. The reaction was carried out in methylene chloride and the n.m.r. spectra of the product were recorded at ambient temperature.

The ^{31}P and ^{19}F n.m.r. spectra of the product were qualitatively the same as those of complexes A(vii) and A(viii) which implied that $[\text{Ir}(\text{PF}_2\text{NMe}_2)_2(\text{PEt}_3)_2(\text{CO})]^+\text{Cl}^-$ (complex A(vi) of Figure A.1) had been formed. The complex was isolated as a colourless intractable oil.

AI.8 The Reaction of a Large Excess of PF_2NMe_2 with $\text{IrI}(\text{CO})(\text{PEt}_3)_2$

This reaction was studied in the hope that complex A(vi) would be formed. However, on warming the reaction to room temperature no reaction was visibly apparent (if complex A(vi) had formed the solution should have become colourless). The reaction medium was therefore maintained at ambient temperature for ca. 2 weeks after that time the toluene solution was still yellow but a colourless solid had precipitated. The solid was found to dissolve in methylene chloride and ^{31}P and ^{19}F n.m.r. spectra were recorded. The n.m.r. parameters for the product are presented in Table A.1.3.

The $^{31}\text{P}\{-^1\text{H}\}$ n.m.r. spectra consisted of two resonances; that to high frequency ($\delta\text{P} = 122$ ppm) was split into a complex second order pattern. The signal to low frequency arising from

the PEt_3 groups was split into a quartet of septets, these splittings were deduced to have arisen from $^2J_{\text{PP}}$ and $^3J_{\text{PF}}$ respectively.

The ^{19}F n.m.r. spectrum consisted of a single resonance split into a complex second order pattern.

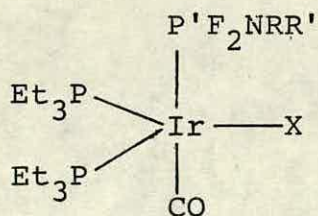
The carbon, hydrogen and nitrogen analyses were reasonably consistent with the formulation $[\text{Ir}(\text{PF}_2\text{NMe}_2)_3(\text{PEt}_3)_2]^+\text{I}^-$.

The i.r. spectrum of the product did not have any bands that could be assigned to ν_{CO} .

From the data collected it was apparent that CO had been displaced by PF_2NMe_2 yielding a cationic five-coordinated iridium (I) complex containing three PF_2NMe_2 and two PEt_3 ligands. (Although no direct evidence that the complex was ionic was obtained it was considered unlikely that the iodide would remain attached to iridium in the light of the results described in AI.4 and AI.5), $[\text{Ir}(\text{PF}_2\text{NMe}_2)_3(\text{PEt}_3)_2]^+\text{I}^-$. The observed splitting pattern for the PEt_3 resonance meant that the PF_2NMe_2 ligands were magnetically equivalent which could only be the case if, either the complex had a trigonal-bipyramidal structure with the PF_2NMe_2 ligands in equatorial positions or the complex was fluxional with ligands undergoing pseudo rotation about the iridium centre. Unfortunately, the possibility of a fluxional molecule was not considered at the time and so no more information regarding the structure of the complex in solution was obtained.

Table A.1.1

N.m.r. parameters for



| Complex | X | R | R' | $\delta\text{P/ppm}$ | $\delta\text{P}'/\text{ppm}$ | $\delta\text{F/ppm}$ | $^1\text{J}_{\text{PF}}/\text{Hz}$ | $^2\text{J}_{\text{PP}'}/\text{Hz}$ | $^3\text{J}_{\text{P}'\text{F}}/\text{Hz}$ |
|---------------|----|----|----|----------------------|------------------------------|----------------------|------------------------------------|-------------------------------------|--|
| A(i) [c] | Cl | Me | Me | 2.0 | 114 | -31.2 | 1108 | 39 | NR |
| A(ii) [a] [c] | Br | Me | Me | -2.5 | 114 | -32.2 | 1105 | 40 | 6.0 |
| A(iii) [d] | I | Me | Me | -9.5 | 114 | -30.6 | 1107 | 41 | NR |
| A(iv) [b] [d] | I | H | Me | -9.9 | 109 | -42.9 | 1134 | 38.3 | 5.7 |
| A(v) [d] | I | H | H | -9.6 | 111 | -30.0 | 1139 | 39 | 6 |

[a] $^3\text{J}_{\text{PH}} = 11.5 \text{ Hz}$

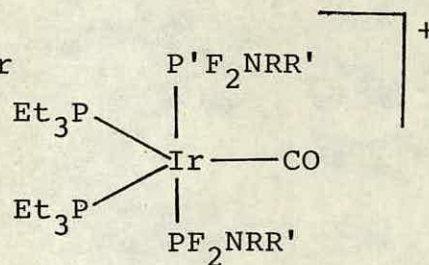
[b] $^2\text{J}_{\text{PH}} = 38.3\text{Hz}; ^3\text{J}_{\text{PH}} = 9.9 \text{ Hz}$

Parameters were recorded in toluene at: [c] 243 K;

[d] room temperature

Table A.1.2

N.m.r. parameters for



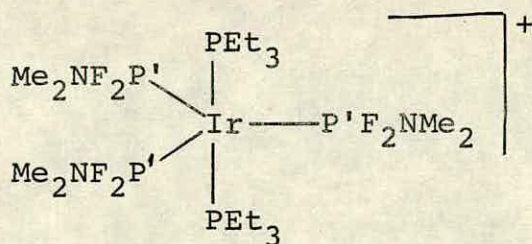
| Complex | R' | R' | $\delta\text{P/ppm}$ | $\delta\text{P' /ppm}$ | $\delta\text{F/ppm}$ | $^1\text{J}_{\text{P}'\text{F}}/\text{Hz}$ [a] | $^2\text{J}_{\text{P}'\text{P}}/\text{Hz}$ [a] | $^2\text{J}_{\text{PP}'}/\text{Hz}$ | $^3\text{J}_{\text{P}'\text{F}}/\text{Hz}$ [a] | $^3\text{J}_{\text{PF}}/\text{Hz}$ |
|-------------|----|----|----------------------|------------------------|----------------------|--|--|-------------------------------------|--|------------------------------------|
| A(vi) [b] | Me | Me | -11.8 | 118.7 | -30.5 | 1130 | 187 | 41.0 | -1 | 2.0 |
| A(vii) [c] | H | Me | -8.9 | 108.1 | -36.4 | 1158 | 293 | 41.1 | -90 | 2.4 |
| A(viii) [b] | H | H | -8.9 | 112.2 | -22.6 | 1168 | 304 | 42.0 | -94 | 2.9 |

[a] Calculated from values obtained in the ^{19}F n.m.r. spectra using expressions described in 3.2.2

Parameters were recorded in: [b] methylene chloride; [c] chloroform, at room temperature

Table A.1.3

N.m.r. parameters for



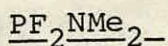
| $\delta P/\text{ppm}$ | $\delta P'/\text{ppm}$ | $\delta F/\text{ppm}$ | $^1J_{P',F'}/\text{Hz}$ [a] | $^2J_{PP'}/\text{Hz}$ | $^3J_{PF}/\text{Hz}$ |
|-----------------------|------------------------|-----------------------|-----------------------------|-----------------------|----------------------|
| -17.8 | 122 | -29.1 | 1050 | 44.9 | 2.2 |

[a] This is a measure of the frequency difference between the two most intense lines in the ^{19}F n.m.r. spectrum

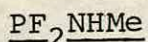
Parameters were recorded in methylene chloride at room temperature.

AI.9 Experimental

AI.9a Preparation of Aminodifluorophosphines



See section 6.5.



PF_2NHMe was prepared using a variation of the literature method⁽¹⁶³⁾ by reaction of PF_2Br with NH_2Me .

Aminodifluorophosphine

PF_2NH_2 was prepared using standard literature methods⁽¹⁶⁴⁾ by reaction of PF_2Br with NH_3 .

AI.9b The Reactions of $\text{PF}_2\text{NRR}'$ with $\text{IrX}(\text{CO})(\text{PEt}_3)_2-$

All reactions described in this section were set up by applying the standard technique for setting up a reaction in a sealed n.m.r. tube (see section 6.4).

AI.9c The Isolation of $\text{IrI}(\text{CO})(\text{PEt}_3)_2(\text{PF}_2\text{NMe}_2)-$

The n.m.r. tube in which the reaction was studied was opened under nitrogen. The contents of the n.m.r. tube were tipped into a Schlenk tube with careful washing with dry degassed toluene. The Schlenk tube was attached to a Schlenk line and all volatiles were pumped off. The resulting gum was triturated with petrol-ether ($40^\circ-60^\circ$) to yield a yellow powder.

Analytical and i.r. spectral data for $\text{IrI}(\text{CO})(\text{PEt}_3)_2-(\text{PF}_2\text{NMe}_2)$ in Tables A.1.4 and A.1.5 respectively.

AI.9d The Isolation of $[\text{Ir}(\text{PF}_2\text{NRR}')_2(\text{PEt}_3)_2(\text{CO})]^+$
 $[\text{R} = \text{R}' = \text{H}, \text{X} = \text{Cl}; \text{R} = \text{H}, \text{R}' = \text{Me}, \text{X} = \text{Cl}]$

The n.m.r. tubes in which the reaction systems were initially studied were opened under nitrogen and the contents transferred to a Schlenk tube, the solids formed in the tubes were carefully washed out with dry degassed methylene chloride. The Schlenk tubes were attached to a vacuum line and sufficient quantities of the appropriate $\text{PF}_2\text{NRR}'$ were condensed into the tube to react with any excess of $\text{IrX}(\text{CO})(\text{PEt}_3)_2$ remaining from the n.m.r. tube reaction. After warming to room temperature all volatiles were pumped off and the products (white microcrystalline solids) were washed with petrol ether ($40^\circ\text{--}60^\circ$) and then maintained under high vacuum for 6 hours to remove any residual solvent.

Analytical and i.r. spectral data for $[\text{Ir}(\text{PF}_2\text{NH}_2)_2(\text{PEt}_3)_2(\text{CO})]^+\text{Cl}^-$ and $[\text{Ir}(\text{PF}_2\text{NHMe})_2(\text{PEt}_3)_2(\text{CO})]^+\text{Cl}^-$ are presented in Tables A.1.4 and A.1.5 respectively.

AI.9e The Preparation of $[\text{Ir}(\text{PF}_2\text{NMe}_2)_2(\text{PEt}_3)_2(\text{CO})]^+\text{Cl}^-$

PF_2NMe_2 (0.2 mmole) was condensed into a Schlenk tube containing a solution of $\text{IrCl}(\text{CO})(\text{PEt}_3)_2$ (0.05 g: 0.1 mmole) in CH_2Cl_2 . After warming to room temperature the volatiles were pumped off leaving an intractable colourless oil which was characterised as $[\text{Ir}(\text{PF}_2\text{NMe}_2)_2(\text{PEt}_3)_2(\text{CO})]^+\text{Cl}^-$ by its n.m.r. spectra.

Table A.1.5 Infra-red spectral data for some complexes described in sections A.1.2 - A.1.9

| | |
|---|--|
| A(iii) $\text{IrI}(\text{CO})(\text{PEt}_3)_2(\text{PF}_2\text{NMe}_2)^{+}[\text{a}]$ | 1938vs, 1305s, 1273m, 1260w, 1190s, 1049s, 990s, 810s, 770s, 750m, 725s, 605m, 540s, 510m, 448m, 360vw. |
| A(vii) $[\text{Ir}(\text{PF}_2\text{NHMe})_2(\text{PEt}_3)_2(\text{CO})]^{+}\text{Cl}^{-}[\text{b}]$ | 1965vs, 1250w, 1105m, 1080m, 1030m, 850m, 780s, 755s, 730m, 580m, 559m, 520m, 480m, 425m, 410m, 380m, 320w. |
| A(viii) $[\text{Ir}(\text{PF}_2\text{NH}_2)_2(\text{PEt}_3)_2(\text{CO})]^{+}\text{Cl}^{-}[\text{b}]$ | 3660w, 3170bw, 2710w, 1962vs, 1571m, 1305w, 1270w, 1150w, 1035m, 965m, 790s, 770s, 735m, 720m, 625w, 525m, 507w, 470w, 463m, 425w, 399m. |
| A(ix) $[\text{Ir}(\text{PF}_2\text{NMe}_2)_3(\text{PEt}_3)_2]^{+}\text{I}^{-}[\text{a}]$ | 1305s, 1240w, 1180s, 1042s, 990vs, 780vs, 760vs, 705vs, 542w, 510s, 450w, 425m, 380m, 360w, 300m |

Abbreviations vs = very strong; s = strong; m = medium; w = weak; b = broad

Data were recorded from either [a] nujol mulls of the solids on CsI plates
or [b] KBr discs .

Table A.1.4 Analytical Data for some complexes described in sections A.1.2 - A.1.9

| Complex | Found | | | Required | | |
|---|-------|-----|-----|----------|-----|--------------------|
| | %C | %H | %N | %C | %H | %N |
| A(iii) $\text{IrI}(\text{CO})(\text{PEt}_3)_2(\text{PF}_2\text{NMe}_2)$ | 25.8 | 5.1 | 1.9 | 26.1 | 5.3 | 2.0 |
| A(vii) $[\text{Ir}(\text{PF}_2\text{NHMe})_2(\text{PEt}_3)_2(\text{CO})]^+\text{Cl}^-$ | 26.3 | 5.4 | 3.9 | 26.1 | 5.5 | 4.0 |
| A(viii) $[\text{Ir}(\text{PF}_2\text{NH}_2)_2(\text{PEt}_3)_2(\text{CO})]^+\text{Cl}^-$ | 23.6 | 5.2 | 4.2 | 24.2 | 5.3 | 4.0 |
| A(ix) $[\text{Ir}(\text{PF}_2\text{NMe}_2)_3(\text{PEt}_3)_2]^+\text{I}^-$ | 25.5 | 5.3 | 3.4 | 24.1 | 5.4 | 4.7 ^[a] |

[a] Sample still slightly wet analyses are better if one assumes ca, 1/7 mole of C_7H_8 per mole of sample

AI.9f The Preparation of $[\text{Ir}(\text{PF}_2\text{NMe}_2)_3(\text{PEt}_3)_2]\text{I}^-$

PF_2NMe_2 (1 mmole) was condensed into a Schlenk tube containing a solution of $\text{IrI}(\text{CO})(\text{PEt}_3)_2$ (0.06 g; 0.1 mmole) in toluene. The reaction medium was warmed to room temperature and then left standing for 2 weeks; a white precipitate drops out of the solution during that time. The supernatant was drawn off using a pasteur pipette and then the solid washed with toluene and petrol-ether ($40^\circ\text{--}60^\circ$). The solid was maintained under high vacuum at room temperature for 3 hours to remove any residual solvent.

Analytical and i.r. spectral data for $[\text{Ir}(\text{PF}_2\text{NMe}_2)_3(\text{PEt}_3)_2]^+\text{I}^-$ are presented in Tables A.1.4 and A.1.5 respectively.

AI.10 Conclusions

The reactions described in this Appendix have confirmed that the aminodifluorophosphines are excellent coordinating ligands. There were a number of interesting observations to be made from the experimental results:

(i) That adducts with single difluorophosphine ligands were detected only when either the fluorophosphine was PF_2NMe_2 or the halide bound to iridium was iodide.

(ii) The stability of the mono- PF_2NMe_2 adducts seemed to be greatest when iodide was bound to iridium; as shown by the exchange of PF_2NMe_2 when X was Cl or Br.

(iii) The greatest tendency to form bis-PF₂NR₂ adducts was observed when the fluorophosphine was PF₂NH₂.

(iv) The lowest tendency to form bis-PF₂NR₂ adducts was observed when the fluorophosphine was PF₂NMe₂; the reaction had to be forced by adding an excess of PF₂NR₂.

(vi) Chloride is displaced fairly easily by the PF₂NR₂ compounds.

The low tendency for displacement of iodide is probably because of the fact that it is a far softer base than the other halides and so it would be difficult to detach it from Ir(I) which is a soft acid.

The different tendencies of the fluorophosphines towards displacement of halides could not be explained. Initially it was thought that they may have been due to the different steric requirements of the three fluorophosphines but this was thought unlikely in the light of results obtained for the reaction of PF₃ with IrCl(CO)(PEt₃)₂ (see A.2) and the fact that it was possible to obtain a complex with three PF₂NMe₂ groups around iridium.

Having shown that it is possible to displace halide ligands from iridium to produce five-coordinate species containing two fluorophosphine ligands, we can propose that the reactions of PF₂OC₃H₅ with Vaska's compound reported by Grosse and Schmutzler using a 1:1 molar ratio of reactants⁽¹⁶²⁾ might have yielded similar complexes (see AI.1); further work would have to be carried out to confirm or refute this postulate.

There are a number of reactions that might be carried out in the light of this work.

(a) Attempts to make $[\text{Ir}(\text{PF}_2\text{NRR}')_3(\text{PEt}_3)_2]^+\text{X}^-$
[R = H, R' = H or Me] should be made.

(b) The reactions of aminodifluorophosphine compounds with more than one fluorophosphine centre might be interesting. These might act as either bridging ligands between iridium centres or in some cases chelating ligands.

(c) The reactions of the metal-bound $\text{PF}_2\text{NRR}'$ with HX might lead to an alternative route for the formation of (PF_2X) -iridium complexes.

A.2 The Reaction of PF_3 with $\text{IrCl}(\text{CO})(\text{PEt}_3)_2$

This reaction was studied in an n.m.r. tube at temperatures from 203 K to ambient temperature and the ^{31}P and ^{19}F n.m.r. spectra of the species formed were recorded. The n.m.r. parameters for this species are presented in Table A.2.

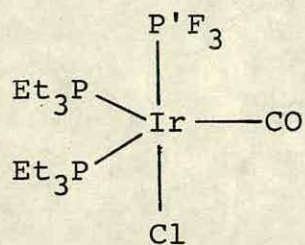
At 203 K, reactions occurred yielding a single product. The $^{31}\text{P}\{-^1\text{H}\}$ n.m.r. spectrum of the product consisted of two resonances. The resonance to high frequency (δP ca. 80 ppm) was split into a quartet ($^1\text{J}_{\text{PF}}$) of triplets ($^2\text{J}_{\text{PP}}$). The signal associated with the PEt_3 groups, at $\delta\text{P} = 5.1$ ppm, was split into a doublet, the magnitude of the coupling being equal to the triplet coupling of the other signal ($^2\text{J}_{\text{PP}}$). The lines constituting the doublet were very broad, presumably because of unresolved $^3\text{J}_{\text{PF}}$.

On warming the reaction system above 243 K the lines constituting the splitting patterns of the $^{31}\text{P}-\{^1\text{H}\}$ n.m.r. signals broaden such that no couplings of a lower order than $^1J_{\text{PF}}$ were resolved. On recooling the system to 203 K, $^{31}\text{P}-\{^1\text{H}\}$ and ^{19}F n.m.r. spectra identical to those originally obtained were collected.

The interpretation of these results was that a reaction completely analogous to those described in A1.2 had taken place forming a five-coordinate iridium(I) complex containing a coordinated PF_3 ligand. The n.m.r. parameters associated with the PF_3 group fall within ranges normally associated with a coordinated PF_3 ligand^(17,46). The splitting pattern observed for the PF_3 resonance implied that the complex contained the $(\text{PF}_3)\text{Ir}-(\text{PEt}_3)_2$ unit. Although we have no direct evidence that either CO or Cl were bound to iridium, it was considered unlikely that they had been displaced to form four-coordinate iridium(I) complexes with a coordinated PF_3 , in the light of results described in A.1.

Table A.2

N.m.r. parameters for



| $\delta\text{P/ppm}$ | $\delta\text{P' /ppm}$ | $\delta\text{F/ppm}$ | $^1\text{J}_{\text{P}'\text{F}}/\text{Hz}$ | $^2\text{J}_{\text{PP}}/\text{Hz}$ | $^3\text{J}_{\text{PF}}/\text{Hz}$ |
|----------------------|------------------------|----------------------|--|------------------------------------|------------------------------------|
| 5.1 | 83.6 | -13.3 | 1377 | 44 | NR |

Parameters were recorded in methylene chloride at 203 K.

APPENDIX 3

Published Material

"Complexes of Iridium with Terminal PF_2 -Ligands",

by E.A.V. Ebsworth, Neil T. McManus, David W.H. Rankin
and John D. Whitelock.

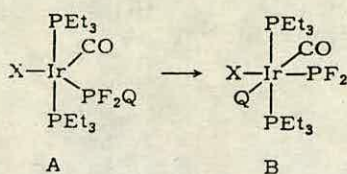
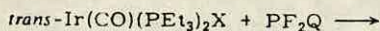
Angew.Chem.Internat. Edn., 20, 801, (1981).

By E. A. V. Ebsworth, Neil T. McManus,
David W. H. Rankin, and John D. Whitlock^[**]

Attempts to prepare complexes containing a metal bound to tricoordinated phosphorus have usually produced bridged species. Some derivatives of chromium and tungsten are known in which terminal PCl₂-groups are bound to the metal^[1], but attempts to prepare PF₂-complexes of platinum have led to the production of dinuclear diplatinum complexes^[2]. Here we report the synthesis and characterization of some complexes of iridium(III) containing terminal PF₂-ligands; these compounds should be suitable for use in the controlled synthesis of mixed-metal bridged complexes.

Reaction of a solution of PF₂H and *trans*-Ir(CO)I(PEt₃)₂ at 233 K in toluene leads to the formation of a PF₂H-complex of pentacoordinated iridium (type A in Scheme 1). Two signals are observed in the ³¹P{¹H}-NMR spectrum (Table 1); a doublet at $\delta = -7$ (²J(PP) = 38 Hz) arising from PEt₃, and a wide triplet from the PF₂-group at $\delta = 142$ (¹J(PF) = 1103 Hz) each line of which is further split into a narrow triplet because of coupling with the P atoms of the two Et₃P-groups. In the non-decoupled spectrum, each line of the PF₂-signal shows an additional doublet splitting of 415 Hz, a typical value for ¹J(PH) in tetracoordinated phosphorus compounds. The ¹H-NMR spectrum shows a resonance at $\delta = 8.4$ with a doublet splitting of 415 Hz, each line is further split into a triplet [due to ²J(FH)] of triplets [due to ³J(PH)].

When the solution was allowed to warm to room temperature, the spectra changed. The P resonance of the PF₂-group shifts from $\delta = 142$ to $\delta = 378$; this implies a significant alteration in the environment of the PF₂-group. Moreover, the magnitude of ²J(PP) becomes smaller and *J*(HPF₂) drops from 415 Hz to 7.5 Hz. In the ¹H-NMR spectrum, the resonance at $\delta = 8.4$ disappears and is replaced by a complex multiplet at $\delta = -16$ that must be due to H bound to Ir. It follows that the pentacoordinated iridium complex (1) (type A) formed initially has rearranged to give a new complex (5) of hexacoordinated iridium(III) (type B in Scheme 1) by oxidative addition of PH, leaving H and a terminal PF₂-group bound to the metal.



| X | Q | Type A | Type B |
|----|----|--------|--------|
| I | H | (1) | (5) |
| Cl | Cl | (2) | (6) |
| Br | Br | (3) | (7) |
| I | I | (4) | (8) |

Scheme 1

Similar reactions occur between PF₂X and *trans*-Ir(CO)X(PEt₃)₂, X = Cl, Br or I. When X = Cl, the ¹⁹F- and ³¹P-NMR spectra show peaks with the multiplet structures expected for a complex of type A; the PF₂-chemical shift ($\delta = 97$) is in the same region as that of PF₂Cl-complexes. When the solution is allowed to warm to room temperature, the PF₂-resonance shifts to $\delta = 364.8$ i.e. the signal for (6) is similar to that for (5). When X = Br, the concentration of the complex (3) (type A) at 193 K is small, and the assignment of the PF₂-resonance is doubtful; when X = I, we were unable to identify any of the signals expected for complex (4). In each case, however, there are resonances due to complexes (7) or (8) (type B); in keeping with the assigned structure, all the PF₂-chemical shifts are very similar (Table 1).

Table 1. NMR data for the complexes of types A and B recorded in [D₈]toluene at 233 K [(1)–(5)] and at 298 K [(6)–(8)]; precision: ± 1 to the last figure quoted (J in Hz).

| Complex | Type | $\delta(\text{PEt}_3)$ | $\delta(\text{PF}_2)$ | $\delta(\text{F})$ | ¹ J(PF) | ² J(PP) | ³ J(PF) |
|---------|------|-------------------------|-----------------------|--------------------|--------------------|--------------------|--------------------|
| (1) [a] | A | – 7.2 | 142 | – 60.8 | 1103 | 38 | [c] |
| (2) | A | – 6.9 | 97 | 4.9 | 1333 | 42 | 9 |
| (3) | A | 0.3 | 110 | 6.2 | 1341 | 45 | [c] |
| (4) | A | resonances not observed | | | | | |
| (5) [b] | B | – 10.8 | 376.7 | – 61.5 | 1111 | 25.9 | 17.1 |
| (6) | B | – 9.3 | 364.8 | – 68.3 | 1106 | 9.2 | 11.6 |
| (7) | B | – 18.1 | 363.1 | – 64.8 | 1108 | 8.5 | 11.1 |
| (8) | B | – 31.9 | 364.8 | – 61.0 | 1112 | 8.3 | 10.6 |

[a] $\delta(\text{H}) = 8.72$. [b] $\delta(\text{H}) = -16.0$; ²J(H(PEt)) = 10, ²J(H(PF)) = 7.5, ³J(HF) = 11.5 Hz. [c] Not resolved.

Complex (5) decomposes slowly in solution at room temperature, but complexes (6)–(8) are stable at room temperature and have been isolated and characterized by elemental analysis, IR-, and NMR-spectroscopy. Addition of B₂H₆ to a solution of (8) in C₇H₈ leads to a shift in the PF₂-resonance in the ³¹P{¹H}-NMR spectrum to $\delta = 250$, together with a marked broadening of the lines. We interpret these observations as evidence that a bridged complex containing the grouping Ir–PF₂–BH₃ has been formed; in confirmation of this view, the ¹⁹F-NMR spectrum consists of a broad doublet, due to ¹J(PF), each line of which is split into a 1:3:3:1 quartet by F–H coupling.

Received: August 18, 1980 [Z 825 IE]
German version: Angew. Chem. 93, 785 (1981)

[1] W. Malisch, R. Alsmann, Angew. Chem. 88, 809 (1976); Angew. Chem. Int. Ed. Engl. 15, 769 (1976).

[2] E. A. V. Ebsworth, D. W. H. Rankin, J. D. Whitlock, unpublished results.

[*] Prof. Dr. E. A. V. Ebsworth, N. T. McManus, Dr. D. W. H. Rankin, Dr. J. D. Whitlock,
Department of Chemistry, University of Edinburgh,
Edinburgh EH9 3JJ (Scotland)

[**] This work was supported by Messrs Johnson Matthey and the Science Research Council

REFERENCES

1. L. Vaska, Science, 140, 809 (1963).
2. L. Vaska, ibid, 152, 769, (1966).
3. L. Vaska, J.Amer.Chem.Soc., 88, 1333 , (1966).
4. L. Vaska and R.E. Rhodes, ibid, 87, 4970 (1965).
5. R.N. Scott, D.F. Schriver and D.D. Lehmann, Inorg.Chim. Acta, 4, 73, (1970).
6. R.N. Scott and D.F. Schriver, J.Amer.Chem.Soc., 90, 1079 (1968).
8. L. Vaska, Acc.Chem.Res., 1, 335, (1968).
9. D.F. Schriver, ibid, 3, 231, (1968).
10. P. Powell and H. Nöth, Chem.Comm., 637, (1966).
11. J.L. Margrave, K.G. Sharp and P.W. Wilson, J.Inorg. and Nuc.Chem., 32, 1815, (1970).
12. C.J. Schack, K.G. Sharp and M.G. Warner, Chem.Comm., 1110, (1969).
13. R.R. Homes and W.P. Gallagher, Inorg.Chem., 2, 433, (1963).
14. D.F. Smith, Science, 141, 1039 (1963).
15. K.G. Sharp and J.L. Margrave, Inorg.Chem., 8, 2655, (1969).
16. J.L. Margrave, K.G. Sharp and P.W. Wilson, J.Inorg. and Nuc.Chem., 32, 1817, (1970).
17. J.F. Nixon, Adv. in Inorg. and Radiochem., 13, 364, (1973), and references therein.

18. J. Emsley and D. Hall, "The Chemistry of Phosphorus", (1976), Harper and Row Ltd., London, and references therein.
19. R. Schmutzler, *Advan. Fluorine Chem.*, Vol. 5, 66, Butterworths, London, (1965).
20. D.B. Denney, D.Z. Denney, B.C. Chang and K.L. Marsi, J.Amer.Chem.Soc., 91, 5243, (1969).
21. D.B. Denney, D.Z. Denney, C.D. Hall and K.L. Marsi, *ibid*, 94, 245, (1972).
22. L. Centofanti and R.W. Parry, Inorg.Chem., 12, 1456, (1973).
23. D.W.H. Rankin and J.G. Wright, J.Chem.Soc. Dalton, 2049, (1980).
24. J.P. Collmann, Acc. Chem. Res., 1, 136, (1968).
25. J.A. Osborn, F.H. Jardine, J.F. Young and G. Wilkinson, J.Chem.Soc. (A), 1711, (1966).
26. D. Evans, G. Yagupsky and G. Wilkinson, J.Chem.Soc. (A), 2660, (1968); D. Evans, J.A. Osborn and G. Wilkinson, *ibid*, 3133, (1968); G. Yagupsky, C.K. Brown and G. Wilkinson, *ibid*, 1392, 2753, (1970).
27. L. Vaska and J.W. Diluzzio, J.Amer.Chem.Soc., 84, 679, (1962).
28. L. Vaska and J.W. Diluzzio, *ibid*, 83, 2784, (1961);
L. Vaska, *ibid*, 88, 5325, (1966).
29. R.F. Heck, *ibid*, 86, 2796, (1964).
30. R.S. Nyholm and K. Vrieze, J.Chem.Soc., 5337, (1965).

31. E.A.V. Ebsworth and T.E. Fraser, J.Chem.Soc. Dalton, 1960, (1979).
32. C.B. Colburn, W.E. Hill and D.W.A. Sharp, Inorg. and Nuc. Chem. Lett., 8, 625, (1972).
33. E.A.V. Ebsworth and T.E. Fraser, J.Chem.Soc., Dalton, 1960, (1979); E.A.V. Ebsworth, H.M. Ferrier and T.E. Fraser, *ibid*, 836, (1981).
34. F. Glockling and W.D. Wilbey, J.Chem.Soc.(A), 1675, (1969).
35. N.J. Pilkington, personal communication.
36. L. Vallerino, J.Inorg. and Nuc. Chem.Lett., 8, 288, (1958).
37. F. de Charentnay, J.A. Osborn and G. Wilkinson, J.Chem.Soc.(A), 787, (1968).
38. E.A.V. Ebsworth, M.R. Ojeda and D.W.H. Rankin, J.Chem.Soc. Dalton, 1513, (1982).
39. M.R. Ojeda, Ph.D. Thesis, (1981).
40. R.B. King and A. Efraty, J.Amer.Chem.Soc., 94, 3768, (1972).
41. T. Krück, Angew.Chem.Internat.Edn., 6, 53, (1967).
42. J.F. Nixon, Endeavour, 32, 19, (1973).
43. T. Krück, K. Bauer and W. Lang, Chem.Ber., 101, 138, (1968).
44. M.A. Bennett and D.L. Milner, Chem.Comm., 581, (1967).
45. D.A. Clement, J.F. Nixon and M.D. Sexton, J.Chem.Soc. Dalton, 1509, (1969).
46. R.A. Head and J.F. Nixon, J.Chem.Soc., Dalton, 885, (1978).
47. C.A. Udovich and R.J. Clark, Inorg.Chem., 8, 939, (1969).

48. E.A.V. Ebsworth, J.D. Whitelock and D.W.H. Rankin,
J.Chem.Soc., Dalton, 840, (1981).
49. J. Grobe and F. Kober, Z. Naturforsch, 246, 1660, (1969).
50. D. Bain, unpublished work.
51. W.M. Douglas and J.K. Ruff, J.Chem.Soc.(A), 3558, (1971).
52. T. Krück, M. Höfler, H. Jung and H. Blume, Angew.Chem.
Internat.Edn., 8, 522, (1969).
53. D.C. Staplin and R.W. Parry, Inorg.Chem., 18, 1473, (1979).
54. J.D. Whitelock, personal communication.
55. R.C. Dobbie and P.R. Mason, J.Chem.Soc., Dalton, 1124, (1973).
56. W.R. Cullen and R.G. Hayter, J.Amer.Chem.Soc., 86, 1030,
(1963).
57. W.R. Cullen, D.J. Patmore, J.R. Sams, M.J. Newlands
and J.K. Thomson, Chem.Comm., 953, (1971).
58. W.R. Cullen, D.J. Patmore and J.R. Sams, Inorg.Chem.,
12, 867, (1973).
59. G.N. Schrauzer and G. Kratell, Angew.Chem.Internat.Edn.,
4, 146, (1965).
60. Y.L. Baay and A.G. MacDiarmid, Inorg.Nuc.Chem.Lett., 3,
159, (1967).
61. P.M. Treichel, W.M. Douglas and W.K. Dean, Inorg.Chem.,
11, 1615, (1972).
62. A.N. Nesmayanov, K. Anisasimov, N. Kolobova and
V.N. Khandozkho, Dokl.Akad.Nauk., S.S.S.R., 156,
863, (1963).

63. J.F. Young, Advan.Inorg.Chem. and Radiochem., 11, 92, (1968), and references therein.
64. M. Cooke, M. Green and D. Kirkpatrick, J.Chem.Soc.(A), 1507, (1968).
65. W. Malisch, and M. Kuhn, J.Organomet.Chem., 73, C1, (1974).
66. W. Malisch and P. Panster, Z. Naturforsch(B), 33B, 1405, (1978).
67. W. Malisch and P. Panster, ibid, 30B, 220, (1975).
68. W. Malisch and P. Panster, Angew.Chem.Internat.Edn., 15, 618, (1976).
69. W. Malisch and P. Panster, Chem.Ber., 108, 700, (1975).
70. W. Malisch and J. Kuhn, Angew.Chem.Internat.Edn., 13, 84, (1974).
71. W. Malisch and P. Panster, J.Organomet.Chem., 76, C7, (1974); 99, 421, (1975).
72. W. Malisch and R. Alsmann, Angew.Chem.Internat.Edn., 15, 769, (1976).
73. W. Malisch, P. Panster and R. Alsmann, Z.Naturforsch(B), 33B, 899, (1978).
74. W. Malisch and R. Maisch, J.Organomet.Chem., 220, C1, (1981).
75. R.J. Haines and C.R. Nolte, J.Organomet.Chem., 36, 163, (1972).
76. W. Malisch and P. Panster, Angew.Chem., 16, 408, (1977).
77. W. Malisch, M. Kuhn, W. Albert and H. Rössner, Chem.Ber., 113, 3318, (1980).

78. W. Malisch and P. Panster, Chem.Ber., 108, 716, (1975).
79. W. Malisch, R. Janta and G. Kuenzel, Z. Naturforsch(B), 34B, 599, (1979).
80. M.J. Barrow and G.A. Sim, J.Chem.Soc. Dalton, 219, (1975).
81. S.J. La Placa and J.A. Ibers, Inorg.Chem., 5, 405, (1966).
82. S.J. La Placa and J.A. Ibers, J.Amer.Chem.Soc., 87, 2581, (1965).
83. J. Chatt, N.P. Johnson and B.L. Shaw, J.Chem.Soc. (A), 1625, (1964).
84. J.F. Nixon and J.R. Swain, J.Inorg. and Nuc. Chem. Lett., 295, (1969).
85. P.W. Rudolph, R.C. Taylor and R.W. Parry, J.Amer.Chem. Soc., 88, 3729, (1966).
86. G.S. Reddy and R. Schmulzler, Inorg.Chem., 6, 823, (1967).
87. D.W.W. Anderson, J.E. Bentham and D.W.H. Rankin, J.Chem.Soc., Dalton, 1215, (1973).
88. P.S. Pregosin and R.W. Kunz, "³¹P and ¹³C n.m.r. of Transition Metal Phosphine Complexes", Springer Verlag, Berlin-Heidelberg-New York, (1979) and references therein.
89. B.E. Mann, C. Masters and B.L. Shaw, J.Chem.Soc. Dalton, 704, (1972).
90. J.F. Nixon and R. Schmutzler, Spectrochim.Acta, 20, 1835, (1964).
91. R.W. Rudolph and R.W. Parry, J.Amer.Chem.Soc., 89, 1621, (1967).

92. E. Müller, E. Nieke and B. Krebs, Mol.Phys., 14, 591, (1968).
93. R.T. Paine, R.W. Light and D.E. Maier, Inorg.Chem., 18, 368, (1979).
94. E.A.V. Ebsworth, D.W.H. Rankin and J.G. Wright, J.Chem.Soc., Dalton, 1065, (1979).
95. R.T. Paine, Inorg.Chem., 16, 2996, (1977).
96. E.L. Lines and L.F. Centofanti, Inorg.Chem., 12, 598, (1973).
97. P.G. Page, personal communication.
98. E.A.V. Ebsworth, D.W.H. Rankin and J.D. Whitelock, J.Chem.Soc, Dalton, 840, (1981); J.D. Whitelock, Ph.D. Thesis, (1980).
99. D.M. Anderson, Ph.D. Thesis, (1982).
100. J. Grosse and R. Schmutzler, J.Chem.Soc., Dalton, 405, (1976).
101. T. Kruck, M. Höfler, K. Baur, P. Junkes and K. Glinka, Chem.Ber., 101, 3827, (1968).
102. D.W.W. Anderson, E.A.V. Ebsworth, G.D. Miekke and D.W.H. Rankin, Mol.Phys., 25, 381, (1973).
103. H.G. Horn and A. Müller, Z.Anorg.Allg.Chem., 346, 266 (1966).
104. A. Müller, E. Nieke and B. Krebs, Mol.Phys., 14, 591, (1968).
105. R.O. Gould, Proc. 7th Euro. Crystallographic Meeting, (1982).
106. J. McFarlane and D.S. Rycroft, J.Chem.Soc., Chem.Comm., 913, (1972).

107. J.A. Nash, Chem.Comm., 913, (1969).
108. T. Moritami, K. Kuchitsu and Y. Morino, Inorg.Chem.,
10, 344, (1971).
109. D.E.J. Arnold and D.W.H. Rankin, J.Fluor.Chem., 405, (1972).
110. V. Schomacker and D.P. Stevenson, J.Amer.Chem.Soc., 63,
37, (1941).
111. J. Grosse, R. Schmutzler and N.S. Sheldrick, Acta.Cryst.(B),
30, 1623, (1976).
112. R.P. Carter and R.R. Holmes, Inorg.Chem., 4, 738, (1965).
113. R.R. Holmes and W.P. Gallagher, Inorg.Chem., 2, 433, (1963).
114. S.C. Peake and R. Schmutzler, J.Chem.Soc.(A), 1049, (1970).
115. R. Schmutzler, J.Amer.Chem.Soc., 86, 4500, (1964).
116. R. Schmutzler, J.Chem.Soc., 5630, (1965).
117. P.M. Treichel, R.A. Goodrich and S.B. Pierce, J.Amer.Chem.
Soc., 89, 2017, (1969).
118. G.S. Reddy and R. Schmutzler, Inorg.Chem., 6, 823, (1967).
119. B. Blaser and K.A. Worms, Z.Anorg.Allg.Chem., 361, 15, (1966).
120. T. Kruck and R. Kobelt, Chem.Ber., 105, 3765, (1972).
121. T. Kruck, G. Sylvester and I. Kunaw, Z.Naturforsch (B),
28B, 38, (1973).
122. T. Kruck and W. Lang, Angew.Chem.Internat.Edn., 6, 454,
(1967).
123. P.L. Timms, Chem.Comm., 1033, (1969).
124. W.M. Douglas and J.K. Ruff, Inorg.Chem., 11, 901, (1972).

125. M.G. Newton, R.B. King, M. Chang and J. Gimeno, J.Amer. Chem.Soc., 100, 326, (1978).
126. N. Ahmad, E.W. Ainscough, T.A. James and S.D. Robinson, J.Chem.Soc., Dalton, 1148, (1973).
127. D.A. Couch, S.D. Robinson and J.N. Wingfield, *ibid*, 1309, (1974).
128. M.P. Brown, R.J. Puddephat, M. Rashidi and K.R. Seddon, *ibid*, 951, (1977).
129. M.C. Cornock and T.A. Stephenson, *ibid*, 683, (1977).
130. D.S. Rycroft, D.W.A. Sharp and J.G. Wright, Inorg. and Nuc. Chem.Lett., 14, 451, (1978).
131. R.K. Harris, J.R. Woplin, R.E. Dunmur, M. Murray and R. Schmutzler, Ber. der Bunsengesellschaft, 76, 44, (1972).
132. P.B. Hitchcock, B. Jacobson and A. Pidcock, J.Chem.Soc., Dalton, 2043, (1977).
133. L. Manojlovic-Muir, K.W. Muir and T. Solumun, J.Organomet. Chem., 142, 265, (1977).
134. L. Manojlovic-Muir, K.W. Muir and R. Walker, J.Chem.Soc. Dalton, 1279, (1976).
135. L. Manojlovic-Muir, K.W. Muir, T. Solamun, D.W. Meek and J. Peterson, J.Organomet.Chem., 146, C26, (1978).
136. R.A. Zelonka and M.C. Baird, Can.J.Chem., 50, 3063, (1972).
137. T. Arthur and T.A. Stephenson, J.Organomet.Chem., 208, 369, (1981).

138. D.R. Robertson, I.W. Robertson and T.A. Stephenson,
J. Organomet.Chem., 202, 309, (1980).
139. R.O. Gould and N.J. Pilkington, unpublished work.
140. J.A. Ibers, D.S. Hamilton and W.H. Baddsey,
Inorg.Chem., 12, 229, (1979).
141. A.J. Schultz, J.V. McArdle and G.P. Khare, J.Organomet.
Chem., 72, 415, (1974).
142. P.D. Brotherton, C.L. Raston, A.H. White and S.B. Wild,
J.Chem.Soc. Dalton, 1799, (1976).
143. L. Aslanov, R. Mason, A.G. Wheeler and P.O. Whimp,
Chem.Comm., 30, (1970).
144. T.G. Appleton, H.C. Clark and L.E. Manzer, Coord.Chem.
Rev., 10, 335, (1973).
145. G.I. Drozd and S.Z. Join, Zh.Obsch.Khim., 38, 1907,
(1968).
146. J.S. Al-Sibori, C. Crocker and B.L. Shaw, J.Chem.Soc.
Dalton, 319, (1981).
147. B.E. Mann, C. Master and B.L. Shaw, J.Chem.Soc.(A),
1104, (1971).
148. R.J. Cross, Proc. Royal Soc.Chem., Dalton Division,
Autumn Meeting, (1982).
149. H.E. Robertson, personal communication.
150. J.F. Nixon and J.R. Swain, J.Organomet.Chem., 72, C15,
(1974).
151. T.H. Brown and P.J. Green, J.Amer.Chem.Soc., 92, 2359,
(1970).

152. B.E. Mann, C. Masters and B.L. Shaw, J.Chem.Soc. Dalton, 704, (1972).
153. G. Pass and H. Sutcliffe, "Practical Inorganic Chemistry", Wm. Cloves and Sons, London, 2nd Edn., (1974).
154. T.E. Fraser, Ph.D. Thesis, (1978).
155. J.L. Herde, J.C. Lampert and C.V. Senoff, Inorg.Synth, XV, 19, (1974).
156. J.G. Morse and K. Cohn, R.W. Rudolph and R.W. Parry, Inorg.Synth., X, 147, (1967).
157. R.W. Rudolph and R.W. Parry, Inorg.Chem., 4, 1339, (1965).
158. A.D. Norman and W.L. Jolly, Inorg.Synth., XI, 15, (1968).
159. K. Brauer, "Handbook of Preparative Inorg. Chem.", Vol. 1, Scripta Technica, New York.
160. J. Chatt, L.M. Vallerino and L.M. Venazzi, J.Chem.Soc., 2496, (1957).
161. J. Chatt and B.L. Shaw, J.Chem.Soc.(A). 1437, (1966).
162. J. Grosse and R. Schmutzler, J.Chem.Soc. Dalton, 412, (1976).
163. S.G.D. Henderson, personal communication;
J.S. Harmann and D.W.A. Sharp, J.Chem.Soc.(A), 1935, (1970).
164. D.W.H. Rankin, J.Chem.Soc.(A), 783, (1971).
165. R.M. Lynden-Bell and R.K. Harris, "Nuclear Magnetic Resonance Spectroscopy", Nelson, London, (1969).

Courses Attended

Inorganic Group Meetings and Seminars.

Programming in Fortran - Dr. C.M. Pounder

Homogeneous Catalysis - Dr. T.A. Stephenson

Inorganic Cage and Cluster Compounds - Dr. A.J. Welch

Attendance at University of Strathclyde Inorganic Club
Conferences (3 years)

Mass Spectrometry - J.H. Beynon